

NEW CARBON-NITROGEN BOND-FORMING REACTIONS OF PALLADIUM

BY

PATRICK S. HANLEY

DISSERTATION

Submitted in partial fulfillment of the requirements
for the degree of Doctor of Philosophy in Chemistry
in the Graduate College of the
University of Illinois at Urbana-Champaign, 2012

Urbana, Illinois

Doctoral Committee:

Professor John F. Hartwig, Chair
Professor Gregory S. Girolami
Professor Thomas B. Rauchfuss
Professor Scott E. Denmark

Abstract

Here we report the synthesis of a series of palladium amido complexes that undergo some of the fundamental reactions of organometallic chemistry. We have discovered two new palladium mediated C-N bond-forming reactions: the migratory insertion of an unactivated alkene into a palladium-nitrogen bond and the reductive elimination of an alkylamine from a low-valent alkylpalladium amido complex. These reactions were previously proposed as steps in palladium catalyzed reactions, however, these are the first examples of isolated palladium complexes that undergo these C-N bond-forming reactions.

The discovery of a series of amidopalladium complexes ligated by a cyclometallated benzylphosphine that react with unactivated alkenes is described. Kinetic and stereochemical analysis indicate that these complexes react by migratory insertion of an alkene into the Pd-N bond. In the presence of ethylene at low temperature (-65°C), an olefin adduct was observed by ^{31}P and ^{13}C NMR spectroscopy that, upon warming to -40 °C, reacted to generate enamines. The final products, enamines, are formed by migratory insertion and subsequent β -hydride elimination.

In a subsequent report, reactions of a family of these complexes containing ancillary ligands having systematically varied electronic and steric properties allowed us to map the effect these properties have on the binding of the alkene and the rate of migratory insertion. Reactions of Pd-amides with functionalized vinylarenes were studied experimentally and computationally to determine the effect of the electronic properties of the alkene on the equilibrium for olefin binding and the rate of insertion. Alkene insertions into Pd-N bonds have been proposed in many catalytic reactions, and these are the first detailed studies of the steric and electronic effects on the migratory insertion step of the reaction of well-defined amido complexes with alkenes.

In the final chapter, we describe the first alkylpalladium amido complexes that undergo C(sp³)-N bond-forming reductive elimination of alkylamines. Three-coordinate norbornylpalladium anilido complexes ligated by bulky monodentate *N*-heterocyclic carbene (NHC) ligands undergo thermal reductive elimination to generate alkylamine products. The stereochemistry of the norbornylamine product suggests that the reductive elimination occurs by a concerted mechanism. The experimentally determined free energy barrier for the reductive elimination of 26 kcal/mol is similar to the computed free energy barrier of 23.9 kcal/mol. Although the reductive elimination of alkylamine to form C(sp³)-N bonds has been proposed to occur in several palladium catalyzed reactions this is first example of isolated low-valent amido complex that undergoes these reactions. We also report preliminary results of reductive elimination of alkylamines from Pd-amido complex ligated by bulky monophosphine ligands.

Acknowledgements

There are many people to thank for supporting me throughout graduate school and during my academic life. Foremost, I owe immense appreciation to my wife Brittany for her loving support over the last 10 years. In July 2008, we moved into a tiny apartment in Champaign; I started graduate school and Brittany started a new path to become a (very good) nurse. Brittany was accepted and graduated from the accelerated nursing program at Illinois State University, and delivered a small portion of the new babies in the Champaign-Urbana area from 2011-2012. Then, we found out we were moving to Berkeley. The last 4.5 years haven't been the easiest, but it has been an awesome experience that I cannot imagine without Brittany. I also owe gratitude to my family. My parents have not studied chemistry, but they have always encouraged me to pursue my interests. The guidance they have provided me has been invaluable.

I am also grateful for the guidance and mentoring of Professor John F. Hartwig. I came to Illinois to work for John, and honestly did not know what I was getting myself into. John is demanding, but I could not be happier to have worked for him. I have learned so much during my time as a member of the Hartwig group. John has shared his expansive knowledge of organometallic chemistry through many subgroups, group meetings, and catalysis lunch sessions. These experiences have been essential to my development as an independent researcher. My approach to thinking about science and problem solving has changed and I feel prepared for the next challenges in my career.

I am fortunate to have a knowledgeable and supportive thesis committee: Professor Thomas B. Rauchfuss, Professor Gregory S. Girolami, and Professor Scott E. Denmark. They have always welcomed my questions and challenged me to think about chemistry from a fundamental

viewpoint. Specifically, Prof. Rauchfuss encouraged me to come to Illinois when I was searching for graduate schools, and served as my advisor when my group left for Berkeley. His support put me at ease during a stressful period: “the move.”

I also owe gratitude to Professor Levi M. Stanley. Levi was an excellent post-doc in the Hartwig group during most of my time in graduate school. In my first year, I asked Levi hundreds of questions, and he was always willing to help me. I feel as though he contributed to my development as an organometallic chemist as much as anyone. I also thank Danielle Gray and Amy Fuller for help collecting x-ray data and solving structures. Dahl Pahls and Professor Thomas Cundari (UNT) assisted with me with computations, and Professor Bill Jones (Rochester) took the time to teach me how to use kinetic simulation software. They are all generous and easy to work with; and the breadth of skills I have acquired during graduate school is more extensive thanks to them.

I also thank Professor Jeffrey Petersen, my research advisor at West Virginia University. Dr. P taught me how to work in a glovebox, but more importantly, he pushed me to attend a great graduate school and pursue science.

Luke Davis and Carl Liskey deserve great thanks for being wonderful friends and classmates. Luke and I became friends on the first day of new student orientation and joined different groups, but remained close throughout graduate school. Luke and I spent many hours late at night discussing chemistry over a beer and these conversations were some the most memorable during my time at Illinois. Carl and I joined the Hartwig lab together in 2008, and have spent plenty time complaining about the rigors of graduate school. It was a little easier to go through prelim, ORP, and moving with someone else who was experiencing the same challenges. In addition, I thank the Hartwig group. I have worked with a diverse group of scientists from many

different backgrounds. Finally, I express thanks to the staff in the chemistry department at the University of Illinois. I have had a wonderful experience and the people in the department made it that much better.

Table of Contents

Chapter 1: Migratory Insertion of Alkenes into Metal-Oxygen and Metal-Nitrogen Bonds.....	1
1.1 Introduction.....	1
1.2 Reactions Involving Migratory Insertion of Olefins into M-O Bonds.....	3
1.3 Reactions Involving Migratory Insertion of Olefins into M-N Bonds.....	12
1.4 Conclusions.....	38
1.5 References.....	40
Chapter 2: Intermolecular Migratory Insertion of Ethylene and Octene into a Palladium-Amide Bond.....	46
2.1 Introduction.....	46
2.2 Results and Discussion.....	48
2.3 Conclusion.....	56
2.4 Experimental.....	57
2.5 References.....	92
Chapter 3: Intermolecular Migratory Insertion of Unactivated Olefins into Palladium-Nitrogen Bonds. Steric and Electronic Effects on the Rate of Migratory Insertion.....	95
3.1 Introduction.....	95
3.2 Results and discussion.....	97

3.3 Summary.....	128
3.4 General Experimental Details.....	130
3.5 References.....	183

Chapter 4: Reductive Elimination of Alkylamines from Low-Valent Alkylpalladium(II)

Amido Complexes.....	186
4.1 Introduction.....	186
4.2 Results and Discussion.....	190
4.3 Summary.....	204
4.4 Experimental.....	205
4.5 References.....	285

Chapter 1: Migratory Insertion of Alkenes into Metal-Oxygen and Metal-Nitrogen Bonds

1.1. Introduction

Migratory insertion is a fundamental organometallic reaction that proceeds by the concerted insertion of an unsaturated ligand into an adjacent metal-ligand bond. A variety of unsaturated ligands undergo migratory insertion, including carbon monoxide, carbon dioxide, alkenes, alkynes, ketones, aldehydes, and imines, and migratory insertion is a common step in numerous catalytic reactions, including hydroformylation,¹⁻² hydrogenation,³⁻⁵ polymerization,⁶⁻⁹ hydroarylation,¹⁰⁻¹⁴ difunctionalization of alkenes,¹⁵⁻¹⁸ and the olefination of aryl halides (commonly termed the Mizoroki-Heck reaction).¹⁹⁻²²

In most cases, the unsaturated ligand inserts into an M-C or M-H bond; related insertions of alkenes into M-O and M-N bonds are much less common. Over the past decade, however, several papers have described palladium-catalyzed alkene alkoxylation and amination reactions with stereochemical evidence for a mechanism involving migratory insertion of an alkene into an M-O or M-N bond. Moreover, the first isolated transition metal-amido complexes that insert unactivated alkenes have been reported in the past few years. These recent publications include information on the factors controlling the rate of insertion.

Although the first examples of insertion of an alkene into a metal-heteroatom bond were reported more than two decades ago, experiments on the insertions of alkenes into isolated metal-amido complexes are rare. An open coordination site is necessary for alkene coordination prior to insertion, and many alkoxo and amido complexes form stable multinuclear structures if the metal center is coordinatively unsaturated. Thus, preparation of monomeric amido complexes with an open coordination site to bind and subsequently insert alkenes is difficult, and the

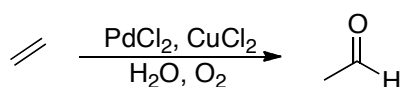
absence of such complexes has meant that the factors that control insertions of alkenes into metal-heteroatom bonds have been poorly understood.

To develop new, selective metal-catalyzed olefin alkoxylation and amination reactions, fundamental knowledge of the factors that control the rate and stereoselectivity of the insertion of alkenes into metal-oxygen and –nitrogen bonds is needed. These factors are just beginning to be revealed. Thus, one aim of this minireview is to provide a perspective on how these recent experiments relate to classic experiments on C-O and C-N bond formation with late-metal alkene complexes and to summarize the existing literature on chemistry involving migratory insertion of alkenes into the M-N and M-O bonds of isolated metal amido and metal alkoxo complexes. We will also describe mechanistic studies of catalytic amination and alkoxylation reactions that offer insight into the migratory insertion step.

We have separated this review into two sections. The first section is divided into two subsections; one subsection describes catalytic reactions with evidence of alkene insertion into an M-O bond, and one describes stoichiometric reactions of alkoxo complexes with alkenes. The second section describes chemistry involving migratory insertions of alkenes into M-N bonds. Because more data have been published on alkene insertions into M-N bonds, this section is divided into three subsections; one subsection describes catalytic reactions involving insertions of alkenes into bonds between nitrogen and lanthanide, actinide, alkaline earth, and early transition metals; one describes catalytic reactions involving the insertion of alkenes into late transition metal-nitrogen bonds; and one describes reactions of amido complexes with alkenes that likely occur by a migratory insertion of the alkene into the metal-nitrogen bond.

1.2. Reactions Involving Migratory Insertion of Olefins into M-O Bonds

The oxidative functionalization of alkenes is the one of the most widely used processes catalyzed by soluble transition metal complexes. The oxidation of ethylene in water with a palladium catalyst, commonly termed the Wacker process is used to produce 2×10^6 tons of acetaldehyde annually (Scheme 1.1).²³ The metal-mediated formation of new C-O bonds by the addition of an oxygen nucleophile to an olefin was thought for many years to occur exclusively by nucleophilic attack of an oxygen nucleophile onto a metal-coordinated olefin. Well-characterized, metal-olefin complexes had been prepared, and alcohols were shown to add to the alkene of these complexes at the face opposite the metal center.²⁴⁻²⁷ Thus, metal-catalyzed additions of oxygen nucleophiles to olefins were typically assumed to occur by *anti*-addition. However, alkoxometal olefin complexes that react by migratory insertion have recently been identified. In this, section we will describe catalytic reactions, including the Wacker process, for which mechanistic data implies that the C-O bond is formed by insertion of an alkene into an M-O bond. Stoichiometric reactions of alkoxo complexes with alkenes will be discussed in detail.



Scheme 1.1 The Wacker process

1.2.1. Catalytic Reactions Involving Alkene Insertion into Metal-Oxygen Bonds

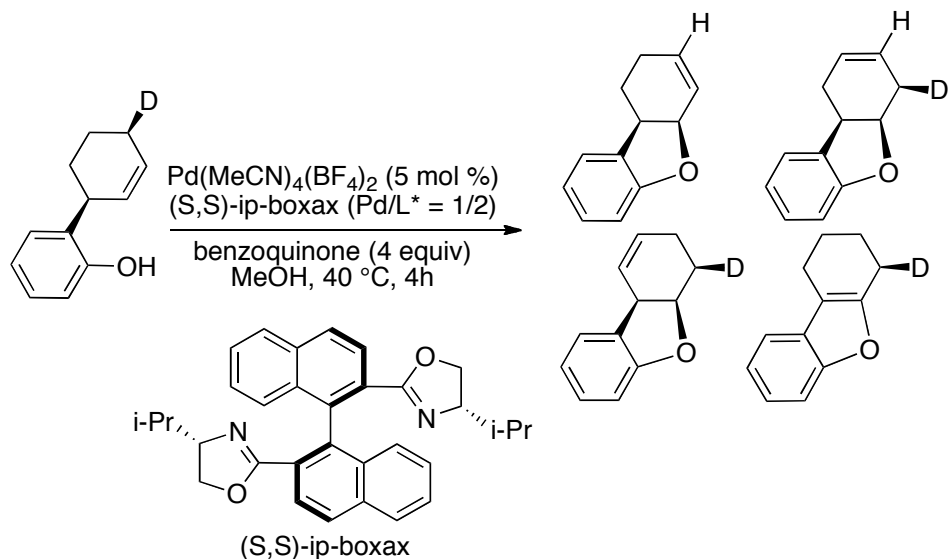
The mechanism of the Wacker process has been disputed for the last four decades. Early kinetic studies of the Wacker oxidation were consistent with a mechanism involving *syn*-addition of a pre-formed palladium-hydroxo complex across ethylene.²⁸ However, experiments conducted by Stille and Bäckvall demonstrated that palladium ligated with deuterium-labeled alkenes

formed products via anti-oxypalladation.²⁹⁻³² For example, the addition of CO to the combination of bis(*cis*-*d*₂-ethylene)PdCl₂ and H₂O in a buffered solution of CuCl₂ and NaOAc led to the formation of lactone products. The stereochemical configuration of the carbon atoms in the lactone indicated that an anti addition of the oxygen atom and palladium to the ethylene had occurred.³⁰ In fact, Bäckvall and Siegbahn stated that a hydroxymetal olefin complex is too unreactive to undergo cis migration of an –OH ligand to a bound alkene.³³

Henry correctly noted that these experiments were conducted under conditions distinct from those of the catalytic Wacker reaction. The Wacker process is typically conducted with low chloride concentrations. Henry examined the hydroxylation of allylic alcohols and demonstrated that the stereochemical outcome of the oxypalladation step is different at high and low concentrations of chloride ion. At high chloride ion concentration, products from anti-oxypalladation were observed, but at low chloride ion concentration, the stereochemical configuration of the observed products indicated that syn-oxypalladation by migratory insertion of an alkene into a metal-alkoxo bond occurred.³⁴⁻³⁹ Because two sets of products with different relative configurations were observed, the hydroxylation of allylic alcohols must occur by two different mechanisms. Despite these results, the mechanism of the Wacker process described in leading textbooks was described as occurring by the attack of a free water molecule on a palladium-bound ethylene.⁴⁰

These studies of Henry relied on allylic alcohols to determine whether the addition occur by a *syn* or *anti* oxypalladation process. Allylic alcohols might give biased results because they contain two binding sites and might isomerize under the reaction conditions. Thus, other researchers more recently have studied the stereochemistry of additional Wacker reactions.

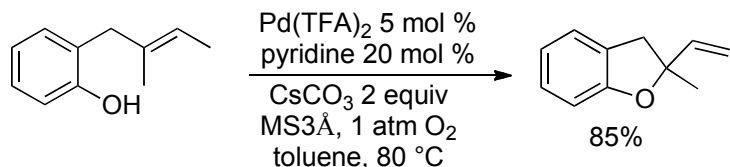
Hayashi assessed the stereochemistry of the oxypalladation step in the oxidative cyclization of an *o*-allylphenol.⁴¹ Stereospecifically deuterated, racemic 6-(2-hydroxy-phenyl)-3-deuteriocyclohexenes underwent cyclization in the presence of $\text{Pd}(\text{MeCN})_4(\text{BF}_4)_2$ as precatalyst and (*S,S*)-2,2'-bis-(4-isopropylloxazolyl)-1,1'binaphthyl as ligand with 4 equiv of benzoquinone in MeOH at 40 °C (Scheme 1.2). In the absence of added LiCl, a series of cyclized products were obtained that would be formed by *syn*-oxypalladation by migratory insertion, followed by a series of β-hydrogen elimination and insertion steps to generate the different product isomers. In the presence of added LiCl, different products formed. Under these conditions, the major cyclized product was resulted from anti addition of the palladium and oxygen across the internal alkene.



Scheme 1.2. Oxidative cyclization of 6-(2-hydroxy-phenyl)-3-deuteriocyclohexene

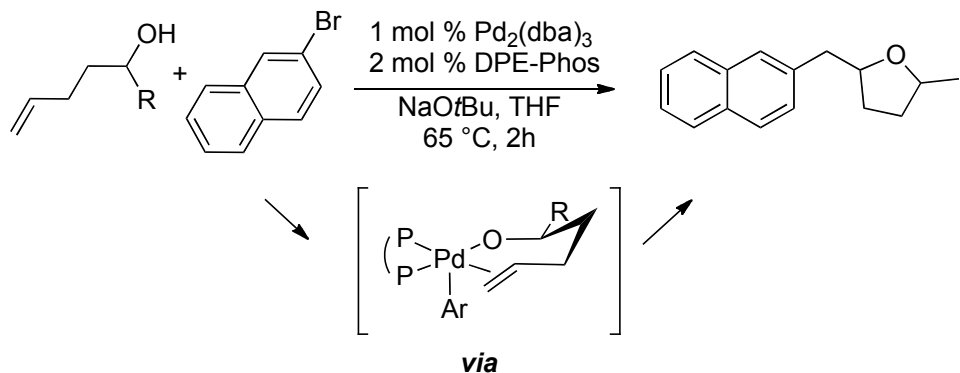
Stereochemical evidence for a *syn*-oxypalladation step also has been gained by Stoltz for similar palladium-catalyzed cyclizations of phenols and primary alcohols.⁴² Treatment of a deuterium-labeled unsaturated alcohol with 10 mol % (pyridine)₂Pd(TFA), 20 mol % pyridine, 2

equiv Na₂CO₃, 1 atm O₂, and 500 mg/mol of MS3Å in toluene at 80 °C for 3 h generated cyclized products in 95% overall yield (Scheme 1.3). Like the products of Hayashi's experiment, the products from Stoltz's experiment are best rationalized by a syn-oxypalladation (migratory insertion of the alkene into the Pd-O bond). However, the stereochemistry of the oxypalladation process was the same, in this case, for reactions conducted with added chloride anion or bidentate ligands.



Scheme 1.3. Oxidative cyclization of *o*-allylphenol

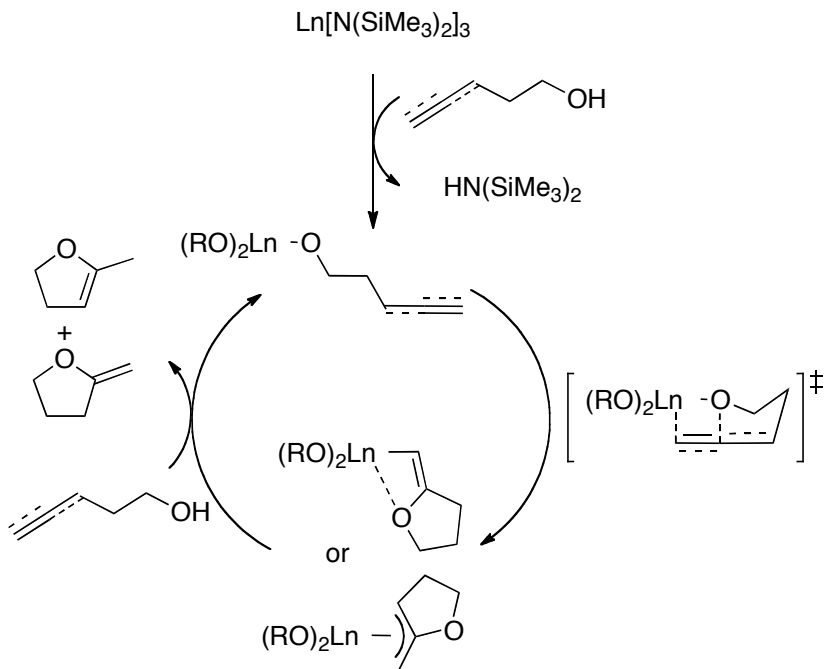
Wolfe published a series of reports of related oxidative cyclizations. The stereochemistry of the products from the Pd-catalyzed reaction of aryl bromides with γ -hydroxy alkenes indicate that these reactions occur by a syn addition of the palladium and of the oxygen atom to the alkene (Scheme 1.4).⁴³⁻⁴⁵ The proposed mechanism for these reactions begins with oxidative addition of the aryl bromide to a bis-phosphine ligated Pd⁰ species, followed by transmetalation to generate a Pd(Ar)(OR) intermediate. This intermediate undergoes selective migratory insertion of the pendant alkene into the Pd-O bond, and the resulting alkylpalladium aryl complex undergoes C-C bond-forming reductive elimination to generate the tetrahydrofuran product.



Scheme 1.4. Pd-catalyzed reaction of aryl bromides with γ -hydroxy alkenes

Catalytic olefin alkoxylation reactions proposed to proceed by a migratory insertion pathway are not limited to palladium-catalyzed reactions; Marks has reported the lanthanide-catalyzed hydroalkoxylation of alkynyl and allenyl alcohols.⁴⁶⁻⁴⁷ The active lanthanide catalyst is formed by rapid protonolysis of the amide ligand of the $\text{Ln}[\text{N}(\text{TMS})_2]_3$ precatalyst to generate a lanthanide alkoxo species that undergoes turnover-limiting migratory insertion of the tethered alkyne into the $\text{Ln}-\text{O}$ bond. The resulting vinyl ether is protonolyzed to release the cyclized product and regenerate the active catalyst.

These reactions were first-order in catalyst and zero-order in alkynyl or allenyl alcohol, which is consistent with the proposed mechanism in Scheme 1.5. Although lanthanide-catalyzed cyclizations of alkenyl alcohols have been reported, these reactions do not proceed through a pathway involving migratory insertion of the alkene into an $\text{Ln}-\text{O}$ bond.⁴⁸ The thermodynamics of the insertion of an alkyne and a terminal alkene into $\text{Ln}-\text{O}$ bonds have been examined by calorimetry; these data predict that the insertion of an alkyne is exothermic ($\Delta H = -13 \text{ kcal/mol}$), but the insertion of a terminal alkene is significantly endothermic ($\Delta H = +22 \text{ kcal/mol}$).⁴⁹

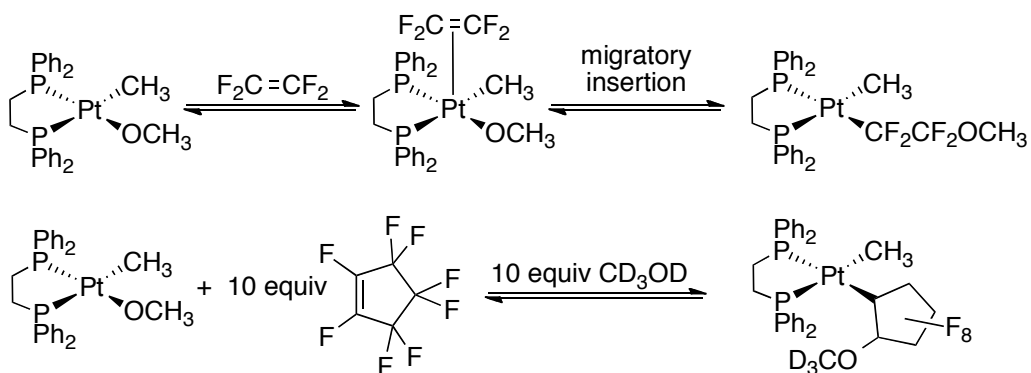


Scheme 1.5. Proposed reaction mechanism of Ln-catalyzed alkyne hydroalkoxylation

1.2.2. Reactions of Metal-Alkoxo Complexes with Alkenes for which Direct Evidence has been Gained on Migratory Insertion into an M-O Bond

Although analysis of catalytic olefin alkoxylation systems provided stereochemical and kinetic evidence for a *syn*-oxypalladation step by migratory insertion of an alkene ligand into a M-O bond, the metal alkoxo complexes that were predicted to insert olefins have not yet been isolated and fully characterized. Until recently, only a single example of an alkoxide complex that reacts with an olefin was reported. Bryndza reported the reaction of (DPPE)Pt(CH₃)(OCH₃) with the highly activated alkene, tetrafluoroethylene (TFE), in THF-*d*₈ at 25 °C to generate (DPPE)Pt(CH₃)(CF₂CF₂OCH₃) in almost quantitative yield.⁵⁰ The reaction is first-order in platinum methoxide and tetrafluoroethylene. At -80 °C, the chemical shift of the tetrafluoroethylene resonance in the ¹⁹F NMR spectrum was found to vary linearly with the quantity of added TFE, indicating that tetrafluoroethylene interacts with the platinum methoxide

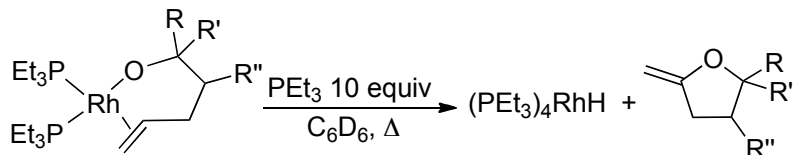
complex. Tetrafluoroethylene is proposed to bind to the Pt methoxide to form a five-coordinate olefin complex. Upon warming to 25 °C, the observed intermediate underwent migratory insertion of the alkene ligand into the Pt-O bond to form an alkylplatinum complex. In addition, a crossover experiment showed that the dppp-ligated platinum complex reacts to form a new alkyl complex in the presence of 10 equiv of CD₃OD and perfluorocyclopentene with less than 8% incorporation of the OCD₃ group (Scheme 1.6). This result indicates that the methoxide ligand does not dissociate from the Pt-complex and subsequently attack a coordinated olefin by an anti-oxyplatination pathway.



Scheme 1.6. Reactions of Pt-methoxide complexes with perfluorinated alkenes

More recently, the first well-characterized alkoxo complexes that undergo migratory insertion of unactivated olefins were reported.⁵¹ A series of triethylphosphine-ligated rhodium alkoxide complexes from the reaction of the Rh(I) silylamido complex (PEt₃)₂RhN(SiMe₃)₂ with enols at room temperature or below formed an alkoxorhodium olefin complex and free HN(SiMe₃)₂. An x-ray crystal structure of the olefin complex of a more stable analog that does not undergo insertion was obtained. This complex adopts a square planar structure, and the alkene moiety of the homoallylic alkoxide ligand is bound perpendicular to square plane. Upon

warming to 25 °C in the presence of added PEt₃, a series of alkoxo olefin complexes formed functionalized tetrahydrofurans and (PEt₃)₄RhH in good yields by sequential migratory insertion of the alkene into the Rh-O bond and β-hydrogen elimination.

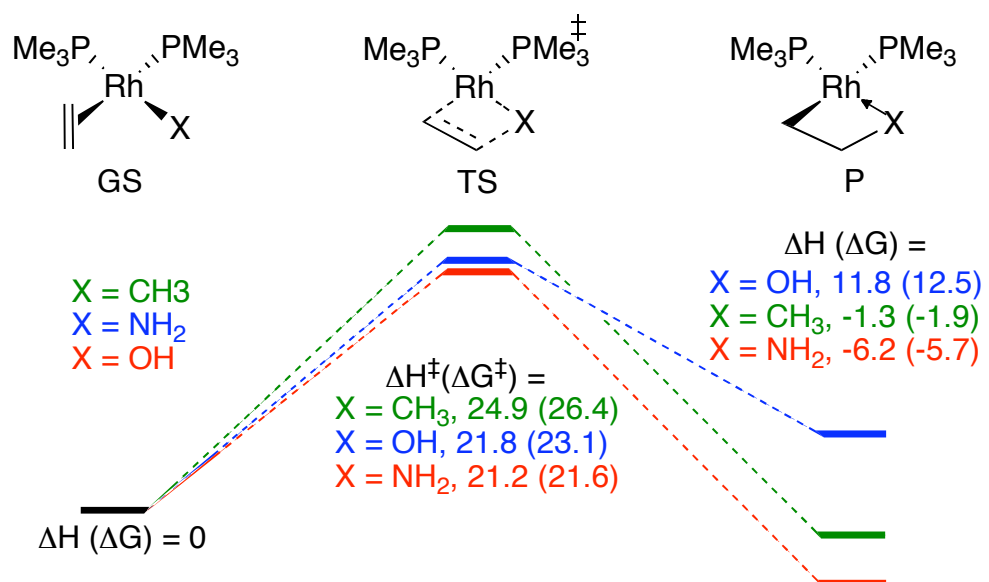


Scheme 1.7. Reactions of alkoxorhodium alkene complexes

The mechanism of the oxypalladation step was assessed by a series of kinetic and stereochemical experiments. The rate of the reaction was first-order in rhodium and zero-order in PEt₃. In addition, the reaction was slightly faster in less-polar solvents, a result that is inconsistent with initial dissociation of the alkoxide ligand to form a zwitterionic intermediate that undergoes nucleophilic attack on a Rh-coordinated olefin. Finally, the reaction of an alkoxo olefin complex containing a deuterium-labeled, dimethyl-substituted alkenyl alcohol generated a single isomer of the *trans*-deutero tetrahydrofuran. The isomer formed is consistent with cyclization by a migratory insertion pathway. Thus, this study provided the first evidence for reaction of an alkene with a directly observed metal-alkoxo complex to form a new C-O bond by migratory insertion of the alkene into a metal-oxygen bond. More important, the modest activation barrier for insertion into an Rh-O bond implies that many catalytic olefin oxidation reactions believed to occur by nucleophilic attack of an alkoxide onto a metal-coordinated olefin might occur, instead, by a migratory insertion pathway.

A series of computational studies on the relative rates for migratory insertion of alkenes into square-planar methyl, amido, and hydroxo complexes of rhodium have also been published.⁵²

The calculated free-energy barriers for migratory insertion of the alkene into the M-X bond of the rhodium complexes $(\text{PMe}_3)_2\text{Rh}(\eta^2\text{-CH}_2=\text{CH}_2)(\text{X})$ ($\text{X}=\text{CH}_3, \text{NH}_2, \text{OH}$) follow the trend Rh-NH₂ < Rh-OH << Rh-CH₃ (Scheme 1.8). This trend was attributed to the presence of an M-X dative bond in the transition state and immediate insertion product. The M-N or M-O bond in the starting complex is transformed from that to an X-type ligand into a bond to an L-type ligand during the insertion step. Because the M-X ($\text{X}=\text{NH}_2, \text{OH}$) bond is transformed to a different type of bond, rather than cleaved, the barrier to migratory insertion is lower when $\text{X}=\text{NH}_2$ and OH than when $\text{X}=\text{CH}_3$. When $\text{X}=\text{CH}_3$, the M-X bond is broken in the product, and the M-X bond order in the transition state is lower.



Scheme 1.8. Optimized ground-state and transition-state energies for ethylene insertion into Rh-alkyl, amido, and hydroxyl bonds.

1.3. Reactions Involving Migratory Insertion of Olefins into M-N Bonds

Catalytic reactions that proceed by migratory insertion of an alkene into an M-N bond are much more common than those that proceed by migratory insertions into M-O bonds. Computational data suggest that migratory insertions into Rh-N bonds occur with a lower barrier than related migratory insertions into Rh-O and M-C bonds,⁵² and this trend in relative barriers apply to other late-transition metal complexes, especially those with similar square-planar geometries. Recently, a number of palladium-amido complexes have been isolated that insert olefins with moderate activation barriers. In addition, thermochemical analysis of the bond enthalpies of bis(pentamethylcyclopentadienyl)samarium complexes shows that insertions into a samarium amide should be considerably less endothermic than insertions into samarium alkoxides.⁴⁹ Thus, there are multiple reports describing lanthanide- and actinide-catalyzed hydroamination reactions that are proposed to occur by migratory insertion of an alkene into the metal-nitrogen bond. In addition, several published reports hypothesize that Group IV transition-metal catalyzed hydroaminations can proceed by a migratory insertion pathway, although the mechanism of the insertion step is still being debated. This section describes examples of catalytic reactions for which experimental evidence has been gained for a migratory insertion step. In addition, we describe in detail the reactions of well-characterized metal-amido complexes with alkenes.

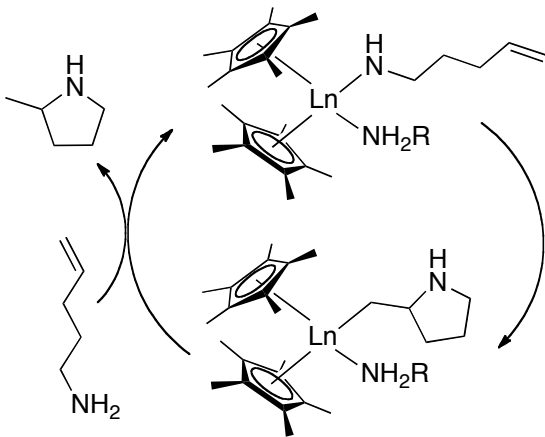
1.3.1. Catalytic Reactions Involving Insertions into Lanthanide, Actinide, Alkaline-Earth and Early-Transition Metal-Nitrogen Bonds

The mechanism of lanthanide-catalyzed hydroamination is typically believed to occur by migratory insertion of an alkene into a lanthanide-nitrogen bond.⁵³⁻⁵⁷ However, closer evaluation

of the kinetic data obtained from many of these systems suggests that aspects of the reaction mechanism should be revised. A large kinetic isotope effect is observed for reactions of *N*-deuterated aminoalkenes in many cases, and these data are inconsistent with a simple migratory insertion as the turnover-limiting step. Assistance by a coordinated amine was proposed initially to account for the kinetic isotope effect. Recent results from Sadow and others on hydroaminations by alkaline-earth and early-transition-metal systems also reveal a large kinetic isotope effect. Sadow proposed that these systems react through a six-membered transition state, not through a simple migratory-insertion pathway.

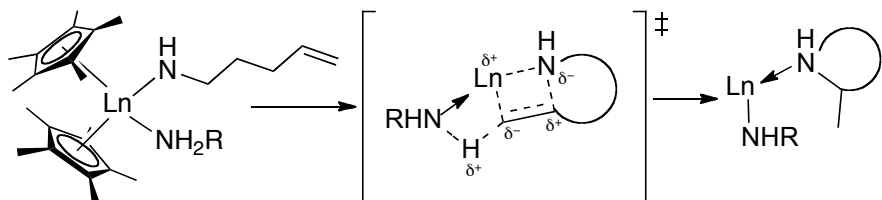
In this section, we present examples of lanthanide and actinide catalyzed hydroamination reactions. Although these reactions were proposed to occur by migratory insertion of an alkene into a M-N bond, it is possible that these systems react through the same six-membered transition state proposed for reaction of the alkaline-earth and early-transition metal systems. We will summarize the mechanistic data collected for each system in light of the recent proposals.

In a seminal report, Marks and co-workers described intramolecular hydroaminations of aminoalkenes catalyzed by a series of bis(pentamethylcyclopentadienyl) lanthanide complexes, including lanthanum, neodymium, samarium, yttrium, and lutetium.⁵³ Reactions with catalysts containing lanthanides having larger ionic radii occurred faster than those with catalysts containing lanthanides having smaller ionic radii. These hydroaminations were found to be first-order in catalyst and zero order in aminoalkene. This result is consistent with rapid proton transfer to generate a lanthanide-amide followed by turnover-limiting migratory insertion of the pendant alkene into the Ln-N bond (Scheme 1.9).



Scheme 1.9. Proposed reaction mechanism of Ln-catalyzed hydroamination.

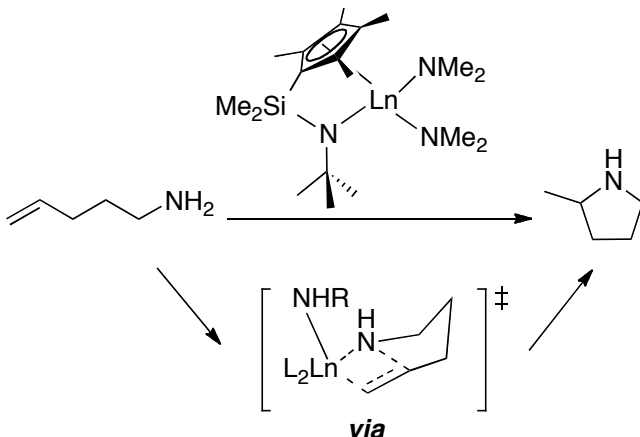
Amido complexes lacking a pendant alkene were prepared from the reaction of $\text{Cp}^*_2\text{LaCH}(\text{TMS})_2$ and HNR_2 . ^1H NMR spectroscopy and x-ray crystallography confirmed the presence of an additional coordinated amine. Eyring analysis of the rate of cyclization of 1-aminopent-4-ene catalyzed by $\text{Cp}^*_2\text{LaCH}(\text{TMS})_2$ over a 25-60 °C temperature range revealed an activation barrier for migratory insertion of $\Delta H^\ddagger = 12.7$ (1.4) kcal/mol and $\Delta S^\ddagger = -27.0$ (4.6) cal/mol. These values are consistent with a highly ordered transition state. Reactions conducted with *N*-deuterium-labeled aminoalkenes revealed a primary KIE of 2.7-5.2. If migratory insertion by a concerted pathway involving a four-membered transition state were turnover-limiting, one would not observe a primary KIE. Therefore, the authors propose that a hydrogen atom on the coordinated-amine ligand stabilizes the transition state for migratory insertion by simultaneously protonating the forming Ln-C bond as the alkene inserts into the Ln-N bond (Scheme 1.10).



Scheme 1.10. Proposed ‘proton-assisted’ mechanism of alkene insertion into an Ln-N bond

Fragalá, Marks and co-workers have also studied the mechanism of these hydroamination reactions by computational methods. They calculated the enthalpic and free energy activation barriers for intramolecular hydroamination of aminoalkenes. The computed barriers indicate that the migratory insertion step is turnover limiting.⁵⁸ The activation parameters computed for the cyclization of 1-aminopent-4ene were $\Delta H^\ddagger = 11.3$ kcal/mol, $\Delta G^\ddagger = 13.4$ kcal/mol, and $\Delta S^\ddagger = -14.6$ cal/mol. Because the catalytic hydroamination requires temperatures higher than room temperature, either the free energy is calculated incorrectly, or migratory insertion is not the turnover-limiting step. In addition, the computed transition state for the migratory-insertion step did not include the proposed proton-assistance from a coordinated-amine ligand to account for the primary isotope effect.

Marks and co-workers also investigated hydroaminations catalyzed by actinide complexes ligated by constrained-geometry ligands (Scheme 1.11). The activity of these organoactinide catalysts is similar to that of the most active lanthanide catalysts and exceeds that of most Group IV transition-metal systems. The scope of these systems includes aminoalkenes, aminoalkynes, aminoallenes, and aminodienes. The catalytic reaction was proposed to occur by migratory insertion of a pendant alkene into an An-N bond.⁵⁹⁻⁶⁰

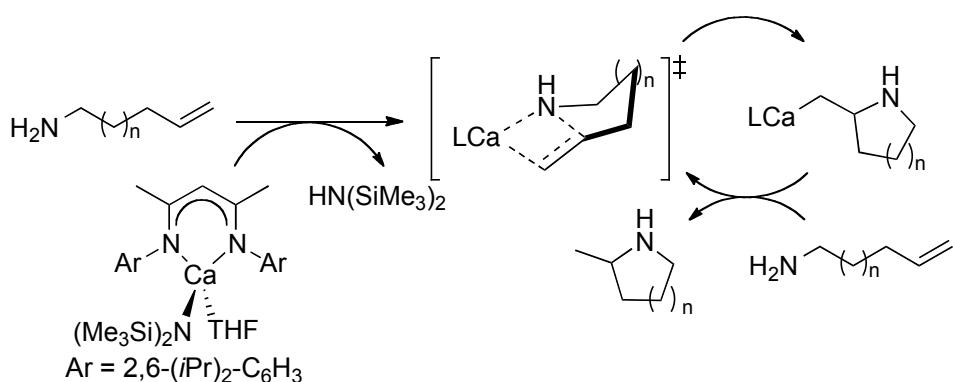


Scheme 1.11. Actinide-catalyzed hydroamination of aminoalkenes.

A series of Group IV complexes that catalyze the cyclization/hydroamination of secondary amines also has been reported recently. Typically, catalysts for hydroaminations catalyzed by early-transition metal complexes react by 2+2 cycloaddition of an alkene across a metal-imido bond.⁶¹⁻⁶² However, complexes reacting through a metal-imido intermediate can only catalyze the hydroamination of primary-amines; a metal-imido complex cannot form from a secondary amine.

However, Hultsch reported the intramolecular hydroamination of secondary aminoalkenes catalyzed by [Cp₂ZrMe]⁺[MeB(C₆F₅)₃]⁻,⁶³ and Marks reported intramolecular hydroaminations of secondary aminoalkenes and aminoalkynes catalyzed by Zr complexes ligated by the same constrained-geometry complex described in Scheme 1.11.⁶⁴ These authors proposed that the new C-N bond forms by migratory insertion through a four-membered transition state in both of these systems. In addition, Odom reported the intramolecular hydroamination of primary aminoalkenes catalyzed by titanium and zirconium dipyrrolylmethane complexes. Based on the competitive formation of products from hydroamination and oxidative amination, these reactions likely occur by insertion of an alkene into an M-N bond.⁶⁵

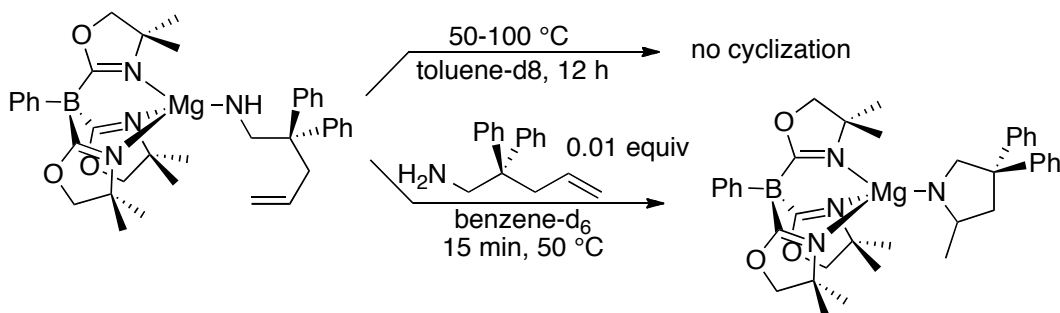
Hill reported the first alkaline earth metal-catalyzed hydroamination of aminoalkenes, and these reactions also are proposed to proceed by migratory insertion of the alkene into the M-N bond. Hill examined the intramolecular hydroamination of aminoalkenes catalyzed calcium and magnesium amido complexes ligated by β -diketiminates.⁶⁶⁻⁶⁷ Kinetic analysis of the reaction catalyzed by the magnesium system revealed a first-order dependence on catalyst concentration and an inverse first-order dependence on the concentration of aminoalkene. Thus, this reaction proceeds by a turnover-limiting alkene insertion into the M-N bond that is inhibited by binding of the substrate to the metal center.



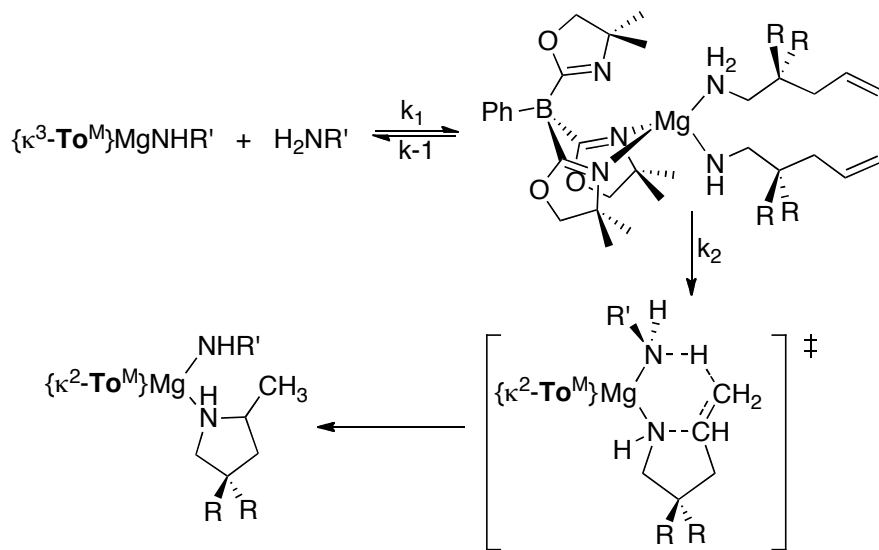
Scheme 1.12. Proposed mechanism of Ca-catalyzed hydroamination of aminoalkenes

More recently, Sadow and co-workers reported the hydroamination of aminoalkenes catalyzed by a magnesium(II) amido complex ligated by tris(4,4-dimethyl-2-oxazolinyl)phenylborate ($[\text{To}^M]$) ligand.⁶⁸ The reaction of $[\text{To}^M]\text{MgMe}$ and aminoalkenes occurs with a large primary KIE, like the KIE Marks obtained for the hydroamination catalyzed by lanthanide metallocene complexes. However, the rate of these hydroaminations are first-order in Mg and first order in aminoalkene, suggesting that binding of the substrate occurs reversibly prior to cyclization. However, the isolated $[\text{To}^M]\text{Mg}$ -primary-amido complex containing a

tethered alkene did not undergo cyclization in the absence of added amine. Instead, the complex underwent cyclization in the presence of a catalytic amount of primary amine to form an amido complex containing the cyclized product bound through the secondary amine function (Scheme 1.13). Thus, an additional amine ligand is necessary to promote cyclization. Based on these data, Sadow proposed that cyclization of the $[To^M]Mg$ -amido complex occurs by substitution of one arm of the To^M ligand for an amine, followed by concerted rate-limiting C-N and C-H bond formation through a six-center transition state (Scheme 1.14). Thus, Sadow proposed that these hydroaminations *do not* proceed through the typical pathway involving migratory insertion of the alkene into a M-N bond.



Scheme 1.13. Reactions of $[To^M]Mg$ -amido complexes in the presence and absences of added amine.



Scheme 1.14. Proposed reaction mechanism of [To^M]Mg-catalyzed hydroamination of aminoalkenes

In addition, Sadow reported that zirconium⁶⁹ and yttrium,⁷⁰ complexes coordinated by similar ligand frameworks catalyze hydroamination through the same six-center transition-state. Schafer and co-workers also proposed a similar transition state for the hydroamination of primary and secondary aminoalkenes catalyzed by zirconium complexes ligated by a tethered bis(ureate).⁷¹⁻⁷²

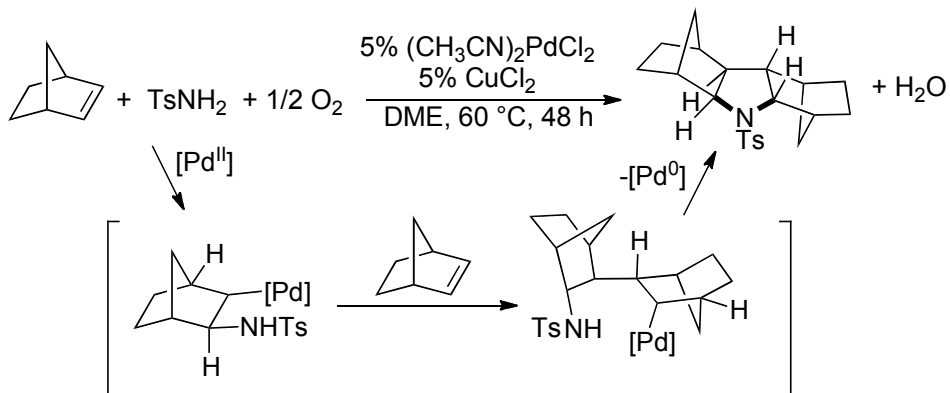
A six-centered transition state better rationalizes the kinetic data obtained for the systems described by Sadow and Schafer, and the Ln and An systems described by Marks. The large KIEs observed for many of these systems suggest that cleavage of the N-H bond occurs in the turnover-limiting step. Although the computed barriers for alkene insertion are reasonable, they do not account for cleavage of an N-H bond during the transition state. Thus, the mechanistic conclusions drawn from computation and experiment are not consistent. The mechanism of Ln-catalyzed hydroamination warrants reevaluation, because a six-centered transition-state proposed by Sadow for related systems better explains the available kinetic data.

1.3.2. Catalytic Reactions Involving Insertions into Palladium-Nitrogen Bonds

Most published literature on catalytic reactions that use palladium catalysts to accomplish the addition of an amine or amide to an olefin, commonly termed the “aza-Wacker” reaction, state that these reactions occur by nucleophilic addition of a nitrogen nucleophile to a metal-coordinated olefin. A number of early, elegant studies demonstrated that the addition of nitrogen nucleophiles to a palladium-coordinated alkene formed new C-N bonds by trans aminopalladation.⁷³⁻⁷⁵ Hegedus and coworkers reported the first catalytic oxidative amination of alkenes that used benzoquinone to regenerate the palladium(II), and researchers proposed that these reactions occurred by trans addition of the palladium and the nucleophile to the alkene.⁷⁶ Over the next two decades, several studies described palladium-catalyzed amination reactions, but no one reported evidence for a syn-aminopalladation by migratory insertion of the alkene into a Pd-N bond.⁷⁷ Thus, migratory insertion was not thought to be part of the mechanism of palladium-catalyzed amination reactions.

During the past ten years, however, this view of the mechanism has changed. Palladium-catalyzed amination reactions now thought to occur by a migratory insertion step including carboaminations,⁷⁸⁻⁸¹ oxidative aminations,⁸²⁻⁸⁴ chloroaminations,⁸⁵ aminoacetoxylations,⁸⁶ diaminations,⁸⁷ and hetero-Heck type transformations.⁸⁸ In some of these examples, stereochemical evidence for *syn*-aminopalladation by migratory insertion has been gained. Because reviews detailing known examples of palladium-catalyzed reactions involving an aminopalladation step are available,⁸⁹⁻⁹⁰ this review focuses on the migratory insertion step. For example, Stahl and co-workers reported the first palladium-catalyzed intermolecular oxidative amination of unactivated alkenes with amides.⁸⁶ The stereochemistry of the product that arises from the palladium-catalyzed amination of norbornene is consistent with a mechanism involving

syn-aminopalladation. The oxidative coupling of two norbornenes and p-toluenesulfonamide in the presence of 5 mol % $(\text{CH}_3\text{CN})_2\text{PdCl}_2$ in DME under 1 atm of O_2 and 5 % CuCl_2 at 60 °C formed cyclized product with relative stereochemistry that is consistent with norbornene insertion into the Pd-N bond (Scheme 1.15).⁹¹



Scheme 1.15. Proposed reaction mechanism of the Pd-catalyzed oxidative amination of norbornene

In subsequent studies, Stahl has investigated the mechanism of palladium-catalyzed oxidative amination reactions using several palladium catalysts under a series of varying reaction conditions.⁸³ In most cases, the products of the oxidative cyclization of a deuterium-labeled sulfonamide-substituted aminoalkene are stereochemically consistent with a syn-aminopalladation step by migratory insertion (Table 1.1). Amination of substrates containing a nosyl group instead of a tosyl group resulted exclusively in products consistent with syn-aminopalladation. Because the N-H proton of the nosyl group is more acidic than the N-H proton of the tosyl group, the palladium amido species is formed more readily with a nosyl-protected amine. Decreased stereoselectivity for the oxidative cyclization of tosyl-substituted carboxamide

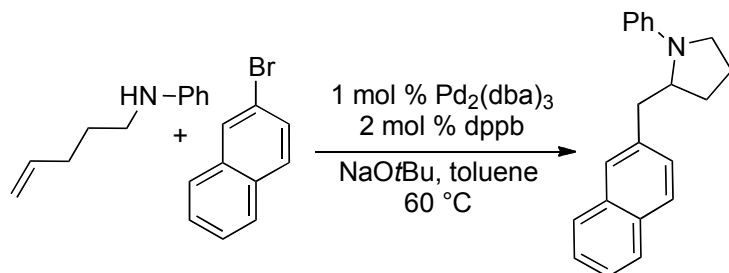
substrates was observed with most catalyst combinations, although the origin of the selectivity is not well understood.

Table 1.1. Oxidative amination of a sulfonamide-substituted aminoalkene

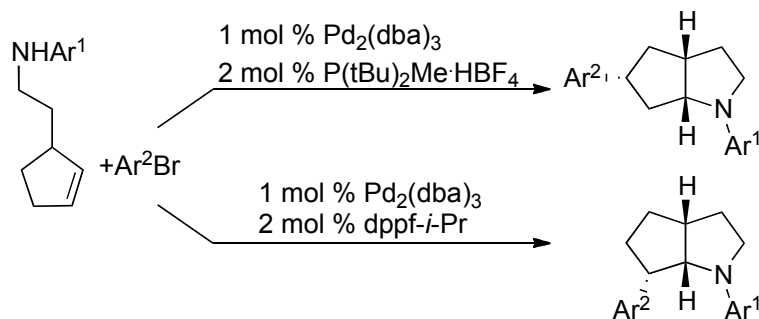
				Product ratio	
Entry	Pd catalyst	Time (h)	Yield (%)	Syn-AP	Anti-AP
1	Pd(OAc) ₂ /DMSO	15	70	100:0	
2	Pd(OAc) ₂ /py	15	84	98:2	
3	Pd(O ₂ CCF ₃) ₂ /py	15	85	88:12	
4	Pd(IMes)(O ₂ CCF ₃) ₂ /BzOH	72	60	43:8	37:12
5	Pd(O ₂ CCF ₃) ₂ /sp	72	72	59:41	

Wolfe investigated the palladium-catalyzed carboamination of *N*-arylaminoalkenes with aryl bromides. The reaction of *N*-arylaminoalkenes with aryl bromides in the presence of 1 mol % Pd₂(dba)₃, 2 mol % dppb ligand, 1.2 equiv NaOtBu, in toluene at 60 °C generated carboaminated products (Scheme 1.16).⁹² They demonstrated that the C-N bond-forming step of these multi-component reactions likely occurs by migratory insertion of the alkene into a Pd-N bond. Careful selection of the phosphine ligand resulted in selective synthesis of either the 5-aryl or 6-aryl carboaminated products (Scheme 1.17).⁷⁹ In combination with Pd₂(dba)₃, the chelating phosphine

dppf-*i*-Pr generated a catalyst that provided primarily the 6-aryl octahydrocyclopenta[b]-pyrrole product. However, analogous reactions conducted with the combination of Pd₂(dba)₃ and P(*t*-Bu)₂Me·HBF₄ generated the 5-aryl regioisomer with high diastereoselectivity.



Scheme 1.16. Pd-catalyzed carboamination of N-arylaminoalkenes with aryl bromides



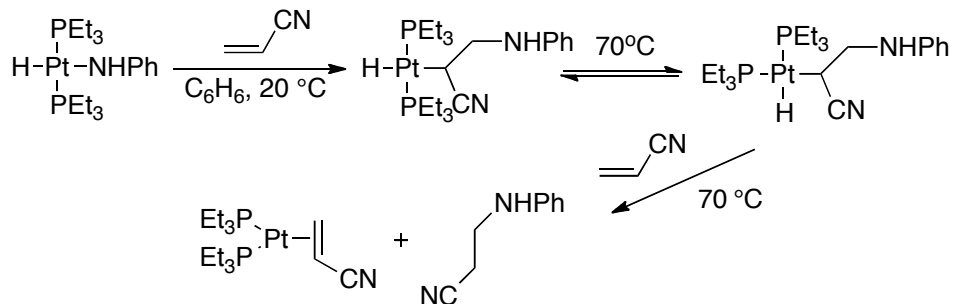
Scheme 1.17. Pd-catalyzed carboamination of N-arylaminoalkenes to form either 5-aryl or 6-aryl products.

1.3.3. Reactions of Metal-Amido Complexes with Alkenes for which Direct Evidence has been Gained on Migratory Insertion into an M-N Bond

Although stereochemical and kinetic analysis of many of the catalysts described in this review provide convincing evidence that these systems react by alkene insertion into an M-N bond, direct evidence of insertion has not been provided for any of these systems. In none of

these cases was a metal amido complex isolated and shown to react with an alkene to transfer an amido group to the olefin. However, a few examples of metal amido complexes that react with alkenes to generate metal alkyl complexes, or organic products with stereochemical evidence for syn-amidometallation.

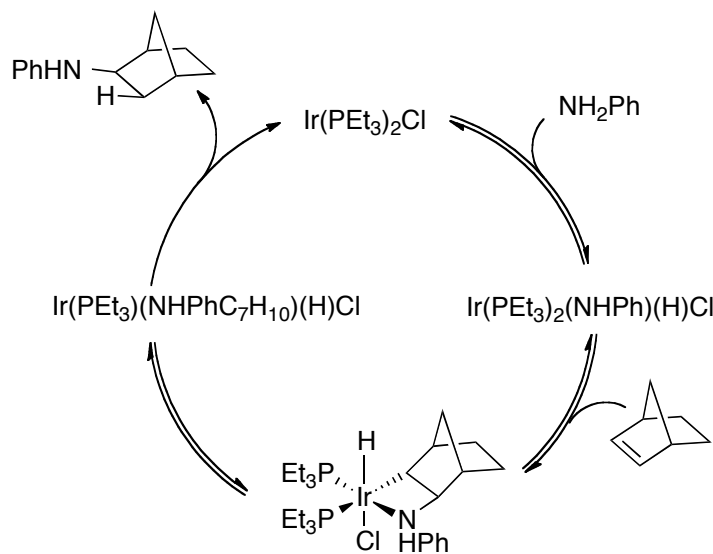
Trogler reported the first example of an isolated metal amido complex that reacts with an alkene to generate products resulting from the “formal” insertion of an unsaturated C-C double bond into an M-N bond.⁹³ The PEt₃ ligated platinum complex (PEt₃)₂Pt(H)(NPh) reacts with acrylonitrile at 20 °C in C₆D₆ to generate an alkyl complex by 2,1-addition to the acrylonitrile (Scheme 1.18). Upon warming to 70 °C, this complex underwent C-H bond-forming reductive elimination to generate hydroaminated product. Although this reaction is reported to occur by a migratory insertion mechanism, no evidence was presented that would rule out direct attack of the amido complex onto the activated acrylonitrile. Reactions with less activated olefins did not occur.



Scheme 1.18. Proposed reaction mechanism of Pt-amides with acrylonitrile

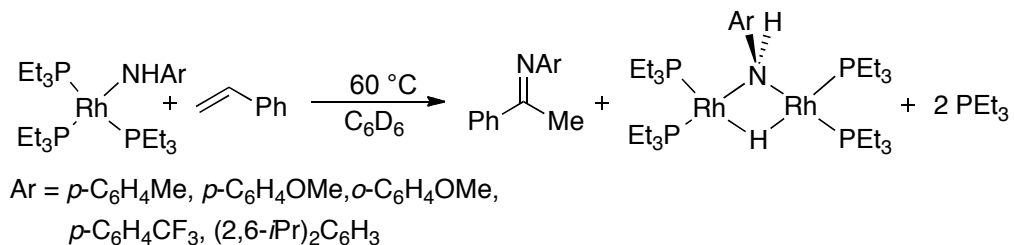
In 1988, Milstein and co-workers reported the first example of migratory insertion of an alkene into a M-N bond as part of studies on an iridium catalyzed addition of aniline to norbornene (Scheme 1.19).⁹⁴ Addition of aniline to a slurry of norbornene and Ir(PEt₃)₂(C₂H₄)₂Cl

in refluxing Et₂O resulted in the formation of a well-characterized azametallacyclic Ir complex. This intermediate is proposed to form by oxidative addition of the N-H bond in aniline to Ir(PEt₃)₂(C₂H₄)₂Cl followed by migratory insertion of the norbornene into the Ir-N bond. The precursor to the insertion step was not observed, but the addition of excess PEt₃ to the azametallacycle, or the reaction of Ir(PEt₃)₃Cl, aniline and norbornene, formed the related, coordinatively saturated complex Ir(PEt)₃(NHPh)(H)Cl. Warming of the azametallacyclic Ir complex to 45 °C resulted in C-H bond-forming reductive elimination to release *exo*-2-(phenylamino)norbornane. Catalytic addition of aniline to norbornene was also observed, with 10 mol% Ir(PEt₃)₂(C₂H₄)₂Cl and 0.2 mol% ZnCl₂ to form *exo*-2-(phenylamino)norbornane with six turnovers. Recently, several examples of enantioselective, iridium-catalyzed hydroamination reactions of strained bicyclic alkenes were reported with evidence that the reactions occur by migratory insertion of the alkene into an Ir-N bond.⁹⁵⁻⁹⁸



Scheme 1.19. Proposed reaction mechanism of Ir-catalyzed addition of aniline to norbornene

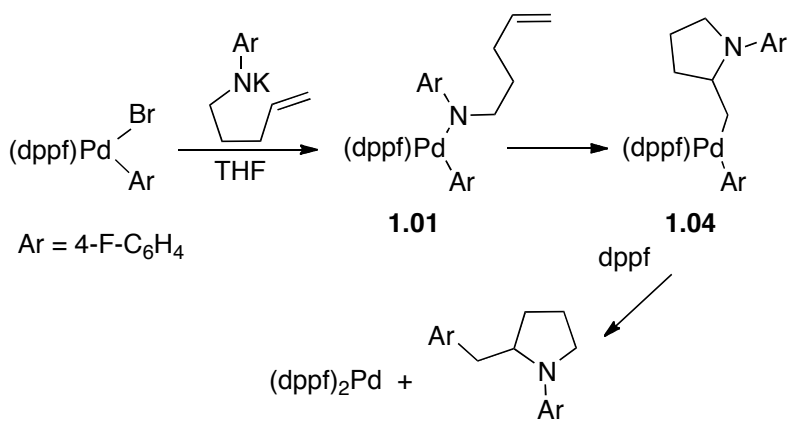
More recently, Hartwig and co-workers reported the transfer of an amido group to alkenes and vinylarenes from an isolated rhodium amido complex.⁹⁹ A series of triethylphosphine-ligated rhodium amido complexes react with vinylarenes at 60 °C to form the corresponding *N*-arylimine and a dimeric hydridorhodium amide complex (Scheme 1.20). These complexes also react with propylene to form *N*-arylimine products at 95 °C. The rate of the reaction of (PEt₃)₃RhNHAr with styrene was determined to be first-order in the concentration of Rh-amide and styrene and inverse first-order in the concentration of PEt₃. These data are consistent with dissociation of PEt₃ from (PEt₃)₃RhNHAr and binding of styrene, and irreversible migratory insertion of the vinylarene into the Rh-N bond.



Scheme 1.20. Reactions of Rh-amides with vinylarenes

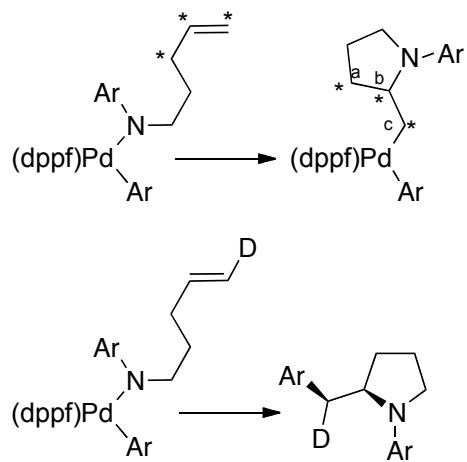
Although the stoichiometric reactions of alkenes with Ir, Pt, and Rh amido complexes demonstrated that alkene insertion into a late transition metal-nitrogen bond is feasible, there were no reports of a palladium amido complex that reacts with an olefin to generate a new C-N bond until recently. In 2010, reports from Wolfe¹⁰⁰ and Hartwig¹⁰¹ described two different phosphine-ligated palladium-amido complexes proposed to react with unactivated alkenes by a migratory insertion pathway. These reports, along with subsequent studies¹⁰²⁻¹⁰³ on the effect of the ancillary and amido ligands on the rate of the insertion step, provided detailed information on the migratory insertion of an alkene into a metal-heteroatom bond.

The Wolfe group has had a longstanding interest in palladium-catalyzed carboamination reactions. To examine the mechanism of these reactions, they prepared a palladium amido complex and studied the migratory insertion of a tethered alkene into the Pd-N bond *in situ*.¹⁰⁰ Upon mixing of (DPPF)Pd(4-F-C₆H₄)Br and KN(4-F-C₆H₄)(CH₂)₃CH=CH₂ in THF at room temperature, the (DPPF)Pd(4-F-C₆H₄)[N(4-F-C₆H₄)(CH₂)₃CH=CH₂] complex was formed. They characterized this complex by the presence of a pair of doublet resonances at δ 24.9 ppm ($J = 38.1$ Hz) and δ 9.0 ppm ($J = 35.5$ Hz) in the ³¹P NMR spectrum and two new resonances at δ -123.7 and -137.3 ppm in the ¹⁹F NMR spectrum. This complex underwent migratory insertion of the pendant alkene into the Pd-N bond to generate a new intermediate proposed to be an alkylpalladium aryl complex. This complex decomposed by C-C bond-forming reductive elimination to form the pyrrolidine product and (DPPF)₂Pd at a rate comparable to that of its formation by migratory insertion.



Scheme 1.21. Proposed reaction mechanism of arylpalladium halide complexes with $\text{KN}(\text{Ar})(\text{CH}_2)_3\text{CH}=\text{CH}_2$

The structure of the alkylpalladium aryl intermediate was cleverly elucidated by preparation of a complex containing an amido ligand and a ^{13}C -labeled pendant alkene (Scheme 1.22). The chemical shifts of the labeled carbon atoms in the proposed alkylpalladium amido intermediate were inconsistent with those of a coordinated alkene. The chemical shift of C_b (δ 61.9 ppm) indicated that it is adjacent to a heteroatom. This connectivity is inconsistent with a six-membered palladacycle that would result from alkene insertion into the Pd-aryl bond. Instead, this connectivity is consistent with alkene insertion into Pd-N bond to form the intermediate **1.04**. Therefore, the authors concluded that this reaction occurs by a pathway involving aminopalladation of the alkene. The stereochemical configuration of the pyrrolidine products formed from the reaction of a palladium amido complex containing a trans-deuterium labeled alkene indicated net *syn*-addition of the aryl group and the nitrogen atom across the alkene.



Scheme 1.22. Reactions of (dppf)Pd-amide complexes containing isotopically labeled alkenes.

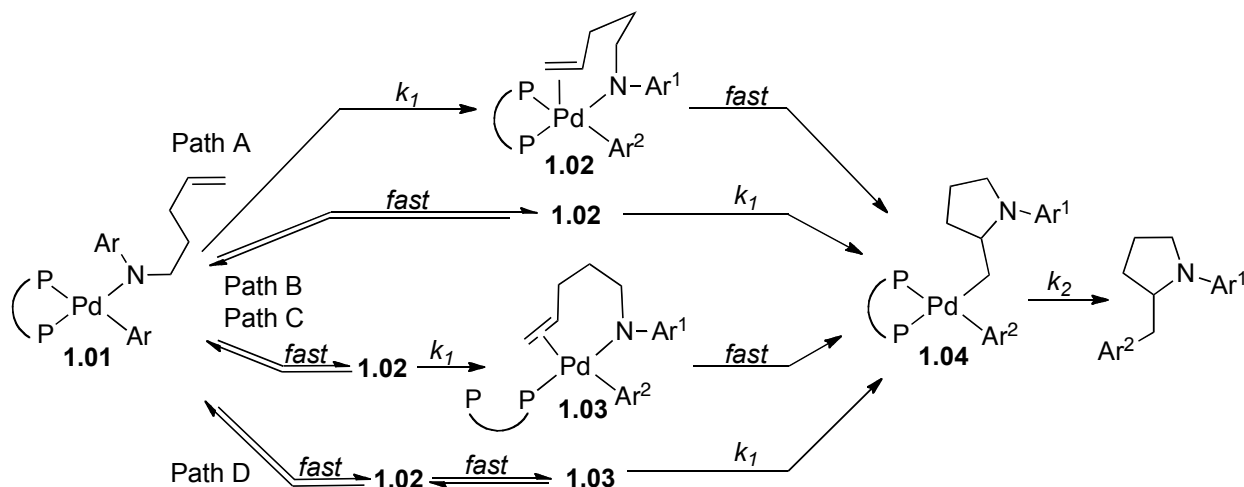
The concentration of the amido complex, alkyl arene intermediate, and pyrrolidine were monitored over the course of the reaction, and because the rates of each step are within an order of magnitude of each other, the rate constant for each step was determined from consecutive

first-order reactions. Eying plot analysis indicated that the enthalpic barrier for alkene insertion into the Pd-N bond was 24.8 kcal/mol.

In a subsequent article, Wolfe investigated the electronic and steric effects of the ancillary, amido, and aryl ligands on the rate constants k_1 and k_2 (Scheme 1.23). Complexes containing electron-donating substituents on the N-(aryl) group underwent conversion from **1.01** to **1.04** and reductive elimination from **1.04** more rapidly than complexes containing electron-withdrawing substituents on the N-aryl group. A Hammett analysis using the σ_p parameters generated linear plots of $\log(k_R/k_H)$ with good fits from which $\rho = -2.5 \pm 0.2$ and $\rho = -9.2 \pm 0.06$ were obtained for k_1 and k_2 , respectively. A clear correlation was not observed between complexes with varying substituents on the aryl ligand. The effect of the electronic properties of the ancillary ligand on the conversion of **1.01** to **1.04** was also investigated. The complex ligated by the least electron donating of the dppf (the ligand containing *p*-CF₃ substituents, dppf-*p*-CF₃) underwent conversion from **1.01** to **1.04** about 1.5 times faster than the complex ligated by dppf.

The effect of bite angle on the reactivity of arylpalladium amido complexes was examined, but quantitative rate data were not obtained. Qualitative studies showed that amido complexes ligated with bisphosphines containing large bite angles (N-methyl-nixanthphos and xantphos) formed pyrrolidine products rapidly at room temperature. In contrast, amido complexes ligated to react at elevated temperatures (60 °C) or decomposed. In addition, the authors demonstrated that a complex containing an amido ligand tethered to a 1,1-disubstituted alkene reacts to generate the corresponding pyrrolidine product, although this reaction occurred more slowly than that of the analogous complex containing a monosubstituted alkene. Complexes containing cis or trans 1,2-disubstituted alkenes did not react.

Several mechanisms were considered for the conversion of the amido complex **1.01** to the aminoalkyl complex **1.04**. Four pathways are outlined in Scheme 1.23, two of which involve a five-coordinate intermediate and two of which involve dissociation of half of the chelating phosphine. Pathways B and D involving reversible coordination of the alkene were determined to be unlikely to occur because neither alkene complex **1.02** or **1.03** was detected spectroscopically and a kinetic isotope effect was not observed for the reaction of complexes containing deuterated alkenes. Because the hybridization of carbon atoms in the alkene change from sp^2 to sp^3 in the transition state for the migratory insertion step, the authors suggested that a secondary kinetic isotope effect should be observed if the aminopalladation were rate limiting.



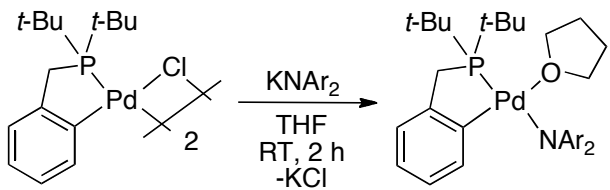
Scheme 1.23. Possible pathways of aminopalladation in dppf-ligated arylpalladium amido complexes

Several pieces of data suggest that the insertion occurs by path C. A positive entropy of activation was measured for the conversion of **1.01** to **1.04**, and one should expect a large, negative entropy of activation for reaction by path A because the overall order of the system is greater in the transition state from **1.01** to **1.04** in this path. Instead, the positive ΔS^\ddagger is consistent

with rate-limiting phosphine dissociation (path C). Moreover, the conversion of **1.01** to **1.04** was faster for complexes containing less-donating bis-phosphine ligands, and dissociation of one arm of a less donating phosphine ligand should be faster than dissociation of one arm of a more donating phosphine.

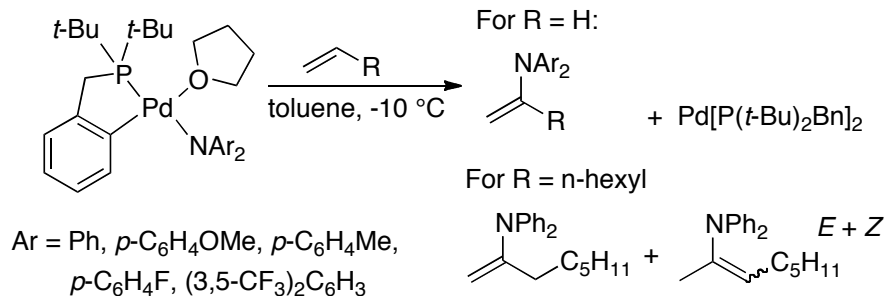
Thus, Wolfe's studies lead to the conclusion that $(P-P)Pd(Ar)[N(Ar)(CH_2)_3CH=CH_2]$ complexes react to generate pyrrolidine products by associative ligand substitution to form a four-coordinate alkene amido complex that undergoes C-N bond forming migratory insertion. The resulting alkylpalladium aryl intermediate then undergoes C-C bond-forming reductive elimination at a rate comparable to that of the phosphine dissociation. Because the rate-limiting step is phosphine dissociation, the study does not reveal an effect of the electronic and steric parameters of the ancillary, amido, or alkene ligand may have on the migratory insertion step.

Concurrent with the work from Wolfe, Hartwig and co-workers described a series of palladium diarylamido complexes that react with unactivated alkenes to form enamine products. These reactions were shown to occur by intermolecular migratory alkene insertion into the Pd-N bond. To promote the formation of monomeric amido complexes and discourage C-N bond-forming reductive elimination, complexes containing a cyclometallated, monoanionic benzylphosphine were studied. Stable THF-ligated amido complexes were prepared from the reaction of $[(P-C)PdCl]_2$ with $KNAr_2$ in THF at room temperature (Scheme 1.24). A series of complexes were synthesized containing different diarylamido ligands; these complexes were isolated and fully characterized by x-ray crystallography.



Scheme 1.24. Synthesis of THF-ligated Pd-diarylamido complexes

The THF-ligated amido complexes react with ethylene at -10 °C and with 1-octene at 80 °C to form enamine products in good yields (Scheme 1.25). Complexes containing more electron-donating amido groups react faster than those containing less electron-donating amido groups. For example, the complex containing a di-*p*-ansiyamide reacts 10 times faster than a complex containing less-electron donating diphenyl or *p*-fluorophenylamide.

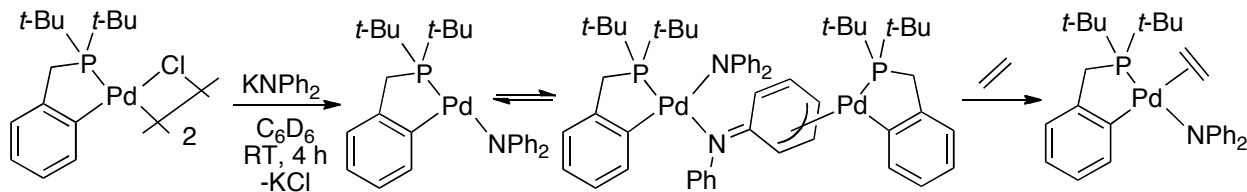


Scheme 1.25. Reactions of THF-ligated Pd-amides with ethylene and octene

The mechanism of the reaction of ethylene with the Pd-amides was examined by kinetic experiments and an assessment of the stereochemical outcome of the insertion step. The reaction was found to be first-order in palladium amide and ethylene, and inverse first-order in THF. These data are consistent with ligand substitution of ethylene for THF followed by migratory insertion of the alkene into the Pd-N bond of a four-coordinate ethylene amido intermediate. Reaction of the palladium amide with *cis*-ethylene-*d*₂ generated products that would be expected

to form from a concerted migratory insertion into the Pd-N bond, followed by β -hydrogen elimination. C-H bond-forming reductive elimination and binding of the added phosphine form the observed Pd(0) product.

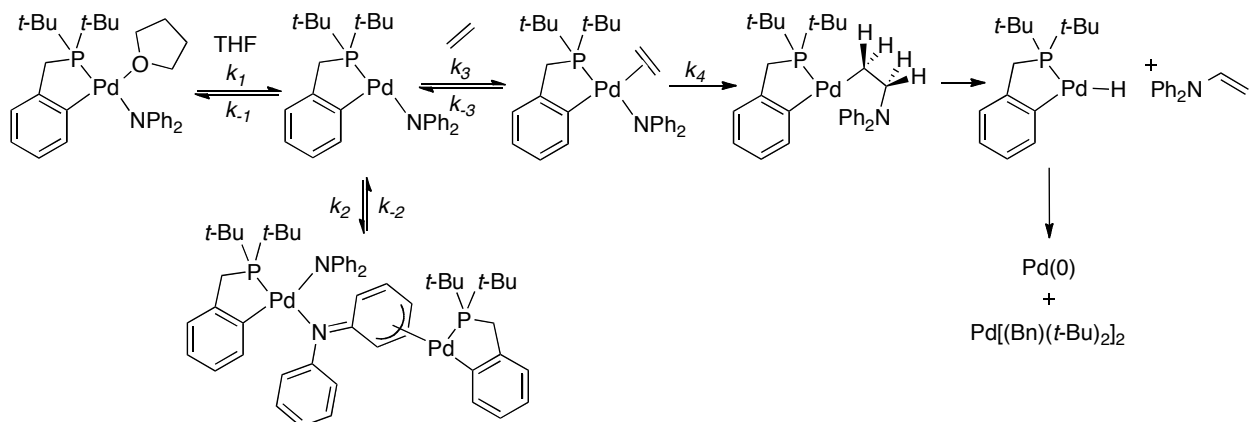
An analogous diarylamido complex lacking a THF ligand was prepared from the reaction of $[(P-C)PdCl]_2$ with $KNAr_2$ in benzene. In solution at room temperature, this complex is a three-coordinate monomer; in solution at low-temperature and in the solid state the complex is an unsymmetrical dinuclear species. Addition of ethylene to the THF-free, three-coordinate palladium amide at -65 °C generates a four-coordinate ethylene amido intermediate that undergoes migratory insertion at -40 °C. The formation of the ethylene amido intermediate was corroborated by the observation of new, broad resonance at δ 106.5 ppm in the ^{13}C NMR spectrum when the THF-free Pd-amide was treated with $^{13}CH_2=^{13}CH_2$ at -65 °C.



Scheme 1.26. Preparation of THF-free and ethylene-bound Pd-amides

A complete overview of the mechanism by which these complexes react with ethylene was recently reported, and the steric and electronic effects imparted by the ancillary ligand on the rate of migratory insertion were described.¹⁰² Addition of varying excess amounts of ethylene to the three-coordinate amido complex revealed that binding of ethylene to form an olefin adduct is rapid and reversible. To ensure that the alkene-amido complex was the major complex in solution so that rate of migratory insertion could be measured directly, a large excess of ethylene

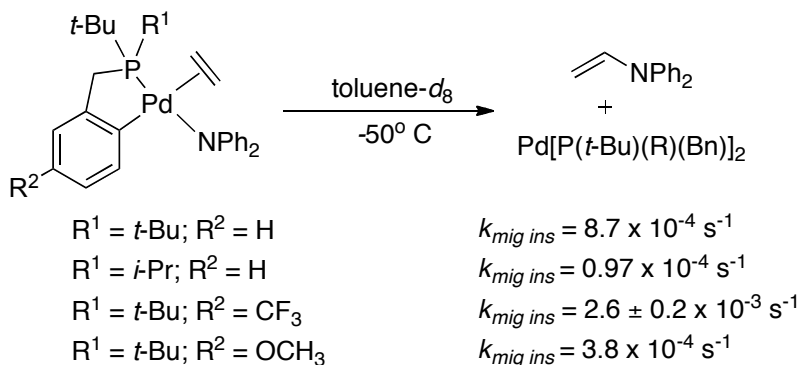
(150 equiv) was necessary. Under these conditions the rate of migratory insertion could be measured directly. The proposed reaction mechanism of these Pd-amides with ethylene is illustrated in Scheme 1.27. The rate constant for the migratory insertion step was found to have a ΔG^\ddagger of 16.0 kcal/mol.



Scheme 1.27. Proposed reaction mechanism of benzylphosphine ligated Pd-amides with ethylene

To examine the steric effects of the ancillary ligand on the rate of migratory insertion, an amido complex ligated by a cyclometallated benzyl(isopropyl)(*tert*-butyl)phosphine ligand was prepared and the reactivity of this complex was compared to that of the 2-(*t*-Bu)₂PCH₂C₆H₄-ligated complex both experimentally and computationally. The rate constant for migratory insertion of the less sterically encumbered 2-(*t*-Bu)(*i*-Pr)PCH₂C₆H₄-ligated complex was almost an order of magnitude smaller than the rate constant for the 2-(*t*-Bu)₂PCH₂C₆H₄-ligated complex (Scheme 1.28). The computed free energy barriers for the reaction of these complexes and for the reaction of an analogous complex ligated by a truncated 2-(CH₃)₂PCH₂C₆H₄ were computed with DFT. The calculated barriers were consistent with those measured experimentally. The bulky substituents on the phosphine create stronger steric interactions in the ground state than in

the transition state for migratory insertion. Thus, the reactions of complexes ligated by bulkier ancillary ligands undergo migratory insertion with a lower barrier than those of complexes ligated by less bulky ancillary ligands. However, this steric effect imparted by the ancillary ligand on the migratory insertion step is counterbalanced by the steric effect on the binding of the alkene to the three coordinate complex. The reactions of the two THF-ligated analogs of these complexes react with similar rate constants at -10 °C.



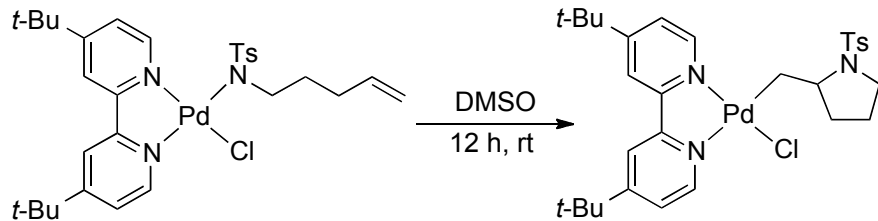
Scheme 1.28. Rate constants for migratory insertion reactions of amidopalladium ethylene complexes

To evaluate the electronic effect of the ancillary ligands on the rate constant for migratory insertion, amido complexes ligated by cyclometallated di-*tert*-butylbenzylphosphine ligands containing *meta*-trifluoromethyl and *meta*-methoxy substituents on the aryl ring were synthesized and their reactivity was compared. Complexes ligated by more weakly donating ancillary ligands, thus containing more electrophilic metal centers, underwent migratory insertion faster than those containing more electron-donating phosphines. The effect of the electronic parameters of the alkene on the rate of insertion was examined by allowing the THF-ligated palladium amide to react with a series of vinylarenes containing different substituents on

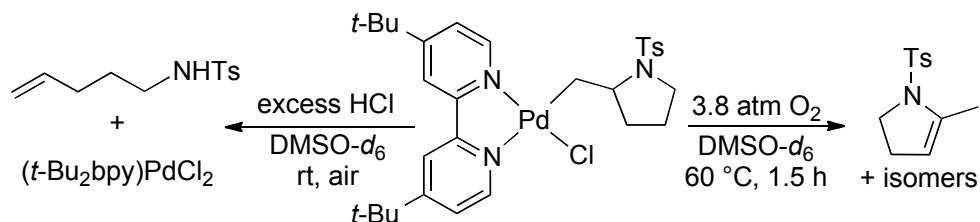
the aryl ring. Migratory insertion reactions of more electron-poor vinylarenes occurred faster than those of more electron-rich vinylarenes. A Hammett analysis revealed a ρ value of 1.04 that indicates a decrease in positive charge on the alkene ligand in the transition state for migratory insertion.

We have provided the most in depth evaluation of the steric and electronic effects of the alkene and the ancillary and amido ligand on the rate of migratory insertion into a Pd-N bond. Rapid β -hydrogen elimination immediately following migratory insertion precludes the observation of the immediate product from the insertion step. In addition, the resulting palladium-hydride formed from β -hydrogen elimination undergoes rapid C-H bond-forming reductive elimination, opening the P-C metallocycle, and limiting this system to stoichiometric reactions.

More recently, Stahl has described the intramolecular migratory insertion of an unactivated olefin into the Pd-N bond of a well-defined palladium sulfonamide complex.¹⁰⁴ The air-stable Pd-amidate complex was prepared from the reaction of (*t*-Bu₂bpy)PdCl₂ and a single equiv of NaN(Ts)[(CH₂)₃CH=CH₂] in DCM at RT, and was fully characterized by NMR spectroscopy and x-ray crystallography. The reaction of the sulfonamide complex in DMSO over 12 h formed an alkylpalladium chloride complex that Stahl proposed to form by dissociation of the chloride ligand followed by migratory insertion of the pendant alkene into Pd-N bond through a four-coordinate intermediate (Scheme 1.29). Under aerobic conditions at 60 °C, the alkyl complex underwent β -hydrogen elimination to yield a mixture of N-tosylpyrrole and N-tosylpyrrolidine products (Scheme 1.30). Reaction of a palladium sulfonamide complex containing a stereochemically defined, deuterium-labeled amido ligand formed products resulting from *syn*-aminopalladation.



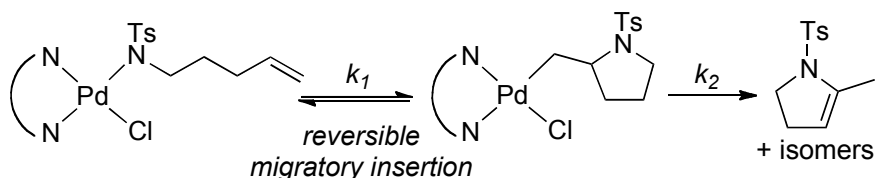
Scheme 1.29. Reaction of Pd-sulfonamidate complex



Scheme 1.30. Reactions of di-*t*-butylpyridine ligated Pd-alkyl complex

Addition of excess HCl to the aminoalkylpalladium chloride complex resulted in the rapid formation of 4-pentenyl tosylamide and $(t\text{-Bu}_2\text{bpy})\text{PdCl}_2$ (Scheme 1.30). Thus, the alkyl complex undergoes de-insertion of the sulfonamide (β -amidate elimination) faster than β -hydrogen elimination, and the resulting Pd-amidate complex is protonated by HCl. This result implies that alkene insertion into the Pd-amidate bond is reversible. Indeed, the reactions of a series of palladium sulfonamidate complexes with different *para*-substituted benzenesulfonamidate groups were monitored by ^1H NMR spectroscopy. These sulfonamide complexes underwent migratory insertion to form an equilibrium mixture of aminoalkyl- and sulfonamidate-palladium complexes. These complexes decayed in concert with the formation of heterocyclic products (Scheme 1.31). The rate constant for the migratory insertion step was measured for each complex, and those complexes containing more electron-donating groups on the amidate ligand

reacted faster than those containing less electron-donation groups. This trend is similar to that observed for the insertion of ethylene into palladium diarylamido bonds.



Scheme 1.31. Proposed reaction mechanism of Pd-sulfonamidate complexes

1.4. Conclusions

Recently, a number of catalytic aminations and alkoxylations of alkenes have been reported that appear to occur by migratory insertion of an alkene into an M-N or M-O bond as step in the proposed catalytic cycle. However, few examples of isolated amido and alkoxo complexes that react with alkenes were reported. The propensity of amido and alkoxo complexes to form stable N-or O-bridged dimeric or oligomeric species precludes the formation of complexes that can undergo migratory insertion of the alkene into an M-N or M-O bond, because an open site is necessary for alkene coordination prior to the insertion step. In the last two years, however, several papers have described a series of palladium-amido complexes that undergo migratory insertion reactions with unactivated olefins. These reports provide direct evidence that migratory insertion of an alkene into a late-metal-nitrogen bond occurs with moderate activation barriers. The systems studied by Stahl, Wolfe, and Hartwig, undergo migratory insertion at or below room temperature, and these moderate activation barriers are similar to those obtained for insertions into metal-carbon bonds. Although most authors have proposed that metal-catalyzed olefin amination and alkoxylation reactions occur by attack of the heteroatom nucleophile on to a

metal-coordinated olefin, many of these reactions likely occur by migratory-insertion of the alkene into an M-O or M-N bond.

Although some of the factors that control the rate and selectivity of migratory insertion of an alkene into a metal-heteroatom bond have been revealed, many of the proposed reactive intermediates that undergo insertion reactions have yet to be isolated or observed. No one has isolated a reactive intermediate involved in the palladium catalyzed alkene alkoxylation. These intermediates have been proposed for over 40 years, but their isolation remains elusive. In addition, a reevaluation of the mechanism of lanthanide-catalyzed hydroamination is necessary. Although Marks has reported some evidence that these reactions occur by alkene insertion into a Ln-amide, an olefin-amido complex that reacts with alkenes has not been observed. Ambiguity remains with regard to the role of the N-H bond on the coordinated amine ligand during the insertion step. Sadow has proposed a six-centered transition state for related hydroaminations catalyzed by rare-earth metals that appears to rationalize better the kinetic data collected for Ln-catalyzed hydroamination.

This review presents the foundation of a new class of fundamental organometallic transformations. Migratory insertion of alkenes into M-O and M-N bonds occur with barriers similar to those of insertions into M-C bonds. Future work investigating the metal-catalyzed addition of amines and alcohols to an alkene must include migratory insertion as possible pathway for the C-N or C-O bond-forming step.

1.5. References

- (1) Herrmann, B. C. a. W. A. *Applied Homogeneous Catalysis with Organometallic Compounds*; Wiley-VCH: Weinheim, 2002; Vol. 1.
- (2) Chaudhari, R. V. *Top. Catal.* **2012**, *55*, 439.
- (3) Evans, D.; Osborn, J. A.; Jardine, F. H.; Wilkinso.G *Nature* **1965**, *208*, 1203.
- (4) Jardine, F. H.; Osborn, J. A.; Wilkinso.G; Young, J. F. *Chem. Ind.* **1965**, *560*.
- (5) Morris, R. H. *Handbook of Homogeneous Hydroamination*; Wiley-VCH: Weinheim, 2007; Vol. 1.
- (6) Grubbs, R. H.; Coates, G. W. *Acc. Chem. Res.* **1996**, *29*, 85.
- (7) Ittel, S. D.; Johnson, L. K.; Brookhart, M. *Chem. Rev.* **2000**, *100*, 1169.
- (8) Gibson, V. C.; Spitzmesser, S. K. *Chem. Rev.* **2003**, *103*, 283.
- (9) Mecking, S. *Angew. Chem., Int. Ed.* **2001**, *40*, 534.
- (10) Thalji, R. K.; Ahrendt, K. A.; Bergman, R. G.; Ellman, J. A. *J. Am. Chem. Soc.* **2001**, *123*, 9692.
- (11) Tan, K. L.; Bergman, R. G.; Ellman, J. A. *J. Am. Chem. Soc.* **2002**, *124*, 13964.
- (12) Periana, R. A.; Liu, X. Y.; Bhalla, G. *Chem. Commun.* **2002**, 3000.
- (13) Oxgaard, J.; Periana, R. A.; Goddard, W. A. *J. Am. Chem. Soc.* **2004**, *126*, 11658.
- (14) Lail, M.; Bell, C. M.; Conner, D.; Cundari, T. R.; Gunnoe, T. B.; Petersen, J. L. *Organometallics* **2004**, *23*, 5007.
- (15) Nakao, Y.; Hirata, Y.; Hiyama, T. *J. Am. Chem. Soc.* **2006**, *128*, 7420.
- (16) Nakao, Y.; Ebata, S.; Yada, A.; Hiyama, T.; Ikawa, M.; Ogoshi, S. *J. Am. Chem. Soc.* **2008**, *130*, 12874.

- (17) Nakao, Y.; Idei, H.; Kanyiva, K. S.; Hiyama, T. *J. Am. Chem. Soc.* **2009**, *131*, 5070.
- (18) Watson, M. P.; Jacobsen, E. N. *J. Am. Chem. Soc.* **2008**, *130*, 12594.
- (19) Beletskaya, I. P.; Cheprakov, A. V. *Chem. Rev.* **2000**, *100*, 3009.
- (20) Amatore, C.; Jutand, A. *Acc. Chem. Res.* **2000**, *33*, 314.
- (21) Heck, R. F. *Acc. Chem. Res.* **1969**, *2*, 10.
- (22) Heck, R. F. *Acc. Chem. Res.* **1979**, *12*, 146.
- (23) Eckert, M. F., G.; Jira, R.; Bolt, H. M.; Golka, K. In *Ullmann's Encyclopedia of Industrial Chemistry*; Wiley-VCH: Weinheim, 2012; Vol. 1, p 191.
- (24) Green, M.; Sarhan, J. K. K.; Alnajjar, I. M. *J. Chem. Soc. Dalton.* **1981**, 1565.
- (25) Shaw, B. L. *Chem. Commun.* **1968**, 464.
- (26) Green, M.; Hancock, R. I. *J. Chem. Soc. A.* **1967**, 2054.
- (27) Stille, J. K.; Morgan, R. A. *J. Am. Chem. Soc.* **1966**, *88*, 5135.
- (28) Henry, P. M. *J. Am. Chem. Soc.* **1964**, *86*, 3246.
- (29) Akermark, B.; Soderberg, B. C.; Hall, S. S. *Organometallics* **1987**, *6*, 2608.
- (30) Stille, J. K.; Divakaruni, R. *J. Am. Chem. Soc.* **1978**, *100*, 1303.
- (31) Backvall, J. E.; Akermark, B.; Ljunggren, S. O. *J. Chem. Soc. Chem. Comm.* **1977**, 264.
- (32) Backvall, J. E.; Akermark, B.; Ljunggren, S. O. *J. Am. Chem. Soc.* **1979**, *101*, 2411.
- (33) Backvall, J. E.; Bjorkman, E. E.; Pettersson, L.; Siegbahn, P. *J. Am. Chem. Soc.* **1984**, *106*, 4369.
- (34) Hamed, O.; Henry, P. M.; Thompson, C. *J. Org. Chem.* **1999**, *64*, 7745.

- (35) Hamed, O.; Thompson, C.; Henry, P. M. *J. Org. Chem.* **1997**, *62*, 7082.
- (36) Hamed, O.; Henry, P. M. *Organometallics* **1997**, *16*, 4903.
- (37) Zaw, K.; Henry, P. M. *Organometallics* **1992**, *11*, 2008.
- (38) Francis, J. W.; Henry, P. M. *Organometallics* **1992**, *11*, 2832.
- (39) Francis, J. W.; Henry, P. M. *Organometallics* **1991**, *10*, 3498.
- (40) Crabtree, R. H. *The Organometallic Chemistry of the Transition Metals*; 5th ed.; John Wiley & Sons: Hoboken, NJ, 2009.
- (41) Hayashi, T.; Yamasaki, K.; Mimura, M.; Uozumi, Y. *J. Am. Chem. Soc.* **2004**, *126*, 3036.
- (42) Stoltz, B. M.; Trend, R. M.; Ramtohul, Y. K. *J. Am. Chem. Soc.* **2005**, *127*, 17778.
- (43) Hay, M. B.; Wolfe, J. P. *J. Am. Chem. Soc.* **2005**, *127*, 16468.
- (44) Hay, M. B.; Hardin, A. R.; Wolfe, J. P. *J. Org. Chem.* **2005**, *70*, 3099.
- (45) Wolfe, J. P.; Rossi, M. A. *J. Am. Chem. Soc.* **2004**, *126*, 1620.
- (46) Seo, S. Y.; Yu, X. H.; Marks, T. J. *J. Am. Chem. Soc.* **2009**, *131*, 263.
- (47) Yu, X. H.; Seo, S.; Marks, T. J. *J. Am. Chem. Soc.* **2007**, *129*, 7244.
- (48) Dzudza, A.; Marks, T. J. *Chem-Eur J* **2010**, *16*, 3403.
- (49) Nolan, S. P.; Stern, D.; Marks, T. J. *J. Am. Chem. Soc.* **1989**, *111*, 7844.
- (50) Bryndza, H. E. *Organometallics* **1985**, *4*, 406.
- (51) Zhao, P. J.; Incarvito, C. D.; Hartwig, J. F. *J. Am. Chem. Soc.* **2006**, *128*, 9642.
- (52) Tye, J. W.; Hartwig, J. F. *J. Am. Chem. Soc.* **2009**, *131*, 14703.
- (53) Gagne, M. R.; Stern, C. L.; Marks, T. J. *J. Am. Chem. Soc.* **1992**, *114*, 275.
- (54) Li, Y. W.; Marks, T. J. *J. Am. Chem. Soc.* **1996**, *118*, 9295.

- (55) Pohlki, F.; Doye, S. *Chem. Soc. Rev.* **2003**, *32*, 104.
- (56) Hong, S.; Marks, T. J. *J. Acc. Chem. Res.* **2004**, *37*, 673.
- (57) Gribkov, D. V.; Hultzsch, K. C.; Hampel, F. *J. Am. Chem. Soc.* **2006**, *128*, 3748.
- (58) Motta, A.; Lanza, G.; Fragala, I. L.; Marks, T. J. *Organometallics* **2004**, *23*, 4097.
- (59) Stubbert, B. D.; Stern, C. L.; Marks, T. J. *Organometallics* **2003**, *22*, 4836.
- (60) Stubbert, B. D.; Marks, T. J. *J. Am. Chem. Soc.* **2007**, *129*, 4253.
- (61) Baranger, A. M.; Walsh, P. J.; Bergman, R. G. *J. Am. Chem. Soc.* **1993**, *115*, 2753.
- (62) Walsh, P. J.; Baranger, A. M.; Bergman, R. G. *J. Am. Chem. Soc.* **1992**, *114*, 1708.
- (63) Gribkov, D. V.; Hultzsch, K. C. *Angew. Chem., Int. Ed.* **2004**, *43*, 5542.
- (64) Stubbert, B. D.; Marks, T. J. *J. Am. Chem. Soc.* **2007**, *129*, 6149.
- (65) Majumder, S.; Odom, A. L. *Organometallics* **2008**, *27*, 1174.
- (66) Crimmin, M. R.; Casely, I. J.; Hill, M. S. *J. Am. Chem. Soc.* **2005**, *127*, 2042.
- (67) Crimmin, M. R.; Arrowsmith, M.; Barrett, A. G. M.; Casely, I. J.; Hill, M. S.; Procopiou, P. A. *J. Am. Chem. Soc.* **2009**, *131*, 9670.
- (68) Dunne, J. F.; Fulton, D. B.; Ellern, A.; Sadow, A. D. *J. Am. Chem. Soc.* **2010**, *132*, 17680.
- (69) Manna, K.; Xu, S. C.; Sadow, A. D. *Angew. Chem., Int. Ed.* **2011**, *50*, 1865.
- (70) Manna, K.; Kruse, M. L.; Sadow, A. D. *Accts. Catal.* **2011**, *1*, 1637.
- (71) Leitch, D. C.; Payne, P. R.; Dunbar, C. R.; Schafer, L. L. *J. Am. Chem. Soc.* **2009**, *131*, 18246.
- (72) Leitch, D. C.; Platel, R. H.; Schafer, L. L. *J. Am. Chem. Soc.* **2011**, *133*, 15453.

- (73) Akerman, B.; Backvall, J. E.; Hegedus, L. S.; Zetterbe.K; Siiralah.K; Sjoberg, K. *J. Organomet. Chem.* **1974**, 72, 127.
- (74) Backvall, J. E. *Tet. Lett.* **1978**, 163.
- (75) Akerman, B.; Zetterberg, K. *J. Am. Chem. Soc.* **1984**, 106, 5560.
- (76) Hegedus, L. S.; McKearin, J. M. *J. Am. Chem. Soc.* **1982**, 104, 2444.
- (77) Zeni, G.; Larock, R. C. *Chem. Rev.* **2004**, 104, 2285.
- (78) Nakhla, J. S.; Kampf, J. W.; Wolfe, J. P. *J. Am. Chem. Soc.* **2006**, 128, 2893.
- (79) Ney, J. E.; Wolfe, J. P. *J. Am. Chem. Soc.* **2005**, 127, 8644.
- (80) Mai, D. N.; Wolfe, J. P. *J. Am. Chem. Soc.* **2010**, 132, 12157.
- (81) Schultz, D. M.; Wolfe, J. P. *Org. Lett.* **2011**, 13, 2962.
- (82) Kotov, V.; Scarborough, C. C.; Stahl, S. S. *Inorg. Chem.* **2007**, 46, 1910.
- (83) Liu, G. S.; Stahl, S. S. *J. Am. Chem. Soc.* **2007**, 129, 6328.
- (84) Liu, G. S.; Yin, G. Y.; Wu, L. *Angew. Chem., Int. Ed.* **2008**, 47, 4733.
- (85) Helaja, J.; Gottlich, R. *Chem. Commun.* **2002**, 720.
- (86) Liu, G. S.; Stahl, S. S. *J. Am. Chem. Soc.* **2006**, 128, 7179.
- (87) Muniz, K.; Hovelmann, C. H.; Streuff, J. *J. Am. Chem. Soc.* **2008**, 130, 763.
- (88) Tsutsui, H.; Narasaka, K. *Chem. Lett.* **1999**, 45.
- (89) Minatti, A.; Muniz, K. *Chem. Soc. Rev.* **2007**, 36, 1142.
- (90) Wolfe, J. P. *Synlett* **2008**, 2913.
- (91) Brice, J. L.; Harang, J. E.; Timokhin, V. I.; Anastasi, N. R.; Stahl, S. S. *J. Am. Chem. Soc.* **2005**, 127, 2868.
- (92) Ney, J. E.; Wolfe, J. P. *Angew. Chem., Int. Ed.* **2004**, 43, 3605.
- (93) Cowan, R. L.; Trogler, W. C. *Organometallics* **1987**, 6, 2451.

- (94) Casalnuovo, A. L.; Calabrese, J. C.; Milstein, D. *J. Am. Chem. Soc.* **1988**, *110*, 6738.
- (95) Dorta, R.; Egli, P.; Zurcher, F.; Togni, A. *J. Am. Chem. Soc.* **1997**, *119*, 10857.
- (96) Zhou, J. R.; Hartwig, J. F. *J. Am. Chem. Soc.* **2008**, *130*, 12220.
- (97) Pan, S. G.; Endo, K.; Shibata, T. *Org. Lett.* **2012**, *14*, 780.
- (98) Sevov, C. S.; Zhou, J. R.; Hartwig, J. F. *J. Am. Chem. Soc.* **2012**, *134*, 11960.
- (99) Zhao, P. J.; Krug, C.; Hartwig, J. F. *J. Am. Chem. Soc.* **2005**, *127*, 12066.
- (100) Neukom, J. D.; Perch, N. S.; Wolfe, J. P. *J. Am. Chem. Soc.* **2010**, *132*, 6276.
- (101) Hanley, P. S.; Markovic, D.; Hartwig, J. F. *J. Am. Chem. Soc.* **2010**, *132*, 6302.
- (102) Hanley, P. S.; Hartwig, J. F. *J. Am. Chem. Soc.* **2011**, *133*, 15661.
- (103) Neukom, J. D.; Perch, N. S.; Wolfe, J. P. *Organometallics* **2011**, *30*, 1269.
- (104) White, P. B.; Stahl, S. S. *J. Am. Chem. Soc.* **2011**, *133*, 18594.

Chapter 2: Intermolecular Migratory Insertion of Ethylene and Octene into a Palladium-Amide Bond.*

2.1 Introduction

Migratory insertions of alkenes are among the most documented organometallic transformations. This class of reaction is a common step in numerous catalytic processes, including the polymerization of alkenes,¹⁻⁴ the hydroarylation of alkenes,⁵⁻⁹ the difunctionalization of alkenes,¹⁰⁻¹³ and the olefination of aryl halides, commonly termed the Mizoroki-Heck reaction.¹⁴⁻¹⁷ Many organometallic complexes react to form new C-C and C-H bonds by the transfer of a transition-metal hydrocarbyl or hydride group to a coordinated olefin.¹⁸ However, the transfer of an amido group from an isolated transition-metal amido complex to an olefin to generate a new C-N bond is much less established.

Many of the prior reactions of alkenes with isolated amido complexes have required activated alkenes. Milstein, Casalnuovo and coworkers reported an iridium(III) arylamido complex that inserts norbornene, but reactions with less-strained olefins were not observed.¹⁹ Trogler et al. reported the transfer of an amido ligand from an isolated platinum-amido complex to acrylonitrile, but this reaction most likely occurs by direct nucleophilic attack of the nitrogen of the amide on the electrophilic acrylonitrile.²⁰ Boncella et al. reported the reaction of a palladium amide with dimethylacetylene dicarboxylate, but alkenes and unactivated alkynes did not react.²¹

* Part of this chapter was previously published in Hanley, P. S.; Markovic, D.; Hartwig, J. F. *J. Am. Chem. Soc.* **2010**, *132*, 6302 and Hanley, P. S. Hartwig, J. F. *J. Am. Chem. Soc.* **2011**, *133*, 15661.

Less-activated alkenes undergo intramolecular insertion into amido complexes characterized in situ, and recent catalytic hydroaminations of secondary aminoalkenes catalyzed by group IV transition metal complexes are thought to occur by alkene insertion into the metal-amide bond.²²²⁴ For example, Marks et al. reported the intramolecular insertion of an olefin into a lanthanide-amide generated in situ,²⁵ and Hultzsch has reported the hydroamination of secondary aminoalkenes catalyzed by cationic zirconocene and titanocene complexes.²⁶ More recently, Wolfe reported the intramolecular insertion of an alkene into a palladium-amido complex generated and characterized in situ.^{27,28}

The authors' group has reported the isolation and full characterization of a series of isolated rhodium(I) amido complexes that react intermolecularly with unactivated alkenes and vinylarenes to generate imine products.²⁹ Potential pathways for the transfer of the amido group were investigated by a series of mechanistic experiments. All the mechanistic data were consistent with a pathway initiated by coordination of the alkene to the metal center, migratory insertion of the olefin into the rhodium-amido bond, and β -hydrogen elimination from the resulting aminoalkene complex.

In addition, migratory insertion has been proposed to occur during several classes of palladium-catalyzed aminations of alkenes, including carboaminations,³⁰⁻³⁴ oxidative aminations,³⁵⁻³⁷ aminoacetoxylations,³⁸ diaminations,³⁹ chloro-aminations,⁴⁰ and hetero-Heck type transformations.⁴¹ Stereochemical evidence for *syn*-aminopalladation by migratory insertion has been obtained during studies of some of these systems. For example, Stahl and coworkers have shown that a complex generated from $\text{Pd}(\text{OAc})_2$ and pyridine catalyzes the oxidative cyclization of deuterium-labeled aminoalkenes to generate products from *syn*-aminopalladation,⁴² and Wolfe and coworkers have shown that the stereochemical outcome of

alkene carboaminations they developed is consistent with a mechanism involving the migratory insertion of an alkene into a metal-amide bond.²⁷ Although data have been reported that imply that alkenes insert into palladium-nitrogen bonds during catalytic reactions, discrete complexes involved in palladium-catalyzed olefin aminations, other than those studied in the current work, have not been isolated. Studies aimed at revealing steric and electronic effects on the insertions of alkenes into the Pd-N bonds of phosphine-ligated intermediates in palladium-catalyzed carboamination reactions were stated to reveal the effect of these properties on the rate of ligand dissociation, rather than the rate of the C-N bond-forming migratory insertion step.²⁸

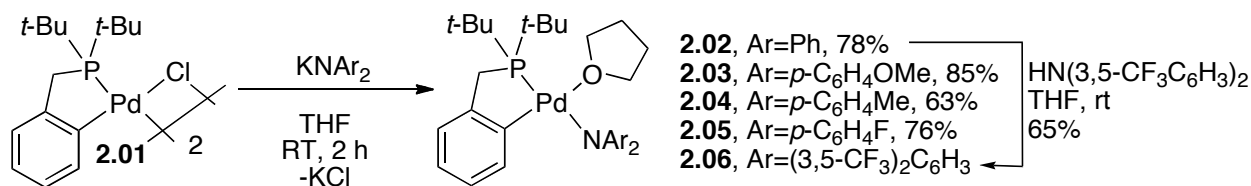
In this chapter, a series of palladium diarylamido complexes that react with unactivated alkenes, including the simplest alkene, ethylene, to form enamine products from initial intermolecular insertion are described. The stereochemistry of the enamine products, along with kinetic data, supports a migratory insertion pathway, and we have obtained spectroscopic evidence at -100 °C for an ethylene amido intermediate that undergoes migratory insertion at -40 °C.

2.2 Results and Discussion

2.2.1 Reaction of Pd-Amides with Ethylene and Octene

The preparation of the palladium-amido complexes in this study **2.02-2.06** is depicted in Scheme 2.1. To generate complexes that are isoelectronic with the rhodium amido complexes reported previously by our group to insert alkenes,²⁹ an anionic ancillary ligand is necessary. To encourage monomeric structures and to discourage C-N reductive elimination from unsaturated arylpalladium amido complexes,⁴³ a cyclometallated complex generated from a hindered benzylic phosphine was studied. The stable THF-ligated Pd-amido complexes **2.02-2.05** were

formed from the reaction of $[(P-C)PdCl]_2$ (**2.01**) with $KNAr_2$ in THF. Complex **2.06** was synthesized by proton transfer between **2.02** and $HN((3,5-CF_3)_2C_6H_3)_2$. The bound THF in **2.02-2.06** was evidenced by broad resonances in the 1H NMR spectrum between δ 3.56-3.32 and 1.35-0.94 ppm that integrated to 1 equiv of THF in C_6D_6 . Apparently, the bulky *tert*-butyl groups and the weak basicity of the diarylamido nitrogen inhibit formation of an *N*-bridged amido dimer.



Scheme 2.1. Preparation of THF ligated amido complexes.

An ORTEP diagram of **2.02** is shown in Figure 1. Complex **2.02** possesses a square planar geometry, and the substituents on the diarylamide lie on either side of the square plane. The Pd-N distance is within error of that of a related three-coordinate diarylamide⁴³ and the average for palladium-amido complexes (2.083 Å) in the CCD. The Pd-C bond is only about 0.03 Å longer than that in the previous arylpalladium diarylamido complex. The P-Pd-C angle (82.4°) is typical for a five-membered palladacycle.

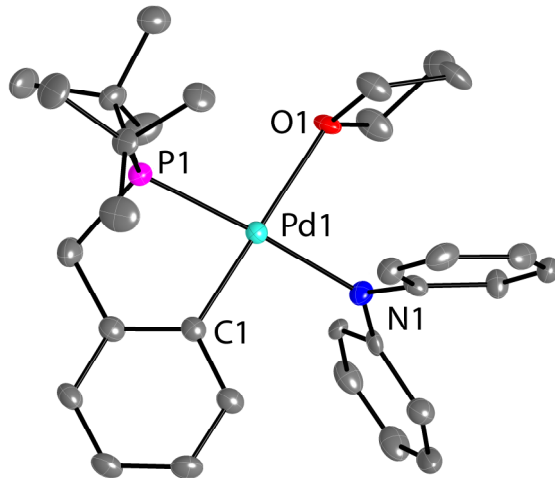


Figure 2.1. An ORTEP drawing of **2.02** with 35% probability ellipsoids. Hydrogen atoms are omitted for clarity. Selected bond angles (degrees) and lengths (\AA): P-Pd-C, 82.4(2); P-Pd-N, 176.5(2); C-Pd-N, 94.2(2); N-Pd-O, 85.8(2); P-Pd-O, 97.59(9); C-Pd-O, 179.4(2); Pd-C, 2.001(5); Pd-P, 2.249(1); Pd-N, 2.082(2); Pd-O, 2.264(3).

Amido complexes **2.02-2.06** reacted with alkenes to form enamine products, and the yields and rate constants for these reactions are shown in Table 2.1. The reaction of **2.02** with ethylene for 2 h at -10 °C formed the *N*-vinyldiarylamine product in 89% yield. The reaction of **2.02** with neat 1-octene at 80 °C for 30 min generated a mixture of three isomeric enamines in 74% yield. Reactions with 1-octene were conducted in both polar and nonpolar solvents, including diethyl ether, DMF, benzene, and toluene; the highest yields were obtained from reactions in toluene or benzene.

Table 2.1. Reactions of ethylene and 1-octene with amides **2.02-2.06**^a

The reaction scheme shows complex **2a-e** reacting with $\text{R}=\text{H}$ or $\text{R}=n\text{-hexyl}$ in the presence of $n \text{ P}(t\text{-Bu})_2\text{Bn}$ ($n=0\text{-}1.5$ equiv) and C_2H_4 or C_8H_{16} . The products are enamines ($\text{R}-\text{CH}(\text{NAr}_2)=\text{CH}_2$) and $\text{Pd}[(\text{P}(t\text{-Bu})_2\text{Bn})]_2$ (7).

entry	complex	For $\text{R} = \text{H}$ (Yield)	for $\text{R} = \text{H}$ $k_{\text{obs}} \times 10^3 (\text{s}^{-1})$	For $\text{R} = \text{C}_6\text{H}_{13}$ (Yield) ^b
1	2.02	89%	0.91	(neat) 74%
2	2.02	-	-	(25 equiv) 69%
3	2.02	-	-	(10 equiv) 48%
4	2.03	94%	9.6	97%
5	2.04	63%	4.3	64%
6	2.05	60%	0.79	52%
7 ^c	2.06	98%	0.053	ND ^d

^aConditions for reactions with 1-octene: benzene, 80 °C for 30 min. Conditions for reactions with ethylene: toluene, -10 °C for 2 h, 20 equiv ethylene. ^bCombined yield for all enamine isomers.

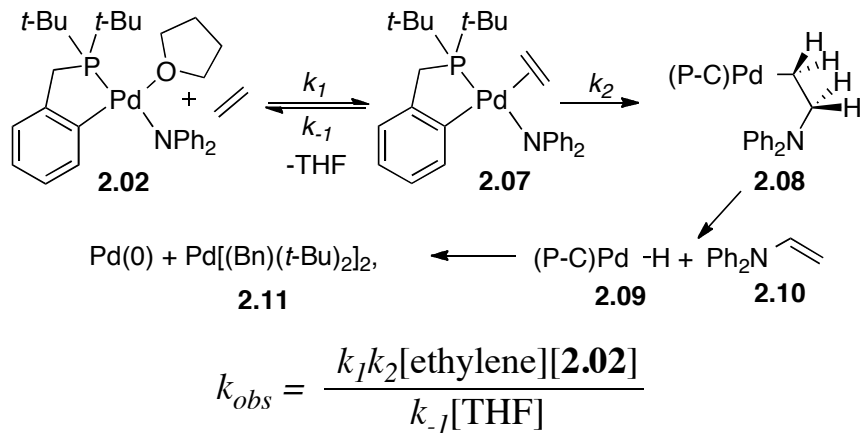
^cReaction at 85 °C. ^dThis reaction did not form detectable amounts of the enamine product.

The data in Table 1 show that the complexes containing the more electron-donating amido groups occurred faster than those containing the less electron-donating amido groups. Complex **2.03** containing the most electron-donating di-*p*-ansiylamido ligand reacted about two times faster than complex **2.04** containing di-*p*-tolylamido groups and ten times faster than complexes **2.02** and **2.05** containing the less electron-donating diphenyl and *p*-fluorophenylamido ligands. Likewise, complexes **2.02** and **2.05** reacted much faster than complex **2.06** containing the bis-trifluoromethyl-substituted diarylamido ligand.

2.2.2 The Mechanism of the Reaction of Ethylene with Pd-amides

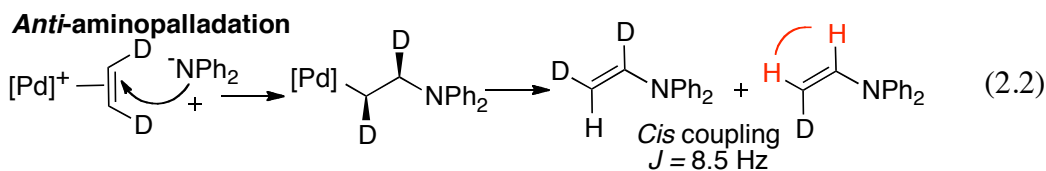
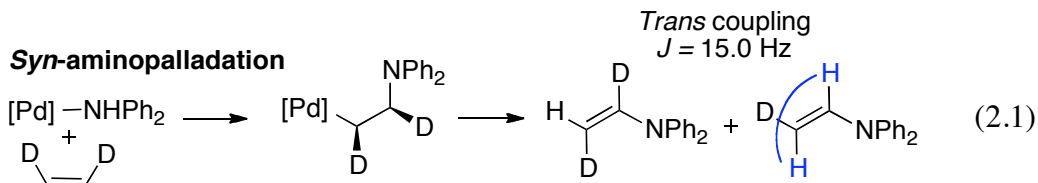
The mechanism of the reaction of ethylene with the amido complexes was examined by kinetic experiments and an evaluation of the stereochemistry of insertion. The decay of diphenylamide **2.02** was monitored during reaction with ethylene at -10 °C by ¹H NMR spectroscopy. An exponential decay of [**2.02**] was observed, indicating a first order dependence

on [2.02] and reaction through the observed monomer. The reaction was first-order in [ethylene] and inverse first-order in [THF]. These data are consistent with exchange of ethylene for THF and reaction through a four-coordinate alkene complex, as summarized in Scheme 2.2.



Scheme 2.2. Proposed mechanism of the reaction of Pd-amide **2.02** with ethylene

To distinguish between *syn*-aminopalladation by migratory insertion within the amido olefin complex **2.07** and *anti*-aminopalladation by alternative pathways, the isomeric composition of the products from the reaction of **2.02** with *cis*-ethylene-*d*₂ was examined. The products of *syn*- and *anti*-aminopalladation are distinguishable by the presence or absence of *trans* or *cis* ³*J* vicinal coupling constants in the enamine and the chemical shift of the uncoupled proton, as shown in eq 2.1 and 2.2. The ¹H NMR spectrum of the product from the reaction of (P-C)Pd(THF)NPh₂ with ethylene is shown below in figure 2.2.



If a *syn*-aminopalladation pathway is active, only the *trans* coupling $J = 15.0 \text{ Hz}$ between H_a and H_c will be observed in the products of the reaction of **2.02** and *cis*- D_2 -ethylene. The coupling between H_a and H_b will no longer be present and the resonance for H_b should be observed as a singlet. Likewise, if a *trans*-aminopalladation pathway is active, only the *cis* coupling $J = 8.5 \text{ Hz}$ between H_a and H_b will be observed in the products of the reaction of **2.02** and *cis*- D_2 -ethylene. The coupling between H_a and H_c will no longer be present and the resonance for H_c should be observed as a singlet.

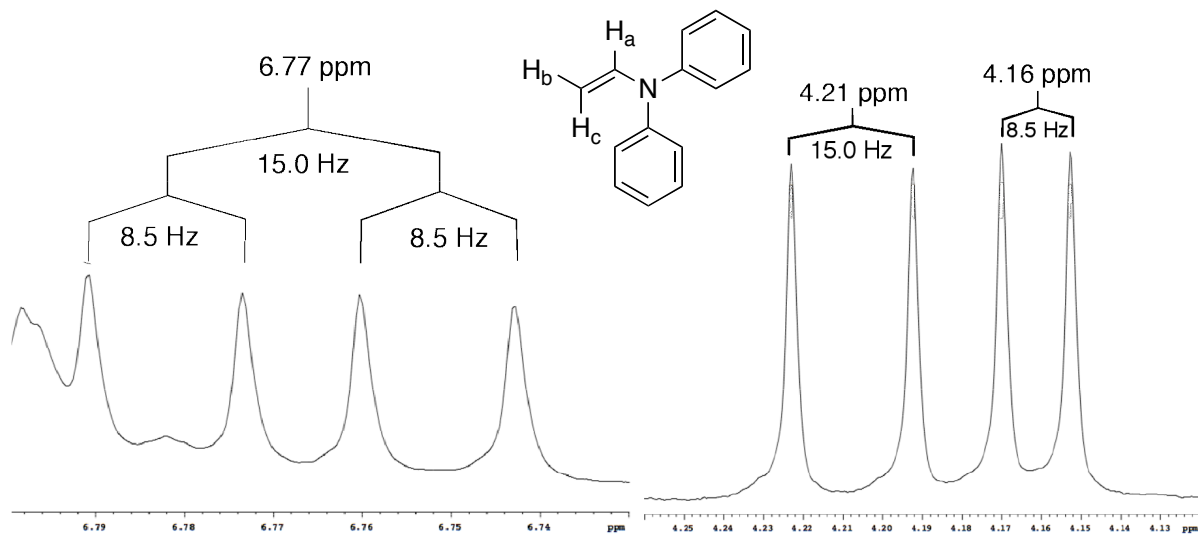


Figure 2.2. Vinylic resonances of N-vinyldiphenylamine in ^1H NMR spectrum. The spectrum is expanded to show δ 6.80 -6.73 ppm and δ 4.26-4.12 ppm.

The product of the reaction of **2.02** with *cis*-ethylene-*d*₂ formed a 72±5:28 ratio of *d*₂:*d*₁ *N*-vinyldiphenylamines in 75% yield, reflecting an isotope effect for the *b*-hydrogen elimination step of 2.7 ± 0.6 . The ¹H NMR spectrum of the product from the reaction of **2.02** with *cis*-*D*₂-ethylene is shown below in Figure 2.3. In this mixture of product isotopomers, one H_c resonated at δ 4.21 as a doublet with a *trans*-coupling of 15 Hz, and H_b resonated at δ 4.16 ppm as a singlet. The internal vinylic proton (H_a) is now observed as simple doublet $J = 15.0$ Hz. These data are consistent with formation of the *Z-d*₂ and *E-d*₁ products in eq 1, and the formation of these stereoisomers is consistent with reaction by a concerted migratory insertion, followed by *b*-hydrogen elimination from a syn coplanar intermediate.

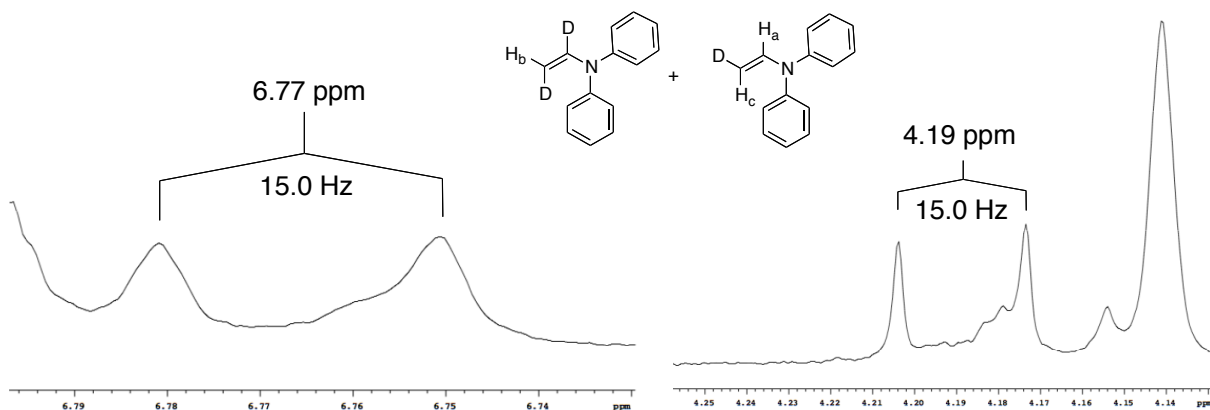
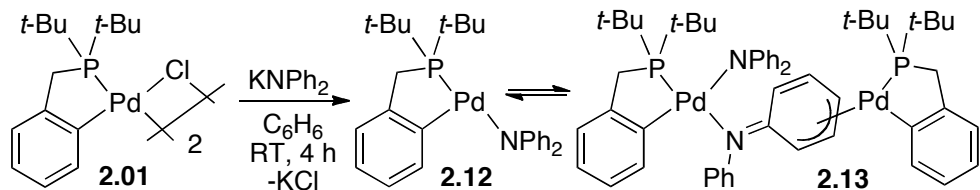


Figure 2.3. Vinylic resonances of the *N*-vinyldiphenylamine in ¹H NMR spectrum. The spectrum is expanded to show δ 6.80 -6.73 ppm and δ 4.26-4.12 ppm.

2.2.3 Spectroscopic Evidence for an Ethylene Amido Intermediate

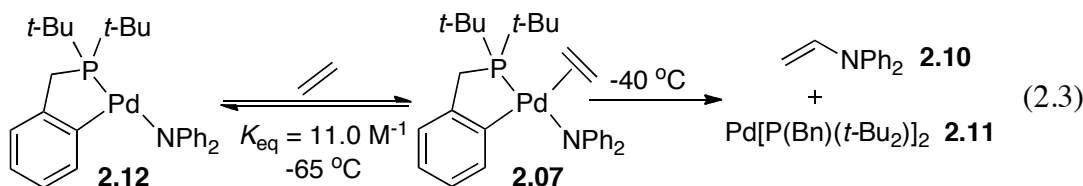
The analogous diarylamido complex **2.12** lacking a bound THF was prepared by the reaction of [(P-C)PdCl]₂ (**2.01**) with KNPh₂ in benzene (Scheme 2.3). At room temperature, this complex is the three-coordinate **2.12**, as revealed by the single ³¹P resonance at δ 101.8 ppm and a simple ¹H NMR spectrum containing one set of aryl resonances. However, at low temperatures, a

mixture of this three-coordinate monomer and a dinuclear species (**2.13**)—were observed by ^1H and ^{31}P NMR spectroscopy. The structure of the dinuclear species—was identified in the solid state by X-ray diffraction. The three-coordinate amido complex reacted with ethylene at -40 °C to generate enamine products in 86% yield. The rate of this insertion and subsequent b-hydrogen elimination to form enamine is remarkably fast, considering the dearth of olefin insertions into transition metal-amido complexes, but modest computed barriers were reported recently for insertions into a rhodium amide.⁴⁴



Scheme 2.3. Preparation of THF-free Pd-amide **2.12/2.13**.

Addition of varying excess amounts of alkene to THF-free complex **2.12/2.13** below -40 °C generated a solution for which the NMR spectrum implied a rapidly equilibrating mixture of **3a** and an olefin adduct, formulated as the olefin amido complex **2.13** in eq 2.3. Addition of increasing amounts of ethylene at -65 °C led to a progressive upfield shift of the ^{31}P NMR resonance from δ 101.8 ppm for **2.12** to δ 90.6 ppm. At -100 °C, distinct signals for the free complex **2.12** and olefin adduct **2.07** were observed, along with 34% of the dinuclear species **2.12**.



To confirm the presence of an ethylene bound species at low temperature, we allow Pd-amide to react with ^{13}C -labeled ethylene. The ^{13}C NMR spectrum (Figure 2.4) of this species generated at -100 °C from $^{13}\text{CH}_2=^{13}\text{CH}_2$ consisted of a broad ^{13}C resonance at 106.5 ppm, which falls in the range of chemical shifts typical for Pd(II) alkene complexes.^{45,46} An equilibrium constant between **2.12** and **2.07** of 11 M^{-1} at -65°C was determined from a plot of the ^{31}P NMR chemical shift vs the concentration of added ethylene. The rate constant for the decay of the observed species and formation of the enamine at -40 °C was $8.7 \times 10^{-4}\text{ s}^{-1}$ (ΔG^\ddagger of 17 kcal/mol).

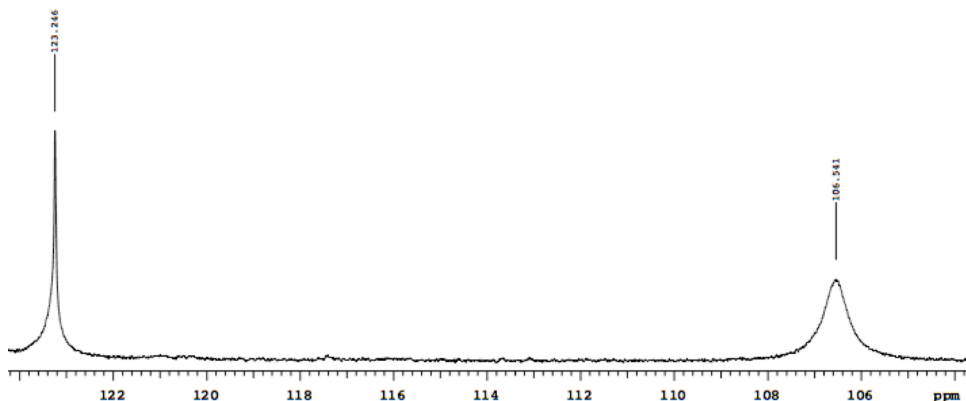


Figure 2.4. ^{13}C NMR spectrum of the Reaction of $^{13}\text{C}=^{13}\text{C}$ ethylene at -100 °C

2.3 Conclusion

In summary, we have reported the first evidence for intermolecular migratory insertion of alkenes into the Pd-N bonds of discrete Pd-amides. These reactions occur by reversible generation of four-coordinate amido alkene complexes by replacement of bound THF or direct coordination to a three-coordinate amido complex. Complexes of electron-rich amides insert much faster than those of electron-poor amides, and the insertion step itself occurs within

minutes, even at -40 °C. Computational studies of the barriers and efforts to design catalytic processes with alternative ancillary ligands are in progress.

2.4 Experimental

2.4.1 General Experimental Details

Unless otherwise noted, all manipulations were carried out under an inert atmosphere in an argon-filled glovebox or by standard Schlenk techniques. THF, CH₂Cl₂, benzene, and toluene were degassed by purging with argon for 45 minutes and dried with a solvent purification system containing a 1 m column of activated alumina. Deuterated solvents (benzene, toluene, and THF), were dried over Na/benzophenone and vacuum distilled prior to use. CpPd(allyl), benzyldi-*tert*butylphosphine, 2-bromo-1-octene, and HN(4-FC₆H₄)₂ were prepared by established literature procedures. 1-octene was stirred over Na/benzophenone overnight and vacuum distilled prior to use. *Cis-d₂*-ethylene was purchased from Cambridge Isotopes Inc. in a break-seal flask and used without further purification. Potassium diarylamides were prepared by addition 1.1 equiv of HMDS to 1 equiv of diarylamine in toluene. The precipitated amides were collected by filtration and washed with pentane.

Analytical gas chromatography (GC) was performed using a Hewlett-Packard 5890 Gas Chromatograph fitted with a flame ionization detector and a Hewlett-Packard HP5 (30m x 0.32 mm) capillary column. NMR spectra were acquired on 500 MHz or 400 MHz Varian Unity or 500 MHz Innova instruments at the University of Illinois VOICE NMR facility. Chemical shifts are reported in ppm relative to residual chloroform (7.26 ppm for ¹H; 77.0 ppm for ¹³C), benzene (7.15 ppm for ¹H; 128.0 ppm for ¹³C), or THF (3.58 ppm for ¹H) or to an external standard

(85% H₃PO₄ = 0 ppm for ³¹P or CFCl₃ = 0 ppm for ¹⁹F). Coupling constants are reported in hertz. Elemental analyses were performed by the University of Illinois at Urbana-Champaign Microanalysis Laboratory or at Roberston Microlit Laboratories, Inc. (Madison, NJ)

2.4.2 General Procedure for the Reaction of Ethylene with 2.02-2.06

To a 4 dram vial was added (P-C)Pd(THF)NPh₂ (0.010 g, 0.017 mmol) and trimethoxybenzene (as the internal standard for NMR integration) (0.0029 g, 0.017 mmol), which were dissolved in 0.4 mL of benzene-*d*₆ or toluene-*d*₈ and carefully transferred into a J-Young tube. The reaction mixture was cooled in a liquid N₂ bath, and the sample tube was evacuated on a high vacuum manifold. A calibrated bulb (3.8 mL) attached to the NMR sample tube was evacuated and filled with ethylene to a pressure of 830 mmHg (0.17 mmol). The ethylene was then condensed in the cold J-Young tube. The reaction mixture was removed from the liquid N₂ and allowed to warm to room temperature. After 20 minutes yields of the organic and palladium products were determined by NMR spectroscopy.

2.4.3 General Procedure for the Reaction of 1-octene with 2.02-2.06

To a 4 dram vial was added (P-C)Pd(THF)NPh₂ (0.0100 g, 0.0172 mmol), which was dissolved in 0.5 mL of benzene. Neat 1-octene 0.12 mL (0.86 mmol) was added to the solution, and the vial was capped with a PTFE-lined silicone septum and heated in an oil bath to 80 °C for 1 h. The reaction was allowed to cool to room temperature, 3.9 µL (0.0172 mmol) of dodecane as internal standard was added to the reaction mixture, and the vial was shaken vigorously. A sample was extracted from the reaction mixture and diluted with dry Et₂O for GC analysis.

2.4.4 General Procedure for Kinetic Analysis

In a glove box, 0.010 g (0.0172 mmol) **2.02** and 0.0029 g TMB was weighed into a 4 dram vial. The mixture was dissolved into 0.40 mL toluene-*d*₈ and a 14.0 μ L (0.172 mmol) aliquot of THF was added via microliter syringe. The reaction mixture was swirled and added to a 9'' NMR tube that was then connected to a NMR sealing assembly. The tube was attached to a high-vacuum line, frozen in a liquid N₂ bath, and argon evaporated under vacuum. An attached 3.86 mL calibrated bulb was filled to a pressure of 621 x 2 torr of ethylene (0.258 mmol). The ethylene was vacuum transferred into the NMR tube, which was then flame sealed. The sealed NMR tube was removed from the liquid N₂ bath and quickly inserted into a dry ice/acetone bath at -78° C. Prior to inserting the NMR tube into a NMR spectrometer set to -10 °C, the tube was vigorously shaken to dissolve the ethylene into the reaction mixture. The NMR tube was inserted into the NMR probe, shimmed, and an array was collected until the **2.02** was consumed >3 half lives (180 min for this run). After completion of the array, the data were integrated and normalized the TMB internal standard. The concentration of **2.02** was plotted versus time and fitted to an exponential decay using KaleidaGraph from which the k_{obs} was extracted.

2.4.5 Determination of Order in Olefin

To determine the order in olefin we followed the general procedure for insertion of ethylene described above, but varied the concentration of added ethylene. A 10.0 mg (0.0172 mmol) sample of **2.02** was allowed to react with 10 (0.172 mmol), 15 (0.258 mmol), 20 (0.346 mmol), 25 (0.435 mmol), and 40 (0.672 mmol) equiv of ethylene at -10 °C for >3 half lives. The concentration of **2.02** was monitored by ¹H NMR spectroscopy was plotted versus time, and fit to an exponential decay using KaleidaGraph from which the k_{obs} was extracted. A linear increase

in the k_{obs} vs [ethylene] was observed which indicates a first-order dependence of the concentration of ethylene.

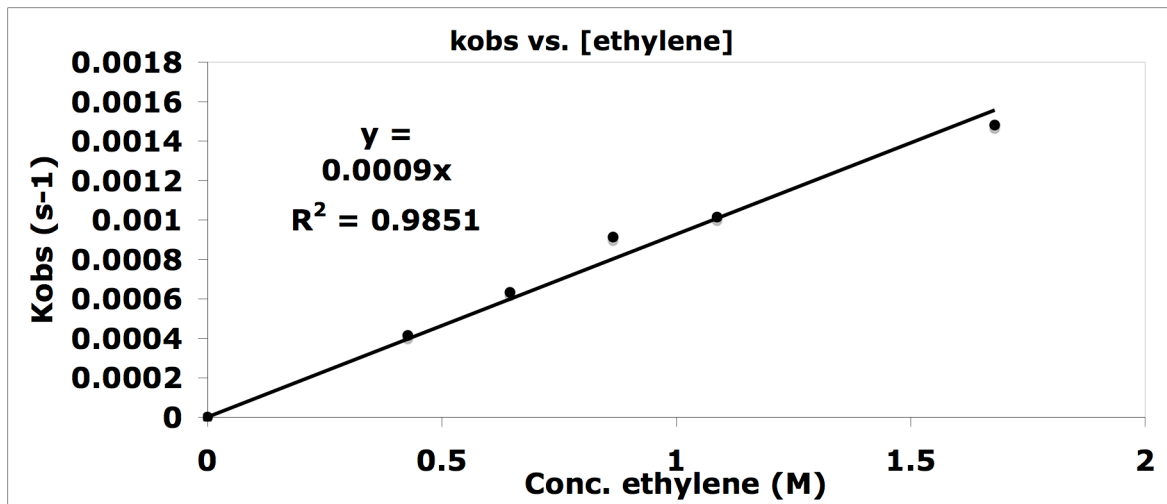


Figure 2.5. Plot of observed rate constant vs [ethylene] for the reaction of **2.02** and ethylene.

2.4.6 Determination of the Order in THF

To determine the order in THF we followed the general procedure for insertion of ethylene described above, but varied the concentration of added THF. Reactions with 10 (0.172 mmol), 12.5 (0.215 mmol), 15 (0.258 mmol), and 20 (0.344 mmol) equiv of THF were conducted at -10 °C for >3 half lives. The concentration of **2.02** was monitored by ¹H NMR spectroscopy, plotted versus time, and fit to an exponential decay using KaleidaGraph from which the k_{obs} was extracted. A linear increase of $1/k_{obs}$ vs [THF] was observed which indicates an inverse first-order dependence of the concentration of THF.

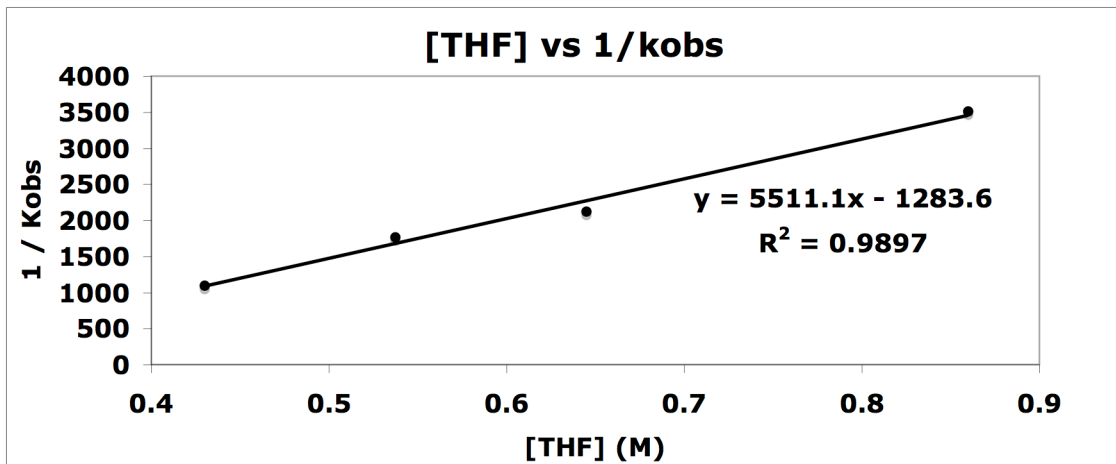


Figure 2.6. Plot of inverse rate constant vs [THF] for the reaction of **2.02** and ethylene

2.4.7 Reaction of *cis*-D₂-ethylene with **2.02**

A 0.010 g sample of **2.02** was dissolved into 0.4 mL of benzene-*d*₆ and added to a J-Young tube. The tube was attached to a high-vacuum line, frozen in a liquid N₂ bath, and the sample tube was evacuated. An attached 3.86 mL calibrated bulb was filled to a pressure of 830 torr of *cis*-D₂-ethylene (0.172 mmol) from a break-seal flask. The *cis*-D₂-ethylene was condensed into the J-Young tube and the reaction mixture was allowed to warm to room temperature. After 20 min the products were analyzed by ¹H NMR spectroscopy.

2.4.8 Reaction of **2.12** and Ethylene

Upon addition of 10 equiv of ethylene at -65 °C to **2.12** a new, broad ³¹P chemical shift was observed (Figure 2.6). We propose that this new resonance is that of the ethylene adduct **2.07**. The chemical shift of the new resonance assigned as **2.07** is directly related to the amount of ethylene added to **2.12**. Thus, in the presence of ethylene at -65 °C complex **2.12** is rapidly equilibrating with complex **2.07** as described in eq 2.4.

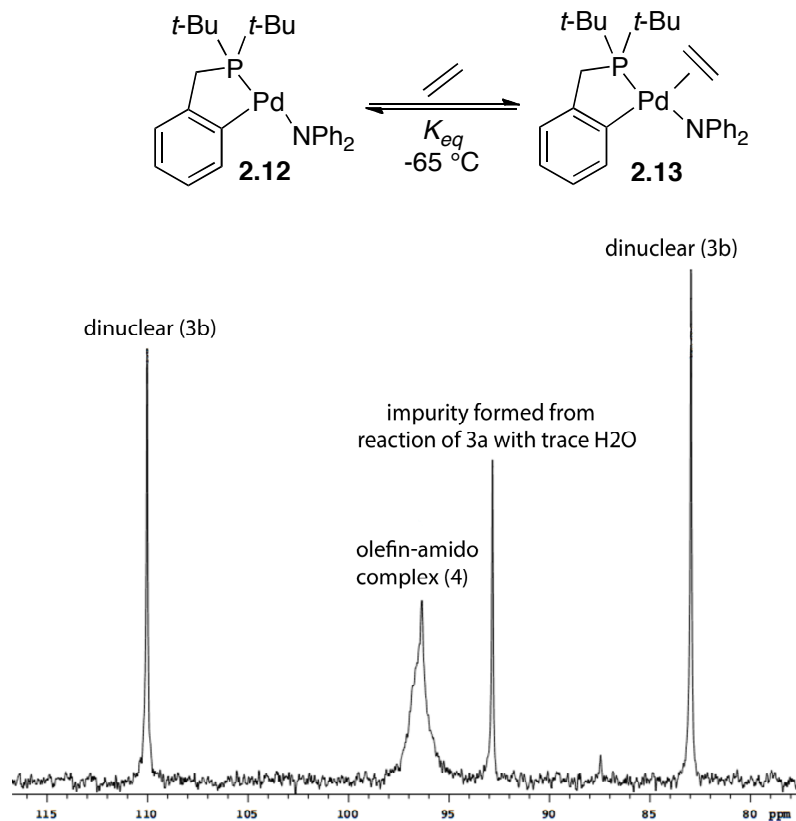


Figure 2.7. ${}^{31}\text{P}$ NMR spectrum of **2.12** and 1 equiv of ethylene at -65°C .

The observed chemical shift of **2.07** is therefore an average of the amount **2.12** and **2.07** present in solution and is described by eq 2.5. To determine the equilibrium constant for ethylene binding to **2.12**, we desired to derive an equation that related the observed chemical shift of **2.07** with the concentration of added ethylene. The concentration of **2.07** is related to the equilibrium constant by eq 2.6, and substituting eq 2.6 into eq 2.5 generates a new expression that relates the observed chemical shift of **2.07** to K_{eq} (eq 2.7). Dividing eq 2.7 by the observed chemical shift of **2.12** generates eq 2.8 from which we plotted the change in ${}^{31}\text{P}$ chemical shift of **(2.07)** vs the concentration of added ethylene at -65°C and calculated the equilibrium constant to be 11.0 M^{-1} and the chemical shift of **(2.07)** to be $\delta 86.8 \text{ ppm}$

$$\delta_{obs} = \frac{\delta_{2.12}[2.12] + \delta_{2.07}[2.07]}{[2.12] + [2.07]} \quad (2.5)$$

$$[2.07] = K_{eq}[2.12][ethylene] \quad (2.6)$$

$$\delta_{obs} = \frac{\delta_{2.11}[2.12] + K_{eq}\delta_{2.07}[2.12][ethylene]}{[2.12] + K_{eq}[2.12][ethylene]} \quad (2.7)$$

$$\delta_{obs} = \frac{\delta_{2.12} + K_{eq}\delta_{2.07}[ethylene]}{1 + K_{eq}[2.12][ethylene]} \quad (2.8)$$

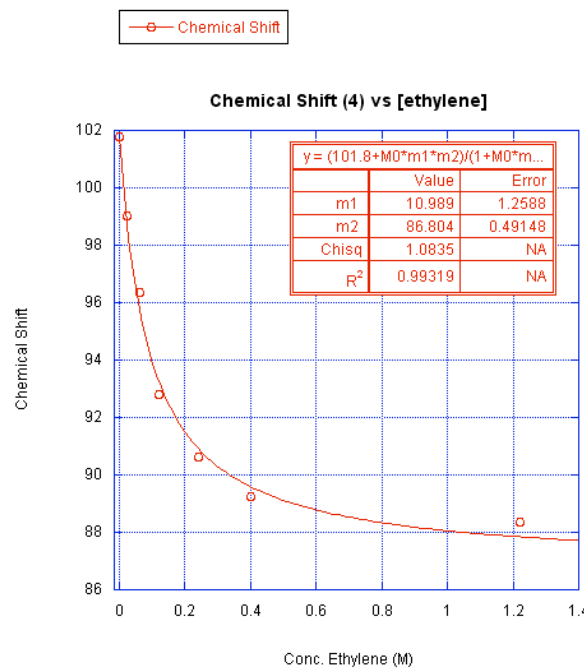


Figure 2.8. Plot of concentration of added ethylene to **2.12** vs observed chemical shift at -65 °C.

Upon addition of 1 equiv of ethylene to **2.12** at -100 °C a new resonance corresponding to **2.07** was identified in the ^{31}P NMR spectrum in addition to the resonance for **2.12**. At -100

°C, binding of ethylene to **2.12** is slower than the NMR timescale, thus resonances for both **2.12** and **2.07** are observed. The ^{31}P NMR spectrum is shown below in Figure 2.9.

Key:

δ 110.0 ppm - dimer (**2.13**)

δ 101.5 ppm - monomer (**2.12**)

δ 92.8 ppm - impurity formed from reaction of **2.12** and trace H_2O (independently identified by x-ray crystallography and NMR spectroscopy.)

δ 87.4 ppm - olefin-amido complex (**2.07**)

δ 83.0 ppm - dimer (**2.13**)

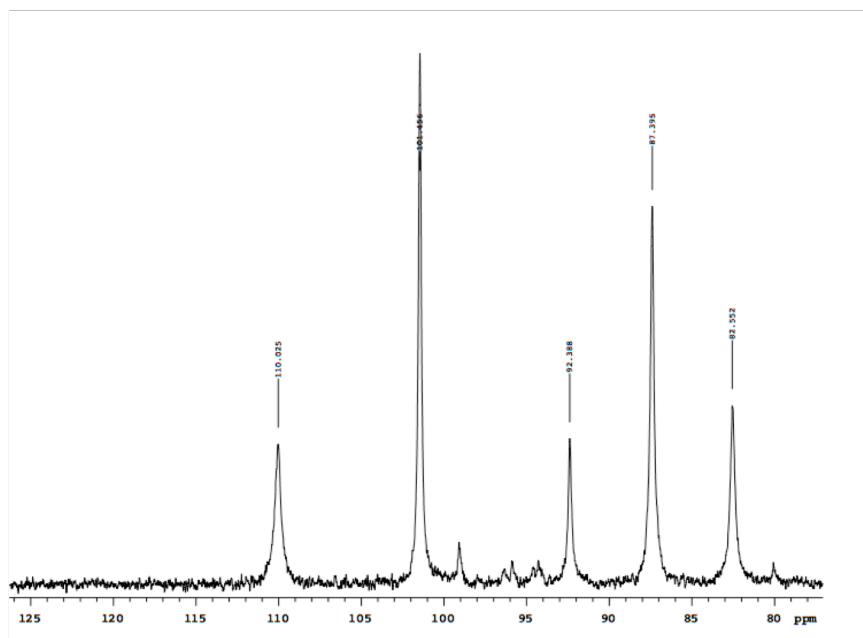
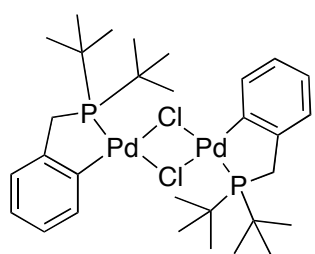


Figure 2.9. ^{31}P NMR spectrum of **2.12** and 1 equiv of ethylene at -100 °C

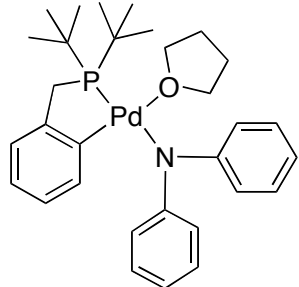
2.4.9 Preparation and Characterization of New Palladium Complexes and Enamine Products

Preparation of *syn/anti*- $[(P-C)PdCl]_2$ (2.01)



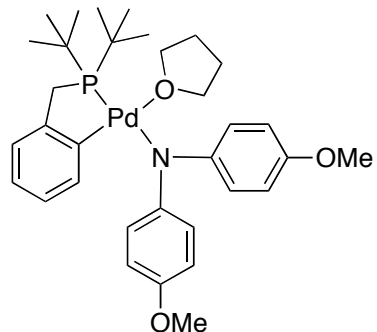
Pd(OAc)₂ (1.00 g, 0.445 mmol) and benzylditertbutylphosphine (1.05 g, 0.445 mmol) were added to a 50 mL round-bottom flask and dissolved in 20 mL of toluene. The reaction mixture was stirred at room temperature for 4 h. The volatile materials were evaporated under vacuum, and a solution of LiCl (1.88 g / 3.81 mmol) in 20 mL of anhydrous methanol was added to the brown residue and the reaction mixture was stirred vigorously for 1 h. A light grey precipitate was collected by filtration and washed with methanol (5 mL x 3) and pentane (5 mL x 3). The crude product was dissolved in a minimum amount of dichloromethane (10 mL) and filtered through a plug of Celite. The yellow solution was layered with pentane (30 mL) and cooled to -35 °C. After 24 h, 1.06 g (63% yield) of yellow crystals were collected by filtration, washed with pentane, and dried by vacuum. The product consisted of a 2:1 mixture of *anti:syn* diastereomers. ¹H NMR (CDCl₃, 500 MHz) δ 7.85-7.69 (m, 2H), 7.02-6.82 (m, 6H), 3.20 (d, *J* = 10.5 Hz, 4H), 1.45-1.35 (m, 36H). ¹³C{¹H} NMR (CDCl₃, 126 MHz) major diastereomer: δ 149.5, 148.5, (d, *J* = 16.6 Hz), 137.3, 124.9, 124.9, 123.2 (d, *J* = 22.6 Hz), 36.0, (d, *J* = 17.6 Hz), 33.7 (d, *J* = 29.4 Hz), 29.3; minor diastereomer: δ 149.2, 148.2 (d, *J* = 16.8 Hz), 136.8, 125.1, 125.0, 123.0 (d, *J* = 22.6 Hz), 35.8 (d, *J* = 17.6 Hz), 33.7 (d, *J* = 29.4 Hz), 29.3. ³¹P NMR (C₆D₆, 200 MHz, with integral *I*) δ 101.5 (s, *I* = 63%), 100.7 (s, *I* = 37%). Anal. Calcd. For C₃₀H₄₈Cl₂P₂Pd: C, 47.76; H, 6.41; found, C, 47.54; H, 6.62.

Preparation of (P-C)Pd(THF)NPh₂ (2.02)



To a 20 mL scintillation vial was added [(P-C)PdCl]₂ (0.177 g, 0.234 mmol) and KNPh₂ (0.0971 g, 0.468 mmol). The mixture was dissolved in 5 mL of THF and stirred for 3 h. The cloudy orange reaction mixture was filtered through a plug of Celite to remove KCl and trace Pd black. THF was slowly evaporated under vacuum until ~1 mL remained. Pentane (15 mL) was carefully layered on top of the THF, and the mixture was cooled at -35 °C. After 2 d, 0.212 g (78% yield) of orange crystals were collected by filtration and washed with a small amount of pentane. The isolated solid was dried under vacuum. ¹H NMR (C₆D₆, 500 MHz) δ 7.99 (d, *J* = 7.5 Hz, 1H), 7.36 (d, *J* = 7.0 Hz, 4H), 7.20 (t, *J* = 7.5 Hz, 4H), 6.94-6.93 (m, 2H), 6.81-6.78 (m, 3H), 3.55 (bs, 4H), 2.68 (d, *J* = 9.5 Hz, 2H), 1.35 (bs, 4H), 0.86 (d, *J* = 13.5 Hz, 18H). ¹³C{¹H} NMR (C₆D₆, 101 MHz) δ 151.8, 150.8, 149.3 (d, *J* = 14.8 Hz), 139.7, 131.8, 125.9, 125.2, 123.6 (d, *J* = 14.8 Hz), 119.8, 117.4, 68.5, 34.2 (d, *J* = 11.8 Hz), 32.8 (d, *J* = 22.2 Hz), 28.8 (d, 4.4 Hz), 25.7. ³¹P NMR (C₆D₆, 202 MHz) δ 98.7. Anal. Calcd. For C₃₁H₄₂NOPPd: C, 63.97; H, 7.27; N, 2.41; found, C, 63.73; H, 7.20; N, 2.39.

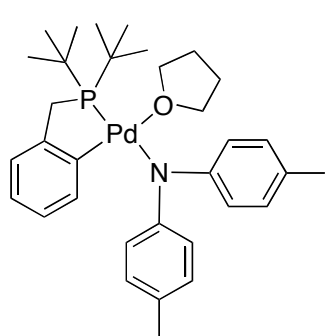
Preparation of (P-C)Pd(THF)N(p-OMe)₂ (2.03)



To a 20 mL scintillation vial was added [(P-C)PdCl]₂ (0.121 g, 0.160 mmol) and KN(p-OMe)₂ (0.0850 g, 0.320 mmol). The mixture was dissolved in 5 mL of THF and stirred for 3 h. The dark red reaction mixture was filtered through a plug of Celite to remove KCl and trace Pd black. THF was slowly evaporated under vacuum until only ~1 mL remained. Pentane (15 mL) was carefully added, and the

mixture cooled at 35 °C. After 2 d, red crystals were collected by filtration and washed with a small amount of pentane, and dried by vacuum. Yield 0.175 g, 85%. ^1H NMR (C_6D_6 , 500 MHz) δ 8.03 (d, $J = 8.0$ Hz, 1H), 7.18 (d, $J = 8.0$ Hz, 4H), 7.01 (d, $J = 7.0$ Hz, 1H), 6.97 (t, $J = 7.5$ Hz, 1H), 6.84 (t, $J = 7.5$ Hz, 1H), 6.81 (d, $J = 8.5$ Hz, 4H), 3.56 (bs, 4H), 3.34 (s, 6H), 2.73, (d, $J = 9.5$ Hz, 2H), 1.40 (bs, 4H), 0.87 (d, $J = 13.5$ Hz, 18H). $^{13}\text{C}\{\text{H}\}$ NMR (C_6D_6 , 101 MHz) δ 154.4, 153.2 (d, $J = 10.1$ Hz), 149.4, (d, $J = 17.2$ Hz), 145.0, 139.6, 125.7, 125.1, 123.6 (d, $J = 17.2$ Hz), 117.9, 117.2, 68.0, 55.0, 34.2 (d, $J = 15.2$ Hz), 33.2 (d, $J = 28.3$ Hz), 28.8 (d, $J = 4.0$ Hz), 25.7. ^{31}P NMR (C_6D_6 , 202 MHz) δ 97.3 Anal. Calcd. For $\text{C}_{33}\text{H}_{46}\text{NO}_3\text{PPd}$: C, 61.73; H, 7.22; N, 2.18; found C, 61.48; H, 7.46; N, 1.97.

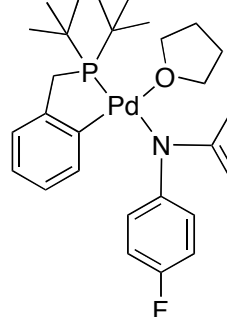
*Preparation of (P-C)Pd(THF)N(*p*-tol)₂ (2.04)*



To a 20 mL scintillation vial was added $[(\text{P-C})\text{PdCl}]_2$ (0.121 g, 0.160 mmol) and $\text{KN}(p\text{-tol})_2$ (0.0750g, 0.320 mmol). The mixture was dissolved in 5 mL THF and stirred for 3 h. The red reaction mixture was filtered through a plug of Celite to remove KCl and trace Pd black. THF was slowly evaporated under vacuum until only ~1 mL remained. Pentane (15 mL) was carefully added and the mixture cooled at -35 °C. After 2 d, 0.123 g, 63% of red crystals were collected by filtration and washed with a small amount of pentane. The isolated solid was dried by vacuum. Yield ^1H NMR (C_6D_6 , 400 MHz) δ 8.06 (d, $J = 7.2$ Hz, 1H), 7.21 (d, $J = 8.0$ Hz, 4H), 7.01 (d, $J = 8.0$ Hz, 4H), 7.02-6.82 (m, 2H), 6.82 (t, $J = 7.6$ Hz, 1H), 3.56 (bs, 4H), 2.70 (d, $J = 12$ Hz, 2H), 2.11 (s, 6H), 1.38 (bs, 4H), 0.84 (d, $J = 13.6$ Hz, 18H). $^{13}\text{C}\{\text{H}\}$ NMR (C_6D_6 , 101 MHz) δ 152.8 (d, $J = 8.4$ Hz), 149.3 (d, $J = 17.7$ Hz), 148.8, 139.7, 132.6, 129.0, 125.8, 125.1, 123.5 (d, $J = 18.3$ Hz), 116.8, 68.1, 33.9 (d, $J = 14.5$

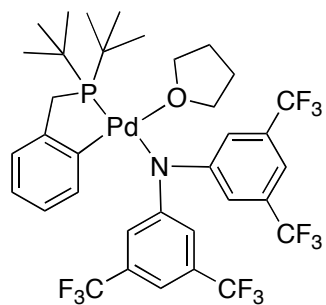
Hz), 33.2 (d, J = 28.3 Hz), 28.7 (d, J = 4.5 Hz), 25.7, 20.8. ^{31}P NMR (C_6D_6 , 162 MHz) δ 97.7. Anal. Calcd. For $\text{C}_{33}\text{H}_{46}\text{NOPPd}$: C, 64.96; H, 7.60; N, 2.30; found C, 64.71; H, 7.82; N, 2.65.

Preparation of (P-C)Pd(THF)N(p-F)₂ (2.05)



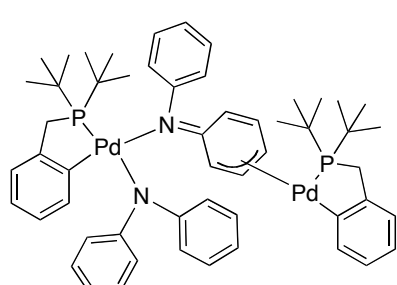
To a 20 mL scintillation vial was added $[(\text{P-C})\text{PdCl}]_2$ (0.181 g, 0.240 mmol) and $\text{KN}(p\text{-F})_2$ (0.116 g, 0.477 mmol). The mixture was dissolved in 5 mL THF and stirred for 3 h. The orange reaction mixture was filtered through a plug of Celite to remove KCl and trace Pd black. THF was slowly evaporated under vacuum until only ~1 mL remained. Pentane (15 mL) was carefully added and the mixture cooled at 35 °C. After 2 d, (0.223 g (76% yield) of orange crystals were collected by filtration and washed with a small amount of pentane. ^1H NMR (C_6D_6 , 500 MHz) δ 7.84 (d, J = 8.0 Hz, 1H), 7.21-7.18 (m, 4H), 6.93-6.85 (m, 6H), 6.81-6.78 (m, 1H), 3.51 (bs, 4H), 2.64 (d, J = 9.5 Hz, 2H), 1.31 (bs, 4H), 0.85 (d, J = 13.5 Hz, 18H). $^{13}\text{C}\{\text{H}\}$ NMR (C_6D_6 , 126 MHz) δ 160.0, 157.3 (d, J = 239 Hz), 149.3, 149.2 (d, J = 17.6 Hz), 139.4, 126.1, 125.4, 123.8, (d, J = 18.5 Hz), 118.7, 117.5, (d, J = 21.7 Hz), 68.6, 34.1, (d, J = 15.8 Hz), 32.4, (d, J = 27.5 Hz), 28.8 (d, J = 4.9 Hz), 25.7. ^{31}P NMR (C_6D_6 , 202 MHz) δ 96.1. ^{19}F NMR (C_6D_6 , 470 MHz) δ -126.7. Anal. Calcd. For $\text{C}_{31}\text{H}_{40}\text{NOF}_2\text{PPd}$: C, 60.24; H, 6.52; N, 2.27; found, C, 59.96; H, 6.42; N, 2.25.

Preparation of (P-C)Pd(THF)N(3,5-CF₃C₆H₃)₂ (2.06)



To a 20 mL vial was added HN(3,5-CF₃C₆H₃)₂ (0.175 g, 0.397 mmol) and (P-C)Pd(THF)NPh₂ (0.080 g, 0.137 mmol), and these solids were dissolved in 3 mL THF. The reaction mixture was stirred for 1 h, over which time its color changed from orange to yellow. The reaction mixture was filtered through Celite, and the THF was evaporated under vacuum. Pentane (15 mL) was added, and the resulting yellow precipitate was collected by filtration. The solid was washed with pentane (3 x 5 mL) and dried under vacuum. Yield: 0.085 g, 65%. ¹H NMR (C₆D₆, 500 MHz) δ 8.26 (s, 4H), 7.40 (d, *J* = 7.5 Hz, 1H), 7.21 (s, 2H), 6.77-6.71 (m, 2H), 6.64 (t, *J* = 7.5 Hz, 1H) 3.25 (bs, 4H), 2.59 (d, *J* = 9.5 Hz 2H), 0.94 (bs, 4H), 0.93 (d, *J* = 13.5 Hz, 18H). ¹³C{¹H} NMR (C₆D₆, 126 MHz) δ 155.1, 148.6 (d, *J* = 17.5 Hz), 141.9, 138.6, 132.5 (q, *J* = 32.3 Hz), 127.0, 125.9, 124.7 (q, *J* = 274.2 Hz), 124.0 (d, *J* = 21.2 Hz), 119.8, 109.7, 71.6, 34.4 (d, *J* = 16.6 Hz), 31.6 (d, *J* = 28.6 Hz), 28.7 (d, *J* = 3.8 Hz), 25.1. ³¹P NMR (C₆D₆, 202 MHz) δ 92.0. ¹⁹F NMR (C₆D₆, 376 MHz) δ -63.4. Anal. Calcd. For C₃₃H₄₆F₆NOPPd: C, 49.22; H, 4.48; N, 1.64; found C, 49.13; H, 4.53; N, 1.68.

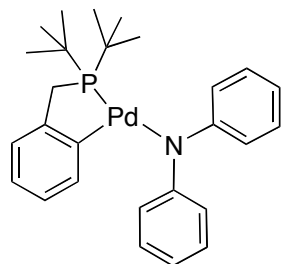
Preparation of (P-C)PdNPh₂ (2.12/2.13)



[(P-C)PdCl]₂ (0.121 g, 0.160 mmol) and KNPh₂ (0.0665 g, 0.320 mmol) were added to a 20 mL scintillation vial and dissolved in 5 mL of benzene. The reaction mixture was stirred at room temperature for 2.5 h, over which time it turned dark red. The mixture was filtered through Celite, and the benzene was evaporated under vacuum until 2 mL of the red solution remained. Pentane (15 mL) was

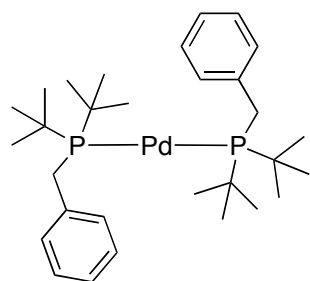
added, leading to the precipitation of a yellow solid, which was removed by filtration through Celite. The resulting dark red solution was cooled at -35 °C. The red crystalline product was collected by filtration and washed with a small amount of pentane (5 mL). Yield: 0.108 g, 66%. ^{31}P NMR ($\text{C}_6\text{D}_5\text{CD}_3$, 202 MHz) δ 110.0 (s), 82.9 (s). ^1H NMR -65 °C (C_6D_6 , 400 MHz, selected distinguishing resonances) δ 6.20 (bs, 1H), 6.09 (bs, 1H), 5.66 (bs, 2H), 4.28 (bs, 1H), bridging phenyl ring; 3.33 (dd, J = 15.5, 5.0 Hz, 1H), 2.86 (dd, J = 17.0, 8.0 Hz, 1H), 2.65 (dd, J = 15.5, 12.0 Hz, 1H), 2.51 (dd, J = 11.0, 11.0 Hz, 1H), benzylic protons; 0.70 (apparent d, J = 12.4 Hz, 36 H), *t*-Bu groups.

*At room temperature in solution, dimer **2.13** is a stable three-coordination Pd-amido complex (2.12)*



^1H NMR 20 °C (C_6D_6 , 500 MHz) δ 8.00 (d, J = 7.5 Hz, 1H), 7.19 (bs, 8H) 6.98-6.94 (m, 2H), 6.84-6.77 (m, 3H), 2.69 (d, J = 9.5 Hz, 2H), 0.81 (d, J = 13.5 Hz, 18H) $^{13}\text{C}\{\text{H}\}$ NMR (C_6D_6 , 126 MHz) δ 152.3, 150.9, 149.4 (d, J = 17.6 Hz), 139.5, 132.3, 125.7, 125.3, 123.7 (d, J = 17.6 Hz), 120.6, 116.6, 34.3 (d, J = 14.7 Hz), 33.1, (d, J = 24.6 Hz), 28.7 (d, J = 4.9 Hz). ^{31}P NMR (C_6D_6 , 202 MHz) δ 101.8. Anal. Calcd. For $\text{C}_{54}\text{H}_{68}\text{N}_2\text{P}_2\text{Pd}$: C, 63.59; H, 6.72; N, 2.75; found, C, 63.42; H, 7.01, N, 2.47.

*Preparation of Pd[P(Bn)(*t*-Bu)₂]₂ (2.10)*



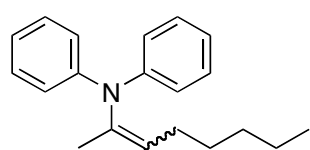
CpPd(allyl) (0.0521 g, 0.245 mmol) and P(Bn)(*t*-Bu)₂ (0.133 g, 0.561 mmol) were added to a 20 mL scintillation vial and dissolved in 5 mL of toluene. The vial was sealed with a Teflon-lined cap. The reaction mixture was heated at 70 °C and stirred for 2.5 h, over which time the

color changed from red to yellow. The reaction mixture was cooled to room temperature and filtered through Celite. The toluene was evaporated in vacuo, leaving a yellow solid. The solid was dissolved in 1 mL of pentane, and the resulting solution was cooled at -35 °C. A white solid was collected by filtration. Yield 0.135 g, 95%. ^1H NMR (C_6D_6 , 500 MHz) δ 8.13 (d, J = 7.5 Hz, 4H), 7.20 (t, J = 7.5 Hz, 4H), 7.09 (t, J = 7.5 Hz, 2H), 2.91 (bs, 4H), 1.29, (t, J = 7.5 Hz, 36H). $^{13}\text{C}\{\text{H}\}$ NMR (C_6D_6 , 126 MHz) δ 140.1, 131.6 (t, J = 4.8 Hz), 127.9, 125.9, 34.6 (t, J = 2.9 Hz), 30.7(t, J = 4.9 Hz), 30.0. ^{31}P NMR (C_6D_6 , 200 MHz) δ 60.1. Anal. Calcd. For $\text{C}_{30}\text{H}_{50}\text{NP}_2\text{Pd}$: C, 62.22; H, 8.70; found, C, 62.28; H, 8.64.

General Procedure for Preparation of Octene Enamine Derivatives

A procedure described by Barluenga⁴⁷ was used to prepare the enamine products using either $\text{Pd}(\text{OAc})_2$ and BINAP or $\text{Pd}_2(\text{dba})_3$ and Xantphos as catalyst. A 50 mL glass reaction vessel attached to a vacuum valve was charged with 0.517 g (2.62 mmol) $\text{HN}(\text{p-tol})_2$, 0.510 g (2.67 mmol) 2-bromo-1-octene, 0.120 g (0.131 mmol) $\text{Pd}_2(\text{dba})_3$, 0.152 g (0.262 mmol) Xantphos or 0.29 g (0.131 mmol) $\text{Pd}(\text{OAc})_2$ and 0.163g (0.262 mmol) BINAP, and 0.352 g (3.67 mmol) NaOtBu . All of the reagents were dissolved in 15 mL of toluene. The reaction mixture was heated at 90 °C for 18 h. The reaction mixture was cooled to room temperature and filtered through Celite (in air). The solvent of the resulting solution was evaporated under vacuum. The enamine product was purified by Kugelrohr distillation.

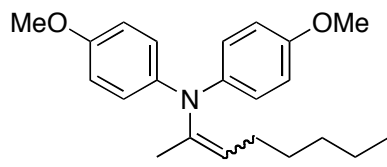
N,N-bis(phenyl)-oct-2-en-2-amine



Prepared according to general procedure using 1.0 g (5.3 mmol) 2-bromo-1-octene, 0.90 g (5.3 mmol) diphenylamine, 0.013 g (0.058

mmol) Pd(OAc)₂, 0.037 g (0.058 mmol) BINAP, and 0.71 g (7.4 mmol) NaOtBu. The product was purified by Kugelrohr distillation (110 °C, 20 mtorr) to give 0.580 g (37% yield) of the product as a mixture of diastereomers; 82% major, 18% minor, and trace terminal enamine. ¹H NMR (C₆D₆, 500 MHz) (major and minor diastereomers) δ 7.12-7.07 (m, 8H), 6.84-6.81 (m, 2H), 5.31 (t, *J* = 7.5 Hz, 0.82H), 5.14 (t, *J* = 7.5 Hz, 0.18H), 1.95 (q, *J* = 7.0 Hz, 1.6H), 1.88 (q, *J* = 7.0 Hz, 0.36H), 1.77 (s, 0.54H), 1.76 (s, 2.5H), 1.25-1.14 (m, 6H), 0.87 (t, *J* = 6.0 Hz, 2.5H), 0.80 (t, *J* = 6.5 Hz, 0.54H). ¹³C{¹H} NMR (C₆D₆, 126 MHz) major diastereomer: δ 147.9, 140.6, 129.3, 125.7, 123.2, 121.9, 31.9, 29.4, 28.9, 22.9, 16.2, 14.3. minor diastereomers: δ 146.5, 143.5, 129.4, 125.0, 121.5, 121.3, 32.0, 28.8, 28.0, 22.8, 20.8, 14.2. Anal. Calcd. For C₂₀H₂₅N: C, 85.97; H, 9.02; N, 5.01; found, C, 86.15; H, 9.30; N, 5.11.

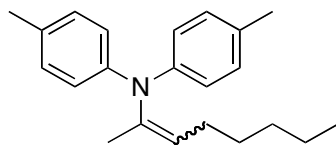
N,N-bis(4-methoxyphenyl)-oct-2-en-2-amine



Prepared according to general procedure using 0.61 g (3.3 mmol) 2-bromo-1-octene, 0.73 g (5.2 mmol), 4,4'-di(4-methoxy)diphenylamine, 0.010 g (0.045 mmol) Pd(OAc)₂, 0.020 g (0.032 mmol) BINAP, and 0.43 g (4.5 mmol) NaOtBu. The product was purified by Kugelrohr distillation (122 °C, 20 mtorr) to give 0.263 g (24% yield) of a mixture of diastereomers (56% major, 44% minor, and trace terminal enamine). ¹H NMR (C₆D₆, 500 MHz) (major and minor diastereomers) δ 7.06-7.01 (m, 4H), 6.76-6.70 (m, 4H), 5.18 (t, *J* = 7.5 Hz, 0.56H), 5.09 (t, 6.5 Hz, 0.44H), 3.55 (s, 3.4H), 3.34 (s, 2.6H), 2.03 (q, *J* = 6.5 Hz, 0.88H), 1.96 (q, *J* = 7.0 Hz, 1.1H), 1.85 (s, 1.3H), 1.83 (s, 1.7H), 1.31-1.12 (m, 6H), 0.87 (t, *J* = 7.0 Hz, 1.3H), 0.81 (t, *J* = 7.0 Hz, 1.7H). ¹³C{¹H} NMR (C₆D₆, 126 MHz) major diastereomer: δ 154.8, 140.8, 138.7, 125.0, 122.6, 114.8, 55.0, 32.0, 29.1, 28.1, 22.8, 21.0, 14.2. minor diastereomer: δ 155.5, 142.0, 141.6, 125.3,

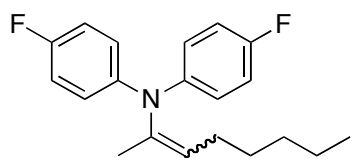
120.8, 114.7, 54.9, 31.9, 29.9, 28.2, 22.9, 16.5, 14.3. Anal. Calcd. For C₂₂H₂₉NO₂: C, 77.84; H, 8.61; N, 4.13; found, C, 78.12; H, 8.88; N, 3.98.

N,N-bis(4-tolylphenyl)-oct-2-en-2-amine



Prepared according to general procedure using 0.52 g (2.6 mmol) HN(p-tol)₂, 0.51 g (2.7 mmol) 2-bromo-1-octene, 0.12 g (0.13 mmol) Pd₂(dba)₃, 0.15 g (0.26 mmol) Xantphos, and 0.35 g (3.7 mmol) NaOtBu.. The product was purified by Kugelrohr distillation (120 °C, 20 mtorr) to give 0.297 g, (37% yield) of a mixture of diastereomers (53% major, 47% minor, and trace terminal enamine). ¹H NMR (C₆D₆, 500 MHz) (major and minor diastereomers) δ 7.08 (d, *J* = 8.0 Hz, 4H), 6.94 (d, *J* = 8.0 Hz, 4H), 5.3 (t, *J* = 7.0 Hz, 0.47H), 5.14 (t, *J* = 7.0 Hz, 0.53H), 2.13 (s, 3.2H), 2.12 (s, 2.8), 2.00 (q, *J* = 7.0 Hz, 0.94H) 1.94 (q, *J* = 7.0 Hz, 1.1H), 1.83 (s, 6H), 1.27-1.11 (m, 6H), 0.88 (t, *J* = 7.0 Hz, 1.4H), 0.80 (t, *J* = 7.0 Hz, 1.6H). ¹³C{¹H} NMR (C₆D₆, 126 MHz) major diastereomer: δ 144.5, 138.5, 130.8, 129.9, 126.2, 121.4, 31.9, 28.9, 28.1, 22.8, 20.9, 20.7, 14.2. minor diastereomer: δ 145.9, 141.1, 131.0, 130.0, 123.7, 123.6, 31.9, 29.7, 28.2, 22.9, 20.8, 16.3, 14.3. Anal. Calcd. For C₂₂H₂₉N: C, 85.94; H, 9.51; N, 4.56; found, C, 85.86; H, 9.23; N, 4.49.

N,N-bis(4-fluorophenyl)-oct-2-en-2-amine



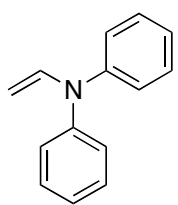
Prepared according to general procedure using 0.52 g (2.6 mmol) 2-bromo-1-octene, 0.56 g (2.6 mmol), 4,4'-di(4-fluoro)diphenylamine, 0.018 g (0.080 mmol) Pd(OAc)₂, 0.048 g (0.077 mmol) BINAP, and 0.35 g (3.7 mmol) NaOtBu. The product was purified by Kugelrohr

distillation (120 °C, 20 mtorr) to give 0.128 g (15% yield) of a mixture of diastereomers (68% major, 32 minor, and trace terminal enamine). ^1H NMR (C_6D_6 , 500 MHz) (major and minor diastereomers) δ 6.78-6.71 (m, 8H), 5.11 (t, J = 7.5 Hz, 0.68H), 5.02 (t, J = 6.5 Hz, 0.32H), 1.92 (q, 7.5 Hz, 1.4H), 1.78 (q, J = 7.0 Hz, 0.64H), 1.65 (s, 2.0H), 1.64 (s, 0.96H), 1.28-1.08 (m, 6H), 0.87 (t, J = 7.0 Hz, 2.0H), 0.82 (t, J = 7.0 Hz, 0.96H). $^{13}\text{C}\{\text{H}\}$ NMR (C_6D_6 , 126 MHz) major diastereomer: δ 158.6 (d, J = 242 Hz), 144.1, 140.8, 124.7 (d, J = 7.4 Hz), 124.1, 115.9 (d, J = 22.2 Hz), 31.8, 29.5, 28.1, 22.9, 16.0, 14.3. minor diastereomer: δ 158.2 (d, 242 Hz), 142.8, 138.1, 126.6, 122.4 (d, J = 8.3 Hz), 116.0 (d, J = 22.2 Hz), 31.9, 28.3, 27.9, 22.8, 20.5, 14.2. Anal. Calcd. For $\text{C}_{20}\text{H}_{23}\text{NF}_2$: C, 76.16; H, 7.35; N, 4.44; found, C, 76.40; H, 7.54; N, 4.50.

Preparation of N-Vinyldiarylamines

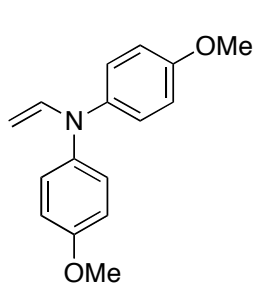
A 4 dram vial was charged with HNPh_2 (0.086 g, 0.500 mmol), $\text{Pd}_2(\text{dba})_3$ (0.0229 g, 0.025 mmol), Xantphos (0.028 g, 0.0500 mmol), and NaOtBu (0.0673 g, 0.700 mmol). These solids were dissolved in 2 mL of toluene. Vinyl bromide (0.50 mL of a 1M solution in THF, 0.50 mmol) was added via syringe and the vial was capped with a PTFE/silicone-lined septa. The reaction mixture was heated to 90 °C for 16 h. The reaction mixture was taken into the glove box, filtered through Celite, and the volatile materials were evaporated under vacuum. A 15 mL sample of pentane was added to the dark residue, and the mixture was stirred for 1 h and filtered through Celite. The pentane was evaporated under vacuum, and the ratio of enamine product to unreacted starting material was determined by NMR analysis.

N-vinyldiphenylamine



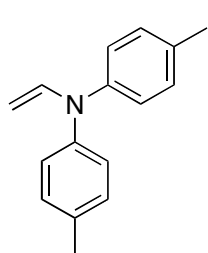
¹H NMR (C₆D₆, 500 MHz) δ 7.05 (t, *J* = 7.5 Hz, 4H), 6.95 (d, *J* = 8.5 Hz, 4H), 6.85 (t, *J* = 7.5 Hz, 2H), 6.77 (dd, *J* = 15.0, 8.5 Hz, 1H), 4.21 (d, *J* = 15.0 Hz, 1H), 4.16, (d, *J* = 8.5 Hz, 1H). Ratio: 79:21.

*N-vinyldi(4,4'-*p*-methoxydiphenyl)amine*



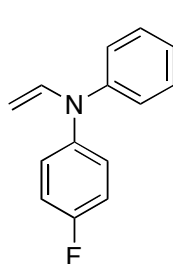
¹H NMR (C₆D₆, 500 MHz) δ 6.96 (d, *J* = 9.0 Hz, 4H), 6.84 (dd, *J* = 15.5, 9.0 Hz, 1H), 6.72 (d, *J* = 9.0 Hz, 4H), 4.24 (d, *J* = 15.0 Hz, 1H), 4.17 (d, *J* = 8.5 Hz, 1H), 3.28 (s, 6H). Ratio: 27:23.

*N-vinyldi(4,4'-*p*-tolyldiphenyl)amine*



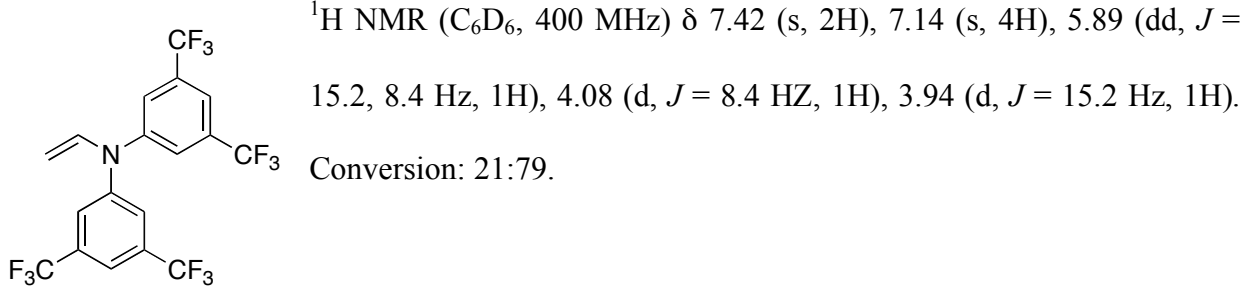
¹H NMR (C₆D₆, 500 MHz) δ 6.96 (d, *J* = 9.0 Hz, 4H), 6.90 (d, *J* = 8.5 Hz, 4H), 6.85 (dd, *J* = 15.0, 9.0 Hz, 1H), 4.27 (d, *J* = 15.5 Hz, 1H), 4.18 (d, *J* = 8.5 Hz, 1H), 2.07 (s, 6H). Ratio: 14:11.

*N-vinyldi(4,4'-*p*-fluorodiphenyl)amine*

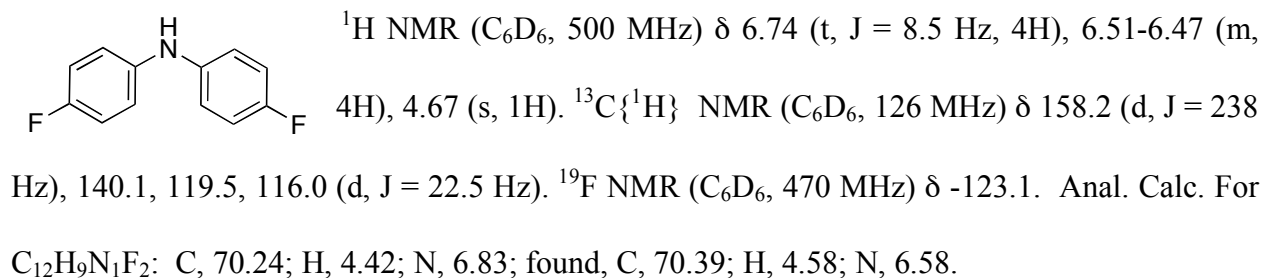


¹H NMR (C₆D₆, 500 MHz) δ 6.70 (t, *J* = 8.5 Hz, 4H), 6.64-6.58 (m, 4H), 6.51 (dd, *J* = 15.5, 9.0 Hz, 1H), 4.10 (d, *J* = 9 Hz, 1H), 4.03 (d, *J* = 15.5 Hz, 1H).
¹⁹F NMR (C₆D₆, 470 MHz) δ -119.5. Ratio: 7:3.

N-vinyldi(3,5-trifluoromethyl diphenyl)amine



Characterization of HN(4-FC₆H₄)₂



2.4.10 X-Ray Crystallographic Analysis of **2.02** and **2.13**

Table 2.2. Crystal data and structure refinement for (P-C)Pd(THF)NPh₂ (**2.02**).

Empirical formula	C ₃₁ H ₄₂ N O P Pd		
Formula weight	582.03		
Temperature	193(2) K		
Wavelength	0.71073 Å		
Crystal system	Orthorhombic		
Space group	P n a 21		
Unit cell dimensions	a = 16.0764(8) Å	b = 20.7006(10) Å	c = 8.5956(4) Å a = 90°. b = 90°. g = 90°.
Volume	2860.5(2) Å ³		
Z	4		
Density (calculated)	1.351 Mg/m ³		
Absorption coefficient	0.728 mm ⁻¹		
F(000)	1216		
Crystal size	0.30 x 0.12 x 0.08 mm ³		
Theta range for data collection	1.60 to 25.36°.		
Index ranges	-16<=h<=19, -24<=k<=21, -7<=l<=10		
Reflections collected	14036		
Independent reflections	4818 [R(int) = 0.0527]		
Completeness to theta = 25.36°	100.0 %		
Absorption correction	Integration		
Max. and min. transmission	0.9588 and 0.9197		
Refinement method	Full-matrix least-squares on F ²		
Data / restraints / parameters	4818 / 1 / 322		
Goodness-of-fit on F ²	1.000		
Final R indices [I>2sigma(I)]	R1 = 0.0380, wR2 = 0.0683		
R indices (all data)	R1 = 0.0606, wR2 = 0.0759		
Absolute structure parameter	-0.05(3)		
Largest diff. peak and hole	0.529 and -0.428 e.Å ⁻³		

Table 2.3. Atomic coordinates ($\times 10^4$) and equivalent isotropic displacement parameters ($\text{\AA}^2 \times 10^3$) for **2.02**. $U(\text{eq})$ is defined as one third of the trace of the orthogonalized U^{ij} tensor.

	x	y	z	$U(\text{eq})$
C(1)	6611(3)	2829(3)	1367(6)	27(1)
C(2)	6777(3)	3395(3)	515(6)	32(1)
C(3)	7274(4)	3383(3)	-798(6)	38(2)
C(4)	7627(4)	2818(3)	-1294(5)	39(2)
C(5)	7471(3)	2260(2)	-485(6)	34(1)
C(6)	6974(3)	2260(2)	829(6)	31(1)
C(7)	6791(4)	1633(3)	1691(7)	40(2)
C(8)	4956(4)	1507(3)	1644(6)	34(1)
C(9)	4162(3)	1817(3)	2299(7)	42(2)
C(10)	4833(4)	779(3)	1534(7)	58(2)
C(11)	5084(4)	1778(3)	10(7)	55(2)
C(12)	6019(4)	1257(2)	4634(6)	36(1)
C(13)	6670(4)	1616(3)	5594(7)	52(2)
C(14)	5219(4)	1200(3)	5580(7)	46(2)
C(15)	6350(4)	578(2)	4260(7)	54(2)
C(16)	6631(3)	4171(2)	3870(5)	26(1)
C(17)	7226(3)	3871(2)	4815(6)	30(1)
C(18)	7952(4)	4167(3)	5230(6)	42(2)
C(19)	8137(4)	4777(3)	4692(7)	47(2)
C(20)	7592(4)	5081(3)	3742(6)	50(2)
C(21)	6837(3)	4793(2)	3308(8)	36(1)
C(22)	5199(3)	4183(2)	3068(7)	26(1)
C(23)	4933(3)	4745(2)	3836(6)	32(1)
C(24)	4177(4)	5027(2)	3478(9)	35(1)
C(25)	3656(4)	4769(3)	2367(7)	41(2)
C(26)	3899(4)	4214(3)	1610(6)	40(2)
C(27)	4651(3)	3928(3)	1954(6)	35(1)
C(28)	4169(3)	3016(3)	5265(6)	46(2)
C(29)	3993(4)	3541(3)	6450(6)	49(2)
C(30)	4615(4)	3398(3)	7686(6)	49(2)
C(31)	5380(4)	3211(3)	6737(6)	49(2)
N(1)	5916(3)	3849(2)	3461(7)	26(1)
O(1)	5053(2)	2868(2)	5382(4)	29(1)
P(1)	5861(1)	1773(1)	2859(1)	28(1)
Pd(1)	5874(1)	2848(1)	3243(1)	23(1)

Table 2.4. Bond lengths [\AA] and angles [$^\circ$] for (P-C)Pd(THF)NPh₂ (**2.02**).

C(1)-C(6)	1.394(7)	C(10)-H(10B)	0.9800
C(1)-C(2)	1.408(7)	C(10)-H(10C)	0.9800
C(1)-Pd(1)	2.001(5)	C(11)-H(11A)	0.9800
C(2)-C(3)	1.383(7)	C(11)-H(11B)	0.9800
C(2)-H(2)	0.9500	C(11)-H(11C)	0.9800
C(3)-C(4)	1.369(7)	C(12)-C(13)	1.525(8)
C(3)-H(3)	0.9500	C(12)-C(14)	1.527(7)
C(4)-C(5)	1.370(6)	C(12)-C(15)	1.537(7)
C(4)-H(4)	0.9500	C(12)-P(1)	1.879(5)
C(5)-C(6)	1.384(7)	C(13)-H(13A)	0.9800
C(5)-H(5)	0.9500	C(13)-H(13B)	0.9800
C(6)-C(7)	1.523(7)	C(13)-H(13C)	0.9800
C(7)-P(1)	1.823(6)	C(14)-H(14A)	0.9800
C(7)-H(7A)	0.9900	C(14)-H(14B)	0.9800
C(7)-H(7B)	0.9900	C(14)-H(14C)	0.9800
C(8)-C(10)	1.523(7)	C(15)-H(15A)	0.9800
C(8)-C(11)	1.527(8)	C(15)-H(15B)	0.9800
C(8)-C(9)	1.535(8)	C(15)-H(15C)	0.9800
C(8)-P(1)	1.875(6)	C(16)-N(1)	1.376(6)
C(9)-H(9A)	0.9800	C(16)-C(17)	1.399(7)
C(9)-H(9B)	0.9800	C(16)-C(21)	1.416(6)
C(9)-H(9C)	0.9800	C(17)-C(18)	1.366(7)
C(20)-C(21)	1.402(7)	C(10)-H(10A)	0.9800
C(20)-H(20A)	0.9500	C(17)-H(17A)	0.9500
C(21)-H(21A)	0.9500	C(18)-C(19)	1.377(7)
C(22)-N(1)	1.386(6)	C(18)-H(18A)	0.9500
C(22)-C(27)	1.404(7)	C(19)-C(20)	1.353(8)
C(22)-C(23)	1.405(6)	C(19)-H(19A)	0.9500
C(23)-C(24)	1.384(7)	C(28)-H(28A)	0.9900
C(23)-H(23A)	0.9500	C(28)-H(28B)	0.9900
C(24)-C(25)	1.377(8)	C(29)-C(30)	1.489(8)
C(24)-H(24A)	0.9500	C(29)-H(29A)	0.9900
C(25)-C(26)	1.378(7)	C(29)-H(29B)	0.9900
C(25)-H(25A)	0.9500	C(30)-C(31)	1.526(8)
C(26)-C(27)	1.378(7)	C(30)-H(30A)	0.9900
C(26)-H(26A)	0.9500	C(30)-H(30B)	0.9900
C(27)-H(27A)	0.9500	C(31)-O(1)	1.461(6)
C(28)-O(1)	1.458(6)	C(31)-H(31A)	0.9900
C(28)-C(29)	1.517(7)	C(31)-H(31B)	0.9900
O(1)-Pd(1)	2.264(3)	N(1)-Pd(1)	2.082(3)
P(1)-Pd(1)	2.2494(13)		
C(6)-C(1)-C(2)	116.9(5)	H(7A)-C(7)-H(7B)	108.6
C(6)-C(1)-Pd(1)	122.1(4)	C(10)-C(8)-C(11)	108.9(5)
C(2)-C(1)-Pd(1)	121.0(4)	C(10)-C(8)-C(9)	109.3(5)
C(3)-C(2)-C(1)	121.3(5)	C(11)-C(8)-C(9)	107.2(5)
C(3)-C(2)-H(2)	119.4	C(10)-C(8)-P(1)	115.2(4)
C(1)-C(2)-H(2)	119.4	C(11)-C(8)-P(1)	107.4(4)
C(4)-C(3)-C(2)	120.5(5)	C(9)-C(8)-P(1)	108.6(4)
C(4)-C(3)-H(3)	119.7	C(8)-C(9)-H(9A)	109.5
C(2)-C(3)-H(3)	119.7	C(8)-C(9)-H(9B)	109.5
C(3)-C(4)-C(5)	119.2(5)	H(9A)-C(9)-H(9B)	109.5

Table 2.4 (cont.)

C(3)-C(4)-H(4)	120.4	C(8)-C(9)-H(9C)	109.5
C(5)-C(4)-H(4)	120.4	H(9A)-C(9)-H(9C)	109.5
C(4)-C(5)-C(6)	121.3(5)	H(9B)-C(9)-H(9C)	109.5
C(4)-C(5)-H(5)	119.3	C(8)-C(10)-H(10A)	109.5
C(6)-C(5)-H(5)	119.3	C(8)-C(10)-H(10B)	109.5
C(5)-C(6)-C(1)	120.8(5)	H(10A)-C(10)-H(10B)	109.5
C(5)-C(6)-C(7)	120.6(5)	C(8)-C(10)-H(10C)	109.5
C(1)-C(6)-C(7)	118.5(5)	H(10A)-C(10)-H(10C)	109.5
C(6)-C(7)-P(1)	106.9(4)	H(10B)-C(10)-H(10C)	109.5
C(6)-C(7)-H(7A)	110.3	C(8)-C(11)-H(11A)	109.5
P(1)-C(7)-H(7A)	110.3	C(8)-C(11)-H(11B)	109.5
C(6)-C(7)-H(7B)	110.3	H(11A)-C(11)-H(11B)	109.5
P(1)-C(7)-H(7B)	110.3	C(12)-C(15)-H(15B)	109.5
C(8)-C(11)-H(11C)	109.5	H(15A)-C(15)-H(15B)	109.5
H(11A)-C(11)-H(11C)	109.5	C(12)-C(15)-H(15C)	109.5
H(11B)-C(11)-H(11C)	109.5	H(15A)-C(15)-H(15C)	109.5
C(13)-C(12)-C(14)	109.1(5)	H(15B)-C(15)-H(15C)	109.5
C(13)-C(12)-C(15)	108.7(5)	N(1)-C(16)-C(17)	120.3(5)
C(14)-C(12)-C(15)	109.3(5)	N(1)-C(16)-C(21)	123.3(5)
C(13)-C(12)-P(1)	104.8(4)	C(17)-C(16)-C(21)	116.3(5)
C(14)-C(12)-P(1)	111.3(4)	C(18)-C(17)-C(16)	122.4(5)
C(15)-C(12)-P(1)	113.4(4)	C(18)-C(17)-H(17A)	118.8
C(12)-C(13)-H(13A)	109.5	C(16)-C(17)-H(17A)	118.8
C(12)-C(13)-H(13B)	109.5	C(17)-C(18)-C(19)	120.6(6)
H(13A)-C(13)-H(13B)	109.5	C(17)-C(18)-H(18A)	119.7
C(12)-C(13)-H(13C)	109.5	C(19)-C(18)-H(18A)	119.7
H(13A)-C(13)-H(13C)	109.5	C(20)-C(19)-C(18)	119.3(6)
H(13B)-C(13)-H(13C)	109.5	C(20)-C(19)-H(19A)	120.4
C(12)-C(14)-H(14A)	109.5	C(18)-C(19)-H(19A)	120.4
C(12)-C(14)-H(14B)	109.5	C(19)-C(20)-C(21)	121.6(6)
H(14A)-C(14)-H(14B)	109.5	C(19)-C(20)-H(20A)	119.2
C(12)-C(14)-H(14C)	109.5	C(21)-C(20)-H(20A)	119.2
H(14A)-C(14)-H(14C)	109.5	C(20)-C(21)-C(16)	119.8(5)
H(14B)-C(14)-H(14C)	109.5	C(20)-C(21)-H(21A)	120.1
C(12)-C(15)-H(15A)	109.5	O(1)-C(28)-H(28B)	110.4
C(16)-C(21)-H(21A)	120.1	C(29)-C(28)-H(28B)	110.4
N(1)-C(22)-C(27)	120.0(5)	H(28A)-C(28)-H(28B)	108.6
N(1)-C(22)-C(23)	123.5(5)	C(30)-C(29)-C(28)	102.1(5)
C(27)-C(22)-C(23)	116.2(5)	C(30)-C(29)-H(29A)	111.3
C(24)-C(23)-C(22)	120.8(5)	C(28)-C(29)-H(29A)	111.3
C(24)-C(23)-H(23A)	119.6	C(30)-C(29)-H(29B)	111.3
C(22)-C(23)-H(23A)	119.6	C(28)-C(29)-H(29B)	111.3
C(25)-C(24)-C(23)	121.6(5)	H(29A)-C(29)-H(29B)	109.2
C(25)-C(24)-H(24A)	119.2	C(29)-C(30)-C(31)	102.2(4)
C(23)-C(24)-H(24A)	119.2	C(29)-C(30)-H(30A)	111.3
C(24)-C(25)-C(26)	118.6(5)	C(31)-C(30)-H(30A)	111.3
C(24)-C(25)-H(25A)	120.7	C(29)-C(30)-H(30B)	111.3
C(26)-C(25)-H(25A)	120.7	C(31)-C(30)-H(30B)	111.3
C(25)-C(26)-C(27)	120.4(5)	H(30A)-C(30)-H(30B)	109.2
C(25)-C(26)-H(26A)	119.8	O(1)-C(31)-C(30)	105.1(5)
C(27)-C(26)-H(26A)	119.8	O(1)-C(31)-H(31A)	110.7
C(26)-C(27)-C(22)	122.3(5)	C(30)-C(31)-H(31A)	110.7
C(26)-C(27)-H(27A)	118.8	O(1)-C(31)-H(31B)	110.7
C(22)-C(27)-H(27A)	118.8	C(30)-C(31)-H(31B)	110.7
O(1)-C(28)-C(29)	106.6(5)	H(31A)-C(31)-H(31B)	108.8

Table 2.4 (cont.)

O(1)-C(28)-H(28A)	110.4	C(16)-N(1)-C(22)	121.1(4)
C(29)-C(28)-H(28A)	110.4	C(8)-P(1)-Pd(1)	112.32(19)
C(16)-N(1)-Pd(1)	122.2(3)	C(12)-P(1)-Pd(1)	116.20(18)
C(22)-N(1)-Pd(1)	116.6(3)	C(1)-Pd(1)-N(1)	94.2(2)
C(28)-O(1)-C(31)	107.7(4)	C(1)-Pd(1)-P(1)	82.42(16)
C(28)-O(1)-Pd(1)	121.1(3)	N(1)-Pd(1)-P(1)	176.48(17)
C(31)-O(1)-Pd(1)	116.5(3)	C(1)-Pd(1)-O(1)	179.37(18)
C(7)-P(1)-C(8)	106.5(3)	N(1)-Pd(1)-O(1)	85.82(17)
C(7)-P(1)-C(12)	104.2(3)	P(1)-Pd(1)-O(1)	97.59(9)
C(8)-P(1)-C(12)	113.0(3)	C(7)-P(1)-Pd(1)	103.31(19)

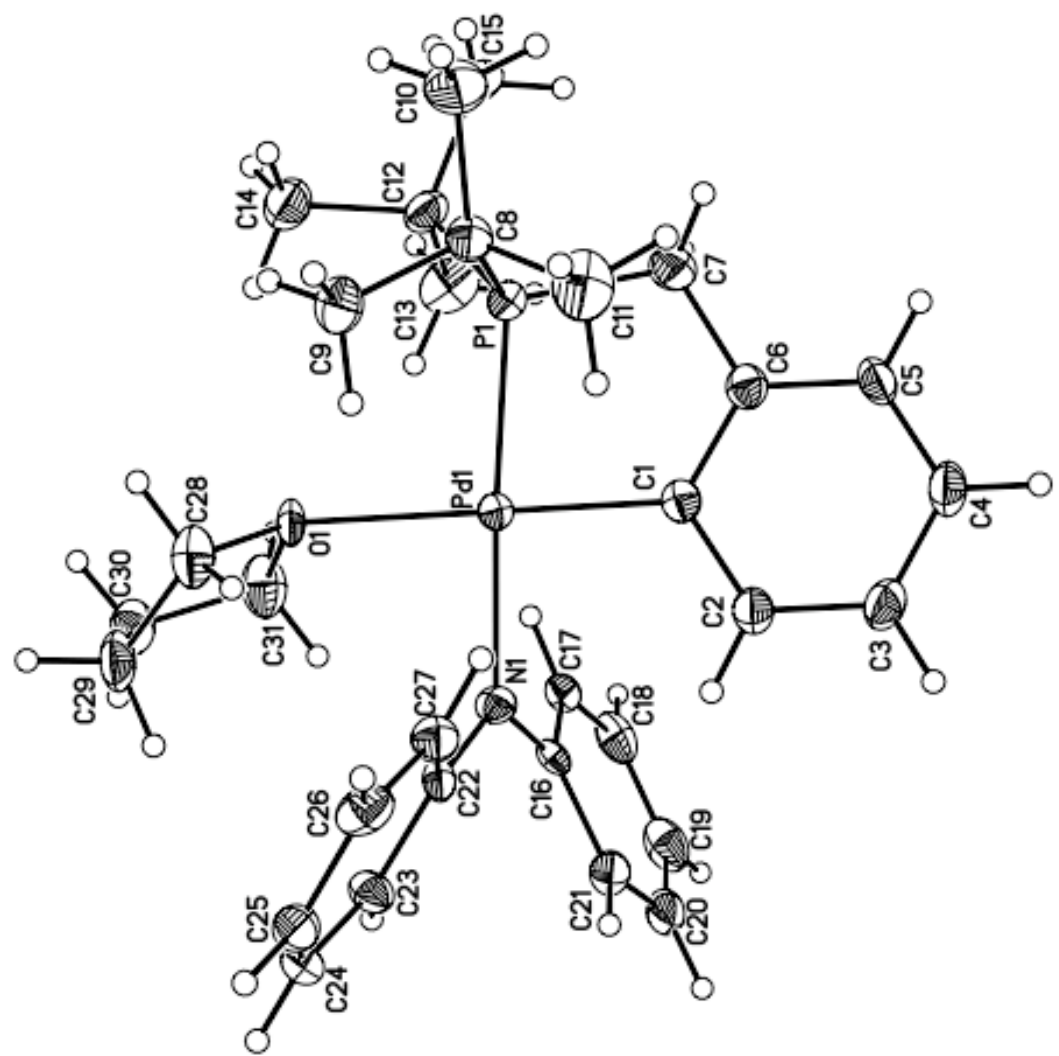


Figure 2.10. ORTEP diagram of (P-C)Pd(THF)NPh₂ (**2.02**) 35 % probability ellipsoids.

Table 2.5. Crystal data and structure refinement for $[(P-C)PdNPh_2]_2$ (**2.13**).

Empirical formula	C ₅₄ H ₆₈ N ₂ P ₂ Pd ₂
Formula weight	1019.84
Temperature	193(2) K
Wavelength	0.71073 Å
Crystal system	Monoclinic
Space group	P2(1)/c
Unit cell dimensions	a = 13.9745(8) Å a= 90°. b = 18.6987(11) Å b= 102.129(4)°. c = 20.4170(12) Å g = 90°.
Volume	5216.0(5) Å ³
Z	4
Density (calculated)	1.299 Mg/m ³
Absorption coefficient	0.785 mm ⁻¹
F(000)	2112
Crystal size	0.446 x 0.335 x 0.306 mm ³
Theta range for data collection	1.49 to 27.19°.
Index ranges	-17<=h<=17, -23<=k<=24, -26<=l<=21
Reflections collected	99103
Independent reflections	11568 [R(int) = 0.0401]
Completeness to theta = 27.19°	99.7 %
Absorption correction	Integration
Max. and min. transmission	0.8640 and 0.8146
Refinement method	Full-matrix least-squares on F ²
Data / restraints / parameters	11568 / 410 / 665
Goodness-of-fit on F ²	1.051
Final R indices [I>2sigma(I)]	R1 = 0.0244, wR2 = 0.0599
R indices (all data)	R1 = 0.0315, wR2 = 0.0624
Largest diff. peak and hole	0.503 and -0.374 e.Å ⁻³

Table 2.6. Atomic coordinates ($\times 10^4$) and equivalent isotropic displacement parameters ($\text{\AA}^2 \times 10^3$) for **2.13**. U(eq) is defined as one third of the trace of the orthogonalized U^{ij} tensor.

	x	y	z	U(eq)
Pd(1)	1577(1)	4471(1)	2417(1)	22(1)
Pd(2)	3226(1)	5683(1)	505(1)	24(1)
P(1)	523(1)	4827(1)	3050(1)	25(1)
P(2)	3490(1)	6845(1)	318(1)	24(1)
N(1)	1385(1)	3331(1)	2425(1)	29(1)
N(2)	2471(1)	4318(1)	1706(1)	24(1)
C(1)	1900(2)	5529(1)	2473(1)	28(1)
C(2)	1270(2)	6032(1)	2675(1)	30(1)
C(3)	1546(2)	6745(1)	2784(1)	38(1)
C(4)	2450(2)	6972(1)	2700(1)	44(1)
C(5)	3076(2)	6491(1)	2493(1)	42(1)
C(6)	2803(2)	5782(1)	2378(1)	35(1)
C(7)	299(2)	5758(1)	2776(1)	34(1)
C(8)	1038(1)	4898(1)	3978(1)	30(1)
C(9)	567(2)	5498(1)	4316(1)	41(1)
C(10)	928(2)	4186(1)	4330(1)	40(1)
C(11)	2137(2)	5064(1)	4076(1)	39(1)
C(12)	-731(1)	4411(1)	2859(1)	36(1)
C(13)	-1438(2)	4761(1)	3244(1)	48(1)
C(14)	-686(2)	3606(1)	2988(1)	53(1)
C(15)	-1136(2)	4514(1)	2107(1)	53(1)
C(16)	1658(13)	2933(10)	3016(7)	27(2)
C(17)	2478(11)	3145(8)	3481(6)	31(2)
C(18)	2771(9)	2808(7)	4097(5)	33(2)
C(19)	2248(10)	2237(6)	4259(5)	35(2)
C(20)	1433(11)	2006(6)	3799(6)	38(2)
C(21)	1124(11)	2351(8)	3190(6)	34(2)
C(16B)	1793(15)	3002(11)	3041(8)	28(2)
C(17B)	2619(11)	3259(8)	3475(7)	26(2)
C(18B)	2950(10)	2969(8)	4109(6)	31(2)
C(19B)	2479(10)	2395(8)	4319(5)	35(2)
C(20B)	1666(11)	2114(7)	3895(6)	38(2)
C(21B)	1334(11)	2404(9)	3260(7)	35(2)
C(22)	1160(1)	2955(1)	1835(1)	28(1)
C(23)	1434(2)	2233(1)	1761(1)	36(1)
C(24)	1316(2)	1924(1)	1133(1)	43(1)
C(25)	941(2)	2297(1)	557(1)	43(1)
C(26)	635(2)	2997(1)	618(1)	37(1)
C(27)	720(1)	3307(1)	1239(1)	31(1)
C(28)	3294(8)	3861(6)	1937(7)	28(1)
C(29)	4037(7)	4080(5)	2461(6)	35(1)
C(30)	4854(6)	3649(5)	2669(4)	42(1)
C(31)	4918(6)	2996(5)	2365(4)	40(2)
C(32)	4169(7)	2761(4)	1859(5)	36(2)
C(33)	3365(7)	3197(5)	1640(5)	33(2)
C(28B)	3249(10)	3809(8)	1833(9)	27(2)
C(29B)	4026(10)	3928(7)	2365(8)	36(2)
C(30B)	4779(8)	3429(7)	2528(6)	40(2)

Table 2.6. (cont.)

C(31B)	4705(8)	2800(6)	2175(7)	38(2)
C(32B)	3917(9)	2660(5)	1661(6)	35(2)
C(33B)	3188(9)	3165(6)	1485(7)	26(2)
C(34)	2269(1)	4595(1)	1098(1)	24(1)
C(35)	2864(1)	4489(1)	601(1)	27(1)
C(36)	2548(2)	4729(1)	-63(1)	33(1)
C(37)	1794(2)	5229(1)	-211(1)	36(1)
C(38)	1216(1)	5353(1)	274(1)	34(1)
C(39)	1425(1)	5049(1)	891(1)	28(1)
C(40)	4524(1)	5788(1)	1163(1)	28(1)
C(41)	4959(1)	6461(1)	1333(1)	29(1)
C(42)	5892(2)	6512(1)	1738(1)	37(1)
C(43)	6404(2)	5903(1)	1977(1)	47(1)
C(44)	5983(2)	5239(1)	1819(1)	47(1)
C(45)	5058(2)	5186(1)	1415(1)	36(1)
C(46)	4392(2)	7119(1)	1059(1)	32(1)
C(47)	4094(1)	6951(1)	-408(1)	30(1)
C(48)	5102(2)	6592(1)	-218(1)	42(1)
C(49)	3500(2)	6556(1)	-1018(1)	40(1)
C(50)	4240(2)	7735(1)	-583(1)	40(1)
C(51)	2439(1)	7477(1)	276(1)	32(1)
C(52)	1876(2)	7220(1)	802(1)	45(1)
C(53)	1756(2)	7451(1)	-415(1)	43(1)
C(54)	2771(2)	8250(1)	443(1)	45(1)

Table 2.7. Bond lengths [Å] and angles [°] for [(P-C)PdNPh₂]₂ (**2.13**).

Pd(1)-C(1)	2.0264(17)	C(2)-C(3)	1.392(3)
Pd(1)-N(2)	2.1228(14)	C(2)-C(7)	1.504(3)
Pd(1)-N(1)	2.1485(15)	C(3)-C(4)	1.377(3)
Pd(1)-P(1)	2.2548(4)	C(3)-H(3A)	0.9500
Pd(2)-C(40)	2.0263(19)	C(4)-C(5)	1.382(3)
Pd(2)-C(36)	2.2291(19)	C(4)-H(4A)	0.9500
Pd(2)-P(2)	2.2492(5)	C(5)-C(6)	1.385(3)
Pd(2)-C(35)	2.3069(17)	C(5)-H(5A)	0.9500
Pd(2)-C(37)	2.375(2)	C(6)-H(6A)	0.9500
P(1)-C(7)	1.8356(19)	C(7)-H(7A)	0.9900
P(1)-C(12)	1.881(2)	C(7)-H(7B)	0.9900
P(1)-C(8)	1.8856(19)	C(8)-C(10)	1.535(3)
P(2)-C(46)	1.828(2)	C(8)-C(9)	1.536(3)
P(2)-C(47)	1.8645(18)	C(8)-C(11)	1.539(3)
P(2)-C(51)	1.8720(19)	C(9)-H(9A)	0.9800
N(1)-C(22)	1.373(2)	C(9)-H(9B)	0.9800
N(1)-C(16)	1.402(5)	C(9)-H(9C)	0.9800
N(1)-C(16B)	1.409(6)	C(10)-H(10A)	0.9800
N(2)-C(34)	1.320(2)	C(10)-H(10B)	0.9800
N(2)-C(28B)	1.428(6)	C(10)-H(10C)	0.9800
N(2)-C(28)	1.431(5)	C(11)-H(11A)	0.9800
C(1)-C(6)	1.400(3)	C(11)-H(11B)	0.9800
C(1)-C(2)	1.408(3)	C(20)-H(20A)	0.9500
C(11)-H(11C)	0.9800	C(21)-H(21A)	0.9500
C(12)-C(14)	1.529(3)	C(16B)-C(17B)	1.385(6)
C(12)-C(13)	1.532(3)	C(16B)-C(21B)	1.408(6)
C(12)-C(15)	1.533(3)	C(17B)-C(18B)	1.389(6)
C(13)-H(13A)	0.9800	C(17B)-H(17B)	0.9500
C(13)-H(13B)	0.9800	C(18B)-C(19B)	1.374(6)
C(13)-H(13C)	0.9800	C(18B)-H(18B)	0.9500
C(14)-H(14A)	0.9800	C(19B)-C(20B)	1.380(6)
C(14)-H(14B)	0.9800	C(19B)-H(19B)	0.9500
C(14)-H(14C)	0.9800	C(20B)-C(21B)	1.391(6)
C(15)-H(15A)	0.9800	C(20B)-H(20B)	0.9500
C(15)-H(15B)	0.9800	C(21B)-H(21B)	0.9500
C(15)-H(15C)	0.9800	C(22)-C(27)	1.407(3)
C(16)-C(17)	1.384(6)	C(22)-C(23)	1.421(3)
C(16)-C(21)	1.407(6)	C(23)-C(24)	1.383(3)
C(17)-C(18)	1.390(6)	C(23)-H(23A)	0.9500
C(17)-H(17A)	0.9500	C(24)-C(25)	1.374(3)
C(18)-C(19)	1.373(6)	C(24)-H(24A)	0.9500
C(18)-H(18A)	0.9500	C(25)-C(26)	1.389(3)
C(19)-C(20)	1.384(6)	C(25)-H(25A)	0.9500
C(19)-H(19A)	0.9500	C(26)-C(27)	1.377(3)
C(20)-C(21)	1.388(6)	C(32B)-H(32B)	0.9500
C(26)-H(26A)	0.9500	C(33B)-H(33B)	0.9500
C(27)-H(27A)	0.9500	C(34)-C(39)	1.442(2)
C(28)-C(29)	1.387(5)	C(34)-C(35)	1.454(2)
C(28)-C(33)	1.394(5)	C(35)-C(36)	1.408(3)
C(29)-C(30)	1.390(5)	C(35)-H(35A)	1.0000
C(29)-H(29A)	0.9500	C(36)-C(37)	1.394(3)
C(30)-C(31)	1.380(6)	C(36)-H(36A)	1.0000
C(30)-H(30A)	0.9500	C(37)-C(38)	1.423(3)
C(31)-C(32)	1.379(6)	C(37)-H(37A)	1.0000

Table 2.7. (cont.)

C(31)-H(31A)	0.9500	C(38)-C(39)	1.356(3)
C(32)-C(33)	1.383(5)	C(38)-H(38A)	0.9500
C(32)-H(32A)	0.9500	C(39)-H(39A)	0.9500
C(33)-H(33A)	0.9500	C(40)-C(45)	1.388(3)
C(28B)-C(29B)	1.382(7)	C(40)-C(41)	1.409(3)
C(28B)-C(33B)	1.392(6)	C(41)-C(42)	1.393(3)
C(29B)-C(30B)	1.394(7)	C(41)-C(46)	1.506(3)
C(29B)-H(29B)	0.9500	C(42)-C(43)	1.377(3)
C(30B)-C(31B)	1.372(8)	C(42)-H(42A)	0.9500
C(30B)-H(30B)	0.9500	C(43)-C(44)	1.382(3)
C(31B)-C(32B)	1.378(7)	C(43)-H(43A)	0.9500
C(31B)-H(31B)	0.9500	C(44)-C(45)	1.383(3)
C(32B)-C(33B)	1.380(6)	C(51)-C(53)	1.529(3)
C(44)-H(44A)	0.9500	C(51)-C(54)	1.535(3)
C(45)-H(45A)	0.9500	C(51)-C(52)	1.537(3)
C(46)-H(46A)	0.9900	C(52)-H(52A)	0.9800
C(46)-H(46B)	0.9900	C(52)-H(52B)	0.9800
C(47)-C(50)	1.533(3)	C(52)-H(52C)	0.9800
C(47)-C(49)	1.533(3)	C(53)-H(53A)	0.9800
C(47)-C(48)	1.535(3)	C(53)-H(53B)	0.9800
C(48)-H(48A)	0.9800	C(53)-H(53C)	0.9800
C(48)-H(48B)	0.9800	C(54)-H(54A)	0.9800
C(48)-H(48C)	0.9800	C(54)-H(54B)	0.9800
C(49)-H(49A)	0.9800	C(54)-H(54C)	0.9800
C(49)-H(49B)	0.9800	C(50)-H(50B)	0.9800
C(49)-H(49C)	0.9800	C(50)-H(50C)	0.9800
C(50)-H(50A)	0.9800		

C(1)-Pd(1)-N(2)	90.83(6)	C(46)-P(2)-C(51)	105.04(9)
C(1)-Pd(1)-N(1)	173.91(7)	C(47)-P(2)-C(51)	112.18(9)
N(2)-Pd(1)-N(1)	87.96(5)	C(46)-P(2)-Pd(2)	103.85(6)
C(1)-Pd(1)-P(1)	81.01(5)	C(47)-P(2)-Pd(2)	110.83(6)
N(2)-Pd(1)-P(1)	168.65(4)	C(51)-P(2)-Pd(2)	117.57(6)
N(1)-Pd(1)-P(1)	100.96(4)	C(22)-N(1)-C(16)	117.0(9)
C(40)-Pd(2)-C(36)	130.27(8)	C(22)-N(1)-C(16B)	122.3(11)
C(40)-Pd(2)-P(2)	82.14(5)	C(22)-N(1)-Pd(1)	120.47(12)
C(36)-Pd(2)-P(2)	138.73(5)	C(16)-N(1)-Pd(1)	121.5(8)
C(40)-Pd(2)-C(35)	102.71(7)	C(16B)-N(1)-Pd(1)	114.4(9)
C(36)-Pd(2)-C(35)	36.11(7)	C(34)-N(2)-C(28B)	115.9(9)
P(2)-Pd(2)-C(35)	174.73(5)	C(34)-N(2)-C(28)	122.8(7)
C(40)-Pd(2)-C(37)	164.61(7)	C(34)-N(2)-Pd(1)	123.37(12)
C(36)-Pd(2)-C(37)	35.06(7)	C(28B)-N(2)-Pd(1)	120.0(9)
P(2)-Pd(2)-C(37)	112.81(5)	C(28)-N(2)-Pd(1)	113.8(7)
C(35)-Pd(2)-C(37)	62.22(7)	C(6)-C(1)-C(2)	116.84(17)
C(7)-P(1)-C(12)	103.74(10)	C(6)-C(1)-Pd(1)	121.24(14)
C(7)-P(1)-C(8)	104.12(9)	C(2)-C(1)-Pd(1)	121.61(14)
C(12)-P(1)-C(8)	112.29(9)	C(3)-C(2)-C(1)	121.24(18)
C(7)-P(1)-Pd(1)	101.25(6)	C(3)-C(2)-C(7)	122.09(17)
C(12)-P(1)-Pd(1)	116.87(6)	C(1)-C(2)-C(7)	116.67(16)
C(8)-P(1)-Pd(1)	116.09(6)	C(4)-C(3)-C(2)	120.34(19)
C(46)-P(2)-C(47)	106.19(9)	C(11)-C(8)-P(1)	107.75(12)
C(4)-C(3)-H(3A)	119.8	C(8)-C(9)-H(9A)	109.5
C(2)-C(3)-H(3A)	119.8	C(8)-C(9)-H(9B)	109.5

Table 2.7. (cont.)

C(3)-C(4)-C(5)	119.56(19)	H(9A)-C(9)-H(9B)	109.5
C(3)-C(4)-H(4A)	120.2	C(8)-C(9)-H(9C)	109.5
C(5)-C(4)-H(4A)	120.2	H(9A)-C(9)-H(9C)	109.5
C(4)-C(5)-C(6)	120.4(2)	H(9B)-C(9)-H(9C)	109.5
C(4)-C(5)-H(5A)	119.8	C(8)-C(10)-H(10A)	109.5
C(6)-C(5)-H(5A)	119.8	C(8)-C(10)-H(10B)	109.5
C(5)-C(6)-C(1)	121.59(19)	H(10A)-C(10)-H(10B)	109.5
C(5)-C(6)-H(6A)	119.2	C(8)-C(10)-H(10C)	109.5
C(1)-C(6)-H(6A)	119.2	H(10A)-C(10)-H(10C)	109.5
C(2)-C(7)-P(1)	105.33(13)	H(10B)-C(10)-H(10C)	109.5
C(2)-C(7)-H(7A)	110.7	C(8)-C(11)-H(11A)	109.5
P(1)-C(7)-H(7A)	110.7	C(8)-C(11)-H(11B)	109.5
C(2)-C(7)-H(7B)	110.7	H(11A)-C(11)-H(11B)	109.5
P(1)-C(7)-H(7B)	110.7	C(8)-C(11)-H(11C)	109.5
H(7A)-C(7)-H(7B)	108.8	H(11A)-C(11)-H(11C)	109.5
C(10)-C(8)-C(9)	109.20(16)	H(11B)-C(11)-H(11C)	109.5
C(10)-C(8)-C(11)	108.01(17)	C(14)-C(12)-C(13)	109.83(18)
C(9)-C(8)-C(11)	107.68(17)	C(14)-C(12)-C(15)	106.88(19)
C(10)-C(8)-P(1)	110.79(14)	C(13)-C(12)-C(15)	108.57(18)
C(9)-C(8)-P(1)	113.23(14)	C(17)-C(16)-C(21)	117.1(5)
C(14)-C(12)-P(1)	111.62(15)	N(1)-C(16)-C(21)	124.4(8)
C(13)-C(12)-P(1)	112.98(15)	C(16)-C(17)-C(18)	122.3(6)
C(15)-C(12)-P(1)	106.69(15)	C(16)-C(17)-H(17A)	118.8
C(12)-C(13)-H(13A)	109.5	C(18)-C(17)-H(17A)	118.8
C(12)-C(13)-H(13B)	109.5	C(19)-C(18)-C(17)	120.0(6)
H(13A)-C(13)-H(13B)	109.5	C(19)-C(18)-H(18A)	120.0
C(12)-C(13)-H(13C)	109.5	C(17)-C(18)-H(18A)	120.0
H(13A)-C(13)-H(13C)	109.5	C(18)-C(19)-C(20)	118.9(5)
H(13B)-C(13)-H(13C)	109.5	C(18)-C(19)-H(19A)	120.5
C(12)-C(14)-H(14A)	109.5	C(20)-C(19)-H(19A)	120.5
C(12)-C(14)-H(14B)	109.5	C(19)-C(20)-C(21)	121.3(5)
H(14A)-C(14)-H(14B)	109.5	C(19)-C(20)-H(20A)	119.3
C(12)-C(14)-H(14C)	109.5	C(21)-C(20)-H(20A)	119.3
H(14A)-C(14)-H(14C)	109.5	C(20)-C(21)-C(16)	120.3(6)
H(14B)-C(14)-H(14C)	109.5	C(20)-C(21)-H(21A)	119.9
C(12)-C(15)-H(15A)	109.5	C(16)-C(21)-H(21A)	119.9
C(12)-C(15)-H(15B)	109.5	C(17B)-C(16B)-C(21B)	116.5(5)
H(15A)-C(15)-H(15B)	109.5	C(17B)-C(16B)-N(1)	123.1(9)
C(12)-C(15)-H(15C)	109.5	C(21B)-C(16B)-N(1)	120.3(9)
H(15A)-C(15)-H(15C)	109.5	C(16B)-C(17B)-C(18B)	122.0(6)
H(15B)-C(15)-H(15C)	109.5	C(16B)-C(17B)-H(17B)	119.0
C(17)-C(16)-N(1)	118.3(9)	C(24)-C(25)-C(26)	118.02(19)
C(18B)-C(17B)-H(17B)	119.0	C(24)-C(25)-H(25A)	121.0
C(19B)-C(18B)-C(17B)	120.5(6)	C(26)-C(25)-H(25A)	121.0
C(19B)-C(18B)-H(18B)	119.7	C(27)-C(26)-C(25)	120.8(2)
C(17B)-C(18B)-H(18B)	119.7	C(27)-C(26)-H(26A)	119.6
C(18B)-C(19B)-C(20B)	119.1(6)	C(25)-C(26)-H(26A)	119.6
C(18B)-C(19B)-H(19B)	120.5	C(26)-C(27)-C(22)	122.43(18)
C(20B)-C(19B)-H(19B)	120.5	C(26)-C(27)-H(27A)	118.8
C(19B)-C(20B)-C(21B)	120.4(6)	C(22)-C(27)-H(27A)	118.8
C(19B)-C(20B)-H(20B)	119.8	C(29)-C(28)-C(33)	119.2(4)
C(21B)-C(20B)-H(20B)	119.8	C(29)-C(28)-N(2)	119.8(6)
C(20B)-C(21B)-C(16B)	121.4(6)	C(33)-C(28)-N(2)	121.0(6)
C(20B)-C(21B)-H(21B)	119.3	C(28)-C(29)-C(30)	119.9(5)
C(16B)-C(21B)-H(21B)	119.3	C(28)-C(29)-H(29A)	120.0

Table 2.7. (cont.)

N(1)-C(22)-C(27)	119.80(16)	C(30)-C(29)-H(29A)	120.0
N(1)-C(22)-C(23)	124.33(18)	C(31)-C(30)-C(29)	120.1(5)
C(27)-C(22)-C(23)	115.54(18)	C(31)-C(30)-H(30A)	119.9
C(24)-C(23)-C(22)	120.9(2)	C(29)-C(30)-H(30A)	119.9
C(24)-C(23)-H(23A)	119.6	C(32)-C(31)-C(30)	120.5(4)
C(22)-C(23)-H(23A)	119.6	C(32)-C(31)-H(31A)	119.8
C(25)-C(24)-C(23)	122.11(19)	C(30)-C(31)-H(31A)	119.8
C(25)-C(24)-H(24A)	118.9	C(31)-C(32)-C(33)	119.5(5)
C(23)-C(24)-H(24A)	118.9	C(28B)-C(33B)-H(33B)	120.1
C(31)-C(32)-H(32A)	120.2	N(2)-C(34)-C(39)	120.41(15)
C(33)-C(32)-H(32A)	120.2	N(2)-C(34)-C(35)	124.22(16)
C(32)-C(33)-C(28)	120.7(5)	C(39)-C(34)-C(35)	115.36(16)
C(32)-C(33)-H(33A)	119.6	C(36)-C(35)-C(34)	121.27(17)
C(28)-C(33)-H(33A)	119.6	C(36)-C(35)-Pd(2)	68.93(10)
C(29B)-C(28B)-C(33B)	119.6(6)	C(34)-C(35)-Pd(2)	95.42(11)
C(29B)-C(28B)-N(2)	118.6(8)	C(36)-C(35)-H(35A)	118.5
C(33B)-C(28B)-N(2)	121.4(8)	C(34)-C(35)-H(35A)	118.5
C(28B)-C(29B)-C(30B)	120.6(7)	Pd(2)-C(35)-H(35A)	118.5
C(28B)-C(29B)-H(29B)	119.7	C(37)-C(36)-C(35)	119.47(18)
C(30B)-C(29B)-H(29B)	119.7	C(37)-C(36)-Pd(2)	78.19(12)
C(31B)-C(30B)-C(29B)	118.6(6)	C(35)-C(36)-Pd(2)	74.96(11)
C(31B)-C(30B)-H(30B)	120.7	C(37)-C(36)-H(36A)	120.2
C(29B)-C(30B)-H(30B)	120.7	C(35)-C(36)-H(36A)	120.2
C(30B)-C(31B)-C(32B)	121.5(6)	Pd(2)-C(36)-H(36A)	120.2
C(30B)-C(31B)-H(31B)	119.3	C(36)-C(37)-C(38)	118.20(18)
C(32B)-C(31B)-H(31B)	119.3	C(36)-C(37)-Pd(2)	66.74(11)
C(31B)-C(32B)-C(33B)	119.8(6)	C(38)-C(37)-Pd(2)	92.34(12)
C(31B)-C(32B)-H(32B)	120.1	C(36)-C(37)-H(37A)	120.3
C(33B)-C(32B)-H(32B)	120.1	C(38)-C(37)-H(37A)	120.3
C(32B)-C(33B)-C(28B)	119.7(6)	Pd(2)-C(37)-H(37A)	120.3
C(32B)-C(33B)-H(33B)	120.1	C(44)-C(45)-H(45A)	119.1
C(39)-C(38)-C(37)	122.36(19)	C(40)-C(45)-H(45A)	119.1
C(39)-C(38)-H(38A)	118.8	C(41)-C(46)-P(2)	107.23(13)
C(37)-C(38)-H(38A)	118.8	C(41)-C(46)-H(46A)	110.3
C(38)-C(39)-C(34)	121.45(17)	P(2)-C(46)-H(46A)	110.3
C(38)-C(39)-H(39A)	119.3	C(41)-C(46)-H(46B)	110.3
C(34)-C(39)-H(39A)	119.3	P(2)-C(46)-H(46B)	110.3
C(45)-C(40)-C(41)	117.50(18)	H(46A)-C(46)-H(46B)	108.5
C(45)-C(40)-Pd(2)	120.24(14)	C(50)-C(47)-C(49)	110.30(17)
C(41)-C(40)-Pd(2)	122.00(14)	C(50)-C(47)-C(48)	108.55(16)
C(42)-C(41)-C(40)	120.60(18)	C(49)-C(47)-C(48)	107.81(17)
C(42)-C(41)-C(46)	121.26(17)	C(50)-C(47)-P(2)	113.09(13)
C(40)-C(41)-C(46)	118.14(17)	C(49)-C(47)-P(2)	109.61(13)
C(43)-C(42)-C(41)	120.33(19)	C(48)-C(47)-P(2)	107.30(13)
C(43)-C(42)-H(42A)	119.8	C(47)-C(48)-H(48A)	109.5
C(41)-C(42)-H(42A)	119.8	C(47)-C(48)-H(48B)	109.5
C(42)-C(43)-C(44)	119.8(2)	H(48A)-C(48)-H(48B)	109.5
C(42)-C(43)-H(43A)	120.1	C(47)-C(48)-H(48C)	109.5
C(44)-C(43)-H(43A)	120.1	H(48A)-C(48)-H(48C)	109.5
C(43)-C(44)-C(45)	120.1(2)	H(48B)-C(48)-H(48C)	109.5
C(43)-C(44)-H(44A)	120.0	C(47)-C(49)-H(49A)	109.5
C(45)-C(44)-H(44A)	120.0	C(47)-C(49)-H(49B)	109.5
C(44)-C(45)-C(40)	121.7(2)	C(51)-C(53)-H(53A)	109.5
H(49A)-C(49)-H(49B)	109.5	C(51)-C(53)-H(53B)	109.5
C(47)-C(49)-H(49C)	109.5	H(53A)-C(53)-H(53B)	109.5

Table 2.7. (cont.)

H(49A)-C(49)-H(49C)	109.5	C(51)-C(53)-H(53C)	109.5
H(49B)-C(49)-H(49C)	109.5	H(53A)-C(53)-H(53C)	109.5
C(47)-C(50)-H(50A)	109.5	H(53B)-C(53)-H(53C)	109.5
C(47)-C(50)-H(50B)	109.5	C(51)-C(54)-H(54A)	109.5
H(50A)-C(50)-H(50B)	109.5	C(51)-C(54)-H(54B)	109.5
C(47)-C(50)-H(50C)	109.5	H(54A)-C(54)-H(54B)	109.5
H(50A)-C(50)-H(50C)	109.5	C(51)-C(54)-H(54C)	109.5
H(50B)-C(50)-H(50C)	109.5	H(54A)-C(54)-H(54C)	109.5
C(53)-C(51)-C(54)	109.67(17)	H(54B)-C(54)-H(54C)	109.5
C(53)-C(51)-C(52)	108.82(17)	C(51)-C(52)-H(52A)	109.5
C(54)-C(51)-C(52)	108.29(17)	C(51)-C(52)-H(52B)	109.5
C(53)-C(51)-P(2)	110.77(14)	H(52A)-C(52)-H(52B)	109.5
C(54)-C(51)-P(2)	112.76(14)	C(51)-C(52)-H(52C)	109.5
C(52)-C(51)-P(2)	106.38(13)	H(52A)-C(52)-H(52C)	109.5
H(52B)-C(52)-H(52C)	109.5		

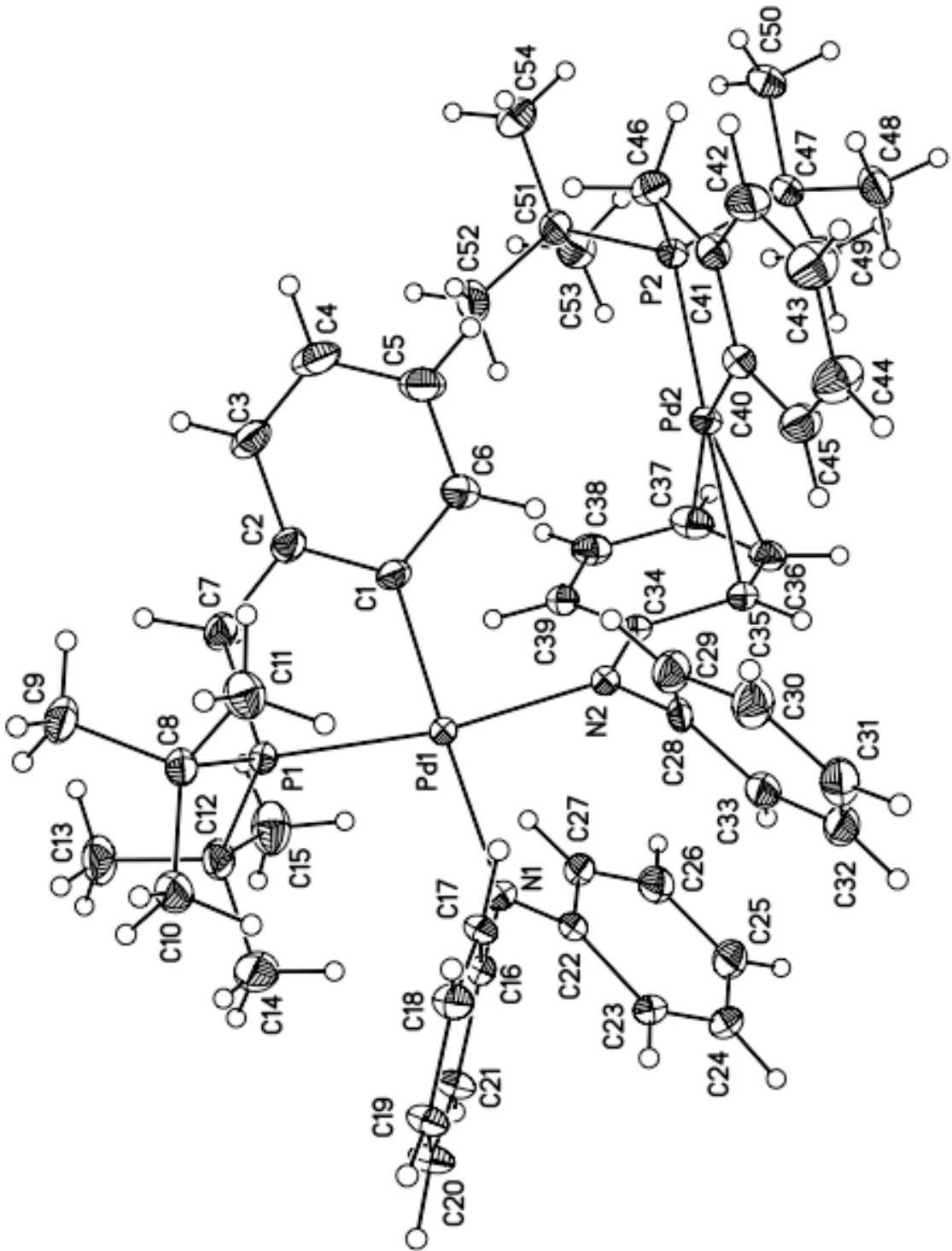


Figure 2.11. ORTEP diagram of $[(P-C)PdNPh_2]$ (2.13) 35 % probability ellipsoids

2.5 References

- (1) Grubbs, R. H.; Coates, G. W. *Acc. Chem. Res.* **1996**, *29*, 85.
- (2) Ittel, S. D.; Johnson, L. K.; Brookhart, M. *Chem. Rev.* **2000**, *100*, 1169.
- (3) Mecking, S. *Angew. Chem., Int. Ed.* **2001**, *40*, 534.
- (4) Gibson, V. C.; Spitzmesser, S. K. *Chem. Rev.* **2003**, *103*, 283.
- (5) Thalji, R. K.; Ahrendt, K. A.; Bergman, R. G.; Ellman, J. A. *J. Am. Chem. Soc.* **2001**, *123*, 9692.
- (6) Periana, R. A.; Liu, X. Y.; Bhalla, G. *Chem. Commun.* **2002**, 3000.
- (7) Tan, K. L.; Bergman, R. G.; Ellman, J. A. *J. Am. Chem. Soc.* **2002**, *124*, 13964.
- (8) Lail, M.; Bell, C. M.; Conner, D.; Cundari, T. R.; Gunnoe, T. B.; Petersen, J. L. *Organometallics* **2004**, *23*, 5007.
- (9) Oxgaard, J.; Periana, R. A.; Goddard, W. A. *J. Am. Chem. Soc.* **2004**, *126*, 11658.
- (10) Nakao, Y.; Hirata, Y.; Hiyama, T. *J. Am. Chem. Soc.* **2006**, *128*, 7420.
- (11) Nakao, Y.; Ebata, S.; Yada, A.; Hiyama, T.; Ikawa, M.; Ogoshi, S. *J. Am. Chem. Soc.* **2008**, *130*, 12874.
- (12) Watson, M. P.; Jacobsen, E. N. *J. Am. Chem. Soc.* **2008**, *130*, 12594.
- (13) Nakao, Y.; Idei, H.; Kanyiva, K. S.; Hiyama, T. *J. Am. Chem. Soc.* **2009**, *131*, 5070.
- (14) Heck, R. F. *Acc. Chem. Res.* **1969**, *2*, 10.
- (15) Heck, R. F. *Acc. Chem. Res.* **1979**, *12*, 146.
- (16) Amatore, C.; Jutand, A. *Acc. Chem. Res.* **2000**, *33*, 314.
- (17) Beletskaya, I. P.; Cheprakov, A. V. *Chem. Rev.* **2000**, *100*, 3009.

- (18) Hartwig, J. F. *Organotransition metal chemistry : from bonding to catalysis*; University Science Books: Sausalito, Calif., 2010.
- (19) Casalnuovo, A. L.; Calabrese, J. C.; Milstein, D. *J. Am. Chem. Soc.* **1988**, *110*, 6738.
- (20) Cowan, R. L.; Trogler, W. C. *Organometallics* **1987**, *6*, 2451.
- (21) Villanueva, L. A.; Abboud, K. A.; Boncella, J. M. *Organometallics* **1992**, *11*, 2963.
- (22) Stubbert, B. D.; Marks, T. J. *J. Am. Chem. Soc.* **2007**, *129*, 6149.
- (23) Majumder, S.; Odom, A. L. *Organometallics* **2008**, *27*, 1174.
- (24) Leitch, D. C.; Payne, P. R.; Dunbar, C. R.; Schafer, L. L. *J. Am. Chem. Soc.* **2009**, *131*, 18246.
- (25) Gagne, M. R.; Stern, C. L.; Marks, T. J. *J. Am. Chem. Soc.* **1992**, *114*, 275.
- (26) Gribkov, D. V.; Hultzsch, K. C. *Angew. Chem., Int. Ed.* **2004**, *43*, 5542.
- (27) Neukom, J. D.; Perch, N. S.; Wolfe, J. P. *J. Am. Chem. Soc.* **2010**, *132*, 6276.
- (28) Neukom, J. D.; Perch, N. S.; Wolfe, J. P. *Organometallics* **2011**, *30*, 1269.
- (29) Zhao, P. J.; Krug, C.; Hartwig, J. F. *J. Am. Chem. Soc.* **2005**, *127*, 12066.
- (30) Ney, J. E.; Wolfe, J. P. *J. Am. Chem. Soc.* **2005**, *127*, 8644.
- (31) Nakhla, J. S.; Kampf, J. W.; Wolfe, J. P. *J. Am. Chem. Soc.* **2006**, *128*, 2893.
- (32) Mai, D. N.; Wolfe, J. P. *J. Am. Chem. Soc.* **2010**, *132*, 12157.
- (33) Neukom, J. D.; Aquino, A. S.; Wolfe, J. P. *Org. Lett.* **2011**, *13*, 2196.
- (34) Schultz, D. M.; Wolfe, J. P. *Org. Lett.* **2011**, *13*, 2962.
- (35) Kotov, V.; Scarborough, C. C.; Stahl, S. S. *Inorg. Chem.* **2007**, *46*, 1910.
- (36) Liu, G. S.; Stahl, S. S. *J. Am. Chem. Soc.* **2007**, *129*, 6328.

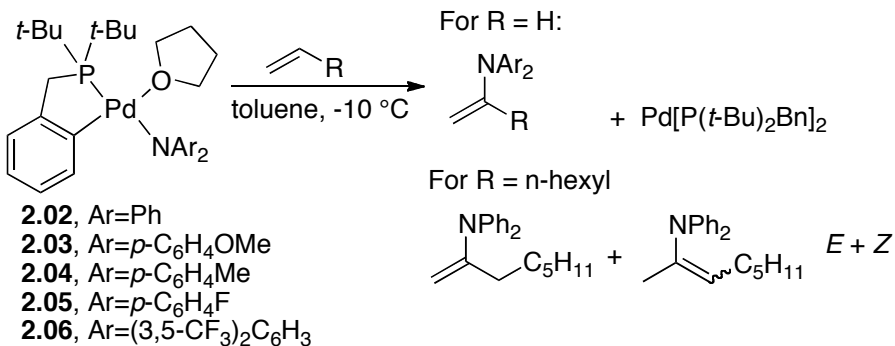
- (37) Liu, G. S.; Yin, G. Y.; Wu, L. *Angew. Chem., Int. Ed.* **2008**, *47*, 4733.
- (38) Liu, G. S.; Stahl, S. S. *J. Am. Chem. Soc.* **2006**, *128*, 7179.
- (39) Muniz, K.; Hovelmann, C. H.; Streuff, J. *J. Am. Chem. Soc.* **2008**, *130*, 763.
- (40) Helaja, J.; Gottlich, R. *Chem. Commun.* **2002**, 720.
- (41) Tsutsui, H.; Narasaka, K. *Chem. Lett.* **1999**, 45.
- (42) Ye, X. A.; Liu, G. S.; Popp, B. V.; Stahl, S. S. *J. Org. Chem.* **2011**, *76*, 1031.
- (43) Yamashita, M.; Hartwig, J. F. *J. Am. Chem. Soc.* **2004**, *126*, 5344.
- (44) Tye, J. W.; Hartwig, J. F. *J. Am. Chem. Soc.* **2009**, *131*, 14703.
- (45) Rix, F. C.; Brookhart, M. *J. Am. Chem. Soc.* **1995**, *117*, 1137.
- (46) Shultz, C. S.; Ledford, J.; DeSimone, J. M.; Brookhart, M. *J. Am. Chem. Soc.* **2000**, *122*, 6351.
- (47) Barluenga, J.; Fernandez, M. A.; Aznar, F.; Valdes, C. *Chem. Comm.* **2002**, 2362.

Chapter 3: Intermolecular Migratory Insertion of Unactivated Olefins into Palladium-Nitrogen Bonds. Steric and Electronic Effects on the Rate of Migratory Insertion^{*}

3.1 Introduction

In Chapter 2, the intermolecular insertion of ethylene and octene into the Pd-N bonds of discrete, isolated palladium diarylamido complexes to form enamine products was described.¹ Stable, THF-bound Pd-amido complexes ligated by a cyclometallated benzylphosphine ligand reacted with ethylene to form *N*-vinyl diarylamine products over 2 h at -10 °C (Scheme 3.1). The stereochemical outcome of the reaction of *trans*-ethylene-*d*₂ implied that the reaction occurred by insertion of the alkene into the metal-amido bond. Reactions of ethylene with a series of amido complexes containing different substituents on the diarylamide showed that the palladium-amido complexes containing more electron-donating amido groups reacted with alkenes faster than those containing less electron-donating amido groups. During these studies, a diarylamido complex lacking the THF ligand also was isolated, and this unsaturated complex reacted with ethylene at -50 °C in toluene-*d*₈ to form vinyl diphenylamine in high yield. Moreover, this amido complex lacking coordinated THF reacted at low temperatures with ¹³C-labeled ethylene to form a species proposed to be the amido ethylene precursor to the actual migratory insertion process.

^{*} Part of this chapter was previously published in Hanley, P. S. Hartwig, J. F. *J. Am. Chem. Soc.* **2011**, *133*, 15661.



Scheme 3.1. Reactions of THF-ligated palladium-amides **2.02-2.06** with ethylene and octene.

These studies on the reactions of alkenes with discrete amidopalladium complexes set the stage for a detailed analysis of the effect of the steric and electronic properties of the ancillary ligand and of the alkene on the rate of insertion. Such effects could then be compared to those known for insertions of alkenes into metal-alkyl complexes, and the effects of the differences in bond polarity, bond strength and the presence or absence of an electron pair could be determined.

In Chapter 3, the synthesis of a series of amidopalladium complexes possessing varied steric and electronic properties and studies on the reactions of these complexes with olefins that reveal detailed information on the insertion process. This series of complexes reacts with ethylene in high yield through a directly observed ethylene amido complex, and they react with vinylarenes having systematically varied electronic properties. This combination of experiments creates a map of the effects of the steric and electronic properties of the system on this new class of alkene insertion reaction. Some of the effects on the rates of these reactions are distinct from those of metal-alkyl complexes, but other effects parallel those observed for insertions into metal-carbon bonds, despite the significant differences in the properties of the reactive metal-ligand bond.

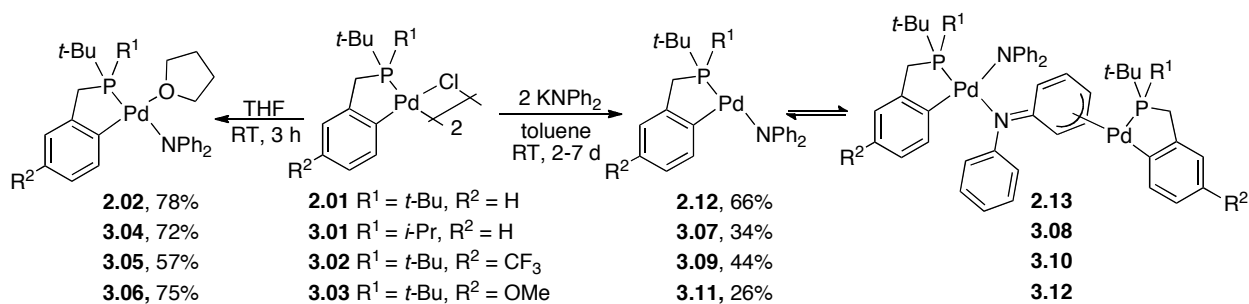
3.2 Results and Discussion

3.2.1 Synthesis and Characterization of Palladium-Diarylamido Complexes

To prepare a series of amidopalladium complexes that undergo migratory insertion reactions with alkenes, we previously targeted complexes that are isoelectronic with the rhodium amides we had shown to undergo intermolecular alkene insertion reactions. To encourage the isolation of monomeric complexes and to discourage C-N bond-forming reductive elimination from unsaturated arylpalladium-amido complexes, cyclometallated species generated from bulky, chelating P-C ligands were synthesized. The synthesis of these complexes was accomplished by a two-step procedure involving initial formation of a dimeric complex with bridging chloride ligands from the reaction of $\text{Pd}(\text{OAc})_2$ with di-*tert*-butylbenzylphosphine and subsequent addition of LiCl in methanol. Reaction of the dimeric chloride complexes with potassium diarylamides generated the diarylamido complexes **2.02-2.06** shown in Scheme 3.1. The characterization of these complexes was reported previously in communication form.¹

To map the effects of the electronic properties of the ligands on the rates of these migratory insertions of alkenes into the Pd-N bonds of the diarylamido complexes, we sought to prepare a series of complexes bearing phosphine ligands with varied steric and electronic properties. Dimeric, cyclometallated palladium-chloride complexes **3.01**, **3.02**, and **3.03** containing different substituents on the cyclometallated benzylphosphine ligand were prepared from the parent benzyl di-*tert*-butylphosphine and from benzyl di-*tert*-butylphosphines containing *meta*-trifluoromethyl and *meta*-methoxy substituents on the phenyl ring. The palladium-diphenylamido complexes were synthesized from the isolated chloride dimers by the addition of KNPh₂ (Scheme 3.2).

Attempts to prepare the analogous amido complexes containing less hindered ligands led to more complicated mixtures of products. Dimeric, cyclometallated palladium chloride complexes containing isopropyl, phenyl, and cyclohexyl groups were synthesized, but attempts to prepare monomeric palladium-diarylamido complexes from these less hindered precursors led to a complex mixture of products. However, less dramatic changes to the steric properties led to isolable species; the monomeric Pd-diarylamido complex **3.04**, which is analogous to **2.02** but containing a ligand derived from benzyl(tert-butyl)(isopropyl)phosphine, was synthesized in pure form by the same route used to prepare **2.02**.



Scheme 3.2. Synthesis of THF ligated palladium-amides **2.02**, **3.04-3.06** and THF-free Pd amides **2.12** and **2.13**; **3.07** and **3.08**; **3.09** and **3.10**; **3.11** and **3.12**.

The structure of the 2-((*t*-Bu)(*i*-Pr))PCH₂C₆H₄-ligated complex **3.04** was determined by X-ray crystallography (Figure 3.1), and this analysis showed that the hydrogen atom in the isopropyl group is directed toward the opposing *tert*-butyl group and that the isopropyl methyl groups face the coordination site occupied by the THF molecule. Thus, the steric effects imparted by the di-*tert*-butylbenzyl phosphine and *tert*-butyl(isopropyl)benzylphosphine on the coordination site that would be occupied by the alkene ligand are not as large as one might first envision. Selected bond angles and lengths of the 2-(*t*-Bu)₂PCH₂C₆H₄-ligated **2.02** and **3.04** are listed in Table 3.1. The structures are similar to each other, but the C(24)-P-C(27) angle between

the quaternary carbon atom of the *tert*-butyl group and the tertiary carbon of the isopropyl group in **3.04** (109.2°) is about 3.8° smaller than the angle between the two quaternary carbons of the *tert*-butyl groups in **2.02** (113.0°). The smaller size of the C-P-C angle in complex **3.04** causes the alkyl substituents on the phosphorus atom of **3.04** to be placed closer to the square plane than they are in complex **2.02**.

While the steric environment around the palladium center of $2-((t\text{-Bu})(i\text{-Pr}))\text{PCH}_2\text{C}_6\text{H}_4^-$ ligated **3.04** is not dramatically different from that of **2.02**, this difference in steric property did affect the structure of the ground state. Significant amounts of the unsymmetrical dinuclear species **3.08** were observed at room temperature by solution NMR spectroscopy, whereas the analogous dinuclear species **2.13** containing di-*tert*-butylphosphino groups was observed in an equilibrium with the THF-free complex **2.12** only at low temperatures.

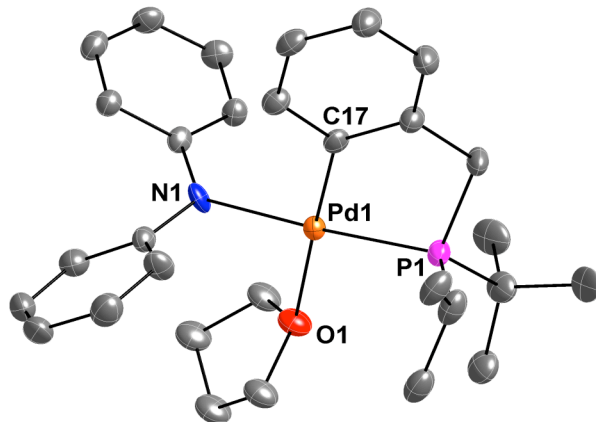


Figure 3.1. ORTEP diagram of **3.04** with 35% probability ellipsoids. Hydrogen atoms are omitted for clarity.

Table 3.1. Selected Bond Distances (\AA) and Angles (degrees) in palladium-amides **2.02** and **3.04**.

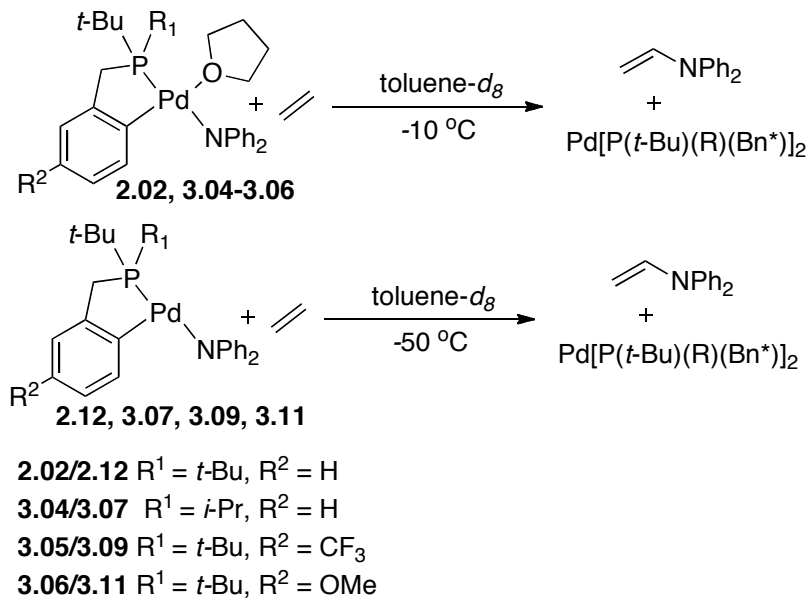
Entry	Parameter	2.02	3.04
1	P-Pd	2.242	2.249(1)
2	P-Pd-C(17)	82.2(3)	82.4(2)
3	P-Pd-N	175.9(2)	176.5(2)
4	C(24)-P-C(27)	109.2	113.0

Three-coordinate amido complexes that lack bound THF would form alkene adducts more readily than the THF-ligated species. To generate amido complexes lacking bound solvent, we conducted the synthesis of the amido complexes in the absence of THF or other basic solvents. The reaction of the cyclometallated palladium chloride dimers with excess KNPh_2 in toluene formed the solvent-free amido complexes **2.12**, **3.07**, **3.09**, and **3.11**. Longer reaction times were needed to prepare **3.07**, **3.09**, and **3.11** than was needed to prepare cyclometallated benzyl phosphine amido complex **2.12**. After one day, all of the chloride complexes **3.01**, **3.02**, and **3.03** were consumed, but intermediates, presumed to be complexes containing bridging chloride and amido groups, were the primary products. After stirring an additional 1-6 days, these intermediates reacted with additional KNPh_2 to generate the desired products. Conducting these reactions at higher temperatures to increase the reaction rate led to the formation of two new, unknown species, as determined by ^{31}P NMR spectroscopy. Recrystallization of the crude material from reactions conducted at room temperature gave pure samples of the THF-free amido complexes in acceptable yields of 26-66%.

3.2.2 Reaction of Palladium-diarylarnido complexes with alkenes

The THF-ligated diarylamido complexes reacted with ethylene and α -olefins to generate enamine products. Reactions of **2.02**, **3.04**, **3.05**, and **3.06** with ethylene in toluene- d_8 occurred at -10 °C to generate *N*-vinyldiphenylamine, $Pd[P(t\text{-}Bu)(R)(Bn^*)]_2$ ($R = t\text{-}Bu$ or *i*-Pr; $Bn^* = -CH_2\text{-}3\text{-}R'\text{-}C_6H_4$, $R' = H, CF_3, OCH_3$) and Pd black. All reactions generated greater than 75% yield of *N*-vinyldiphenylamine. The enamine was characterized by comparison of the 1H NMR spectrum to that of genuine material prepared independently. The Pd(0) complex $Pd[P(t\text{-}Bu)(R)(Bn^*)]_2$ was the only species detected by ^{31}P NMR spectroscopy, and no palladium black was formed in the presence of 1 additional equivalent of $P(t\text{-}Bu)_2(Bn)$.

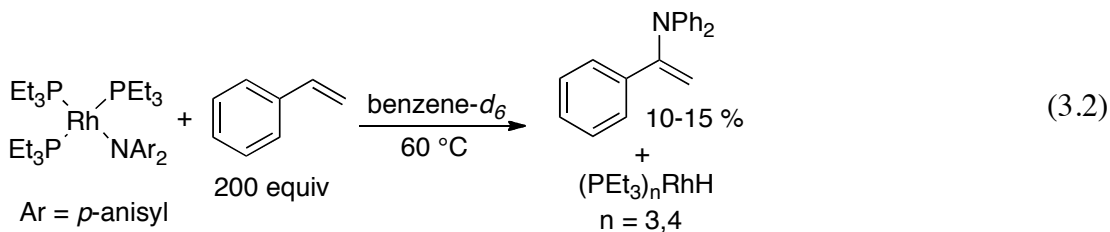
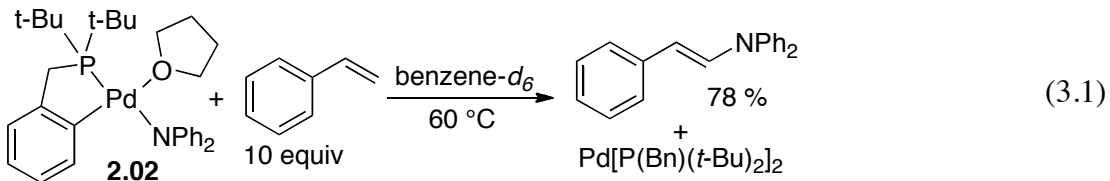
The THF-free amido complexes **2.12**, **3.07**, **3.09**, and **3.11** also reacted with ethylene to generate *N*-vinyl diphenylamine and $Pd[P(t\text{-}Bu)(R)(Bn^*)]_2$ in toluene- d_8 . These reactions occurred below room temperature (-50 °C) to form enamine products in greater than 75% yield. Again, $Pd[P(t\text{-}Bu)(R)(Bn^*)]_2$ was the only palladium product detected by ^{31}P NMR spectroscopy. The rates of the reactions of **2.12**, **3.07**, **3.09**, and **3.11** at -50 °C were similar to those of the THF-ligated species at the higher temperature of -10 °C.



Scheme 3.3. Reactions of THF ligated Pd-Amides **2.02**, **3.04-3.06** and THF-free palladium-amides **2.12**, **3.07**, **3.09**, and **3.11** with Ethylene

Complex **2.02** also reacted with vinylarenes in high yield, but the product of this occurred with regioselectivity distinct from the reactions of alkenes. The reaction of palladium-amide **2.02** with 10 equiv of styrene in benzene- d_6 at $60\text{ }^\circ\text{C}$ generated (*E*)-*N*-benzylidene-1,1-diphenylmethanamine in 78% yield (eq 3.1). In contrast to the reaction of 1-octene with **2.02** that forms enamine products from 1,2-insertion into the metal-nitrogen bond, followed by β -hydrogen elimination (Figure 3.1),¹ the reaction of styrene formed only the enamine product from initial 2,1 insertion into the metal nitrogen bond. Presumably, the formation of this isomer is favored by a combination of the steric interaction of the aryl group on the alkene with the two aryl substituents at nitrogen and the electronic preference for formation of an intermediate with the aryl group located α to the palladium center.² The identity of the organic products from reaction with substituted styrenes was confirmed by independent synthesis through palladium-catalyzed coupling of the corresponding *trans*- α -bromostyrene with HNPh_2 . The regioselectivity

of this process contrasts with that for reaction of $[\text{Rh}(\text{PEt}_3)_3(\text{NAr})]$ and $[\text{Rh}(\text{PEt}_3)_3(\text{NAr}_2)]$ complexes with styrene that formed the ketimine and branched enamine, respectively.³



Palladium amido complex **2.02** containing the cyclometallated benzylphosphine ligand is much more reactive toward alkene insertion than the isoelectronic $[\text{Rh}(\text{PEt}_3)_3(\text{N}(p\text{-anisyl})_2)]$ complex.³ This rhodium complex reacted with styrene to form only 10-15% of the enamine product in the presence of 200 equivalents of styrene at 60 °C (eq 3.2), whereas the palladium complexes formed the enamine product at room temperature in good yield with less than 10 equiv of styrene.

3.2.3 Non-Productive Reactions of Amide 2.02.

To obtain high yields of the enamine from the reactions of alkenes and vinylarenes with amido complexes **2.02**, **3.04-3.06**, **2.12**, **3.07**, **3.09**, and **3.11**, the reactions must be conducted under strictly anhydrous conditions. Preparation of the amido complex in solvents that were not carefully dried generated palladium hydroxo complex **3.13** shown in Figure 3.2. (identified by NMR spectroscopy and X-ray diffraction, see experimental section for more details.) Reactions of the amido complex with ethylene in the presence of adventitious water generated the same hydroxo amido complex.

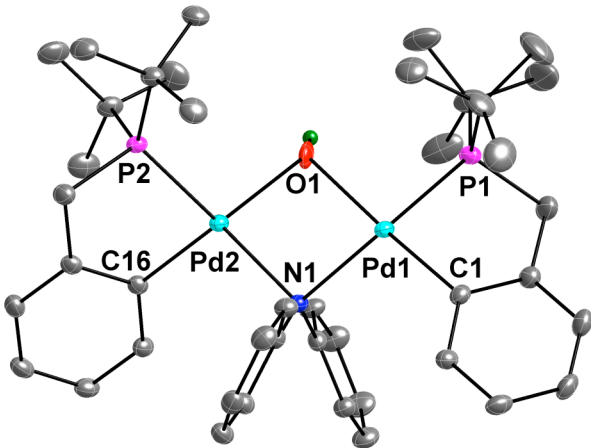
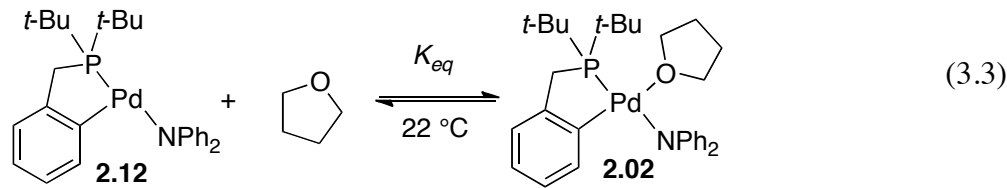


Figure 3.2. ORTEP drawing of **3.13** with 35% probability ellipsoids (The hydrogen atoms, except for the hydroxyl hydrogen, were omitted for clarity).

3.2.4 Comparison of Ethylene and THF Binding to Palladium-amide **2.12**

To measure the rate of migratory insertion directly, the equilibrium constants for dissociation of THF and binding of ethylene to the unsaturated species are needed to ensure that kinetic measurements are conducted under conditions in which the alkene-amido complex is the major species and the observed rate constants correspond as close as possible to that for the migratory insertion step. The THF-bound amido complex **2.02** equilibrates with the combination of free THF and the three-coordinate amido species **2.12** on the NMR timescale (eq 3). This equilibration was revealed by the large difference in ^{31}P NMR chemical shifts of the THF-ligated amide **2.02** in THF- d_8 (δ 88.0 ppm) and benzene- d_6 (δ 98.7 ppm). For reference, the ^{31}P NMR chemical shift of **2.12** in benzene- d_6 was δ 101.7 ppm. The equilibrium constant for dissociation of THF from **2.02** at 22 °C was determined more precisely by obtaining spectra of samples of **2.02** containing different concentrations of THF in toluene- d_8 . The equilibrium constant was

determined to be 6.8 M^{-1} at room temperature from a fit of the plot (Figure 3.3) of the ^{31}P chemical shift vs. the concentration of added THF to eq 3.4.



$$\delta_{obs} = \frac{\delta_{2.12} + K_1 \delta_{2.02} [\text{THF}]}{1 + K_1 [\text{2.12}][\text{THF}]} \quad (3.4)$$

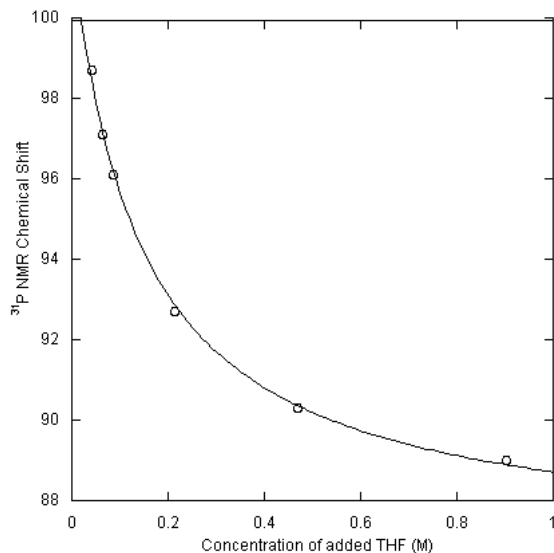


Figure 3.3. Plot of ^{31}P NMR chemical shift of **2.12** vs. concentration of added THF. The data were fit to eq 3.4.

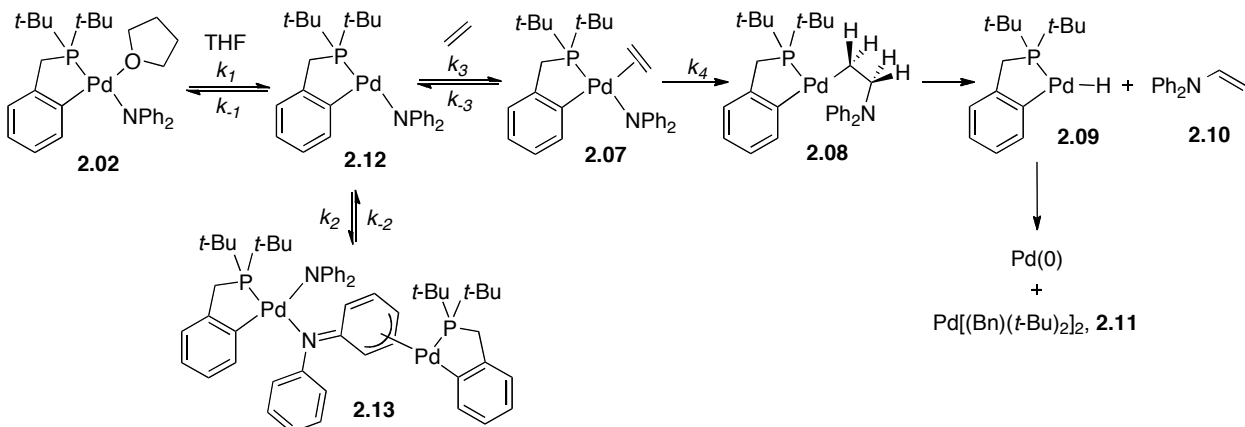
The chemical shift of THF-bound **2.02** also depended on temperature, due to the change in the equilibrium constant for dissociation of THF with temperature. The chemical shift at $-60 \text{ }^\circ\text{C}$ was δ 88.0 ppm; the chemical shift at $40 \text{ }^\circ\text{C}$ (101.1 ppm) was closer to that of the THF-free species **2.12**. From the observed chemical shifts at various temperatures, the equilibrium

constants for the association of THF shown in eq 3.3 were determined (see experimental section), and from the temperature dependence of the equilibrium constants, the enthalpy and entropy were found to be $\Delta H = -11.3$ kcal/mol and $\Delta S = -34.0$ cal/mol. The enthalpy corresponds to the Pd-O bond strength.

We previously reported that the THF-free complex **2.12** equilibrates with the ethylene-amido complex **8** in the presence of ethylene, and determined that the equilibrium constant for ethylene binding at -65 °C is 0.09 ($\Delta G = 1.0$ kcal/mol).¹ If we assume the entropy for binding of ethylene is similar to that for binding of THF, then the Pd-ethylene bond dissociation enthalpy is -6.1 kcal/mol, and the Pd-ethylene bond is weaker than the Pd-THF bond. These data are consistent with the observation by ^{31}P NMR spectroscopy of only complex **2.02** from the reaction of THF-ligated amido complex **2.02** with 50 equiv of ethylene at -10 °C.

3.2.5 Reaction Mechanism of Reaction of Ethylene with Palladium-Amide 2.02

As previously reported, the addition of ethylene to the THF-free amido species **2.12** at -65 °C generates a rapidly equilibrating mixture of **2.12** and ethylene amido complex **2.07** (Scheme 3.4). In addition, the monomeric Pd-amido species **2.12** partially converts to the unsymmetrical dimer **2.13** in an equilibrium process at low temperature. The olefin-amido complex undergoes insertion at -50 °C. At -50 °C, two resonances corresponding to the dinuclear species are observed in the ^{31}P NMR spectrum in addition to the resonance observed for **2.07**. These two complexes decay in concert, implying that the equilibrium between **2.12** and **2.13** is established faster than the olefin insertion process



Scheme 3.4. Proposed reaction mechanism of the reaction of Pd-amides **2.02** and **2.12** with ethylene.

The equilibria involving binding of THF and ethylene to amido complex **2.12** described in this paper, along with the previously reported data concerning the reaction of ethylene amido species **2.07**, support the mechanism shown in Scheme 3.4 for the reaction of palladium-diarylamides **2.02** and **2.12** with ethylene. In this mechanism, THF rapidly and reversibly dissociates from complex **2.02**, and the resulting THF-free complex **2.12** binds ethylene to generate the olefin-amido adduct **2.07**. Although square-planar complexes typically undergo ligand exchange by associative processes, the direct observation of the equilibrium for dissociation of THF suggests that complex **2.02** equilibrates with ethylene by a dissociative process. Complex **2.07** then undergoes migratory insertion to generate the proposed alkylpalladium intermediate **2.08**. Intermediate **2.08** then rapidly decomposes by β -hydrogen elimination to form a Pd-hydride complex (**2.09**), and complex **2.09** undergoes C-H bond-forming reductive elimination to generate Pd[P(Bn)(*t*-Bu)₂]₂ (**2.11**) and Pd black. In the presence of excess P(Bn)(*t*-Bu)₂, the unsaturated product of reductive elimination binds the phosphine,

and $\text{Pd}[\text{P}(\text{Bn})(\text{t-Bu})_2]_2$ is the only product observed by ^{31}P NMR spectroscopy. Intermediates **2.08** and **2.09** were not observed during the course of the reaction.

3.2.6 Reactions of Alkene-Amido Complex.

To gain information on the rate constant of the individual insertion step (k_4), the observed rate constant for the reaction of the pure olefin-amido complex **2.07** was measured at different concentrations of ethylene. If the mechanism in Scheme 3.4 is followed, then the value of k_{obs} should approach the value of the insertion step under conditions in which the equilibrium lies far toward the ethylene amido complex **2.07**. The approximate observed rate constant was determined by plotting the decay of the concentration of the ethylene adduct **2.07** vs. time and fitting the curve to an exponential decay. A good fit was observed, but the decay of **2.07** is not precisely first-order due to the presence of a small amount of dimer **2.13**. The order of the reaction is not an integer value, and the observed rate constant for the decay of the concentration of **2.07** changes over the course of the reaction. A more detailed treatment of the data, including kinetic simulations, are presented later in this section and rigorously determine the rate constant for the insertion step. A plot of the approximate k_{obs} for the reaction of **2.12** vs. the concentration of ethylene is shown in Figure 3.4. At low concentrations of ethylene, the rate is positively dependent on the concentration of ethylene, but at high concentrations the rate constant approaches a constant value.

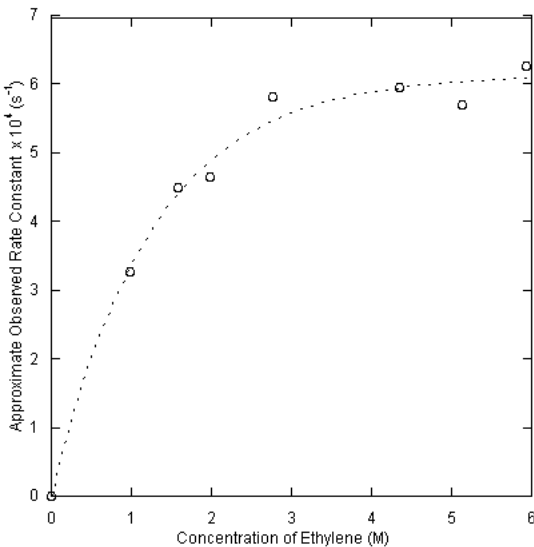
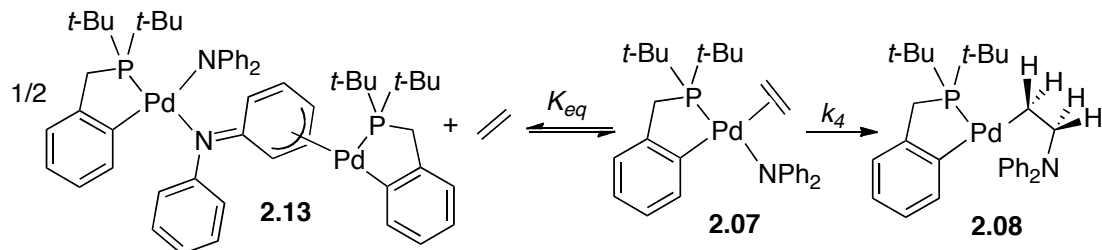


Figure 3.4. Approximate Observed Rate Constant for the reaction of **2.12** with ethylene vs. the concentration of Added Ethylene.

Under conditions in which **2.12** is allowed to react with high concentrations of ethylene (150 equiv), the concentration of the olefin adduct is much larger than the concentration of the three-coordinate monomer **2.12**, and the kinetic expression corresponding to the mechanism in Scheme 3.4 can be simplified. However, fitting of the dependence of k_{obs} on [ethylene] is complicated by the equilibrium between **2.12** and the unsymmetrical dimer **2.13**. Fortunately, the olefin adduct **2.07** equilibrates with the unsymmetrical dimer **2.13** and free ethylene faster than it undergoes migratory insertion. During the reaction of **2.12** with 150 equiv of ethylene, 15 % of the unsymmetrical dimer **2.13** was observed by ^{31}P NMR spectroscopy, and the resonances for **2.13** decay in concert with that observed for the ethylene adduct **2.07**.

To determine precisely the rate constant for the migratory insertion step (k_4), we simulated the kinetic data of the simplified process in Scheme 3.5 with the software KINSIM⁴ and iteratively fit the experimentally collected decays of **2.13** and **2.07** over time to the simulated

data with the software FITSIM.⁵ The experimental data fit the simulated decay curves well (see Figure 3.5), and this analysis showed the rate constant for the C-N bond-forming migratory insertion step (k_4) to be $8.7 \pm 0.5 \times 10^{-4} \text{ s}^{-1}$.



Scheme 3.5. Simulated reaction mechanism of Pd-amide **2.12** with ethylene

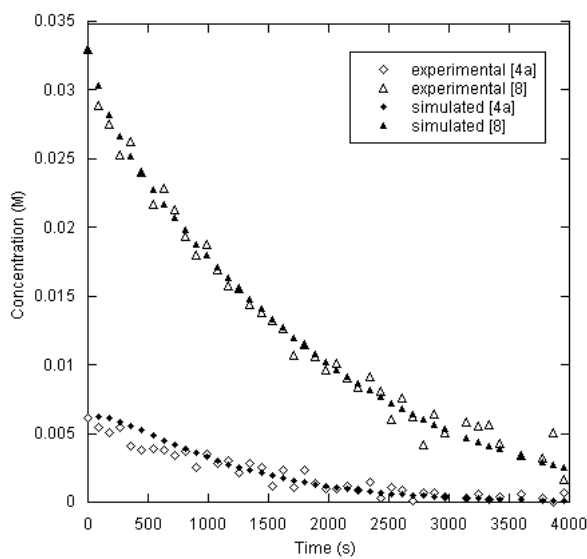
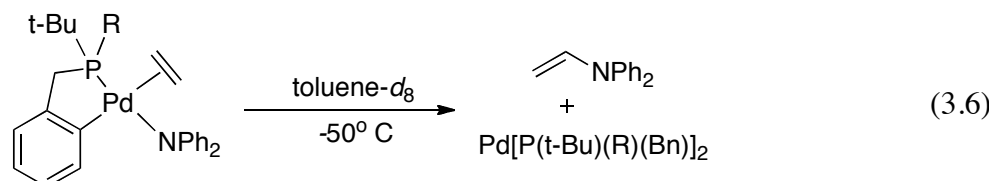
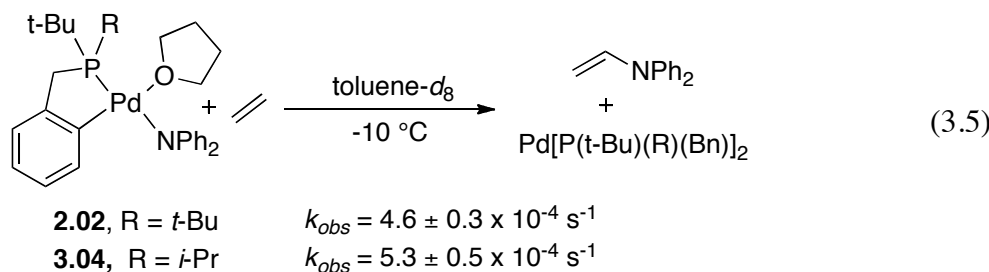


Figure 3.5. Experimental and Simulated Decay Curves of the reaction of **2.12** with ethylene

3.2.7 Steric Effects of the Ancillary Ligand

To evaluate the steric effects of the ancillary ligand on the migratory insertion step, we compared the structure and reactivity of amido complex **3.04** ligated with a cyclometallated (*tert*-butyl)(isopropyl)benzylphosphine ligand to those of the complex **2.02** ligated by the

cyclometallated di(*tert*-butyl)benzylphosphine ligand. The rate constants for the reactions of THF-ligated complexes **2.02** and **3.04** with ethylene are shown in eq 3.5. These observed rate constants correspond to the product of the equilibrium constant for the exchange of ethylene for THF and the rate constant for the migratory insertion step. The reaction of the less hindered **3.04** was faster than that of **2.02**, but by approximately the sum of the standard deviations. The similarity in the rate constant for reaction of **2.02** and **3.04** could be due to similar equilibrium constants for binding and insertion of ethylene by the two complexes or to counterbalancing steric effects on the binding and insertion step. The following experiments and computations distinguish between these possibilities



The rate constants for migratory insertion of ethylene into the Pd-N bond of complexes **2.12** and **3.07** are shown in eq 3.6. In contrast to the reactions of **2.12**, the reaction of the 2-((*t*-Bu)(*i*-Pr))PCH₂C₆H₄ ligated **3.07** with ethylene at -50 °C did not contain measurable quantities of the unsymmetrical dimer **3.02.07** after the pre-equilibrium for binding of ethylene had been

established. After addition of ethylene, the amount of the ethylene adduct **3.07** was small, but after approximately 20 min (vs a $t_{1/2} = 2$ h for the insertion process), the dinuclear species **3.08** was completely converted to the ethylene adduct of **3.07**. Thus, the decay of this adduct was measured after the pre-equilibrium had been established, and this portion of the data were fit to an exponential decay to determine the rate constant for migratory insertion. The rate constant for insertion of ethylene into the less sterically encumbered amido complex **3.07** was 0.97×10^{-4} s⁻¹ ($\Delta G^\ddagger = 17.0$ kcal/mol). This rate constant is almost an order of magnitude smaller than the rate constant for insertion of ethylene into the more sterically encumbered complex **2.12** (8.7×10^{-4} s⁻¹, $\Delta G=16.0$ kcal/mol). These results suggest that steric hindrance at the phosphorus atom decreases the barrier to the C-N bond-forming step of the migratory insertion process.

3.2.8 Computed Free Energy Barriers for Insertion of Ethylene into the Pd-N Bonds of Amido Complexes **2.12** and **3.07**.

To evaluate further the effect of the steric environment around the palladium atom on the migratory insertion process, a series of computations were performed on the reaction of olefin amido complexes **2.12** and **3.07**. These computations were conducted using density functional theory as implemented by the Gaussian 09 package.⁶ The B3LYP functional with polarized triple- ζ basis sets has been shown to generate accurate results for many palladium systems⁷⁻⁹ and was, therefore, used for calculations of the reactivity of **2.12**, **3.07**, and an analogous complex ligated by a truncated 2-(CH₃)₂PCH₂C₆H₄ ligand.

Because the precise structure of the ethylene amido complex **2.07** is unknown, reactions of the two isomers of **2.07** with the alkene *cis* or *trans* to the phosphorus atom were computed. The *cis* isomer contains the alkene in the coordination site of the THF in complex **2.02**. The ground state

of the *cis* isomer is lower than that of the *trans* isomer by 2.4 kcal/mol, and the free energy of activation from the *cis* ground state to the *cis* transition state was 0.5 kcal/mol lower than the free energy of activation from the *trans* ground state to the *trans* transition state. Thus, to determine the steric effect of the ancillary ligand on the migratory insertion step, the reactions of ethylene with the *cis* isomers of a series of olefin amido complexes ligated by $2-((t\text{-Bu})(i\text{-Pr}))\text{PCH}_2\text{C}_6\text{H}_4$ and $2-(\text{CH}_3)_2\text{PCH}_2\text{C}_6\text{H}_4$ were computed.

The optimized ground-state structure of **2.07**, and the structure of the transition state for the insertion reaction of **2.07** are shown in Figure 3.6. In the ground-state structure of **2.07**, the centroid of the ethylene ligand lies in the square plane, and the C-C double bond is oriented perpendicular to that of the square plane. The computed distance of the Pd-ethylene bond is 2.50 Å. In the transition state structure for insertion, the olefin has rotated approximately 90° and lies parallel to the Pd-N bond. The distance between the palladium and the closest ethylene carbon is 2.27 Å, and the C-N distance is 2.04 Å. The hydrogen atoms on the ethylene are splayed away from the Pd-center, and the H-C-H angle is 106°, which is less than the 109° of an sp^3 hybridized carbon.

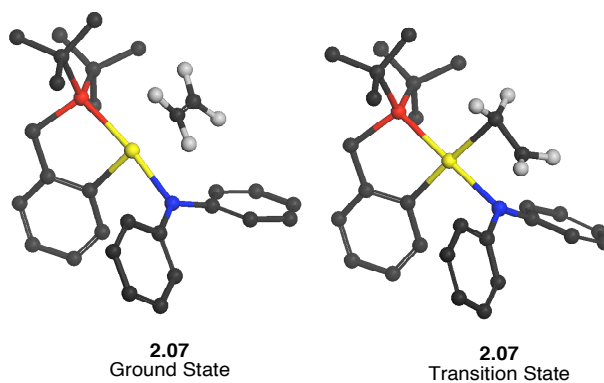


Figure 3.6. Optimized Ground State and Transition State Structure of the Olefin Amido Adduct **2.07**.

The immediate product from the insertion process has an azametallocyclobutane structure in which the nitrogen atom forms a dative bond to the palladium center. The angles at the β -carbon of this product indicate that the ethylene carbons are hybridized in an sp^3 fashion. The Pd-C distance (2.14 Å) is typical for a palladium-carbon bond, and the C-N distance (1.52 Å) is typical for a C-N single bond.

The computed free energies for migratory insertion of ethylene into the amido complexes containing the three cyclometallated ligands, $2-(t\text{-Bu})_2\text{PCH}_2\text{C}_6\text{H}_4$, $2-((t\text{-Bu})(i\text{-Pr}))\text{PCH}_2\text{C}_6\text{H}_4$, and $2-(\text{CH}_3)_2\text{PCH}_2\text{C}_6\text{H}_4$, are shown in Figure 3.7. The free energy of activation for reaction of complex **2.07**, which is ligated by the bulkiest ligand $2-(t\text{-Bu})_2\text{PCH}_2\text{C}_6\text{H}_4$ was computed to be the lowest (15.6 kcal/mol). The free energy barrier for reaction of the $2-((t\text{-Bu})(i\text{-Pr}))\text{PCH}_2\text{C}_6\text{H}_4$ -ligated complex was computed to be about 1 kcal/mol higher (16.5 kcal/mol) than that of the $2-(t\text{-Bu})_2\text{PCH}_2\text{C}_6\text{H}_4$ -ligated complex, and the free energy barrier for reaction of the least bulky complex ligated by $2-(\text{CH}_3)_2\text{PCH}_2\text{C}_6\text{H}_4$ to be the highest (12.14.0 kcal/mol). These computed free energies are consistent with the activation barriers measured experimentally. The difference in free energies determined experimentally for reaction of **2.12** and **3.07** was 1.0 kcal/mol. Thus, both the experimental and computational results indicate that greater steric bulk on the phosphorus atom leads to a lower barrier for migratory insertion, even though the coordination number of the complex does not change during insertion of an alkene into an amido complex.

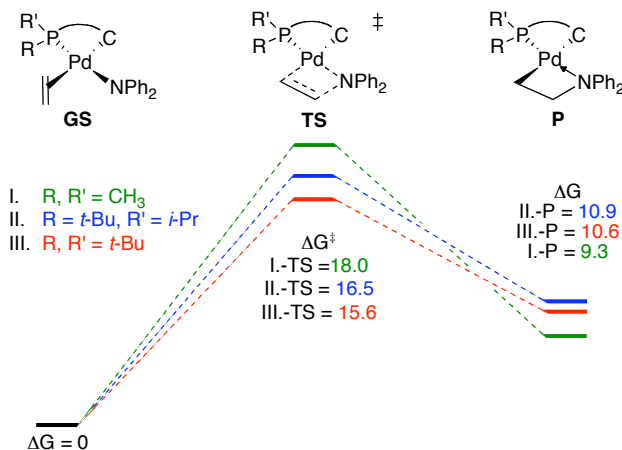


Figure 3.7. Optimized Ground State and Transition State Energies for Ethylene Insertion into P-C Ligated Pd-amido Complexes

An analysis of the computed structures of the ground and transition states provides a rationalization for the steric effect. In the computed ground-state structure, the olefin is located *cis* to the phosphorus atom, and the steric interactions between the ethylene hydrogens and the alkyl groups on the phosphorus atom are greater than they would be in other conformations. As the complex adopts the structure of the transition state in which the C-C bond lies parallel to the Pd-N bond, the distance between the alkene carbons and the phosphorus atom increases, and the steric interactions between the alkyl groups on the phosphorus atom and the alkene ligand decrease. This decrease in steric interaction from the ground to transition state is consistent with the lower barrier for reaction of the more hindered complex.

Although the barrier for the migratory insertion step is lower for the more sterically congested complex than for the less sterically congested compound, the reactions of ethylene with the THF-ligated amides **2.02** and **3.04** are not faster for the more hindered complex than for the less hindered compound. The difference between the rates of reaction of the sterically more and less hindered complexes containing and lacking bound THF results from a difference in

binding energy of ethylene and THF to the more and less hindered amido palladium fragments. The data from which these equilibrium constants were determined for **3.07** are provided in the experimental section and the data from which they were determined for **2.12** are presented in chapter 2. The K_{eq} at 22 °C for binding of THF to the less sterically congested **3.07** is 14 M⁻¹ whereas the K_{eq} for binding of THF to the more hindered **2.12** is 6.8 M⁻¹ (ratio of K_{eq} values =2). The K_{eq} at -65 °C for binding of ethylene to **3.07** is 149 M⁻¹, whereas the K_{eq} for binding of ethylene to **2.12** is 11 M⁻¹ (ratio of K_{eq} values =13). These data demonstrate that the binding affinity of THF to the less sterically congested **3.07** is two times greater than the binding affinity of THF to **2.12**. However, the binding affinity of ethylene to **3.07** is about 13 times greater than the binding affinity of ethylene to **2.12**. Although the ethylene adduct of the THF-free amido complex **3.07** has a 1.0 kcal/mol higher barrier for the migratory insertion step than the ethylene adduct of **2.12**, the difference in binding of ethylene to **3.07** and **2.12** is larger than that for binding of THF, and this difference leads to the slightly faster overall rate for the reaction of **3.04** with ethylene than for the reaction of **2.02** with ethylene.

Steric effects on migratory insertion reactions have rarely been evaluated.^{10,11} The binding equilibrium and the migratory insertion step are rarely separated, and the direct precursor to insertion is rarely observed directly.¹²⁻¹⁶ In one study, Bercaw did report similar results to those we obtained for insertions of propene into niobium–hydride and tantalum–hydride bonds.¹¹ The rate constants measured for insertion of permethylmetallocene and unsubstituted metallocene propylene hydride complexes followed the trend Cp*₂Nb(CH₂=CHCH₃)H > Cp₂Nb(CH₂=CHCH₃)H > Cp*₂Ta(CH₂=CHCH₃)H > Cp₂Ta(CH₂=CHCH₃)H. The authors attribute this trend to the greater steric interactions between the methyl group of the propene and the methyl groups on the Cp* ligands in the ground states than in the transition states. In the

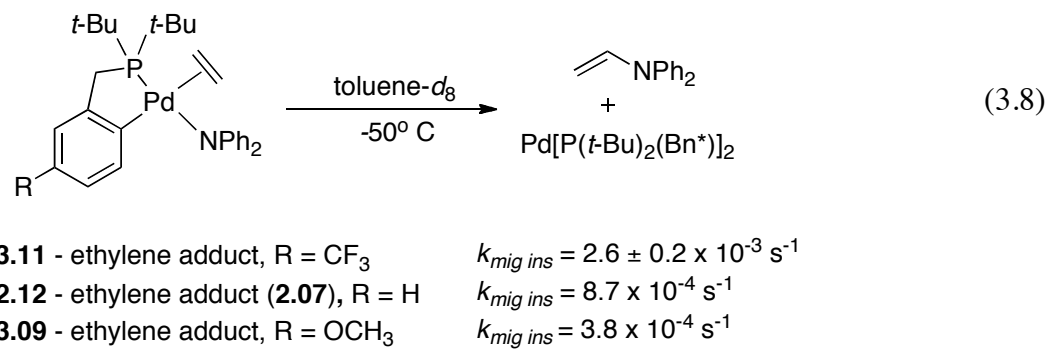
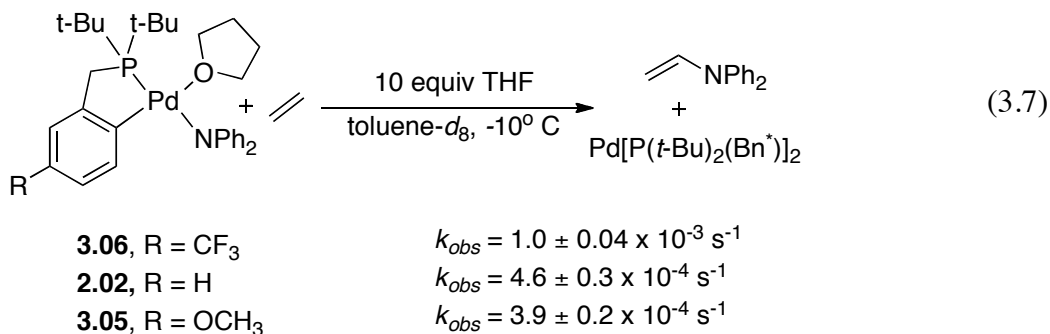
ground state, the olefin lies in the plane bisecting the two Cp* ligands and the hydrogen atoms and methyl group on the alkene are pointed toward the methyl groups on the Cp* ligand. The transition state structure is less sterically congested because the methyl group becomes more distant from the Cp rings as the product alkyl ligand emerges. This change in structure and accompanying decrease in steric effects from the ground to transition state leads to the faster rate for insertion of the permethylmetallocene derivatives.

3.2.9 Electronic Effects of the Ancillary Ligand

To examine the electronic effect of the ancillary ligand on the rate of migratory insertion, THF-ligated, palladium-diarylamido complexes were synthesized that contain substituents in the 3-position of the benzylphosphine aryl ring. Complex **3.06**, which contains an electron-withdrawing trifluoromethyl group and complex **3.05**, which contains an electron-donating methoxy group in this position on the benzylic aryl ring, were allowed to react with ethylene in toluene at -10 °C. The decay of the palladium-amide was monitored by ¹H NMR spectroscopy, and the rate constants for reactions of these complexes and the unsubstituted complex **2.02** are shown in eq 7. Trifluoromethyl-substituted **3.06** reacted about 2.5 times faster than the parent complex **2.02**, and complex **2.02** reacted slightly faster than methoxy-substituted **3.05**.

These observed rate constants are a composite of the equilibrium constants for exchange of ethylene for THF and the rate constant for insertion. Thus, to measure the electronic effects of the ancillary ligand on the individual migratory insertion step, the reactions of ethylene with the benzylphosphine-ligated amido complexes **2.12**, **3.09**, and **3.11** lacking a THF were conducted. Complexes **2.12**, **3.09**, and **3.11**, were allowed to react with a large excess of ethylene at -50 °C, and the decay was monitored by ³¹P NMR spectroscopy. The rate constants for the migratory

insertion step with complexes **2.12** and **3.09** were determined by kinetic simulation as detailed earlier in this paper. Because the reaction of **3.11** with ethylene did not form an observable amount of dimer **4h**, the rate constant for migratory insertion could be determined directly from the exponential decay of the ethylene adduct of **3.11**. The reaction rates and the free energies of activation are listed in eq 3.8. The trifluoromethyl-substituted complex **3.11** reacted about two times faster than the unsubstituted complex **2.12**, and complex **2.12** reacted about two times faster than the methoxy-substituted complex **3.09**. These kinetic data indicate that the complexes in this series containing a more electron-poor metal center undergo the elementary migratory insertion step faster than those containing a more electron-rich metal center.



The trend observed for the insertions of ethylene into the metal-nitrogen bond of palladium-amido complexes parallels the trends observed for insertion of ethylene into metal-carbon and metal-hydrogen bonds. Generally, complexes containing more electrophilic metal centers

undergo migratory insertion faster than those containing less electrophilic centers.^{17,18} However, it is difficult to deduce whether the equilibrium constant for binding of the olefin or the rate constant for migratory insertion is responsible for the faster rates typically observed for the insertions of more electron-poor metal centers because increasing the electrophilicity of the metal center typically results in stronger binding of the olefin.

A comparison of the rates of migratory insertion of the palladium–amido complexes and more electrophilic lanthanide and group IV amido complexes can be made, although one must appreciate that there are multiple differences between the structures and the reactions of the early-metal systems and the palladium complexes. The amido groups in the more electrophilic amido complexes (general alkylamides) are different from those in the palladium amido complexes reported here (diarylamides), and the reactions of the lanthanide systems are intramolecular, whereas the reactions of the palladium amides are intermolecular. Despite these differences, the two types of complexes undergo insertion of alkenes into metal-amido linkages with similar rates.

Marks and coworkers reported computational and experimental studies of the mechanism of the cyclization of aminoalkenes catalyzed by organolanthanide complexes containing permethylcyclopentyldienyl ligands.^{19,20} This work showed that the free energy of activation (ΔG^\ddagger) of the intramolecular migratory insertion of an alkene unit within a lanthanide aminoalkene complex is roughly 21-24 kcal/mol. They have also studied the insertion step computationally and found a free energy of barrier $\Delta G^\ddagger = 12.5$ kcal/mol.²⁰ However, the reaction was conducted above room temperature. Thus, this free energy is calculated incorrectly, or migratory insertion is not the turnover limiting step.

Thus, the free energies of activation for insertions of alkenes into the more electrophilic lanthanide-amido complexes are higher than the 16 kcal/mol free energy barrier for insertion of ethylene within the amidopalladium olefin complex **2.07**. However, the entropic contribution to the ΔG^\ddagger for insertion into the lanthanide amides was found to be large. The ΔH^\ddagger barrier for the migratory insertion of ethylene within complex **2.07** was computed to be 14.0 kcal/mol and this enthalpic barrier is that is similar to the experimentally measured ΔH^\ddagger barrier of 12.7 kcal/mol for organolanthanide complexes. Of these two values, ΔH^\ddagger would be most affected by the electronic properties of the two systems. Perhaps the effect of the greater electrophilicity of the lanthanide amide complexes and the greater bond strength of the lanthanide amides counterbalance each other.

The free energy barriers for insertions of alkenes into group IV amides are also higher than those for the palladium amides. The hydroamination of an aminoalkene catalyzed by constrained-geometry *ansa*-ligated Zr complexes occurred over days at 100-120 °C.²¹ This reaction was proposed to occur by turnover-limiting insertion of the alkene into the metal-amido bond. The elevated temperatures and long times required for cyclization indicate that the barrier for insertions of alkenes into the Zr-N bond is much higher than that for insertion into both the lanthanide-amide and palladium-amide bonds. This higher barrier for reaction of the zirconium complex likely results from an increased strength of the metal-nitrogen bond due to π -donation of the amide lone pair to the d⁰ metal center.^{22,23} This comparison of the barriers to group IV amides is made tentatively because the entropy and enthalpy of activation for insertions into the group IV amido complexes have not been reported.

3.2.10 Electronic Effects of the Olefin on the Rate of Insertion

The reactions of **2.02** with a series of vinylarenes was conducted to reveal the effect of the electronic properties of the vinylarene on the rates of insertion. Amido complex **2.02** was allowed to react with a series of vinylarenes containing electron-donating and electron-withdrawing substituents at the *meta* and *para*-positions, and the rate constants for these reactions were measured by ^1H NMR spectroscopy. The yields and rate constants for these reactions are summarized in Table 3.2.

In general, reactions of Pd-amide **2.02** with electron-poor vinylarenes generated enamine products in higher yields than reactions of **2.02** with electron-rich vinylarenes. The reaction of **2.02** with *p*-(trifluoromethyl)styrene gave 95 % yield of the (*E*)- β -aminoethylarene, whereas the reaction of amide **2.02** with *p*-methoxystyrene gave only 11% yield of the enamine product. In the latter case, decomposition of the amido complex by protonation of the palladium-nitrogen bond was faster than migratory insertion.

Consistent with the difference in reaction yields, the reactions of complex **2.02** with vinylarenes containing electron-withdrawing substituents were faster than those containing electron-donating substituents. For example, the reaction of **2.02** with *p*-(trifluoromethyl)styrene was more than three times faster than the reaction of **2.02** with styrene. Likewise, the reaction of **2.02** with styrene was almost two times faster than the reaction of **2.02** with the more electron-rich *p*-methylstyrene. Figure 3.8 shows a Hammett plot of $\log(k_x/k_h)$ versus σ derived from the data in Table 3.2. The ρ value is 1.04 ($r = 0.988$). This positive ρ value indicates an accumulation of negative charge or a decrease in the partial positive charge on the olefin in the transition state for migratory insertion.

Table 3.2. Reactivity of palladium-amide **2.02** with functionalized

Entry	Styrene	Product	Yield (%)	k_{obs} (s ⁻¹)
1			11	-
2			40	0.94×10^{-3}
3			78	1.5×10^{-3}
4			61	1.7×10^{-3}
5			87	4.3×10^{-3}
6			95	4.9×10^{-3}

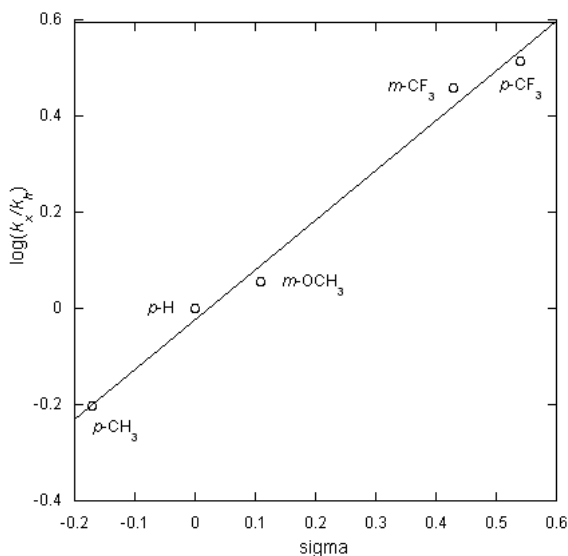


Figure 3.8. Hammett plot of the reaction of palladium-amide **2.02** with substituted styrenes.

To begin to determine the origin of the the observed electronic effects, we evaluated the relative binding affinities of the different vinylarenes. We attempted to generate the amido styrene complex from the reaction of amido complex **2.12** lacking THF with styrene in benzene-*d*₈, but no change in the ³¹P or ¹H NMR signals of complex **2.12** was observed. To assess independently the potential accumulation of a styrene amido complex, we compared the relative rates for reactions of **2.02** with two vinylarenes in separate reactions with the ratio of products from the reaction of **2.02** with two vinylarenes together. In the absence of the accumulation of an amidopalladium vinylarene complex as an intermediate, one would expect the reaction with the two vinylarenes together to form about a 2:1 ratio of (*E*)-*N*-phenyl-*N*-(3-methoxy)styryl)aniline to (*E*)-*N*-phenyl-*N*-(4-methyl)styryl)aniline. If a vinylarene complex accumulates, this ratio would likely be different and be skewed toward the complex that forms the more stable adduct. In the event, the reaction of **2.02** with 5 equiv of 4-methylstyrene and 5 equiv of 3-methoxystyrene generated enamine products in a total yield 60% yield consisting of a ~2:1 ratio

of (*E*)-*N*-phenyl-*N*-(3-methoxy)styryl)aniline to (*E*)-*N*-phenyl-*N*-(3-methyl)styryl)aniline. This experiment corroborates the lack of accumulation of a stable amidopalladium vinylarene complex determined by the lack of a change in the NMR spectroscopic signals of **2.02** upon addition of styrene.

Thus, we assessed the relative binding energies of the vinylarenes to the benzylphosphine-ligated palladium-amido fragments using density functional theory. Although the differences in binding energies of the different vinylarenes are not large, the ground state energies should be reliable, and the relative, rather than absolute, binding energies are the important values for this analysis.

The energies of the vinylarene-amido complexes containing 4-methylstyrene and 3-methoxystyrene were minimized. The initial structures were generated by replacing ethylene in the computed structures of the ethylene amido complex **2.07** with a vinylarene. The energies of four isomers with different orientations of the vinylarenes were minimized, and the same isomer was found to have the lowest energy for both vinylarenes complexes. The palladium-styrene bond is relatively long for a Pd-alkene bond (2.72 Å). The alkene unit is oriented perpendicular to the square plane, and the aryl group of the styrene is located *cis* to the phosphorus atom.

The computed relative free energies (ΔG°) of the styrene-amido complexes are shown in the free energy diagram for reaction of THF-complex **2.02** with 4-methylstyrene and 3-methoxystyrene (Figure 9). The complex of the more electron-rich vinylarene, 4-methylstyrene, was computed to be 1.2 kcal/mol more stable than the complex of 3-methoxystyrene, whereas the experimental free energy barrier (ΔG^\ddagger) for reaction of the 3-methoxystyrene complex was found to be 0.4 kcal/mol lower than that of 4-methylstyrene. As depicted in Figure 3.9, this combination of experimental and computational data imply that the free energy barrier for the

elementary migratory insertion step of the 3-methoxystyrene complex is 1.6 kcal/mol smaller than that for the same reaction of the 4-methylstyrene complex.

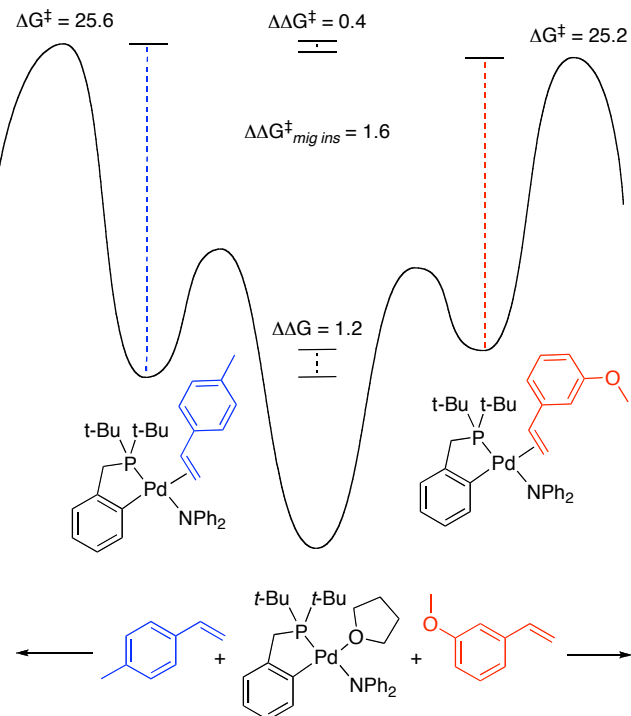
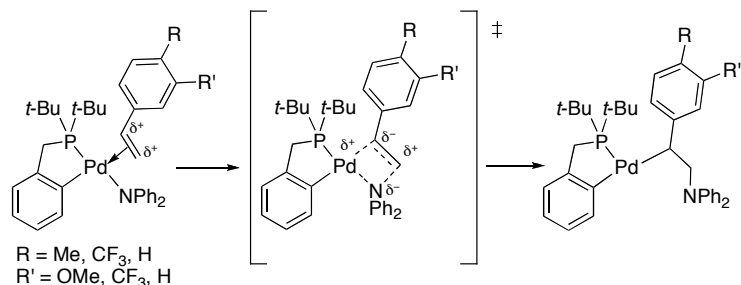


Figure 3.9. Energy Diagram for the reaction of palladium-amide **2.02** with substituted styrenes.

The relative energies of the DFT-optimized, ground-state styrene complexes are shown. All energies have the units of kcal/mol.

Because electron-rich vinylarenes bind more strongly to the palladium center than electron-poor vinylarenes, the coordination of alkenes to this Pd(II) center involves a net flow of electrons from the alkene to the metal. Typically, the alkene in palladium-olefin complexes acts primarily as a sigma donor.^{24,25} The immediate product from insertion of the olefin into the metal-nitrogen bond is an aryl-substituted 2-aminoalkyl ligand that places a negative charge on the Pd-bound carbon. Therefore, we propose that the observed electronic effect results from a positively

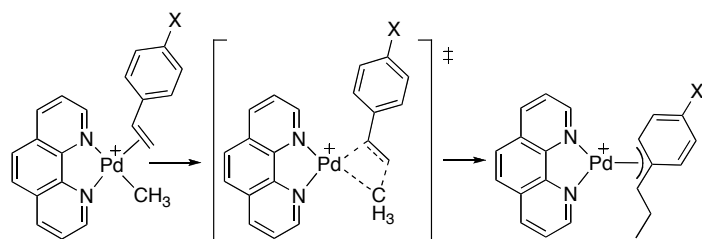
charged alkene ligand becoming a negatively charged alkyl ligand through a transition state that reflects this overall change in the property of the α -carbon of the vinylarene (Scheme 3.6).



Scheme 3.6. Reaction of palladium-amide **2.02** with substituted vinylarenes

3.2.11 Comparison of the electronic effects of the alkene to those of insertions of alkenes into metal-hydride and metal-alkyl bonds.

The ρ value observed for the insertion of substituted styrenes into the palladium-nitrogen bonds of palladium-amides ($\rho = 1.04$, $r = 0.988$) was similar to the ρ value obtained by Brookhart and coworkers ($\rho = 1.1 \pm 0.1$, $r = 0.991$) during a study of the electronic effects of the migratory insertion of *para*-substituted vinylarenes into methylpalladium complexes (Scheme 3.7).²⁶ In this study, the binding affinities of the *para*-substituted styrenes were measured, and the relative free energies of activation ($\Delta\Delta G^\ddagger$) were determined. These data indicate that the effect of the electronic properties of the olefin on the relative energies of the ground states was larger than the effect of the electronic properties of the olefin on the relative energies of the transition states. This result parallels the trend we deduced from our studies of the rates of migratory insertion of substituted vinylarenes into Pd-N bonds.



Scheme 3.7. Reaction of *para*-substituted styrenes with methyl palladium complexes

The electronic effects on the coordination and insertion steps of the reaction of substituted vinylarenes with $\text{RhH}_2\text{Cl}(\text{PPh}_3)_3$ measured during early studies by Halpern were different from those deduced for the insertions into palladium amide and alkyl bonds.²⁷ Electron-poor styrenes bind to these rhodium complexes more strongly than do electron-rich styrenes, and the insertion of the styrene into the Rh-H bond was slower for electron-poor styrenes than for electron-rich styrenes. Similarly, Bercaw studied the binding of vinylarenes to a cyclopentadienyl-ligated niobium hydride complex and the subsequent migratory insertion of the styrene into the Nb-H bond. The ρ values for binding of the styrene to the Nb center and for the insertion reaction of *endo*- $\text{Cp}_2\text{NbH}(4\text{-X-C}_6\text{H}_4\text{CH=CH}_2)$ were +2.2, and -1.06, respectively.^{11,28} These results demonstrate that the more electron-poor, *p*-substituted vinylarenes form more stable adducts to these niobium complexes, (most likely due to increased π -backbonding from the metal to the alkene unit of the more electron-poor vinylarene), but the complex of the more electron-poor vinylarene underwent the migratory insertion step more slowly than did the complex of the more electron-rich vinylarene.¹¹ Thus, the electronic effects observed for the migratory insertion of vinylarenes into the palladium-amides in the current work are the opposite of those observed for the insertions of vinylarenes into the metal-hydride bonds of hydridometal vinylarene complexes of niobium(III) and rhodium(III). Instead, they parallel the electronic effects on the insertions of vinylarenes into the palladium-carbon bonds of cationic Pd(II) vinylarene complexes.

3.3 Summary

In this chapter, studies on the migratory insertions of unactivated olefins into the Pd-N bond of isolated palladium-diarylamido complexes that reveal the steric and electronic effects of the ancillary ligand and olefin on the rate of migratory insertion. By varying the electronic and steric properties of the ancillary benzylphosphine ligand, we revealed the effects of the structure of the ancillary ligand on the individual steps of alkene binding and insertion into the Pd-N bond. In addition, by conducting the reactions with a series of vinylarenes and computing the relative binding energies of the vinylarenes, we also revealed the effect of the olefin electronics on the individual steps of olefin binding and insertion. Understanding these effects on this new class of organometallic transformation is necessary for the rational design of new catalysts for the amination of olefins. The following conclusions drawn from these studies:

3.3.1 Steric Effects On the Insertion Process

- (1) Bulky substituents on the phosphine create stronger steric interactions in the ground state than in the transition state for migratory insertion into the palladium amides. In the transition state, the alkene lies along the Pd-N bond, and the steric interactions between the alkene hydrogens and the alkyl groups on the phosphorus atom in the ancillary ligand are weaker than they are in the ground state. Because the steric interactions are greater in the ground state than in the transition state, the barrier for migratory insertion is lower for the complexes ligated with the bulkier phosphine than for the complex ligated by the smaller phosphine, as deduced by both experimental and computational work.
- (2) The effect of the phosphine steric properties on binding of the alkene prior to the migratory insertion counterbalances the effect of these steric properties on the C-N bond-

forming step, and this combination of effects causes the reactions initiated by the THF-ligated species with larger and smaller ligands to be similar to each other. Thus, careful balancing of the size of the ancillary ligand is needed to increase the reaction rate of reaction of amido complexes with alkenes.

(3) The complex containing the more hindered ancillary ligand adopts more of the monomeric structure than the complex containing the less hindered ancillary ligand. Because insertion involves binding of the olefin *cis* to a terminal amide and the dimeric structures form stable, unreactive amido species, monomeric amides are necessary for facile formation of the olefin-amido adduct.

3.3.2 Electronic Effects on the Insertion Process

(1) The amido complexes in this study containing the more weakly donating ancillary ligands, and therefore the more electrophilic metal centers, inserted alkenes faster than those containing the more strongly donating ancillary ligands. This result parallels the general trend in prior studies showing that alkene insertions into metal-alkyl bonds of complexes containing more electrophilic metal centers are faster than those into metal-alkyl bonds of complexes containing more electron-rich metal centers.

(2) The rates of insertions of alkenes into the palladium-amides in this study are similar to those for insertions into the much more electrophilic lanthanide and Group IV amido alkene complexes. The similarity of these rates suggests that insertions of alkenes into metal-amide bonds could be as broad in scope as insertions of alkenes into metal-carbon bonds.

(3) The THF-ligated benzylphosphine-ligated palladium-amides reacted with electron-poor vinylarenes slightly faster than with electron-rich vinylarenes. The relative ground state energies

of styrene-bound amidopalladium complexes were assessed by DFT methods, and the complex of the more electron-donating 4-methylstyrene was computed to be more stable than the complex of the less electron-donating 3-methoxystyrene. This combination of the experimentally measured free energies of activation for the reaction of THF-ligated palladium amide with the different vinylarenes and the computed relative ground-state energies of the vinylarene complexes show that the elementary step of migratory insertion is faster for complexes of electron-poor vinylarenes than for complexes of electron-rich vinylarenes and that the difference in free energies of activation for this step is larger than that for the overall reaction initiated with the THF-ligated palladium amide.

Thus, we have provided in this article the first detailed account of the effect of the steric and electronic properties of the alkene and ancillary ligand on the rate and scope of the insertion of alkenes into palladium-nitrogen bonds. These complexes are the only metal-amido complexes that form directly observable olefin adducts. Because of the ability to detect these amidopalladium alkene complexes, we were able to probe the effect of the steric and electronic properties of the amido complex and the alkene reactant on the elementary migratory insertion step. Future work will focus on expanding the scope of insertions of alkenes into metal-heteroatom bonds and developing new palladium-catalyzed reactions that involve insertions of alkenes into metal-nitrogen bonds.

3.4 General Experimental Details

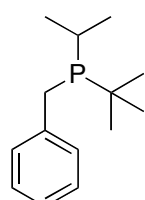
Unless otherwise noted, all manipulations were carried out under an inert atmosphere in an argon-filled glovebox or by standard Schlenk techniques. THF, CH₂Cl₂, benzene, and toluene were degassed by purging with argon for 45 minutes and dried with a solvent purification system

containing a 1 m column of activated alumina. Deuterated solvents (benzene, toluene, and THF), were dried over 3 Å molecular sieves. *tert*-Butyl(isopropyl)chlorophosphine, [2-(CH₂P(*t*-Bu)₂C₆H₄]Pd(THF)NPh₂, and [2-(CH₂P(*t*-Bu)₂C₆H₄]PdNPh₂ were prepared by literature procedures. Styrene was dried over Na and distilled prior to use. Potassium diphenylamide was prepared by addition 1.1 equiv of HMDS to 1 equiv of diphenylamine in toluene. The precipitated amide was collected by filtration and washed with pentane.

Analytical gas chromatography (GC) was performed using a Hewlett-Packard 5890 Gas Chromatograph fitted with a flame ionization detector and a Hewlett-Packard HP5 (30m x 0.32 mm) capillary column. NMR spectra were acquired on 500 MHz or 400 MHz Varian Unity or 500 MHz Innova instruments at the University of Illinois VOICE NMR facility. Chemical shifts are reported in ppm relative to residual chloroform (7.26 ppm for ¹H; 77.0 ppm for ¹³C), dichloromethane (5.32 ppm for ¹H; 54.0 ppm for ¹³C), benzene (7.15 ppm for ¹H; 128.0 ppm for ¹³C), or THF (3.58 ppm for ¹H) or to an external standard (85% H₃PO₄ = 0 ppm for ³¹P or CFCl₃ = 0 ppm for ¹⁹F). Coupling constants are reported in hertz. Elemental analyses were performed by Roberston Microlit Laboratories, Inc. (Madison, NJ) or the Microanalysis Laboratory of The University of Illinois at Urbana-Champaign.

3.4.1 Preparation of palladium amido complexes and insertion products

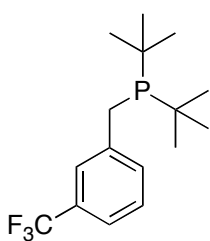
Preparation of benzyl(*tert*-butyl)(isopropyl)phosphine



tert-Butyl(isopropyl)chlorophosphine (1.5 g, 9.0 mmol) was added to a 500 mL glass reaction vessel and dissolved in 50 mL THF. A 5.4 mL aliquot of benzylmagnesium chloride (2.0 M in THF) was added via syringe, and the reaction

mixture was heated to 80 °C for 2 d. The reaction mixture was cooled to room temperature and transferred to a 100 mL round-bottom flask. A 20 mL portion of a freshly degassed saturated aqueous NH₄Cl solution was transferred via cannula into the flask containing the reaction mixture, which was briefly stirred (1 min). The organic layer was extracted into another degassed 100 mL round-bottom flask containing anhydrous MgSO₄. The mixture was taken into the glovebox, and the MgSO₄ was removed by filtration. The volatile materials were evaporated under vacuum. The product was purified by distillation at 80 °C / 20 mtorr to give 0.865 g of product as a colorless oil; 43%. ¹H NMR (C₆D₆, 500 MHz) δ 7.36 (d, J = 7.5 Hz, 2H), 7.15 (t, J = 7.5 Hz, 2H), 7.03 (t, J = 7.5 Hz, 1H), 2.73-2.63 (m, 2H), 1.61 (dsext, J = 7.0, 2.5 Hz, 1H), 1.04 (dd, J = 15, 7.5 Hz, 3H), 0.98 (d, J = 11 Hz, 9H), 0.98 (d, J = 16.5 Hz, 7.0 Hz, 3H). ¹³C{¹H} NMR (C₆D₆, 126 MHz) δ 141.1 (d, J = 11.1 Hz), 129.9 (d, J = 8.3 Hz), 128.5, 125.7, 29.2 (d, J = 24.1 Hz), 28.6 (d, J = 13.0 Hz), 23.9 (d, J = 21.2 Hz), 23.0 (d, J = 22.2 Hz), 20.4 (d, J = 7.3 Hz). ³¹P NMR (C₆D₆, 202 MHz) δ 22.6. Anal. Calc'd. For C₁₄H₂₃P: C, 75.64; H 10.43; found, C, 75.38; H, 10.23.

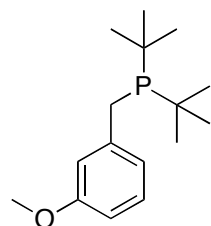
Preparation of di-tert-butyl(3-trifluoromethylbenzyl)phosphine



To a 2-neck 500 mL round-bottom flask with an attached reflux condenser charged with 150 mL of Et₂O, was added 0.622 g (25.6 mmol) of Mg metal. A 3.05 mL (20.0 mmol) aliquot of 3-trifluoromethylbenzylbromide was added via syringe dropwise. The reaction mixture was heated to reflux (50 °C) for 6 h, cooled to room temperature, and transferred to a 500 mL glass reaction vessel containing 3.29 mL (17.3 mmol) of P(t-Bu)₂Cl in 50 mL of Et₂O by cannula. The reaction mixture was heated at reflux for 72 h. The reaction mixture was cooled to RT, and the volatile

materials were evaporated under vacuum until the total volume was 50 mL. A 30 mL aliquot of freshly degassed NH₄Cl (aq) solution was added to the flask containing the reaction mixture, which was briefly stirred (1 min). The organic layer was extracted via cannula into another degassed 100 mL round-bottom flask containing anhydrous MgSO₄. The mixture was taken into a glovebox, and the MgSO₄ was removed by filtration. The volatile materials were evaporated under vacuum. The product was purified by distillation at 100 °C/200 mtorr to give 2.88 g of the product as a colorless oil; 47%. ¹H NMR (C₆D₆, 500 MHz): δ 7.65 (s, 1H), 7.34 (d, *J* = 7.5 Hz, 1H), 7.20 (s, *J* = 8.0 Hz, 1H), 6.92 (t, *J* = 7.5 Hz, 1H), 2.52 (d, *J* = 2.5 Hz, 2H), 0.94 (d, *J* = 11.0 Hz, 18 H). ¹³C{¹H} NMR (C₆D₆, 126 MHz): δ 143.5 (d, *J* = 13.9 Hz), 133.3 (d, *J* = 10.2 Hz), 130.6 (q, *J* = 31.4 Hz), 128.8, 126.6 (m), 125.1 (q, *J* = 273 Hz), 122.3 (m), 31.8 (d, *J* = 24.1 Hz), 29.7 (d, *J* = 13.9 Hz), 28.6 (d, *J* = 25.8 Hz). ³¹P NMR (C₆D₆, 162 MHz): δ 35.4. ¹⁹F NMR (C₆D₆, 376 MHz): δ -62.6. This isolated compound contained 5% 3-trifluoromethyltoluene, and was used in this form to prepare the corresponding palladium complexes.

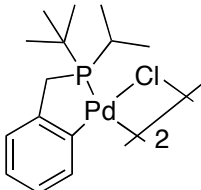
Preparation of di-tert-butyl(3-methoxybenzyl)phosphine



To a 500 mL glass reaction vessel equipped with a vacuum valve was added chlorodi-*tert*-butylphosphine (1.00 g, 5.53 mmol), which was dissolved in 5 mL THF. A 27.8 mL (6.64 mmol) aliquot of 3-methoxybenzylmagnesium chloride solution (0.25 M in THF) was added, and the vessel was capped and heated at 80 °C for 60 h. The reaction was cooled to room temperature and transferred to a 100 mL round-bottom flask. A 20 mL portion of a freshly degassed saturated aqueous NH₄Cl solution was cannula transferred into the flask containing the reaction mixture. The resulting mixture was briefly stirred (1 min). The organic layer was extracted via cannula into another

degassed 100 mL round-bottom flask containing anhydrous MgSO₄. The mixture was taken into a glovebox, and the MgSO₄ was removed by filtration. The volatile materials were evaporated under vacuum. The product was purified by distillation at 110 °C/100 mtorr to give 0.734 g of product as a colorless oil; 50%. ¹H NMR (CDCl₃, 500 MHz): δ 7.19 (s, 1H), 7.11 (t, *J* = 8.0 Hz, 1H), 7.06 (d, *J* = 7.5 Hz, 1H), 6.66 (dd, *J* = 8.0 Hz, 1.5 Hz, 1H), 3.37 (s, 3H), 2.73 (d, *J* = 2.5 Hz, 2H), 1.05 (d, *J* = 11.0 Hz, 18H). ¹³C{¹H} NMR (CDCl₃, 126 MHz): δ 160.2, 143.6 (d, *J* = 13.0 Hz), 129.4, 122.4 (d, *J* = 8.3 Hz), 115.9 (d, *J* = 10.2 Hz), 111.1, 54.6, 31.7 (d, *J* = 24.1 Hz), 29.9 (d, *J* = 13.0 Hz), 29.1 (d, *J* = 25.8 Hz). ³¹P NMR (CDCl₃, 202 MHz): δ 33.3. Anal. Calc'd. for C₁₆H₂₇OP: C, 72.15; H 10.22; found, C, 72.05; H, 10.04.

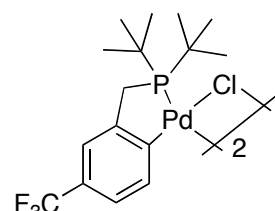
*Preparation of {[2-(CH₂P(*t*-Bu)(*i*-Pr)-C₆H₄]PdCl}₂ (**3.01**)*



Pd(OAc)₂ (0.300 g, 1.34 mmol) and benzyl(tert-butyl)(isopropyl)phosphine (0.297 g, 1.34 mmol) were added to a 20 mL scintillation vial and dissolved in 6 mL of toluene. The reaction mixture was stirred at RT for 4 h. The volatile materials were evaporated under vacuum, and a solution of LiCl (0.388 g, 9.38 mmol) in 10 mL anhydrous methanol was added to the brown residue and stirred vigorously for 30 min. A light grey precipitate was collected by filtration and washed with methanol (5mL x 3) and pentane (5 ml x 3), and dried under vacuum. Yield 0.426 g, 88 %. The product consisted of a 1.2 : 1 mixture of *anti:syn* diastereomers. ¹H NMR (CD₂Cl₂, 500 MHz): δ 7.71-7.62 (m, 2H), 7.05-7.04 (m, 2H), 6.98-6.84 (m, 4H), 3.25-3.14 (m, 4H), 2.40-2.24 (m, 2H), 1.60-1.50 (m, 6H), 1.34 (t, *J* = 14.0 Hz, 18H), 1.19-1.12 (m, 6H). ¹³C{¹H} NMR (CDCl₃, 126 MHz) major diastereomer: δ 149.4, 147.5 (d, *J* = 16.6 Hz), 137.1, 125.1, 125.0, 123.4 (d, *J* = 22.2 Hz), 33.6 (d, *J* = 22.1 Hz), 32.8 (d, *J* = 30.5 Hz), 28.2, 25.1 (d, *J* = 21.2 Hz), 22.3, 18.9. ³¹P NMR (CD₂Cl₂, 202 MHz, with

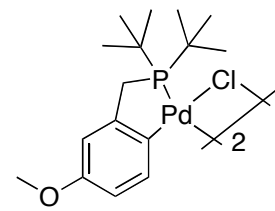
integral *I*): δ 97.9 (s, *I* = 55%) 97.2 (s, *I* = 45%). Anal. Calc'd. for $C_{28}H_{44}ClPPd$: C, 46.30; H 6.11; found, C, 46.43; H, 5.89.

*Preparation of {[2-(CH₂P(*t*-Bu)₂-4-CF₃C₆H₃]PdCl}₂ (3.02)}*



Pd(OAc)₂ (0.200 g, 0.891 mmol) and 3-trifluoromethyl-di-*tert*-butylbenzylphosphine (0.511 g, 1.43 mmol) were added to a 20 mL scintillation vial and dissolved in 5 mL of toluene. The reaction mixture was stirred at RT for 3 h. The volatile materials were evaporated from the light orange reaction mixture under vacuum, and a solution of LiCl (0.286 g, 6.81 mmol) in 10 mL anhydrous methanol was added to the residue and stirred vigorously for 30 min. A light yellow precipitate was collected by filtration and washed with methanol (5mL x 3) and pentane (5 ml x 3), and dried under vacuum. Yield 0.283 g, 71%. The product consisted of a 1.7 : 1 mixture of *anti:syn* diastereomers. ¹H NMR (CDCl₃, 400 MHz): δ 7.96-7.87 (m, 2H), 7.26-7.10 (m, 4H) 3.24 (d, *J* = 12.5 Hz, 4H), 1.41 (m, 36H). ¹³C{¹H} NMR (CDCl₃, 126 MHz) major diastereomer: δ 154.3, 148.7 (d, *J* = 16.5 Hz), 137.5, 127.1 (q, *J* = 31.4 Hz), 124.6 (q, *J* = 272 Hz), 121.3, 119.4 (d, *J* = 23.1 Hz), 36.3 (d, *J* = 18.5 Hz), 33.5 (d, *J* = 29.5 Hz), 29.2. ³¹P NMR (CDCl₃, 162 MHz, with integral *I*): δ 102.7 (s, *I* = 63%) 1 02.3 (s, *I* = 37%). Anal. Calc'd. for C₃₂H₄₆F₃PClPd: C, 43.17; H, 5.21; found, C, 43.17; H, 5.14

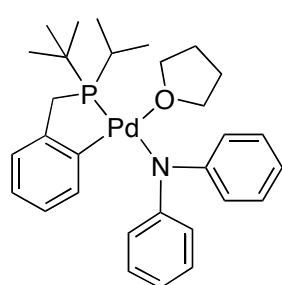
*Preparation of {[2-(CH₂P(*t*-Bu)₂-4-OCH₃C₆H₃]PdCl}₂ (3.03)}*



Pd(OAc)₂ (0.169 g, 0.753 mmol) and di-*tert*-butyl(3-methoxybenzyl)phosphine (0.201 g, 0.753 mmol) were added to a 20 mL scintillation vial and dissolved in 6 mL of toluene. The reaction mixture

was stirred at RT for 4 h. The volatile materials were evaporated under vacuum, and a solution of LiCl (0.223 g, 5.27 mmol) in 10 mL anhydrous methanol was added to the brown residue and stirred vigorously for 30 min. A light grey precipitate was collected by filtration and washed with methanol (5mL x 3) and pentane (5 ml x 3), and dried under vacuum. The product consisted of a 1.2 : 1 mixture of *anti:syn* diastereomers. Yield: 0.290 g, 95%. ¹H NMR (CDCl₃, 400 MHz): δ 7.73 (dd, *J* = 8.8, 4 Hz, minor diastereomer, 0.9H), 7.66 (dd, *J* = 8.8, 3.6 Hz, major diastereomer, 1.1H), 6.64-6.49 (m, 4H), 3.72 (s, 6H), 3.14 (d, *J* = 12 Hz, 4H), 1.41 (m, 36H). ¹³C{¹H} NMR (CDCl₃, 126 MHz) major diastereomer: δ 157.5, 148.8 (d, *J* = 18.5 Hz), 139.4, 137.6, 110.7, 109.1 (d, *J* = 23.1 Hz), 55.0, 38.8 (m), 33.6 (d, *J* = 30.4 Hz), 29.2; minor diastereomer: δ 157.6, 148.4 (d, *J* = 17.5 Hz), 139.2, 137.1, 110.7, 109.2 (d, *J* = 23.1 Hz), 55.0, 38.8(m), 33.6 (d, *J* = 30.4 Hz), 29.2. ³¹P NMR (CDCl₃, 162 MHz, with integral *I*): δ 100.6 (s, *I* = 55%) 100.3 (s, *I* = 45%). Anal. Calc'd. for C₃₂H₅₂OPClPd: C, 47.19; H, 6.44; found, C, 47.43; H, 6.52.

*Preparation of [2-(CH₂P(*t*-Bu)(*i*-Pr))C₆H₄]Pd(THF)NPh₂ (3.04)*



To a 20 mL scintillation vial was added {[2-(CH₂P(*t*-Bu)(*i*-Pr))C₆H₄]PdCl}₂ (0.100 g, 0.138 mmol) and KNPh₂ (0.0571 g, 0.275 mmol). The mixture was dissolved in 2 mL of THF and stirred for 1.5 h. Pentane (15 mL) was added, and the reaction mixture was filtered through a syringe filter to remove KCl and trace Pd black. The filtrate was cooled to -35 °C. After 3 d, 0.115g (72 %) of orange crystals were collected by filtration and washed with pentane. The isolated solid was dried under vacuum. ¹H NMR (THF-*d*₈, 500 MHz): δ 7.49 (d, *J* = 8.0 Hz, 4H), 7.38 (d, *J* = 8.0 Hz, 1H), 6.90 (t, *J* = 7.5 Hz, 5H), 6.72

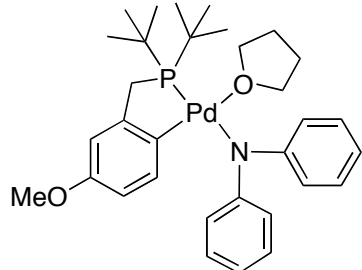
(t, $J = 7.0$ Hz, 1H), 6.56 (t, $J = 8.0$ Hz, 1H), 6.34 (t, $J = 7.0$ Hz, 2H), 3.62, (m, 4H), 3.25 (dd, $J = 16.5, 9$ Hz, 1H), 3.09 (dd, $J = 17.0, 11.0$ Hz, 1H), 2.24 (m, 1H), 1.77 (m, 4H), 1.43 (dd, $J = 17.0, 7.0$ Hz, 3H), 1.34 (d, $J = 13.5$ Hz, 9H), 1.16 (dd, $J = 13.5, 8.0$ Hz, 3H). $^{13}\text{C}\{\text{H}\}$ NMR (THF- d_8 , 126 MHz): δ 156.2, 149.1 (d, $J = 18.4$ Hz), 144.7, 140.6, 128.9, 126.0, 124.9, 123.7 (d, $J = 20.3$ Hz), 121.1, 115.5, 68.2, 32.4 (d, $J = 29.5$ Hz), 32.4 (d, $J = 21.3$ Hz), 27.9 (d, $J = 3.7$ Hz), 26.4, 25.0, 22.9 (d, $J = 6.4$ Hz), 19.7. ^{31}P NMR (THF- d_8 , 202 MHz): δ 82.4 s. Anal. Calc'd. for $\text{C}_{30}\text{H}_{40}\text{NOPPd}$: C, 63.43; H 7.10; N, 2.47; found, C, 63.18; H, 6.97; N, 2.37.

*Preparation of [2-(CH₂P(t-Bu)₂-4-CF₃C₆H₃]Pd(THF)NPh₂ (**3.05**)*

To a 20 mL scintillation vial was added {[2-(CH₂P(t-Bu)₂-4-CF₃C₆H₄]PdCl}₂ (0.080 g, 0.090 mmol) and KNPh₂ (0.0373 g, 0.180 mmol). The mixture was dissolved in 2 mL of THF and stirred for 24 h. Pentane (15 mL) was added, and the reaction mixture was filtered through a syringe filter to remove KCl and trace Pd black.

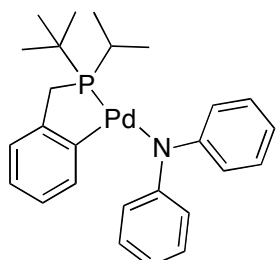
The filtrate was cooled to -35 °C. After 3 d, 0.065 g (57 %) of orange crystals were collected by filtration and washed with pentane. The isolated solid was dried under vacuum. ^1H NMR (C₆D₆, 500 MHz): δ 7.93 (d, $J = 8.5$ Hz, 1H), 7.25-7.15 (m, 9H), 6.93 (d, $J = 8.0$ Hz, 1H), 6.78 (t, $J = 7.0$ Hz, 2H), 3.54 (m, 4H), 2.51 (d, $J = 9.5$ Hz), 1.36 (m, 4H), 0.82 (d, $J = 13.5$ Hz, 18H). $^{13}\text{C}\{\text{H}\}$ NMR (C₆D₆, 126 MHz): δ 156.9, 151.4, 150.0 (d, $J = 18.6$ Hz), 139.8, 132.0, 126.6 (q, $J = 31$ Hz), 121.9, 121.4 (q, $J = 271$ Hz), 120.2, 119.9 (d, $J = 18.6$ Hz), 117.0, 68.4, 34.3 (d, $J = 15.6$ Hz), 32.8 (d, $J = 28.4$ Hz), 28.7 (d, $J = 4.9$ Hz), 25.7. ^{31}P NMR (C₆D₆, 202 MHz): δ 97.6 s. Anal. Calc'd. for C₃₂H₄₁F₃NOPPd: C, 59.12; H 6.36; N, 2.15; found, C, 59.51; H, 6.77; N, 2.25.

*Preparation of [2-(CH₂P(t-Bu)₂-4-OCH₃C₆H₃]Pd(THF)NPh₂ (**3.06**)*



To a 20 mL scintillation vial was added {[2-(CH₂P(t-Bu)₂-4-OCH₃C₆H₃]PdCl}₂ (0.120 g, 0.147 mmol) and KNPh₂ (0.0610 g, 0.294 mmol). The mixture was dissolved in 2 mL of THF and stirred for 3 h. Pentane (15 mL) was added and the reaction mixture was filtered through a syringe filter to remove KCl and trace Pd black, the reaction mixture cooled to -35 °C. After 3d , 0.135 g (75 %) of orange crystals were collected by filtration and washed with pentane. The isolated solid was dried under vacuum. ¹H NMR (C₆D₆, 500 MHz): δ 7.85 (d, *J* = 8.5 Hz, 1H), 7.32 (bs, 4H), 7.21 (t, *J* = 7.5 Hz, 4H), 6.81 (t, *J* = 6.5 Hz, 2H), 6.77 (d, *J* = 2.5 Hz, 1H), 6.32 (dd, *J* = 8.5, 2.5 Hz, 1H), 3.55 (m, 4H), 3.30 (s, 3H), 2.64 (d, *J* = 9.5 Hz, 2H), 1.37 (m, 4H), 0.85 (d, *J* = 13.5 Hz, 18H). ¹³C{¹H} NMR (C₆D₆, 126 MHz): δ 158.2, 153.0, 149.5 (d, *J* = 19.5 Hz), 140.3, 138.1, 130.9, 118.6, 118.6, 111.0, 110.7 (d, *J* = 20.5 Hz), 69.3, 54.5, 34.2 (d, *J* = 14.7 Hz), 32.4 (d, *J* = 28.4 Hz), 28.9 (d, *J* = 3.9 Hz), 25.6. ³¹P NMR (C₆D₆, 202 MHz): δ 98.7 s. Anal. Calc'd. for C₃₂H₄₄NO₂PPd: C, 62.79; H 7.25; N, 2.29; found, C, 62.84; H, 7.40; N, 2.21.

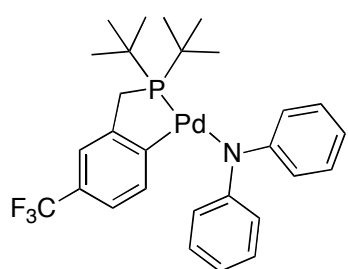
*Preparation of [2-(CH₂P(t-Bu)(i-Pr))C₆H₄]PdNPh₂ (**3.07**)*



To a 20 mL scintillation vial was added {[2-(CH₂P(t-Bu)(i-Pr))C₆H₄]PdCl}₂ (0.120 g, 0.165 mmol) and KNPh₂ (0.0685 g, 0.330 mmol). The mixture was dissolved in 11 mL of toluene and stirred for 2 d. The toluene was slowly evaporated until ~1.5 mL remained. Pentane (15 mL) was carefully added, and the mixture was filtered through a Chromafil syringe filter and cooled to -35 °C. After 4 days, the precipitated solid was collected by filtration,

washed with pentane (2×5 mL) and dried under vacuum. Yield 0.0553 g, 34%. *This complex exists as mixture of the monomeric structure shown and the unsymmetrical dimer **3.08** at room temperature. Because the dimer exists as a set of diastereomers, many signals in the ^1H and ^{13}C NMR spectra overlap.* ^1H NMR (C_6D_6 , 500 MHz): δ 8.15-6.70 (m), 6.60-5.75 (m), 4.67-4.62 (m), 3.54-2.47 (m), 1.15-0.45 (m). ^{31}P NMR (C_6D_6 , 202 MHz): δ 101.3 (m, $I = 35\%$), 94.3 (s, $I = 30\%$), 79.0 (m, $I = 35\%$). Anal. Calc'd. for $\text{C}_{26}\text{H}_{32}\text{NPPd}$: C, 62.97; H, 6.50; N, 2.82; found, C, 62.87; H, 6.51; N, 2.71.

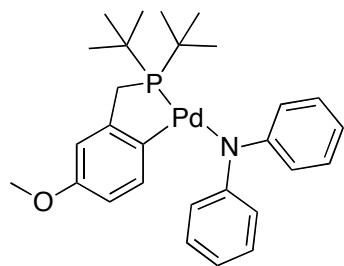
*Preparation of [2-($\text{CH}_2\text{P}(t\text{-Bu})_2$)-4- $\text{CF}_3\text{C}_6\text{H}_3]\text{PdNPh}_2$ (**3.09**)*



To a 20 mL scintillation vial was added {[2-($\text{CH}_2\text{P}(t\text{-Bu})_2$)-4- $\text{CF}_3\text{C}_6\text{H}_4]\text{PdCl}}_2 (0.150 g, 0.168 mmol) and KNPh₂ (0.0790 g, 0.370 mmol). The mixture was dissolved in 11 mL of toluene and stirred for 3 d. The toluene was slowly evaporated until ~1.5 mL remained.$

Pentane (15 mL) was carefully added, and the mixture was filtered through a Chromafil syringe filter and cooled to -35 °C. After 4 days, the precipitated solid was collected by filtration, washed with pentane (2×5 mL) and dried under vacuum. Yield 0.0858 g, 44%. ^1H NMR (C_6D_6 , 500 MHz): δ 7.93 (d, $J = 8.0$ Hz, 1H), 7.22 (s, 1H), 7.15 (m, 5H), 7.04 (m, 4H), 6.93 (d, $J = 8.0$ Hz, 1H), 6.82 (t, 7.0 Hz, 2H), 2.52 (d, 9.5 Hz, 2H), 0.76 (d, 13.5 Hz, 18H). $^{13}\text{C}\{\text{H}\}$ NMR (C_6D_6 , 126 MHz): δ 158.4 (d, $J = 8.3$ Hz), 150.1 (d, $J = 18.5$ Hz), 139.7, 132.2, 128.5 (d, 2.8 Hz), 127.1 (q, 31.4 Hz), 125.7 (q, $J = 272$ Hz), 121.7 (d, $J = 3.7$ Hz), 121.1, 120.0, 116.4, 34.4 (d, $J = 24.0$ Hz), 33.0 (d, $J = 28.6$ Hz), 28.6 (d, $J = 4.5$ Hz). ^{31}P NMR (C_6D_6 , 202 MHz): δ 100.9 s. ^{19}F NMR (C_6D_6 , 470 MHz): δ -61.9 s. Anal. Calc'd. for $\text{C}_{28}\text{H}_{33}\text{NF}_3\text{PPd}$: C, 58.19; H, 5.76; N, 2.42; found, C, 58.28; H, 5.93; N, 2.26.

Preparation of [2-(CH₂P(t-Bu)₂)₂-4-OCH₃C₆H₃]PdNPh₂ (3.11)



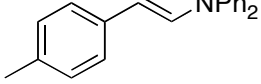
To a 20 mL scintillation vial was added {[2-(CH₂P(t-Bu)₂)₂-4-OCH₃C₆H₃]PdCl}₂ (0.120 g, 0.147 mmol) and KNPh₂ (0.0760 g, 0.366 mmol). The mixture was dissolved in 11 mL of toluene and stirred for 7 d. The toluene was slowly evaporated until ~1.5 mL remained. Pentane (15 mL) was carefully added, and the mixture was filtered through a Chromafil syringe filter and cooled to -35 °C. After 4 days, the precipitated solid was collected by filtration, washed with pentane (2 × 5 mL) and dried under vacuum. Yield 0.0415 g, 26%. ¹H NMR (C₆D₆, 400 MHz): δ 7.85 (d, *J* = 8.8 Hz, 1H), 7.20 (bs, 8H), 6.82 (t, *J* = 4 Hz, 2H), 6.79 (d, *J* = 2.4 Hz, 1H), 6.32 (dd, *J* = 8.4, 2.4 Hz, 1H), 3.31 (s, 3H), 2.64 (d, *J* = 12 Hz, 2H), 0.82 (d, *J* = 13.6 Hz, 18H). ¹³C{¹H} NMR (C₆D₆, 126 MHz): δ 158.3, 150.9, 149.9 (d, *J* = 18.6 Hz), 142.3, 139.8, 132.4, 120.6, 116.6, 110.8 (d, *J* = 18.5 Hz) 110.6, 54.6, 34.2 (d, *J* = 15.6 Hz) 33.0 (d, *J* = 31.5 Hz) 28.7 (d, *J* = 4.9 Hz). ³¹P NMR (C₆D₆, 202 MHz): δ 100.7 s. Anal. Calc'd. for C₂₈H₃₆NOPPd: C, 62.28; H, 6.72; N, 2.59; found, C, 62.39; H, 6.71; N, 2.40.

Independent Synthesis of Enamine Derivatives

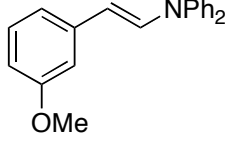
A procedure described by Barluenga was used to prepare the enamine products using Pd₂(dba)₃ and Xantphos as a catalyst.²⁹ Vinyl bromides (*E*)-1-(2-bromovinyl)-4-methoxybenzene and (*E*)-1-(2-bromovinyl)-3-methoxybenzene were prepared by the procedure described by Marciniec and coworkers.³⁰ (*E*)-1-(2-bromovinyl)-4-trifluorobenzene and (*E*)-1-(2-bromovinyl)-3-trifluorobenzene were prepared by addition of excess CuBr₂ to the corresponding (*E*)-vinyl boronic acid in MeOH/H₂O. In an Ar-filled glove box, a 50 mL glass reaction glass reaction vessel attached to a vacuum valve was charged with 0.711 g (3.61 mmol) of (*E*)-1-(2-

bromovinyl)-4-methylbenzene, 0.614 g (3.61 mmol) of HNPh₂, 0.163 g (0.180 mmol) of Pd₂(dba)₃, 0.209 g (0.361 mmol) of Xantphos, and 0.485 g (5.05 mmol) of NaOt-Bu. All reagents were dissolved in 10 mL of toluene. The reaction mixture was heated at 90 °C for 36 h. The reaction mixture was cooled to RT, and 40 mL of hexanes was added. The reaction mixture was filtered through a Celite (in air). The solvent was removed by vacuum, and the product was purified by Kugelrohr distillation (146 °C, 20 mtorr).

(E)-N-phenyl-N-(4-methylstyryl)aniline

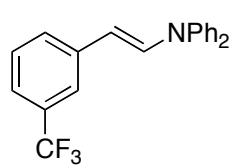
 Yield 0.575 g, 56%. ¹H NMR (C₆D₆, 500 MHz): δ 7.28 (d, *J* = 14.5 Hz, 1H), 7.08-7.02 (m, 6H), 7.00-6.94 (m, 6H), 6.88 (t, *J* = 7.5 Hz, 2H), 5.85 (d, *J* = 14 Hz, 1H), 2.12 (s, 3H). ¹³C{¹H} NMR (C₆D₆, 126 MHz): δ 146.0, 135.8, 134.6, 133.2, 129.7, 129.6, 125.0, 124.1, 123.9, 110.4, 21.1. Anal. Calc'd. for C₂₁H₁₉N: C, 88.38; H, 6.71; N, 4.91; found, C, 88.28; H, 6.58; N, 4.68.

(E)-N-phenyl-N-(3-methoxystyryl)aniline

 Prepared according to general procedure using 0.395 g (1.85 mmol) of (*E*)-1-(2-bromovinyl)-3-methoxybenzene, 0.315 g (1.85 mmol) of HNPh₂, 0.0847 g (0.0925 mmol) of Pd₂(dba)₃, 0.107 g (0.185 mmol) of Xantphos, and 0.249 g (2.59 mmol) of NaOt-Bu. The product was purified by Kugelrohr distillation (150 °C and 25 mtorr) to give 0.331 g (60% yield) of enamine. ¹H NMR (C₆D₆, 500 MHz): δ 7.33 (d, *J* = 14 Hz, 1H), 7.09-7.04 (m, 5H), 6.97 (d, *J* = 7.5 Hz, 4H), 6.88 (t, *J* = 7.0 Hz, 2H), 6.80-6.79 (m, 2H), 6.65 (d, *J* = 8.0 Hz, 1H), 5.85 (d, *J* = 14 Hz, 1H), 3.30 (s, 3H). ¹³C{¹H} NMR (C₆D₆, 126

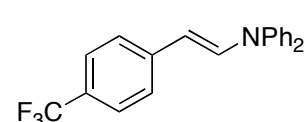
MHz): δ 159.9, 145.3, 139.7, 133.9, 129.5, 129.5, 124.0, 123.7, 117.1, 110.6, 109.8, 108.9, 55.1. Anal. Calc'd. for $C_{21}H_{19}NO$: C, 83.69; H, 6.35; N, 4.65; found, C, 83.57; H, 6.44; N, 4.66.

(E)-N-phenyl-N-(3-trifluoromethyl)styryl)aniline



Prepared according to general procedure using 0.530 g (2.11 mmol) of (*E*)-1-(2-bromovinyl)-3-trifluoromethylbenzene, 0.359 g (2.11 mmol) of HNPh₂, 0.0966 g (0.106 mmol) of Pd₂(dba)₃, 0.122 g (0.211 mmol) of Xantphos, and 0.284 g (2.95 mmol) of NaOt-Bu. The product was purified by Kugelrohr distillation (149 °C and 25 mtorr) to give 0.429 g (60% yield) of enamine. ¹H NMR (C_6D_6 , 500 MHz): δ 7.32 (s, 1H), 7.16-7.15 (m, 1H), 7.13 (d, J = 14.5 Hz, 1H), 7.07-7.03 (m, 4H), 6.93-6.85 (m, 8H), 5.61 (d, J = 14 Hz, 1H). ¹³C{¹H} NMR ($CDCl_3$, 126 MHz): δ 145.0, 139.2, 134.8, 130.9 (q, J = 32.4 Hz), 129.6, 128.9, 127.2, 124.4, 124.3 (q, J = 272 Hz), 123.8, 121.1 (q, J = 3.6 Hz), 120.9 (q, J = 3.8 Hz), 107.0. ¹⁹F NMR (C_6D_6 , 470 MHz): δ -62.7. Anal. Calc'd. for $C_{21}H_{16}F_3N$: C, 74.33; H, 4.75; N, 4.13; found, C, 74.20; H, 4.74; N, 4.03.

(E)-N-phenyl-N-(4-trifluoromethyl)styryl)aniline



Prepared according to general procedure using 0.600 g (2.39 mmol) of (*E*)-1-(2-bromovinyl)-4-trifluoromethylbenzene, 0.406 g (2.39 mmol) of HNPh₂, 0.109 g (0.120 mmol) of Pd₂(dba)₃, 0.138 g (0.239 mmol) of Xantphos, and 0.322 g (3.35 mmol) of NaOt-Bu. The product was purified by Kugelrohr distillation (155 °C and 50 mtorr) to give 0.527 g (65% yield) of enamine. ¹H NMR (C_6D_6 , 500 MHz): δ 7.31 (d, J = 8.0 Hz, 2H), 7.20 (d, J = 14 Hz, 1H), 7.06 (t, J = 8.0 Hz, 4H), 6.93-6.88 (m, 6H), 6.78 (d, J = 8.0 Hz, 2H), 5.60 (d, J = 14 Hz, 1H). ¹³C{¹H} NMR ($CDCl_3$, 126 MHz): δ 144.9, 142.1, 135.4, 129.6,

126.2 (q, $J = 33.2$ Hz), 125.5 (q, $J = 3.7$ Hz), 124.5 (q, $J = 272$ Hz), 124.5, 124.1, 123.8, 106.8. ^{19}F NMR (C_6D_6 , 470 MHz): δ -62.0. Anal. Calc'd. for $\text{C}_{21}\text{H}_{16}\text{F}_3\text{N}$: C, 74.33; H, 4.75; N, 4.13; found, C, 74.09; H, 4.85; N, 4.18.

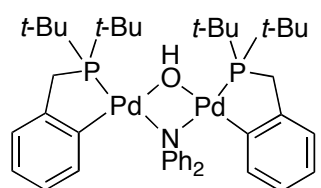
3.4.2 General Procedure for Kinetic Analysis of the Reactions of the THF-ligated Pd-amides with ethylene

In a glove box, 0.0172 mmol of THF-ligated Pd-amide and 0.0029 g 1,3,5-trimethoxybenzene was weighed into a 4 dram vial. The mixture was dissolved into 0.40 mL toluene- d_8 , and a 14.0 μL (0.172 mmol) aliquot of THF was added via microliter syringe. The reaction mixture was swirled and added to a 9" NMR tube, which was then connected to a NMR sealing assembly. The tube was attached to a high-vacuum line, frozen in a liquid N_2 bath, and argon evaporated under vacuum. An attached 3.86 mL calibrated bulb was filled to a pressure of 621 torr of ethylene and condensed into the NMR tube. The bulb was filled to a pressure of 621 torr of ethylene a second time and condensed into the NMR tube to by vacuum transfer so that a total of 0.258 mmol of ethylene was added to the NMR tube. Following the addition of ethylene, the NMR tube was flame sealed. The sealed NMR tube was removed from the liquid N_2 bath and quickly inserted into a dry ice/acetone bath at -78° C, and vigorously shaken to dissolve the ethylene into the reaction mixture prior to inserting the NMR tube into a NMR spectrometer set to -10 °C,. The NMR tube was inserted into the NMR probe, shimmed, and a series of ^1H NMR spectra were collected until the reaction had progressed to >3 half lives. After data collection was complete, the spectra were integrated, and the integrals were normalized against the internal standard. The concentration of the palladium-amide was plotted versus time, and the data were fit to an exponential decay.

3.4.3. General Procedure for Kinetic Analysis of THF-free Pd-amides

In a glove box, 0.0172 mmol of the THF-free Pd-amides were weighed into a 4 dram vial. The Pd-amide was dissolved into 0.40 mL toluene-*d*₈ and added to a 9" medium walled NMR tube. The tube was then connected to an NMR sealing assembly. The tube was attached to a high-vacuum line, frozen in a liquid N₂ bath, and argon evaporated under vacuum. An attached 61 mL calibrated bulb was filled to a pressure of 786 torr of ethylene (2.58 mmol). The ethylene was vacuum transferred into the NMR tube, which was then flame sealed. The sealed NMR tube was left submerged in the liquid N₂ bath until immediately before insertion into the NMR spectrometer. The NMR tube was quickly inserted into a dry ice/acetone bath at -78° C and vigorously shaken to dissolve the ethylene into the reaction mixture. The NMR tube was then inserted into the spectrometer set to -50 °C, and a series of ³¹P NMR spectra were collected until the reaction had progressed to >3 half lives. After data collection was complete, the tube was ejected from the probe and immediately frozen in liquid N₂. Once frozen, the tube was opened and allowed to warm to RT. *NMR tubes containing this concentration of ethylene were never allowed to warm to RT while sealed.* After integration of the spectra, the concentration of the palladium-amide was plotted versus time, and the data were fit to an exponential decay.

3.4.4. Identification of Complex 3.13



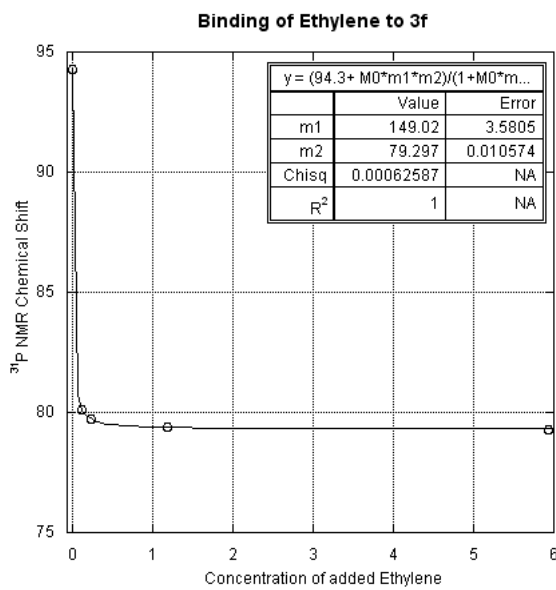
Monitoring reactions of the **2.02** with ethylene by ³¹P NMR spectroscopy revealed the presence of a minor species at δ 92.7 ppm. This same resonance was also observed in the crude reaction mixture of **2.12** before crystallization. In addition to the numerous red crystals obtained during a second recrystallization of the mother liquor of a toluene solution of **2.12**, several small yellow crystals

were present from which single x-ray crystallography revealed the structure of **3.13** to be a bridging hydroxylamido palladium complex. The ^{31}P NMR spectrum of yellow crystals consists of a singlet at δ 92.7 ppm. Solid-state stuctural details are given below.

*3.4.5. Binding of THF to Pd-amide **3.07***

To detemine the equilibrium constant for THF binding to complex **3.07**, the ^{31}P NMR spectra of samples of **3.07** containing different concentration of THF in toluene-d8 at 22 °C were obtained. The equilibrium constant was determined to be 14 M-1 at 22 °C from a fit of the plot of the ^{31}P chemical shift vs. the concentration of added THF to equation 3.9.

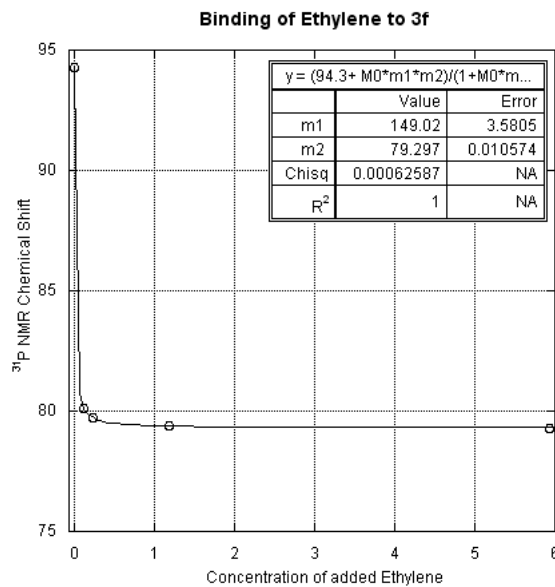
$$\delta_{obs} = \frac{\delta_{3.07} + K_{eq} \delta_{3.04} [THF]}{1 + K_{eq} [3.07][THF]} \quad (3.9)$$



3.4.6 Binding of Ethylene to Pd-Amide 3.07

To determine the equilibrium constant for ethylene binding to complex **3.07**, the ^{31}P NMR spectra of samples of **3.07** containing different concentrations of ethylene in toluene- d_8 at -65 °C were obtained. The equilibrium constant was determined to be 149 M⁻¹ at -65 °C from a fit of the plot (shown below) of the ^{31}P chemical shift vs. the concentration of added THF to equation 3.10.

$$\delta_{obs} = \frac{\delta_{3.07} + K_{eq} \delta_{3.07_ethylene\ adduct} [ethylene]}{1 + K_{eq} [2.07] [ethylene]} \quad (3.10)$$



3.4.7 Van't Hoff Analysis

The ^{31}P NMR spectrum of the THF ligated Pd-amide **2.02** was collected at temperatures between +40 °C and -60 °C. To determine the K_{eq} (eq 3.11) for the binding of THF to complex **2.12** at each temperature, the concentration of **2.02**, **2.12**, and THF at each temperature is needed. To determine the concentration of **2.02**, eq 3.12 was derived which relates the observed ^{31}P

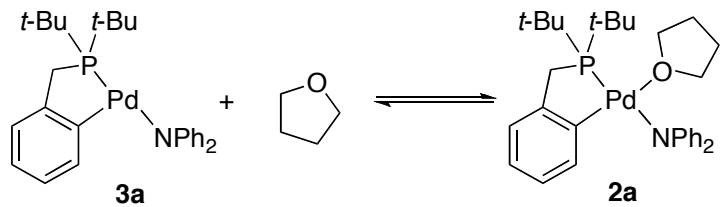
chemical shift to the concentration of **2.02**. The concentration of **2.12** and THF was then determined with eq 3.13 by knowing the initial concentration of **2.02**, the concentration of **2.02** at equilibrium, and stoichiometry of the reaction. The natural log of K_{eq} was plotted vs. $1/T$ (Van't Hoff plot) and a linear relationship was observed. The slope of the line indicated $\Delta H = -11.3$ kcal/mol, and the intercept indicated $\Delta S = -34$ cal/mol for the binding of THF to **2.12**.

$$K_{eq} = \frac{[2a]}{[3a][THF]} \quad (3.11)$$

$$[2a] = \frac{\delta_{obs}[3a] - \delta_{3a}[3a]}{\delta_{2a} - \delta_{obs}} \quad (3.12)$$

$$[2a] + [3a] = 0.043M \quad (3.13)$$

Table 3.3. Binding of THF to complex **2.12**



Temp (° C)	δ_{obs} (ppm)	K_{eq} (M^{-1})	ΔG (kcal/mol)
40	100.1	3.29	-0.74
20	98.2	9.97	-1.34
0	95.1	37.0	-1.96
-20	91.9	160	-2.55
-40	89.3	1140	-3.25
-60	87.9	18400	-4.15

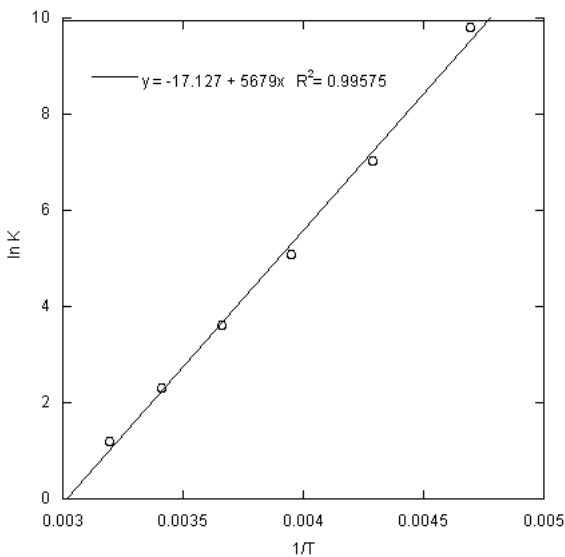


Figure 3.10. Van't Hoff Plot ($\ln K$ vs $1/T$) of data from Table 3.2: ($\Delta H = -11.3$ kcal/mol, and $\Delta S = -34$ cal/mol.)

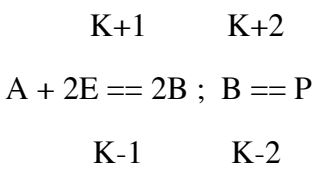
3.4.8 Kinetic Simulation Details

The proper determination of the rate constant for migratory insertion for the reactions of complexes **2.12** and **3.09** with ethylene at -50 °C is complicated by the presence of unsymmetrical dimers **2.13** and **4g**, respectively. To account for the small percentage of dimer (15% for **2.12** and 13% for **3.09**), kinetic simulations using KINSIM and FITSIM were used to rigorously determine the rate constant for insertion. The decay of the concentrations of the ethylene adduct and dimer were monitored over the course of the reaction and the experimental data was fit to the proposed mechanism. The pre-equilibrium ($K1$) between the ethylene adducts and their corresponding dinuclear species and free ethylene were determined in each case from their respective concentrations after 180 s had elapsed, and the relative difference between $K+1$ and $K-1$ was fixed during the fit.

Kinetic Simulation for the Reaction of 2.12 with Ethylene

Mechanism Description:

A = **2.13**; E = ethylene; B = **8**; P = Product

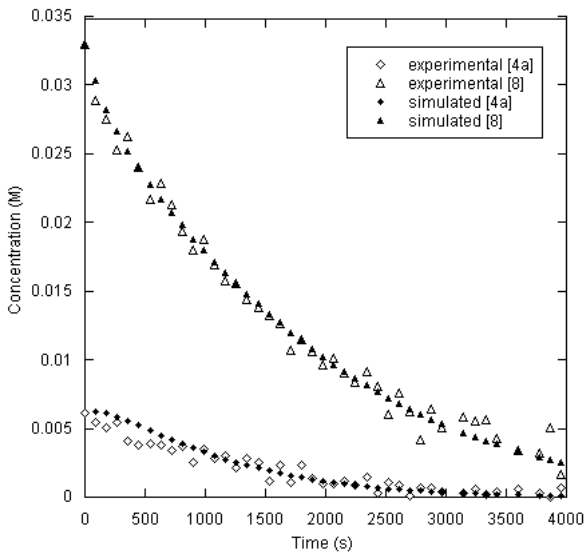


	Rate Constant (s-1)	error
K+2	8.72E-04	9.83E-06

Observed and Fitted Data using FITSIM for the Reaction of 2.12 with Ethylene				
Time (s)	Exp [2.13]	Sim [2.13]	Exp [2.07]	Sim [2.07]
0	6.09E-03	0.00E+00	3.30E-02	3.30E-02
90	5.45E-03	6.21E-03	2.89E-02	3.03E-02
180	5.04E-03	6.09E-03	2.75E-02	2.82E-02
270	5.42E-03	5.85E-03	2.53E-02	2.66E-02
360	4.12E-03	5.54E-03	2.63E-02	2.52E-02
450	3.84E-03	5.21E-03	2.40E-02	2.39E-02
540	3.89E-03	4.86E-03	2.17E-02	2.28E-02
630	3.78E-03	4.52E-03	2.29E-02	2.17E-02
720	3.37E-03	4.18E-03	2.13E-02	2.07E-02
810	3.67E-03	3.87E-03	1.94E-02	1.98E-02
900	2.49E-03	3.56E-03	1.80E-02	1.88E-02
990	3.50E-03	3.28E-03	1.88E-02	1.80E-02
1080	2.81E-03	3.01E-03	1.69E-02	1.71E-02
1170	3.04E-03	2.76E-03	1.58E-02	1.63E-02
1260	2.17E-03	2.53E-03	1.56E-02	1.55E-02

1350	2.83E-03	2.31E-03	1.44E-02	1.48E-02
1440	2.51E-03	2.11E-03	1.38E-02	1.41E-02
1530	1.18E-03	1.92E-03	1.32E-02	1.33E-02
1620	2.38E-03	1.75E-03	1.26E-02	1.27E-02
1710	1.04E-03	1.59E-03	1.07E-02	1.20E-02
1800	2.34E-03	1.44E-03	1.15E-02	1.14E-02
1890	1.38E-03	1.31E-03	1.06E-02	1.08E-02
1980	9.54E-04	1.18E-03	9.67E-03	1.02E-02
2070	1.01E-03	1.07E-03	1.01E-02	9.67E-03
2160	1.21E-03	9.65E-04	9.09E-03	9.14E-03
2250	9.14E-04	8.69E-04	8.41E-03	8.63E-03
2340	1.44E-03	7.82E-04	9.19E-03	8.15E-03
2430	3.21E-04	7.03E-04	8.08E-03	7.69E-03
2520	1.06E-03	6.31E-04	6.01E-03	7.24E-03
2610	8.62E-04	5.65E-04	7.54E-03	6.82E-03
2700	1.32E-04	5.06E-04	6.27E-03	6.42E-03
2790	6.41E-04	4.52E-04	4.14E-03	6.04E-03
2880	7.22E-04	4.04E-04	6.42E-03	5.68E-03
2970	4.02E-04	3.60E-04	5.06E-03	5.33E-03
3150	2.73E-04	2.85E-04	5.87E-03	4.70E-03
3240	6.25E-04	2.53E-04	5.53E-03	4.40E-03
3330	1.55E-04	2.24E-04	5.69E-03	4.13E-03
3420	3.85E-04	1.99E-04	4.30E-03	3.86E-03
3600	5.66E-04	1.55E-04	3.41E-03	3.38E-03
3780	2.91E-04	1.21E-04	3.21E-03	2.95E-03
3870	8.80E-06	1.06E-04	5.02E-03	2.76E-03
3960	6.59E-04	9.36E-05	1.64E-03	2.58E-03

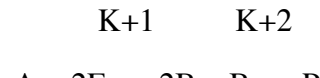
R-Squared Value = .9951



Kinetic Simulation of the Reaction of 3.09 with ethylene

Mechanism Description:

$A = \mathbf{4g}$; $E = \text{ethylene}$; $B = \mathbf{3.09}$ -ethylene adduct; $P = \text{Product}$



	Rate Constant (s^{-1})	Error (s^{-1})
K+2	3.75E-04	2.35E-06

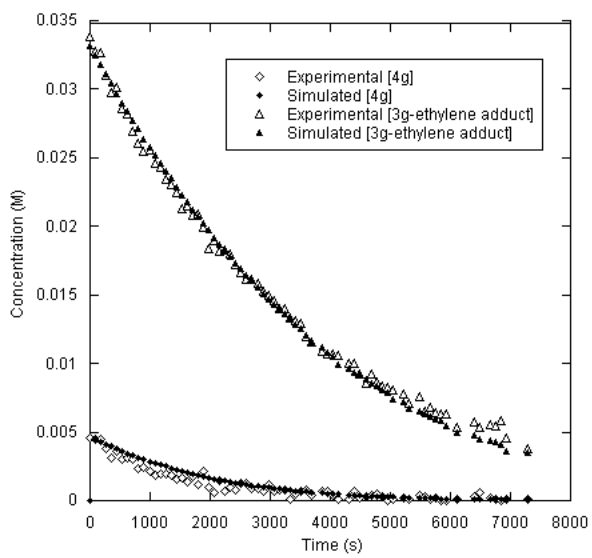
Observed and Fitted data using FITSIM for the Reaction of 3.09 with Ethylene				
Time (s)	Exp [4g]	Sim [4g]	Exp [3.09-adduct]	Sim [3.09-adduct]
0	4.62E-03	0.00E+00	3.38E-02	3.32E-02
90	4.48E-03	4.51E-03	3.28E-02	3.25E-02

180	4.49E-03	4.32E-03	3.27E-02	3.18E-02
270	3.81E-03	4.13E-03	3.10E-02	3.11E-02
360	3.14E-03	3.95E-03	2.98E-02	3.04E-02
450	3.60E-03	3.78E-03	3.01E-02	2.97E-02
540	3.03E-03	3.61E-03	2.86E-02	2.90E-02
630	3.16E-03	3.45E-03	2.82E-02	2.84E-02
720	2.98E-03	3.30E-03	2.69E-02	2.77E-02
810	2.37E-03	3.15E-03	2.61E-02	2.71E-02
900	2.48E-03	3.00E-03	2.55E-02	2.64E-02
990	2.11E-03	2.87E-03	2.56E-02	2.58E-02
1080	1.83E-03	2.73E-03	2.46E-02	2.52E-02
1170	1.97E-03	2.61E-03	2.43E-02	2.46E-02
1260	1.94E-03	2.49E-03	2.34E-02	2.40E-02
1350	1.86E-03	2.37E-03	2.30E-02	2.35E-02
1440	1.60E-03	2.26E-03	2.25E-02	2.29E-02
1530	1.64E-03	2.15E-03	2.13E-02	2.23E-02
1620	1.41E-03	2.05E-03	2.15E-02	2.18E-02
1710	1.75E-03	1.95E-03	2.08E-02	2.12E-02
1800	1.19E-03	1.85E-03	2.09E-02	2.07E-02
1890	2.14E-03	1.76E-03	1.99E-02	2.02E-02
1980	1.01E-03	1.67E-03	1.84E-02	1.97E-02
2070	6.20E-04	1.59E-03	1.90E-02	1.92E-02
2160	1.43E-03	1.51E-03	1.82E-02	1.87E-02
2250	6.64E-04	1.44E-03	1.83E-02	1.82E-02
2340	1.02E-03	1.36E-03	1.80E-02	1.78E-02
2430	7.85E-04	1.29E-03	1.72E-02	1.73E-02
2520	1.22E-03	1.23E-03	1.66E-02	1.69E-02
2610	1.28E-03	1.17E-03	1.61E-02	1.64E-02
2700	9.04E-04	1.11E-03	1.61E-02	1.60E-02
2790	8.52E-04	1.05E-03	1.59E-02	1.56E-02

2880	7.22E-04	9.94E-04	1.53E-02	1.51E-02
2970	1.20E-03	9.41E-04	1.50E-02	1.47E-02
3060	6.58E-04	8.92E-04	1.46E-02	1.43E-02
3150	7.72E-04	8.45E-04	1.40E-02	1.40E-02
3240	7.45E-04	8.00E-04	1.40E-02	1.36E-02
3330	1.12E-04	7.57E-04	1.33E-02	1.32E-02
3420	4.72E-04	7.16E-04	1.31E-02	1.28E-02
3510	6.93E-04	6.77E-04	1.29E-02	1.25E-02
3600	7.72E-04	6.41E-04	1.20E-02	1.21E-02
3690	4.01E-04	6.06E-04	1.16E-02	1.15E-02
3870	6.45E-04	5.41E-04	1.09E-02	1.12E-02
3960	6.54E-04	5.11E-04	1.07E-02	1.08E-02
4050	3.59E-04	4.83E-04	1.07E-02	1.05E-02
4140	1.04E-04	4.56E-04	1.06E-02	9.94E-03
4320	8.70E-05	4.06E-04	9.97E-03	9.66E-03
4410	6.73E-04	3.83E-04	9.97E-03	9.38E-03
4500	1.92E-04	3.61E-04	9.28E-03	9.11E-03
4590	3.20E-04	3.41E-04	8.58E-03	8.84E-03
4680	4.19E-04	3.21E-04	9.27E-03	8.59E-03
4770	5.00E-04	3.03E-04	8.61E-03	8.34E-03
4860	3.15E-04	2.85E-04	8.40E-03	8.09E-03
4950	4.71E-05	2.69E-04	8.30E-03	7.85E-03
5040	1.37E-04	2.53E-04	8.08E-03	7.40E-03
5220	1.67E-04	2.25E-04	7.80E-03	7.18E-03
5310	5.80E-05	2.12E-04	7.15E-03	6.76E-03
5490	3.49E-04	1.87E-04	7.59E-03	6.55E-03
5580	3.21E-04	1.76E-04	6.52E-03	6.36E-03
5670	1.04E-04	1.66E-04	6.78E-03	6.16E-03
5760	1.84E-04	1.56E-04	6.42E-03	5.98E-03
5850	2.17E-06	1.47E-04	6.32E-03	5.80E-03

5940	4.06E-05	1.38E-04	6.32E-03	5.45E-03
6120	1.30E-04	1.22E-04	5.37E-03	4.96E-03
6390	3.22E-04	1.01E-04	5.70E-03	4.81E-03
6480	5.64E-04	9.51E-05	5.34E-03	4.52E-03
6660	2.31E-04	8.39E-05	5.57E-03	4.38E-03
6750	1.16E-04	7.88E-05	5.42E-03	4.24E-03
6840	2.90E-05	7.40E-05	5.83E-03	4.11E-03
6930	7.61E-05	6.94E-05	4.56E-03	3.62E-03
7290	1.20E-04	5.39E-05	3.77E-03	3.51E-03

R-Squared Value = .9985



3.4.9 DFT Calculation Details

Computations with density functional theory were conducted with the Gaussian 09 package.⁶

The B3LYP functional with polarized triple- ζ basis sets was used. The LANL TZ basis set was used for Pd and P atoms. This method has been shown to generate accurate results for palladium systems.⁷

I. [2-(CH₂P(*t*-Bu)₂C₆H₄)Pd(CH₂=CH₂)NPh₂] (2.07)

C	0.128010	-1.141272	1.274444	C	-0.984854	-1.353596	2.100781
H	-1.909232	-0.834016	1.897825	C	-0.929507	-2.235537	3.178857
H	-1.810032	-2.376256	3.796663	C	0.242164	-2.932458	3.458731
H	0.288945	-3.620726	4.29544	C	1.358219	-2.733224	2.65446
H	2.278870	-3.269431	2.866363	C	1.312309	-1.847545	1.571586
C	2.539602	-1.657908	0.715882	H	2.587541	-2.434060	-0.053400
H	3.465434	-1.727292	1.292998	C	3.246709	1.262657	0.975996
C	2.901124	2.689305	0.508091	H	3.380334	3.408553	1.180676
H	1.825648	2.868723	0.545161	H	3.255621	2.902254	-0.501987
C	4.775127	1.102777	1.047787	H	5.162343	1.774859	1.821156
H	5.265597	1.372889	0.111401	H	5.077734	0.088753	1.319284
C	2.662820	1.073018	2.391672	H	3.060670	1.863001	3.037485
H	2.937524	0.113864	2.832658	H	1.574668	1.144286	2.398011
C	3.372857	-0.321460	-1.805922	C	2.510426	-1.269569	-2.667684
H	3.003118	-1.416942	-3.634467	H	1.512350	-0.873432	-2.851465
H	2.394891	-2.253711	-2.208828	C	3.587043	0.998243	-2.568806
H	4.043969	0.782169	-3.540263	H	4.259107	1.675043	-2.038133
H	2.650668	1.526627	-2.760449	C	4.736650	-1.004974	-1.577799
H	5.172333	-1.246891	-2.553490	H	4.642535	-1.942731	-1.026847
H	5.448798	-0.370489	-1.053396	C	-2.781064	-0.908257	-0.715993
C	-2.174525	-1.825020	-1.603476	H	-1.155444	-1.637775	-1.925165
C	-2.840568	-2.960860	-2.048134	H	-2.333732	-3.639108	-2.727448
C	-4.143875	-3.232806	-1.636225	H	-4.664769	-4.115668	-1.987832
C	-4.757061	-2.347002	-0.750225	H	-5.763201	-2.547344	-0.395308
C	-4.095979	-1.214435	-0.291586	H	-4.591026	-0.560834	0.415390
C	-2.695178	1.345839	0.203830	C	-3.880861	1.862136	-0.373461
H	-4.359656	1.314412	-1.175567	C	-4.428664	3.063094	0.058392
H	-5.333981	3.428869	-0.415877	C	-3.826269	3.808961	1.073555
H	-4.260201	4.745266	1.404346	C	-2.656756	3.320526	1.651710
H	-2.172017	3.876240	2.448267	C	-2.103958	2.113937	1.232962
H	-1.202868	1.738353	1.705041	N	-2.066413	0.190552	-0.252223
P	2.385567	-0.026907	-0.172990	Pd	0.043647	0.187425	-0.288453
C	-0.053146	2.287480	-1.644585	C	-0.379096	1.286537	-2.488051
H	0.947065	2.700129	-1.622679	H	-0.804870	2.796531	-1.054386
H	0.351089	0.865596	-3.168929	H	-1.402390	0.956969	-2.603764

I-TS. [2-(CH₂P(*t*-Bu)₂C₆H₄)Pd(CH₂=CH₂)NPh₂

C	0.162531	-0.637633	1.561908	C	-1.017632	-0.666891	2.316385
H	-1.948843	-0.341505	1.870770	C	-1.033541	-1.110161	3.638504
H	-1.967084	-1.117618	4.191870	C	0.143643	-1.539853	4.245959
H	0.139802	-1.882725	5.274953	C	1.328542	-1.527406	3.517529
H	2.249815	-1.867480	3.982836	C	1.344249	-1.087126	2.188860
C	2.633603	-1.126459	1.401355	H	2.819363	-2.141202	1.036625
H	3.505150	-0.844125	1.998781	C	3.167623	1.671092	0.386650
C	2.752852	2.720724	-0.662322	H	3.114608	3.704615	-0.344707
H	1.667072	2.774402	-0.757382	H	3.171877	2.519509	-1.649230
C	4.697783	1.669831	0.545740	H	5.012156	2.643947	0.935918
H	5.215177	1.519501	-0.402704	H	5.042549	0.912048	1.253538
C	2.531222	2.061121	1.736906	H	2.854177	3.075750	1.993522
H	2.836099	1.399622	2.549751	H	1.441843	2.051033	1.690205
C	3.494551	-0.926077	-1.448455	C	2.671693	-2.151788	-1.898970
H	3.239930	-2.704300	-2.655103	H	1.716482	-1.859894	-2.335136
H	2.465110	-2.839804	-1.075669	C	3.730256	-0.010437	-2.662848
H	4.195014	-0.593417	-3.465317	H	4.404676	0.815949	-2.430888
H	2.799364	0.404236	-3.051969	C	4.851389	-1.426038	-0.911922
H	5.365235	-1.969041	-1.712754	H	4.737367	-2.118992	-0.075876
H	5.507117	-0.616085	-0.595563	C	-2.738216	-1.060262	-0.668546
C	-2.160513	-2.173296	-1.311427	H	-1.186388	-2.069188	-1.774024
C	-2.792952	-3.410275	-1.325534	H	-2.313828	-4.242866	-1.829864
C	-4.019665	-3.591356	-0.689641	H	-4.509772	-4.557792	-0.696754
C	-4.591013	-2.508530	-0.027329	H	-5.532800	-2.628978	0.497859
C	-3.967939	-1.263770	-0.013401	H	-4.430235	-0.450193	0.528816
C	-2.714386	1.352185	-0.251198	C	-3.972410	1.709089	-0.775986
H	-4.478775	1.031423	-1.452683	C	-4.569429	2.918869	-0.439448
H	-5.539459	3.167343	-0.856873	C	-3.927000	3.814695	0.415347
H	-4.394518	4.757612	0.674674	C	-2.674861	3.482460	0.924339
H	-2.158628	4.167448	1.588412	C	-2.074786	2.268819	0.594753
H	-1.104262	2.008559	0.999124	N	-2.041735	0.170900	-0.661334
P	2.436182	-0.040960	-0.104051	Pd	0.159727	0.038675	-0.395767
C	-1.387494	0.639622	-2.533561	C	0.016796	0.679395	-2.566185
H	-1.944787	1.568812	-2.523824	H	-1.914465	-0.197974	-2.977201
H	0.492556	1.652738	-2.629461	H	0.523925	-0.115600	-3.104059

I-P. [2-(CH₂P(*t*-Bu)₂C₆H₄]Pd(C₂H₄NPh₂)

C	-0.271284	-1.358048	1.177122	C	0.811055	-2.186621	1.519289
C	0.722821	-3.168518	2.507560	C	-0.473060	-3.358070	3.195285
C	-1.569508	-2.559646	2.881716	C	-1.472605	-1.574894	1.891970
C	-2.673280	-0.703691	1.586684	C	-3.299818	-1.047284	-1.354241
C	-2.874459	-0.655401	-2.781967	C	-4.834100	-1.020013	-1.242663
C	-2.809078	-2.485350	-1.083946	C	-3.273622	1.810786	0.082957
C	-2.328700	2.671730	0.948491	C	-3.430915	2.479629	-1.293690
C	-4.646041	1.736915	0.782316	C	2.430854	1.519767	0.285009
C	2.470517	2.901853	0.082811	C	2.799757	3.758021	1.135821
C	3.099587	3.253582	2.394739	C	3.057825	1.873322	2.599342
C	2.722504	1.016183	1.561132	C	3.077361	-0.445876	-1.018746
C	4.444014	-0.187035	-0.886443	C	5.376291	-1.171515	-1.207922
C	4.958198	-2.415191	-1.673513	C	3.595248	-2.670837	-1.814233
C	2.659715	-1.694825	-1.485121	N	2.079166	0.580307	-0.763925
P	-2.416520	0.096881	-0.084313	Pd	-0.172135	0.129505	-0.323133
C	1.581884	1.203076	-2.063921	C	0.133161	1.597526	-1.847595
H	1.755427	-2.081806	0.994584	H	1.585500	-3.787812	2.734618
H	-0.554076	-4.120516	3.962715	H	-2.506597	-2.704278	3.413440
H	-2.745500	0.110564	2.314639	H	-3.619514	-1.250738	1.635062
H	-1.789846	-0.694614	-2.892745	H	-3.205894	0.345543	-3.060505
H	-3.318252	-1.362034	-3.491954	H	-5.256268	-0.060387	-1.545389
H	-5.184039	-1.249622	-0.233037	H	-5.250099	-1.782099	-1.910801
H	-3.133469	-2.862925	-0.112700	H	-1.721366	-2.556916	-1.121221
H	-3.224967	-3.144490	-1.853788	H	-2.179588	2.248557	1.944905
H	-2.770801	3.666057	1.075418	H	-1.348660	2.783414	0.484458
H	-2.486793	2.506533	-1.838930	H	-3.767711	3.512595	-1.153183
H	-4.177073	1.977541	-1.912838	H	-5.038862	2.753919	0.890589
H	-4.579192	1.310413	1.785311	H	-5.379299	1.163353	0.216699
H	2.234405	3.328168	-0.881177	H	2.819759	4.827690	0.958333
H	3.354307	3.922168	3.208878	H	3.274964	1.460412	3.578065
H	2.665894	-0.049680	1.738083	H	4.777888	0.778583	-0.528449
H	6.433867	-0.958982	-1.097651	H	5.685981	-3.179484	-1.920641
H	3.255593	-3.638226	-2.166646	H	1.597646	-1.896217	-1.569402
H	2.285909	1.984766	-2.386848	H	1.647602	0.406146	-2.803039
H	0.018245	2.622122	-1.484337	H	-0.449174	1.482228	-2.763673

II. [2-(CH₂P(*t*-Bu)(*i*-Pr)C₆H₄]Pd(CH₂=CH₂)NPh₂

Pd	0.155141	0.234531	-0.271250	P	2.484550	0.082452	-0.107103
N	-1.953254	0.173704	-0.263699	C	-2.617434	1.270030	0.280033
C	-2.064654	1.952266	1.387876	H	-1.166623	1.552317	1.845697
C	-2.652394	3.104577	1.901431	H	-2.197307	3.594820	2.756330
C	-3.819354	3.620485	1.342556	H	-4.280456	4.514082	1.746675
C	-4.383821	2.958855	0.250088	H	-5.286408	3.348782	-0.209939
C	-3.801114	1.812995	-0.275865	H	-4.250339	1.330904	-1.135261
C	-2.631491	-0.901322	-0.826234	C	-3.948766	-1.267294	-0.460548
H	-4.476058	-0.681369	0.281580	C	-4.571998	-2.374776	-1.022161
H	-5.581573	-2.623236	-0.709883	C	-3.917651	-3.175787	-1.958002
H	-4.409600	-4.039322	-2.390120	C	-2.611393	-2.845073	-2.313923
H	-2.072664	-3.457513	-3.030240	C	-1.982666	-1.733678	-1.765632
H	-0.960267	-1.500841	-2.044438	C	0.264224	-1.220783	1.172994
C	1.458463	-1.938691	1.395798	C	1.523339	-2.916478	2.394808
H	2.450974	-3.459244	2.551856	C	0.415671	-3.197678	3.186242
H	0.476034	-3.957181	3.957960	C	-0.765764	-2.491374	2.979067
H	-1.639195	-2.697115	3.588681	C	-0.839909	-1.517251	1.984657
H	-1.771281	-0.991941	1.833949	C	2.673272	-1.650001	0.549207
H	2.702018	-2.314654	-0.319636	H	3.610135	-1.790367	1.094001
C	3.281146	1.228309	1.180610	H	4.352683	1.234689	0.955311
C	3.096491	0.719138	2.619013	H	3.570170	1.425047	3.308241
H	3.551782	-0.257927	2.783833	H	2.040906	0.645239	2.886518
C	2.743337	2.663662	1.062846	H	3.256215	3.306486	1.784732
H	1.673862	2.696060	1.284452	H	2.896437	3.096099	0.072984
C	3.647361	0.121173	-1.635079	C	3.033878	-0.774472	-2.729007
H	3.668606	-0.740648	-3.620659	H	2.033866	-0.446026	-3.015164
H	2.964251	-1.819172	-2.419048	C	5.043562	-0.418704	-1.269551
H	5.682534	-0.393741	-2.158887	H	5.007933	-1.453735	-0.924042
H	5.536802	0.181256	-0.501378	C	3.786693	1.555889	-2.173958
H	4.397614	1.542623	-3.082599	H	4.282447	2.216753	-1.459981
H	2.821896	1.994184	-2.436553	C	-0.228438	1.461547	-2.381866
C	0.013227	2.414933	-1.457066	H	0.547952	1.118764	-3.055972
H	-1.231297	1.103015	-2.570134	H	0.990863	2.868626	-1.355825
H	-0.787766	2.850135	-0.873109				

II-TS. [2-(CH₂P(*t*-Bu)(*i*-Pr)C₆H₄]Pd(CH₂=CH₂)NPh₂

Pd	0.263391	0.157088	-0.366164	P	2.530777	0.108501	-0.083497
N	-1.935102	0.204199	-0.640243	C	-2.673729	1.281775	-0.084526
C	-2.091359	2.104600	0.890252	H	-1.113089	1.841036	1.274272
C	-2.756886	3.230122	1.371803	H	-2.284198	3.841571	2.133090
C	-4.018786	3.566779	0.890741	H	-4.537183	4.440784	1.267965
C	-4.604599	2.766647	-0.090255	H	-5.581071	3.022539	-0.487814
C	-3.942104	1.646023	-0.578956	H	-4.405362	1.044556	-1.351803
C	-2.559718	-1.050145	-0.828063	C	-3.800596	-1.398370	-0.260882
H	-4.329681	-0.686205	0.357110	C	-4.350039	-2.662102	-0.458479
H	-5.303473	-2.897154	0.003110	C	-3.692392	-3.620749	-1.224024
H	-4.126811	-4.601803	-1.375753	C	-2.452741	-3.298214	-1.772809
H	-1.906329	-4.034713	-2.352491	C	-1.892726	-2.042227	-1.574290
H	-0.906020	-1.830860	-1.969478	C	0.308171	-0.803181	1.469966
C	1.505916	-1.336622	1.992101	C	1.526052	-1.968859	3.240534
H	2.459384	-2.368217	3.627951	C	0.359086	-2.097775	3.986510
H	0.381209	-2.589894	4.952871	C	-0.835058	-1.593561	3.477426
H	-1.754935	-1.694179	4.044398	C	-0.854599	-0.957275	2.236387
H	-1.798846	-0.581353	1.863256	C	2.768236	-1.255901	1.165905
H	2.904711	-2.181418	0.596807	H	3.668826	-1.117590	1.770043
C	3.236274	1.681332	0.707094	H	4.317745	1.648954	0.533579
C	2.987495	1.727207	2.222466	H	3.382876	2.665954	2.622761
H	3.472861	0.909434	2.756392	H	1.920129	1.686135	2.449207
C	2.661621	2.944880	0.045675	H	3.142012	3.831510	0.471129
H	1.587565	3.017461	0.231566	H	2.813454	2.969673	-1.033725
C	3.719971	-0.348099	-1.514352	C	3.105988	-1.538674	-2.274051
H	3.774128	-1.833167	-3.090375	H	2.136533	-1.282687	-2.703921
H	2.966913	-2.412496	-1.632970	C	5.100646	-0.750732	-0.960340
H	5.767692	-0.988779	-1.795881	H	5.047877	-1.635009	-0.322307
H	5.571316	0.054073	-0.389872	C	3.890380	0.838421	-2.480320
H	4.497313	0.520670	-3.33486	H	4.406794	1.677569	-2.009736
H	2.934512	1.195420	-2.86689	C	0.106015	1.184844	-2.365291
C	-1.283007	0.974736	-2.416737	H	0.727715	0.569237	-3.008244
H	0.461143	2.199968	-2.218743	H	-1.957742	1.815892	-2.308790
H	-1.674946	0.150857	-3.005042				

II-P. [2-(CH₂P(*t*-Bu)(*i*-Pr)C₆H₄]Pd(C₂H₄NPh₂)

Pd	-0.291199	-0.268418	-0.268253	P	-2.533806	-0.108527	-0.169591
N	1.986629	-0.746742	-0.602104	C	2.524452	-1.245731	0.641191
C	3.374096	-0.447355	1.421390	C	3.861605	-0.909357	2.639628
C	3.518412	-2.173562	3.111144	C	2.676352	-2.970288	2.341542
C	2.182145	-2.518268	1.120619	C	2.827798	0.237517	-1.274911
C	4.118400	-0.112510	-1.687681	C	4.898370	0.801668	-2.387813
C	4.399170	2.071469	-2.679207	C	3.116974	2.418650	-2.265407
C	2.329821	1.504089	-1.563917	C	-0.440892	1.522196	0.854966
C	-1.653470	2.250494	0.881113	C	-1.785294	3.426778	1.626817
C	-0.713535	3.912928	2.370859	C	0.488613	3.209246	2.373523
C	0.612813	2.035955	1.627900	C	-2.826741	1.719262	0.085051
C	-3.318215	-0.995754	1.310144	C	-3.235860	-0.175766	2.606814
C	-2.684754	-2.379908	1.525065	C	-3.604051	-0.564131	-1.688629
C	-2.927816	0.037769	-2.935397	C	-5.027361	0.009268	-1.549072
C	-3.683240	-2.093573	-1.842856	C	0.030731	-2.062142	-1.361925
C	1.510408	-1.821612	-1.591089	H	3.661129	0.535006	1.071943
H	4.516933	-0.270247	3.220981	H	3.900203	-2.530546	4.060368
H	2.394955	-3.958455	2.688688	H	1.516209	-3.155682	0.557722
H	4.509256	-1.096222	-1.454460	H	5.896690	0.522724	-2.706076
H	5.008819	2.783940	-3.223341	H	2.722372	3.404963	-2.481720
H	1.334738	1.767825	-1.225934	H	-2.729709	3.964834	1.631335
H	-0.819800	4.824591	2.949173	H	1.327495	3.569516	2.961502
H	1.557281	1.503303	1.66697	H	-2.858774	2.172376	-0.911483
H	-3.791855	1.921424	0.557708	H	-4.374671	-1.124637	1.049803
H	-3.758741	0.779206	2.538758	H	-2.199613	0.028663	2.882131
H	-3.695842	-0.747703	3.419039	H	-1.636739	-2.276837	1.815449
H	-2.720080	-3.007807	0.634604	H	-3.212898	-2.903516	2.328572
H	-2.889145	1.129361	-2.896552	H	-3.500560	-0.238210	-3.827477
H	-1.907679	-0.330958	-3.052369	H	-5.618554	-0.278745	-2.425229
H	-5.029883	1.100051	-1.497724	H	-5.547344	-0.375748	-0.667879
H	-4.202816	-2.334535	-2.776629	H	-4.245833	-2.557760	-1.029657
H	-2.692813	-2.548818	-1.883167	H	-0.498754	-2.169308	-2.310105
H	-0.178979	-2.941770	-0.746615	H	1.674096	-1.389223	-2.577193
H	2.173151	-2.692739	-1.502064				

III. [2-(CH₂P(CH₃)₂C₆H₄]Pd(CH₂=CH₂)NPh₂

C	-1.261323	0.919107	0.875712	C	-0.411949	1.479816	1.837735
H	0.620919	1.165297	1.885550	C	-0.873428	2.448841	2.727747
H	-0.192459	2.866924	3.461478	C	-2.196096	2.880266	2.675882
H	-2.556387	3.633772	3.367492	C	-3.056724	2.334940	1.728948
H	-4.089606	2.667164	1.682549	C	-2.601662	1.364631	0.830288
C	-3.538261	0.775057	-0.200394	H	-3.502320	1.339173	-1.139383
H	-4.580101	0.746466	0.132011	C	-3.602373	-2.004094	0.745722
C	-3.672966	-1.492412	-2.114830	C	1.910641	1.187559	-0.676443
C	1.230583	1.825055	-1.737488	H	0.340438	1.352616	-2.140004
C	1.663601	3.039110	-2.257323	H	1.108509	3.493881	-3.071821
C	2.798581	3.669610	-1.750615	H	3.139547	4.612923	-2.160921
C	3.479126	3.061812	-0.695643	H	4.353700	3.542390	-0.268310
C	3.047924	1.853798	-0.161814	H	3.584172	1.420436	0.672987
C	2.239077	-0.914569	0.511057	C	3.575381	-1.178299	0.124413
H	4.009957	-0.613579	-0.690983	C	4.329052	-2.155675	0.761228
H	5.347846	-2.332958	0.431123	C	3.793234	-2.919078	1.800566
H	4.388571	-3.679549	2.292183	C	2.478134	-2.678764	2.192181
H	2.039618	-3.252155	3.002821	C	1.716975	-1.695091	1.567572
H	0.701070	-1.504957	1.896956	N	1.420356	-0.001158	-0.147207
P	-2.864219	-0.913917	-0.552962	Pd	-0.596424	-0.546334	-0.402848
H	-4.692981	-2.015162	0.675055	H	-3.303593	-1.627551	1.724592
H	-3.224136	-3.022019	0.636512	H	-3.375878	-0.844896	-2.941310
H	-4.761475	-1.472068	-2.018145	H	-3.360479	-2.513164	-2.343739
C	0.048929	-2.704027	-1.382022	C	0.210916	-1.762619	-2.339582
H	-0.846404	-3.314010	-1.333959	H	0.856510	-2.974526	-0.713528
H	-0.550432	-1.580517	-3.090333	H	1.157477	-1.255561	-2.470345

III-TS. [2-(CH₂P(CH₃)₂C₆H₄]Pd(CH₂=CH₂)NPh₂

Pd	-0.712332	-0.582833	-0.479810	P	-2.882499	-1.078906	-0.492873
N	1.594807	-0.411290	-0.674120	C	2.283937	-1.105459	0.410647
C	1.662132	-1.255015	1.647996	H	0.668215	-0.847701	1.791936
C	2.310829	-1.926047	2.684579	H	1.812578	-2.037525	3.640905
C	3.583832	-2.453890	2.492211	H	4.084999	-2.980228	3.296587
C	4.210983	-2.302058	1.256381	H	5.204706	-2.705266	1.096369
C	3.567269	-1.629821	0.221757	H	4.069352	-1.503889	-0.730052
C	2.073394	0.931845	-0.944673	C	3.111729	1.521439	-0.217554
H	3.606609	0.972726	0.570847	C	3.515394	2.828566	-0.494366
H	4.321481	3.263476	0.086210	C	2.899248	3.567061	-1.496386
H	3.215674	4.581684	-1.707905	C	1.852348	2.987993	-2.213375
H	1.339370	3.555419	-2.981832	C	1.437184	1.692595	-1.936981
H	0.587490	1.280815	-2.467413	C	-1.411589	1.007299	0.743490
C	-2.794467	1.310723	0.795663	C	-3.289177	2.335514	1.609232
H	-4.355990	2.542008	1.635683	C	-2.421092	3.103198	2.380956
H	-2.808467	3.898048	3.009465	C	-1.053796	2.841704	2.333086
H	-0.365516	3.438784	2.923726	C	-0.567543	1.810318	1.528450
H	0.505051	1.639547	1.512302	C	-3.742150	0.517901	-0.085727
H	-3.917532	1.035532	-1.036736	H	-4.720867	0.344206	0.374110
C	-3.403967	-2.252199	0.838439	C	-3.710301	-1.746169	-2.004745
C	0.128083	-2.069158	-1.731095	C	1.436180	-1.322657	-1.908097
H	-0.376133	-2.243156	-2.683956	H	0.255076	-3.023485	-1.212846
H	2.335930	-1.941106	-2.002617	H	1.402237	-0.667198	-2.775820
H	-2.907145	-3.212892	0.695612	H	-4.487733	-2.396371	0.829979
H	-3.098288	-1.840661	1.800877	H	-3.288564	-2.723008	-2.246556
H	-3.523768	-1.073976	-2.843435	H	-4.788432	-1.844946	-1.851563

III-TS. [2-(CH₂P(CH₃)₂C₆H₄]Pd(C₂H₄NPh₂)

Pd	-0.717819	-0.502887	-0.542891	P	-2.951974	-0.805275	-0.598750
N	1.476662	-0.251955	-0.468777	C	2.217856	-1.065597	0.430172
C	1.562085	-1.753031	1.460797	H	0.503893	-1.575630	1.613297
C	2.253555	-2.638719	2.285215	H	1.721113	-3.151599	3.078958
C	3.615027	-2.861205	2.101159	H	4.152559	-3.547745	2.745111
C	4.277983	-2.193012	1.071619	H	5.336170	-2.364976	0.905728
C	3.591480	-1.314091	0.241372	H	4.117410	-0.814420	-0.563284
C	1.966912	1.029040	-0.816441	C	3.004350	1.679804	-0.122646
H	3.471666	1.196905	0.724547	C	3.424934	2.954215	-0.492865
H	4.221075	3.427894	0.071978	C	2.834171	3.624611	-1.560092
H	3.166321	4.616459	-1.843195	C	1.791472	3.001091	-2.242596
H	1.297071	3.510669	-3.062908	C	1.360197	1.732249	-1.876151
H	0.517322	1.287771	-2.392467	C	-1.262642	0.817928	0.968592
C	-2.601502	1.248984	1.113010	C	-2.966908	2.125533	2.140162
H	-4.001530	2.442665	2.236929	C	-2.012425	2.602768	3.033109
H	-2.301566	3.283386	3.826502	C	-0.685959	2.200782	2.895558
H	0.068677	2.570582	3.582307	C	-0.322274	1.320308	1.876700
H	0.717032	1.027479	1.790437	C	-3.633565	0.765143	0.115274
H	-3.740749	1.473857	-0.714496	H	-4.625954	0.620198	0.553798
C	-3.577887	-2.146212	0.510042	C	-3.853170	-1.100884	-2.185620
C	-0.094366	-1.812143	-2.248774	C	1.253815	-1.426005	-2.10226
H	-0.647593	-1.393009	-3.085201	H	-0.353807	-2.835418	-1.993964
H	1.971060	-2.143531	-1.721050	H	1.674123	-0.681236	-2.769326
H	-3.187610	-3.109934	0.179131	H	-4.670585	-2.177007	0.509077
H	-3.219009	-1.954596	1.521829	H	-3.537325	-2.053455	-2.614635
H	-3.612213	-0.306477	-2.893525	H	-4.933738	-1.122561	-2.021864

4-methylstyrene

C	-0.422223	0.858214	0.130572	C	0.283823	-0.342582	0.295357
C	1.669798	-0.375879	0.210861	C	2.413733	0.782444	-0.041177
C	1.713043	1.981351	-0.205022	C	0.326524	2.017935	-0.121325
C	-1.887675	0.954656	0.210008	H	-0.253051	-1.263200	0.492873
H	2.187108	-1.320759	0.343993	C	3.919068	0.744373	-0.141304
H	2.259957	2.898709	-0.400301	H	-0.191578	2.962768	-0.252028
C	-2.760128	-0.029660	0.441754	H	-2.281192	1.957685	0.057890
H	-3.824514	0.168587	0.476488	H	-2.456444	-1.057859	0.604314
H	4.255529	1.002884	-1.150663	H	4.309239	-0.247624	0.094671
H	4.381498	1.459314	0.545908				

3-methoxystyrene

C	-0.454175	0.944908	0.110264	C	0.243963	-0.220389	0.437253
C	1.639138	-0.241914	0.457091	C	2.363206	0.914799	0.146701
C	1.668898	2.079216	-0.179987	C	0.281453	2.102093	-0.200156
C	-1.925060	1.009211	0.077882	H	-0.273152	-1.138986	0.684398
O	2.203315	-1.439214	0.791438	H	2.227003	2.977174	-0.420971
H	-0.243554	3.015628	-0.456282	C	-2.788484	0.025113	0.338974
H	-2.326212	1.983246	-0.193219	H	-3.857022	0.193926	0.282016
H	-2.471961	-0.974274	0.616095	C	3.619453	-1.533743	0.831953
H	3.444549	0.919386	0.156305	H	4.065430	-1.326277	-0.147371
H	3.840528	-2.561359	1.116004	H	4.047613	-0.853507	1.576929

[2-(CH₂P(CH₃)₂C₆H₄]Pd(CH₂=CH₂-4-CH₃C₆H₄)NPh₂

C	2.224990	0.895912	-0.886082	C	3.403056	0.139246	-0.919256
H	3.447222	-0.816911	-0.420072	C	4.530459	0.598884	-1.599228
H	5.428383	-0.009721	-1.609864	C	4.504316	1.823481	-2.259832
H	5.379458	2.182897	-2.789697	C	3.342791	2.586967	-2.231103
H	3.313831	3.545818	-2.740645	C	2.204339	2.137717	-1.551910
C	0.952978	2.979930	-1.541149	H	0.356512	2.777155	-2.435687
H	1.169226	4.051580	-1.539130	C	0.441176	3.600966	1.375345
C	-0.131179	3.039237	2.691507	H	0.201169	2.013490	2.861354
H	-1.221288	3.057225	2.720297	H	0.229988	3.649243	3.526424
C	0.004613	5.065341	1.197718	H	-1.077941	5.188735	1.250402
H	0.356126	5.491120	0.254720	H	0.438655	5.664408	2.005634
C	1.980474	3.551776	1.466050	H	2.466916	3.988816	0.592467
H	2.349485	2.531777	1.579426	H	2.293848	4.126783	2.343989
C	-1.887852	2.809195	-0.661552	C	-2.253268	1.658085	-1.623050
H	-1.571092	1.591501	-2.474084	H	-3.258920	1.832117	-2.020373
H	-2.257017	0.692857	-1.116047	C	-2.869695	2.788222	0.521647
H	-3.893662	2.831962	0.136494	H	-2.734214	3.641309	1.188360
H	-2.782309	1.870447	1.104344	C	-2.026507	4.145148	-1.418294
H	-3.061765	4.245277	-1.762538	H	-1.389254	4.190199	-2.303406
H	-1.805730	5.011107	-0.795359	C	1.249878	-2.518584	-0.990628
C	0.298822	-2.249798	-2.000422	H	-0.429335	-1.464503	-1.828478
C	0.293991	-2.947274	-3.202239	H	-0.452432	-2.705279	-3.952353
C	1.230492	-3.950690	-3.449057	H	1.223128	-4.498362	-4.384240
C	2.183595	-4.225368	-2.469189	H	2.936417	-4.987145	-2.646065
C	2.202477	-3.525736	-1.268096	H	2.967999	-3.749084	-0.535849
C	1.790709	-2.259498	1.366082	C	1.658184	-3.612434	1.761274
H	1.162626	-4.310447	1.097893	C	2.133386	-4.055228	2.988429
H	2.003058	-5.098786	3.257264	C	2.756661	-3.180264	3.880252
H	3.124604	-3.533215	4.836517	C	2.893427	-1.844581	3.511996
H	3.379536	-1.143267	4.182881	C	2.426427	-1.391532	2.280967
H	2.555832	-0.351338	2.003265	N	1.243812	-1.763582	0.180996
P	-0.085258	2.457155	-0.081228	Pd	0.599609	0.231324	0.129774
C	-1.248304	-0.585074	2.042755	C	-1.808722	-1.441417	1.166973
H	-1.803317	0.232792	2.487449	H	-0.255116	-0.772395	2.434668
C	-3.194207	-1.442518	0.681520	H	-1.179818	-2.234980	0.776860
C	-4.227845	-0.721480	1.302480	C	-5.524105	-0.764758	0.809815
C	-5.848847	-1.531658	-0.317790	C	-4.823942	-2.257057	-0.931039
C	-3.523536	-2.219986	-0.438796	H	-4.019856	-0.141055	2.194030
H	-6.304711	-0.203985	1.314590	H	-2.744623	-2.792757	-0.931063
C	-7.268403	-1.599176	-0.823799	H	-5.046076	-2.863597	-1.802971
H	-7.307171	-1.946482	-1.858169	H	-7.756958	-0.622555	-0.773925
H	-7.866181	-2.291884	-0.221268				

[2-(CH₂P(CH₃)₂C₆H₄]Pd(CH₂=CH₂-3-OCH₃C₆H₄)NPh₂

C	-2.149107	0.903368	-1.097005	C	-2.398078	2.279259	-1.184185
H	-1.802843	2.974138	-0.611479	C	-3.405580	2.774561	-2.011419
H	-3.574051	3.845124	-2.059118	C	-4.185374	1.906629	-2.769783
H	-4.969415	2.289366	-3.413666	C	-3.951246	0.538644	-2.691286
H	-4.556016	-0.147354	-3.277406	C	-2.943532	0.028129	-1.864743
C	-2.703253	-1.459260	-1.806388	H	-2.035580	-1.763449	-2.617882
H	-3.624439	-2.037155	-1.919790	C	-3.195129	-2.235462	1.069978
C	-2.584953	-2.248765	2.484917	H	-2.105034	-1.296311	2.716558
H	-1.853837	-3.046387	2.623271	H	-3.385023	-2.405614	3.216222
C	-3.930090	-3.561095	0.805195	H	-3.291386	-4.432623	0.957080
H	-4.347779	-3.609933	-0.203450	H	-4.767433	-3.646568	1.506224
C	-4.218442	-1.082599	1.003165	H	-4.754192	-1.052316	0.052925
H	-3.748355	-0.109780	1.151946	H	-4.958548	-1.228822	1.797225
C	-0.767210	-3.400893	-0.651219	C	0.443624	-2.881387	-1.454721
H	0.141115	-2.330178	-2.348704	H	1.047912	-3.734493	-1.781152
H	1.080948	-2.231115	-0.855114	C	-0.256997	-4.105475	0.616266
H	0.444954	-4.894870	0.328536	H	-1.063462	-4.574171	1.182728
H	0.280568	-3.420373	1.272631	C	-1.539843	-4.411199	-1.522408
H	-0.873310	-5.247394	-1.760168	H	-1.862855	-3.979124	-2.471278
H	-2.413974	-4.823388	-1.019919	C	0.977998	2.558385	-0.772602
C	1.507309	1.674336	-1.741219	H	1.349266	0.609336	-1.607841
C	2.187021	2.138842	-2.860838	H	2.562471	1.423560	-3.586496
C	2.384224	3.504694	-3.062845	H	2.917568	3.866585	-3.934054
C	1.861453	4.394246	-2.124762	H	1.978934	5.463510	-2.270497
C	1.168170	3.940532	-1.008642	H	0.753871	4.660351	-0.314418
C	0.100842	2.773123	1.488724	C	1.126424	3.572132	2.048467
H	2.063671	3.679005	1.516501	C	0.960526	4.204549	3.273946
H	1.775240	4.800695	3.672754	C	-0.223715	4.071657	4.000643
H	-0.345651	4.568167	4.956135	C	-1.243640	3.286448	3.469190
H	-2.177594	3.170482	4.009966	C	-1.090142	2.653816	2.238732
H	-1.899885	2.058125	1.832516	N	0.263829	2.048780	0.306317
P	-1.814138	-1.843853	-0.212629	Pd	-0.707853	0.189545	0.142841
C	0.792527	-0.578669	2.306762	C	1.909858	-0.343680	1.591514
H	0.529409	-1.567852	2.662264	H	0.191931	0.248321	2.668121
C	2.933283	-1.316806	1.182219	H	2.099470	0.680957	1.291707
C	3.069367	-2.575637	1.780417	C	4.069933	-3.444528	1.350246
C	4.942497	-3.078800	0.334383	C	4.828009	-1.815566	-0.261054
C	3.830192	-0.938765	0.166923	H	2.421593	-2.863059	2.599171
H	4.180424	-4.414517	1.822213	O	5.731722	-1.536549	-1.238160
H	3.721738	0.040660	-0.280433	H	5.729356	-3.741075	-0.005313
C	5.704295	-0.246349	-1.841931	H	4.751174	-0.056019	-2.345181
H	6.507860	-0.248195	-2.576156	H	5.886577	0.542914	-1.105183

3.4.10 Crystallographic Data for 3.04 and 3.13

Table 3.4. Crystal data and structure refinement for 3.04

Empirical formula	C ₃₀ H ₄₀ NOPPD
Formula weight	568.00
Temperature	193(2) K
Wavelength	0.71073 Å
Crystal system	Orthorhombic
Space group	Pca2(1)
Unit cell dimensions	a = 19.6710(14) Å a= 90°. b = 8.7480(7) Å b= 90°. c = 15.9812(11) Å g = 90°.
Volume	2750.1(4) Å ³
Z	4
Density (calculated)	1.372 Mg/m ³
Absorption coefficient	0.755 mm ⁻¹
F(000)	1184
Crystal size	0.216 x 0.161 x 0.092 mm ³
Theta range for data collection	2.07 to 25.38°
Index ranges	-22<=h<=23, -10<=k<=10, -19<=l<=19
Reflections collected	26326
Independent reflections	4958 [R(int) = 0.0743]
Completeness to theta = 25.38°	99.9 %
Absorption correction	Integration
Max. and min. transmission	0.9593 and 0.8869
Refinement method	Full-matrix least-squares on F ²
Data / restraints / parameters	4958 / 370 / 428
Goodness-of-fit on F ²	1.009
Final R indices [I>2sigma(I)]	R1 = 0.0387, wR2 = 0.0699
R indices (all data)	R1 = 0.0639, wR2 = 0.0773
Absolute structure parameter	-0.02(3)
Largest diff. peak and hole	0.463 and -0.404 e.Å ⁻³

Table 3.5. Atomic coordinates ($\times 10^4$) and equivalent isotropic displacement parameters ($\text{\AA}^2 \times 10^3$) for **3.04**. U(eq) is defined as one third of the trace of the orthogonalized U^{ij} tensor.

	x	y	z	U(eq)
Pd(1)	7152(1)	3270(1)	9605(1)	28(1)
P(1)	8269(1)	3771(1)	9651(2)	34(1)
N(1)	6100(2)	2932(4)	9621(5)	33(1)
O(1)	7230(30)	1150(40)	8830(30)	46(3)
C(1)	7140(30)	960(50)	7940(30)	48(3)
C(2)	6770(20)	-460(50)	7840(20)	52(3)
C(3)	6398(19)	-700(40)	8650(20)	51(3)
C(4)	6890(30)	-160(80)	9240(20)	46(3)
O(1B)	7189(5)	1212(8)	8779(6)	43(1)
C(1B)	7059(5)	1385(9)	7893(6)	47(2)
C(2B)	6598(4)	161(10)	7667(4)	53(2)
C(3B)	6715(5)	-1083(9)	8305(6)	57(2)
C(4B)	6847(7)	-190(14)	9047(5)	47(2)
C(5)	5755(2)	3338(6)	8896(3)	32(1)
C(6)	5966(3)	4599(7)	8436(3)	43(1)
C(7)	5656(3)	5014(7)	7688(3)	56(2)
C(8)	5131(3)	4172(8)	7372(3)	57(2)
C(9)	4919(3)	2897(8)	7800(4)	51(2)
C(10)	5226(3)	2497(10)	8542(4)	49(2)
C(11)	5767(2)	2367(6)	10311(3)	29(1)
C(12)	5072(3)	2528(8)	10465(4)	32(2)
C(13)	4782(3)	1973(6)	11167(4)	42(2)
C(14)	5156(3)	1231(6)	11766(3)	42(2)
C(15)	5832(3)	1076(6)	11635(3)	40(1)
C(16)	6146(2)	1633(6)	10936(3)	36(1)
C(17)	7110(2)	5096(6)	10349(3)	30(1)
C(18)	7691(2)	5635(6)	10753(3)	38(1)
C(19)	7656(3)	6947(7)	11245(4)	48(2)
C(20)	7063(3)	7749(7)	11331(4)	50(2)
C(21)	6486(3)	7241(6)	10944(3)	41(1)
C(22)	6505(2)	5936(6)	10453(3)	35(1)
C(23)	8348(3)	4815(8)	10639(4)	45(2)
C(24)	8540(50)	5130(60)	8850(30)	52(4)
C(25)	8360(40)	6840(60)	8720(60)	55(6)
C(26)	8470(40)	4320(80)	7990(50)	53(6)
C(24B)	8570(9)	5045(14)	8826(7)	49(2)
C(25B)	8341(7)	6696(13)	9021(13)	59(3)
C(26B)	8263(10)	4600(20)	7963(9)	62(3)
C(27)	8881(7)	2214(15)	9741(8)	46(2)
C(28)	8651(10)	1200(20)	10453(13)	61(4)
C(29)	9585(6)	2900(20)	9936(12)	57(3)
C(30)	8938(9)	1240(20)	8938(10)	54(4)
C(27B)	8917(15)	2140(30)	9718(15)	49(3)
C(28B)	8569(16)	870(30)	10200(20)	53(5)
C(29B)	9618(14)	2480(50)	10110(20)	55(5)
C(30B)	9040(20)	1610(60)	8804(13)	59(5)

Table 3.6. Bond lengths [\AA] and angles [$^\circ$] for **3.04**.

Pd(1)-C(17)	1.993(5)	C(14)-H(14A)	0.9500
Pd(1)-N(1)	2.091(3)	C(15)-C(16)	1.367(7)
Pd(1)-O(1B)	2.234(4)	C(15)-H(15A)	0.9500
Pd(1)-O(1)	2.234(9)	C(16)-H(16A)	0.9500
Pd(1)-P(1)	2.2422(11)	C(17)-C(18)	1.395(6)
P(1)-C(27)	1.823(16)	C(17)-C(22)	1.407(6)
P(1)-C(24B)	1.824(7)	C(18)-C(19)	1.393(7)
P(1)-C(24)	1.825(11)	C(18)-C(23)	1.490(7)
P(1)-C(23)	1.832(6)	C(19)-C(20)	1.369(7)
P(1)-C(27B)	1.91(3)	C(19)-H(19A)	0.9500
N(1)-C(11)	1.374(8)	C(20)-C(21)	1.366(7)
N(1)-C(5)	1.388(8)	C(20)-H(20A)	0.9500
O(1)-C(1)	1.447(17)	C(21)-C(22)	1.386(7)
O(1)-C(4)	1.467(18)	C(21)-H(21A)	0.9500
C(1)-C(2)	1.446(19)	C(22)-H(22A)	0.9500
C(1)-H(1A)	0.9900	C(23)-H(23A)	0.9900
C(1)-H(1B)	0.9900	C(23)-H(23B)	0.9900
C(2)-C(3)	1.50(2)	C(24)-C(25)	1.55(2)
C(2)-H(2A)	0.9900	C(24)-C(26)	1.559(19)
C(2)-H(2B)	0.9900	C(24)-H(24A)	1.0000
C(3)-C(4)	1.43(2)	C(25)-H(25A)	0.9800
C(3)-H(3A)	0.9900	C(25)-H(25B)	0.9800
C(3)-H(3B)	0.9900	C(25)-H(25C)	0.9800
C(4)-H(4A)	0.9900	C(26)-H(26A)	0.9800
C(4)-H(4B)	0.9900	C(26)-H(26B)	0.9800
O(1B)-C(1B)	1.445(7)	C(26)-H(26C)	0.9800
O(1B)-C(4B)	1.464(7)	C(24B)-C(25B)	1.545(11)
C(1B)-C(2B)	1.449(9)	C(24B)-C(26B)	1.556(10)
C(1B)-H(1C)	0.9900	C(24B)-H(24B)	1.0000
C(1B)-H(1D)	0.9900	C(25B)-H(25D)	0.9800
C(2B)-C(3B)	1.510(10)	C(25B)-H(25E)	0.9800
C(2B)-H(2C)	0.9900	C(25B)-H(25F)	0.9800
C(2B)-H(2D)	0.9900	C(26B)-H(26D)	0.9800
C(3B)-C(4B)	1.443(10)	C(26B)-H(26E)	0.9800
C(3B)-H(3C)	0.9900	C(26B)-H(26F)	0.9800
C(3B)-H(3D)	0.9900	C(27)-C(28)	1.515(11)
C(4B)-H(4C)	0.9900	C(27)-C(29)	1.541(10)
C(4B)-H(4D)	0.9900	C(27)-C(30)	1.546(12)
C(5)-C(6)	1.389(7)	C(28)-H(28A)	0.9800
C(5)-C(10)	1.395(8)	C(28)-H(28B)	0.9800
C(6)-C(7)	1.390(7)	C(28)-H(28C)	0.9800
C(6)-H(6A)	0.9500	C(29)-H(29A)	0.9800
C(7)-C(8)	1.366(8)	C(29)-H(29B)	0.9800
C(7)-H(7A)	0.9500	C(29)-H(29C)	0.9800
C(8)-C(9)	1.373(8)	C(30)-H(30A)	0.9800
C(8)-H(8A)	0.9500	C(30)-H(30B)	0.9800
C(9)-C(10)	1.377(8)	C(30)-H(30C)	0.9800
C(9)-H(9A)	0.9500	C(27B)-C(28B)	1.517(17)
C(10)-H(10A)	0.9500	C(27B)-C(29B)	1.546(16)
C(11)-C(12)	1.397(7)	C(27B)-C(30B)	1.554(17)
C(11)-C(16)	1.400(7)	C(28B)-H(28D)	0.9800
C(12)-C(13)	1.349(8)	C(28B)-H(28E)	0.9800
C(12)-H(12A)	0.9500	C(28B)-H(28F)	0.9800

Table 3.6. (cont.)

C(13)-C(14)	1.371(7)	C(29B)-H(29D)	0.9800
C(13)-H(13A)	0.9500	C(29B)-H(29E)	0.9800
C(14)-C(15)	1.352(7)	C(30B)-H(30E)	0.9800
C(29B)-H(29F)	0.9800	C(30B)-H(30F)	0.9800
C(30B)-H(30D)	0.9800		

C(17)-Pd(1)-N(1)	93.69(19)	C(4B)-O(1B)-Pd(1)	119.1(7)
C(17)-Pd(1)-O(1B)	179.4(3)	O(1B)-C(1B)-C(2B)	106.2(6)
N(1)-Pd(1)-O(1B)	85.8(3)	O(1B)-C(1B)-H(1C)	110.5
C(17)-Pd(1)-O(1)	176.6(17)	C(2B)-C(1B)-H(1C)	110.5
N(1)-Pd(1)-O(1)	87.4(13)	O(1B)-C(1B)-H(1D)	110.5
O(1B)-Pd(1)-O(1)	3.3(19)	C(2B)-C(1B)-H(1D)	110.5
C(17)-Pd(1)-P(1)	82.23(14)	H(1C)-C(1B)-H(1D)	108.7
N(1)-Pd(1)-P(1)	175.92(17)	C(1B)-C(2B)-C(3B)	105.6(6)
O(1B)-Pd(1)-P(1)	98.3(3)	C(1B)-C(2B)-H(2C)	110.6
O(1)-Pd(1)-P(1)	96.7(13)	C(3B)-C(2B)-H(2C)	110.6
C(27)-P(1)-C(24B)	107.4(6)	C(1B)-C(2B)-H(2D)	110.6
C(27)-P(1)-C(24)	111(3)	C(3B)-C(2B)-H(2D)	110.6
C(27)-P(1)-C(23)	104.4(5)	H(2C)-C(2B)-H(2D)	108.8
C(24B)-P(1)-C(23)	106.9(5)	C(4B)-C(3B)-C(2B)	101.1(7)
C(24)-P(1)-C(23)	105(2)	C(4B)-C(3B)-H(3C)	111.6
C(24B)-P(1)-C(27B)	106.2(8)	C(2B)-C(3B)-H(3C)	111.6
C(24)-P(1)-C(27B)	109(3)	C(4B)-C(3B)-H(3D)	111.6
C(23)-P(1)-C(27B)	105.4(8)	C(2B)-C(3B)-H(3D)	111.6
C(27)-P(1)-Pd(1)	120.2(3)	H(3C)-C(3B)-H(3D)	109.4
C(24B)-P(1)-Pd(1)	114.5(6)	C(3B)-C(4B)-O(1B)	107.2(6)
C(24)-P(1)-Pd(1)	113(3)	C(3B)-C(4B)-H(4C)	110.3
C(23)-P(1)-Pd(1)	102.05(19)	O(1B)-C(4B)-H(4C)	110.3
C(27B)-P(1)-Pd(1)	120.6(6)	C(3B)-C(4B)-H(4D)	110.3
C(11)-N(1)-C(5)	122.0(3)	O(1B)-C(4B)-H(4D)	110.3
C(11)-N(1)-Pd(1)	122.1(4)	H(4C)-C(4B)-H(4D)	108.5
C(5)-N(1)-Pd(1)	115.9(4)	N(1)-C(5)-C(6)	120.0(4)
C(1)-O(1)-C(4)	107.0(16)	N(1)-C(5)-C(10)	124.6(6)
C(1)-O(1)-Pd(1)	129(4)	C(6)-C(5)-C(10)	115.3(5)
C(4)-O(1)-Pd(1)	112(4)	C(7)-C(6)-C(5)	122.1(5)
C(2)-C(1)-O(1)	105.5(17)	C(7)-C(6)-H(6A)	118.9
C(2)-C(1)-H(1A)	110.7	C(5)-C(6)-H(6A)	118.9
O(1)-C(1)-H(1A)	110.7	C(8)-C(7)-C(6)	120.6(6)
C(2)-C(1)-H(1B)	110.7	C(8)-C(7)-H(7A)	119.7
O(1)-C(1)-H(1B)	110.7	C(6)-C(7)-H(7A)	119.7
H(1A)-C(1)-H(1B)	108.8	C(7)-C(8)-C(9)	118.9(5)
C(1)-C(2)-C(3)	105.7(19)	C(7)-C(8)-H(8A)	120.5
C(1)-C(2)-H(2A)	110.6	C(9)-C(8)-H(8A)	120.5
C(3)-C(2)-H(2A)	110.6	C(8)-C(9)-C(10)	120.2(6)
C(1)-C(2)-H(2B)	110.6	C(8)-C(9)-H(9A)	119.9
C(3)-C(2)-H(2B)	110.6	C(10)-C(9)-H(9A)	119.9
H(2A)-C(2)-H(2B)	108.7	C(9)-C(10)-C(5)	122.9(7)
C(4)-C(3)-C(2)	101(2)	C(9)-C(10)-H(10A)	118.6
C(4)-C(3)-H(3A)	111.6	C(5)-C(10)-H(10A)	118.6
C(2)-C(3)-H(3A)	111.6	N(1)-C(11)-C(12)	124.8(5)
C(4)-C(3)-H(3B)	111.6	N(1)-C(11)-C(16)	118.9(4)
C(2)-C(3)-H(3B)	111.6	C(12)-C(11)-C(16)	116.2(5)
H(3A)-C(3)-H(3B)	109.4	C(13)-C(12)-C(11)	121.6(6)

Table 3.6. (cont.)

C(3)-C(4)-O(1)	106(2)	C(13)-C(12)-H(12A)	119.2
C(3)-C(4)-H(4A)	110.6	C(11)-C(12)-H(12A)	119.2
O(1)-C(4)-H(4A)	110.6	C(12)-C(13)-C(14)	121.6(5)
C(3)-C(4)-H(4B)	110.6	C(12)-C(13)-H(13A)	119.2
O(1)-C(4)-H(4B)	110.6	C(14)-C(13)-H(13A)	119.2
H(4A)-C(4)-H(4B)	108.7	C(15)-C(14)-C(13)	117.9(5)
C(1B)-O(1B)-C(4B)	107.0(5)	C(15)-C(14)-H(14A)	121.1
C(1B)-O(1B)-Pd(1)	119.2(7)	C(13)-C(14)-H(14A)	121.1
C(14)-C(15)-C(16)	122.3(5)	C(28)-C(27)-C(30)	108.7(7)
C(14)-C(15)-H(15A)	118.8	C(29)-C(27)-C(30)	108.5(7)
C(16)-C(15)-H(15A)	118.8	C(28)-C(27)-P(1)	107.6(9)
C(15)-C(16)-C(11)	120.4(5)	C(29)-C(27)-P(1)	108.6(9)
C(15)-C(16)-H(16A)	119.8	C(30)-C(27)-P(1)	113.2(11)
C(11)-C(16)-H(16A)	119.8	C(28B)-C(27B)-C(29B)	109.6(13)
C(18)-C(17)-C(22)	117.4(5)	C(28B)-C(27B)-C(30B)	109.0(12)
C(18)-C(17)-Pd(1)	120.8(4)	C(29B)-C(27B)-C(30B)	107.6(12)
C(22)-C(17)-Pd(1)	121.6(4)	C(28B)-C(27B)-P(1)	106.0(16)
C(19)-C(18)-C(17)	120.0(5)	C(29B)-C(27B)-P(1)	118.3(19)
C(19)-C(18)-C(23)	120.5(5)	C(30B)-C(27B)-P(1)	106(2)
C(17)-C(18)-C(23)	119.5(5)	C(27B)-C(28B)-H(28D)	109.5
C(20)-C(19)-C(18)	121.4(5)	C(27B)-C(28B)-H(28E)	109.5
C(20)-C(19)-H(19A)	119.3	H(28D)-C(28B)-H(28E)	109.5
C(18)-C(19)-H(19A)	119.3	C(27B)-C(28B)-H(28F)	109.5
C(21)-C(20)-C(19)	119.7(5)	H(28D)-C(28B)-H(28F)	109.5
C(21)-C(20)-H(20A)	120.1	H(28E)-C(28B)-H(28F)	109.5
C(19)-C(20)-H(20A)	120.1	C(27B)-C(29B)-H(29D)	109.5
C(20)-C(21)-C(22)	120.1(5)	C(27B)-C(29B)-H(29E)	109.5
C(20)-C(21)-H(21A)	119.9	H(29D)-C(29B)-H(29E)	109.5
C(22)-C(21)-H(21A)	119.9	C(27B)-C(29B)-H(29F)	109.5
C(21)-C(22)-C(17)	121.3(5)	H(29D)-C(29B)-H(29F)	109.5
C(21)-C(22)-H(22A)	119.3	H(29E)-C(29B)-H(29F)	109.5
C(17)-C(22)-H(22A)	119.3	C(27B)-C(30B)-H(30D)	109.5
C(18)-C(23)-P(1)	105.7(4)	C(27B)-C(30B)-H(30E)	109.5
C(18)-C(23)-H(23A)	110.6	H(30D)-C(30B)-H(30E)	109.5
P(1)-C(23)-H(23A)	110.6	C(27B)-C(30B)-H(30F)	109.5
C(18)-C(23)-H(23B)	110.6	H(30D)-C(30B)-H(30F)	109.5
P(1)-C(23)-H(23B)	110.6	H(30E)-C(30B)-H(30F)	109.5
H(23A)-C(23)-H(23B)	108.7	P(1)-C(24B)-H(24B)	109.6
C(25)-C(24)-C(26)	108(2)	C(24B)-C(25B)-H(25D)	109.5
C(25)-C(24)-P(1)	132(6)	C(24B)-C(25B)-H(25E)	109.5
C(26)-C(24)-P(1)	107(4)	H(25D)-C(25B)-H(25E)	109.5
C(25)-C(24)-H(24A)	102.1	C(24B)-C(25B)-H(25F)	109.5
C(26)-C(24)-H(24A)	102.1	H(25D)-C(25B)-H(25F)	109.5
P(1)-C(24)-H(24A)	102.1	H(25E)-C(25B)-H(25F)	109.5
C(25B)-C(24B)-C(26B)	107.5(9)	C(24B)-C(26B)-H(26D)	109.5
C(25B)-C(24B)-P(1)	109.3(11)	C(24B)-C(26B)-H(26F)	109.5
C(26B)-C(24B)-P(1)	111.1(10)	H(26D)-C(26B)-H(26F)	109.5
C(25B)-C(24B)-H(24B)	109.6	H(26E)-C(26B)-H(26F)	109.5
C(26B)-C(24B)-H(24B)	109.6	C(28)-C(27)-C(29)	110.3(8)
C(24B)-C(26B)-H(26E)	109.5	H(26D)-C(26B)-H(26E)	109.5

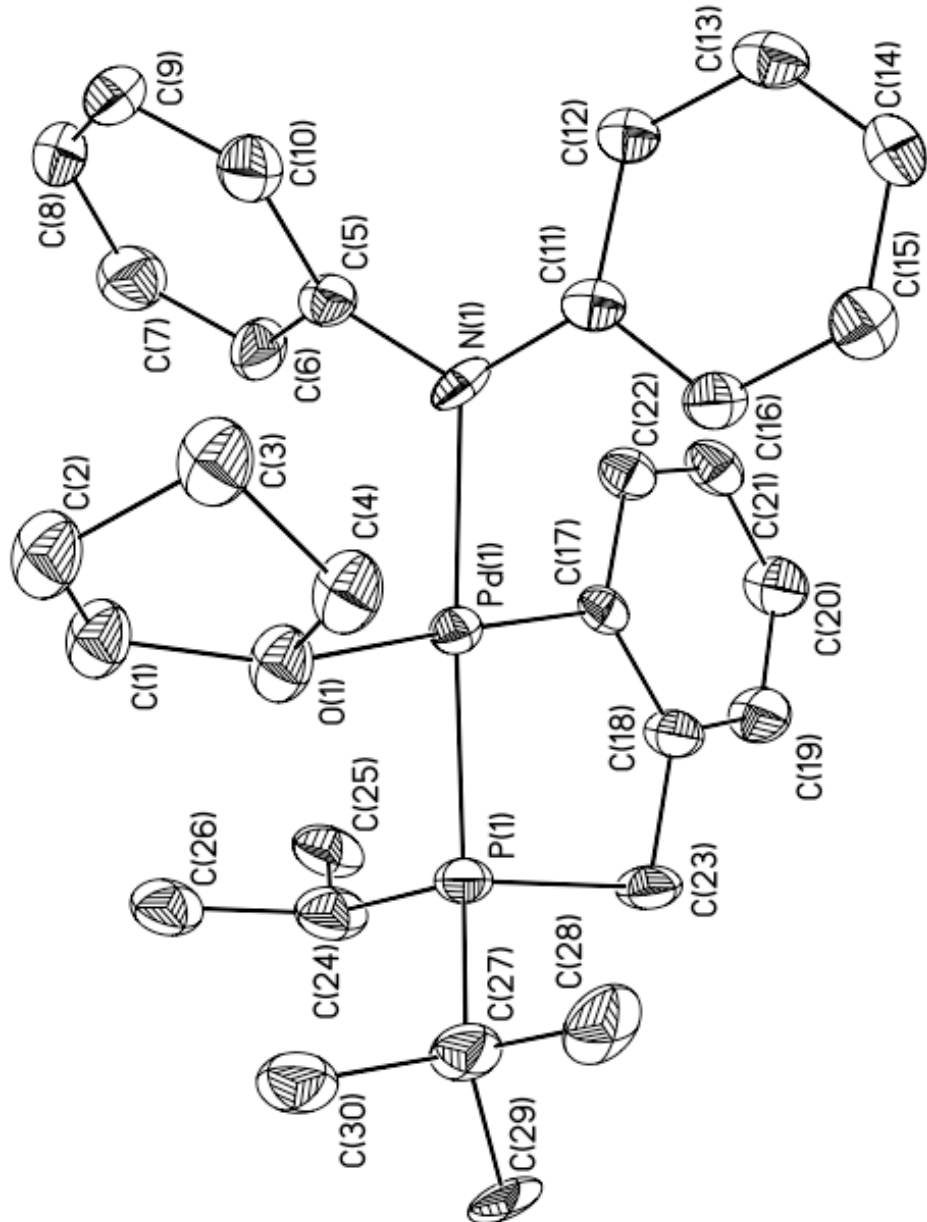


Figure 3.11. ORTEP diagram of **3.04** with 35 % probability ellipsoids.

3.4.11 Crystallographic Data for 3.13

Table 3.7. Crystal data and structure refinement for 3.13.

Empirical formula	C ₄₂ H ₅₉ NOP ₂ Pd ₂
Formula weight	868.64
Temperature	193(2) K
Wavelength	0.71073 Å
Crystal system	Monoclinic
Space group	P2(1)/c
Unit cell dimensions	a = 21.2843(15) Å b = 9.3814(7) Å c = 20.7994(14) Å
Volume	4140.6(5) Å ³
Z	4
Density (calculated)	1.393 Mg/m ³
Absorption coefficient	0.977 mm ⁻¹
F(000)	1792
Crystal size	0.564 x 0.309 x 0.068 mm ³
Theta range for data collection	1.92 to 27.10°
Index ranges	-27<=h<=27, -12<=k<=11, -26<=l<=26
Reflections collected	58747
Independent reflections	9102 [R(int) = 0.0613]
Completeness to theta = 27.10°	99.7 %
Absorption correction	Integration
Max. and min. transmission	0.9545 and 0.6951
Refinement method	Full-matrix least-squares on F ²
Data / restraints / parameters	9102 / 5 / 448
Goodness-of-fit on F ²	1.026
Final R indices [I>2sigma(I)]	R1 = 0.0369, wR2 = 0.0723
R indices (all data)	R1 = 0.0613, wR2 = 0.0802
Largest diff. peak and hole	0.739 and -0.513 e.Å ⁻³

Table 3.8. Atomic coordinates ($\times 10^4$) and equivalent isotropic displacement parameters ($\text{\AA}^2 \times 10^3$) for **3.13**. U(eq) is defined as one third of the trace of the orthogonalized U^{ij} tensor.

	x	y	z	U(eq)
Pd(1)	1863(1)	6095(1)	4764(1)	22(1)
Pd(2)	3130(1)	4183(1)	4656(1)	22(1)
P(2)	3746(1)	3575(1)	3884(1)	23(1)
P(1)	1048(1)	6728(1)	4101(1)	31(1)
O(1)	2323(1)	4890(3)	4050(1)	35(1)
N(1)	2625(1)	5185(3)	5430(1)	22(1)
C(1)	1417(2)	7292(3)	5393(2)	26(1)
C(2)	789(2)	7733(4)	5259(2)	30(1)
C(3)	483(2)	8566(4)	5696(2)	36(1)
C(4)	784(2)	8949(4)	6276(2)	36(1)
C(5)	1408(2)	8560(4)	6415(2)	36(1)
C(6)	1717(2)	7756(4)	5979(2)	30(1)
C(7)	446(2)	7269(5)	4630(2)	43(1)
C(8)	1208(2)	8315(4)	3596(2)	45(1)
C(9)	660(2)	8669(6)	3098(2)	83(2)
C(10)	1336(2)	9577(4)	4054(2)	60(1)
C(11)	1813(2)	8049(5)	3248(2)	50(1)
C(12)	672(2)	5191(5)	3626(2)	48(1)
C(13)	1020(2)	4844(5)	3027(2)	60(1)
C(14)	-24(2)	5452(7)	3425(2)	82(2)
C(15)	741(2)	3905(5)	4083(2)	65(1)
C(16)	3836(2)	3290(3)	5212(2)	24(1)
C(17)	4436(2)	3075(3)	4988(2)	25(1)
C(18)	4907(2)	2362(4)	5361(2)	32(1)
C(19)	4792(2)	1811(4)	5957(2)	34(1)
C(20)	4201(2)	1987(4)	6181(2)	32(1)
C(21)	3732(2)	2700(3)	5812(2)	28(1)
C(22)	4531(2)	3585(4)	4314(2)	31(1)
C(23)	3608(2)	1732(4)	3553(2)	33(1)
C(24)	2911(2)	1584(4)	3299(2)	50(1)
C(25)	4036(2)	1335(4)	3024(2)	49(1)
C(26)	3726(2)	671(4)	4113(2)	44(1)
C(27)	3787(2)	4938(4)	3226(2)	30(1)
C(28)	3255(2)	4767(4)	2686(2)	40(1)
C(29)	3711(2)	6404(4)	3540(2)	39(1)
C(30)	4432(2)	4911(4)	2936(2)	42(1)
C(31)	2284(2)	4237(3)	5816(2)	26(1)
C(32)	2136(2)	4510(4)	6450(2)	29(1)
C(33)	1771(2)	3580(4)	6774(2)	37(1)
C(34)	1542(2)	2346(4)	6489(2)	45(1)
C(35)	1673(2)	2045(4)	5858(2)	44(1)
C(36)	2043(2)	2972(4)	5536(2)	32(1)
C(37)	3072(2)	6147(3)	5731(2)	23(1)
C(38)	3424(2)	5899(4)	6322(2)	29(1)
C(39)	3867(2)	6875(4)	6564(2)	32(1)
C(40)	3982(2)	8116(4)	6247(2)	33(1)
C(41)	3648(2)	8378(4)	5660(2)	34(1)

Table 3.8. (cont.)

C(42)	3201(2)	7412(4)	5411(2)	29(1)
-------	---------	---------	---------	-------

Table 3.9. Bond lengths [\AA] and angles [$^\circ$] for **3.13**.

Pd(1)-C(1)	2.016(3)	C(17)-C(18)	1.391(4)
Pd(1)-O(1)	2.161(2)	C(17)-C(22)	1.510(4)
Pd(1)-P(1)	2.2119(9)	C(18)-C(19)	1.381(5)
Pd(1)-N(1)	2.221(2)	C(18)-H(18)	0.9500
Pd(2)-C(16)	2.006(3)	C(19)-C(20)	1.386(5)
Pd(2)-O(1)	2.156(2)	C(19)-H(19)	0.9500
Pd(2)-N(1)	2.214(2)	C(20)-C(21)	1.383(4)
Pd(2)-P(2)	2.2239(9)	C(20)-H(20)	0.9500
P(2)-C(22)	1.833(3)	C(21)-H(21)	0.9500
P(2)-C(23)	1.875(3)	C(22)-H(22A)	0.9900
P(2)-C(27)	1.880(3)	C(22)-H(22B)	0.9900
P(1)-C(7)	1.826(4)	C(23)-C(25)	1.529(5)
P(1)-C(8)	1.868(4)	C(23)-C(26)	1.538(5)
P(1)-C(12)	1.889(4)	C(23)-C(24)	1.541(5)
O(1)-H(1)	0.83(2)	C(24)-H(24A)	0.9800
N(1)-C(37)	1.421(4)	C(24)-H(24B)	0.9800
N(1)-C(31)	1.432(4)	C(24)-H(24C)	0.9800
C(1)-C(6)	1.401(5)	C(25)-H(25A)	0.9800
C(1)-C(2)	1.407(5)	C(25)-H(25B)	0.9800
C(2)-C(3)	1.398(5)	C(25)-H(25C)	0.9800
C(2)-C(7)	1.510(5)	C(26)-H(26A)	0.9800
C(3)-C(4)	1.369(5)	C(26)-H(26B)	0.9800
C(3)-H(3)	0.9500	C(26)-H(26C)	0.9800
C(4)-C(5)	1.387(5)	C(27)-C(29)	1.537(5)
C(4)-H(4)	0.9500	C(27)-C(30)	1.541(5)
C(5)-C(6)	1.385(5)	C(27)-C(28)	1.541(5)
C(5)-H(5)	0.9500	C(28)-H(28A)	0.9800
C(6)-H(6)	0.9500	C(28)-H(28B)	0.9800
C(7)-H(7A)	0.9900	C(28)-H(28C)	0.9800
C(7)-H(7B)	0.9900	C(29)-H(29A)	0.9800
C(8)-C(10)	1.530(6)	C(29)-H(29B)	0.9800
C(8)-C(9)	1.536(5)	C(29)-H(29C)	0.9800
C(8)-C(11)	1.545(6)	C(30)-H(30A)	0.9800
C(9)-H(9A)	0.9800	C(30)-H(30B)	0.9800
C(9)-H(9B)	0.9800	C(30)-H(30C)	0.9800
C(9)-H(9C)	0.9800	C(31)-C(36)	1.401(5)
C(10)-H(10A)	0.9800	C(31)-C(32)	1.402(4)
C(10)-H(10B)	0.9800	C(32)-C(33)	1.378(5)
C(10)-H(10C)	0.9800	C(32)-H(32)	0.9500
C(11)-H(11A)	0.9800	C(33)-C(34)	1.373(5)
C(11)-H(11B)	0.9800	C(33)-H(33)	0.9500
C(11)-H(11C)	0.9800	C(34)-C(35)	1.391(5)
C(12)-C(14)	1.528(6)	C(34)-H(34)	0.9500
C(12)-C(13)	1.534(5)	C(35)-C(36)	1.381(5)
C(12)-C(15)	1.536(6)	C(35)-H(35)	0.9500
C(13)-H(13A)	0.9800	C(36)-H(36)	0.9500
C(13)-H(13B)	0.9800	C(37)-C(42)	1.399(4)
C(13)-H(13C)	0.9800	C(37)-C(38)	1.407(4)
C(14)-H(14A)	0.9800	C(38)-C(39)	1.382(5)
C(14)-H(14B)	0.9800	C(38)-H(38)	0.9500
C(14)-H(14C)	0.9800	C(39)-C(40)	1.370(5)
C(15)-H(15A)	0.9800	C(39)-H(39)	0.9500
C(15)-H(15B)	0.9800	C(40)-C(41)	1.386(5)

Table 3.9. (cont.)

C(15)-H(15C)	0.9800	C(40)-H(40)	0.9500
C(16)-C(21)	1.399(4)	C(41)-C(42)	1.386(5)
C(16)-C(17)	1.408(4)	C(42)-H(42)	0.9500
C(41)-H(41)	0.950		
C(1)-Pd(1)-O(1)	176.91(11)	H(7A)-C(7)-H(7B)	108.6
C(1)-Pd(1)-P(1)	82.48(10)	C(10)-C(8)-C(9)	109.9(4)
O(1)-Pd(1)-P(1)	94.95(7)	C(10)-C(8)-C(11)	107.6(4)
C(1)-Pd(1)-N(1)	99.62(11)	C(9)-C(8)-C(11)	109.6(4)
O(1)-Pd(1)-N(1)	83.15(9)	C(10)-C(8)-P(1)	107.4(3)
P(1)-Pd(1)-N(1)	172.65(7)	C(9)-C(8)-P(1)	112.9(3)
C(16)-Pd(2)-O(1)	173.11(11)	C(11)-C(8)-P(1)	109.2(3)
C(16)-Pd(2)-N(1)	98.16(11)	C(8)-C(9)-H(9A)	109.5
O(1)-Pd(2)-N(1)	83.40(9)	C(8)-C(9)-H(9B)	109.5
C(16)-Pd(2)-P(2)	81.49(9)	H(9A)-C(9)-H(9B)	109.5
O(1)-Pd(2)-P(2)	98.30(7)	C(8)-C(9)-H(9C)	109.5
N(1)-Pd(2)-P(2)	168.65(7)	H(9A)-C(9)-H(9C)	109.5
C(22)-P(2)-C(23)	107.15(17)	H(9B)-C(9)-H(9C)	109.5
C(22)-P(2)-C(27)	105.01(16)	C(8)-C(10)-H(10A)	109.5
C(23)-P(2)-C(27)	112.00(15)	C(8)-C(10)-H(10B)	109.5
C(22)-P(2)-Pd(2)	102.31(11)	H(10A)-C(10)-H(10B)	109.5
C(23)-P(2)-Pd(2)	114.60(12)	C(8)-C(10)-H(10C)	109.5
C(27)-P(2)-Pd(2)	114.50(11)	H(10A)-C(10)-H(10C)	109.5
C(7)-P(1)-C(8)	106.5(2)	H(10B)-C(10)-H(10C)	109.5
C(7)-P(1)-C(12)	103.80(18)	C(8)-C(11)-H(11A)	109.5
C(8)-P(1)-C(12)	113.78(19)	C(8)-C(11)-H(11B)	109.5
C(7)-P(1)-Pd(1)	104.58(12)	H(11A)-C(11)-H(11B)	109.5
C(8)-P(1)-Pd(1)	113.31(13)	C(8)-C(11)-H(11C)	109.5
C(12)-P(1)-Pd(1)	113.64(15)	H(11A)-C(11)-H(11C)	109.5
Pd(2)-O(1)-Pd(1)	98.13(10)	H(11B)-C(11)-H(11C)	109.5
Pd(2)-O(1)-H(1)	109.5(16)	C(14)-C(12)-C(13)	109.3(3)
Pd(1)-O(1)-H(1)	114(3)	C(14)-C(12)-C(15)	109.8(4)
C(37)-N(1)-C(31)	120.0(3)	C(13)-C(12)-C(15)	107.9(4)
C(37)-N(1)-Pd(2)	104.13(18)	C(14)-C(12)-P(1)	112.6(3)
C(31)-N(1)-Pd(2)	116.0(2)	C(13)-C(12)-P(1)	112.0(3)
C(37)-N(1)-Pd(1)	117.52(19)	C(15)-C(12)-P(1)	105.1(3)
C(31)-N(1)-Pd(1)	102.16(18)	C(12)-C(13)-H(13A)	109.5
Pd(2)-N(1)-Pd(1)	94.66(9)	C(12)-C(13)-H(13B)	109.5
C(6)-C(1)-C(2)	116.3(3)	H(13A)-C(13)-H(13B)	109.5
C(6)-C(1)-Pd(1)	122.1(2)	C(12)-C(13)-H(13C)	109.5
C(2)-C(1)-Pd(1)	121.6(2)	H(13A)-C(13)-H(13C)	109.5
C(3)-C(2)-C(1)	121.2(3)	H(13B)-C(13)-H(13C)	109.5
C(3)-C(2)-C(7)	120.4(3)	C(12)-C(14)-H(14A)	109.5
C(1)-C(2)-C(7)	118.3(3)	C(12)-C(14)-H(14B)	109.5
C(4)-C(3)-C(2)	120.7(3)	H(14A)-C(14)-H(14B)	109.5
C(4)-C(3)-H(3)	119.6	C(12)-C(14)-H(14C)	109.5
C(2)-C(3)-H(3)	119.6	H(14A)-C(14)-H(14C)	109.5
C(3)-C(4)-C(5)	119.3(3)	H(14B)-C(14)-H(14C)	109.5
C(3)-C(4)-H(4)	120.3	C(12)-C(15)-H(15A)	109.5
C(5)-C(4)-H(4)	120.3	C(12)-C(15)-H(15B)	109.5
C(6)-C(5)-C(4)	120.2(3)	H(15A)-C(15)-H(15B)	109.5
C(6)-C(5)-H(5)	119.9	C(12)-C(15)-H(15C)	109.5
C(4)-C(5)-H(5)	119.9	H(15A)-C(15)-H(15C)	109.5
C(5)-C(6)-C(1)	122.2(3)	H(15B)-C(15)-H(15C)	109.5

Table 3.9. (cont.)

C(5)-C(6)-H(6)	118.9	C(21)-C(16)-C(17)	116.7(3)
C(1)-C(6)-H(6)	118.9	C(21)-C(16)-Pd(2)	121.1(2)
C(2)-C(7)-P(1)	106.7(2)	C(17)-C(16)-Pd(2)	121.8(2)
C(2)-C(7)-H(7A)	110.4	C(18)-C(17)-C(16)	121.2(3)
P(1)-C(7)-H(7A)	110.4	C(18)-C(17)-C(22)	121.9(3)
C(2)-C(7)-H(7B)	110.4	C(16)-C(17)-C(22)	116.9(3)
P(1)-C(7)-H(7B)	110.4	C(27)-C(29)-H(29B)	109.5
C(19)-C(18)-C(17)	120.8(3)	H(29A)-C(29)-H(29B)	109.5
C(19)-C(18)-H(18)	119.6	C(27)-C(29)-H(29C)	109.5
C(17)-C(18)-H(18)	119.6	H(29A)-C(29)-H(29C)	109.5
C(18)-C(19)-C(20)	119.0(3)	H(29B)-C(29)-H(29C)	109.5
C(18)-C(19)-H(19)	120.5	C(27)-C(30)-H(30A)	109.5
C(20)-C(19)-H(19)	120.5	C(27)-C(30)-H(30B)	109.5
C(21)-C(20)-C(19)	120.5(3)	H(30A)-C(30)-H(30B)	109.5
C(21)-C(20)-H(20)	119.8	C(27)-C(30)-H(30C)	109.5
C(19)-C(20)-H(20)	119.8	H(30A)-C(30)-H(30C)	109.5
C(20)-C(21)-C(16)	121.9(3)	H(30B)-C(30)-H(30C)	109.5
C(20)-C(21)-H(21)	119.0	C(36)-C(31)-C(32)	116.3(3)
C(16)-C(21)-H(21)	119.0	C(36)-C(31)-N(1)	118.6(3)
C(17)-C(22)-P(2)	105.5(2)	C(32)-C(31)-N(1)	125.0(3)
C(17)-C(22)-H(22A)	110.6	C(33)-C(32)-C(31)	121.3(3)
P(2)-C(22)-H(22A)	110.6	C(33)-C(32)-H(32)	119.3
C(17)-C(22)-H(22B)	110.6	C(31)-C(32)-H(32)	119.3
P(2)-C(22)-H(22B)	110.6	C(34)-C(33)-C(32)	121.2(3)
H(22A)-C(22)-H(22B)	108.8	C(34)-C(33)-H(33)	119.4
C(25)-C(23)-C(26)	108.4(3)	C(32)-C(33)-H(33)	119.4
C(25)-C(23)-C(24)	110.1(3)	C(33)-C(34)-C(35)	119.2(3)
C(26)-C(23)-C(24)	107.4(3)	C(33)-C(34)-H(34)	120.4
C(25)-C(23)-P(2)	113.8(3)	C(35)-C(34)-H(34)	120.4
C(26)-C(23)-P(2)	107.9(2)	C(36)-C(35)-C(34)	119.5(4)
C(24)-C(23)-P(2)	109.2(3)	C(36)-C(35)-H(35)	120.3
C(23)-C(24)-H(24A)	109.5	C(34)-C(35)-H(35)	120.3
C(23)-C(24)-H(24B)	109.5	C(35)-C(36)-C(31)	122.5(3)
H(24A)-C(24)-H(24B)	109.5	C(35)-C(36)-H(36)	118.8
C(23)-C(24)-H(24C)	109.5	C(31)-C(36)-H(36)	118.8
H(24A)-C(24)-H(24C)	109.5	C(42)-C(37)-C(38)	116.5(3)
H(24B)-C(24)-H(24C)	109.5	C(42)-C(37)-N(1)	118.6(3)
C(23)-C(25)-H(25A)	109.5	C(38)-C(37)-N(1)	124.9(3)
C(23)-C(25)-H(25B)	109.5	C(39)-C(38)-C(37)	120.8(3)
H(25A)-C(25)-H(25B)	109.5	C(39)-C(38)-H(38)	119.6
C(23)-C(25)-H(25C)	109.5	C(37)-C(38)-H(38)	119.6
H(25A)-C(25)-H(25C)	109.5	C(40)-C(39)-C(38)	121.9(3)
H(25B)-C(25)-H(25C)	109.5	C(40)-C(39)-H(39)	119.0
C(23)-C(26)-H(26A)	109.5	C(38)-C(39)-H(39)	119.0
C(23)-C(26)-H(26B)	109.5	C(39)-C(40)-C(41)	118.5(3)
H(26A)-C(26)-H(26B)	109.5	C(39)-C(40)-H(40)	120.7
C(23)-C(26)-H(26C)	109.5	C(41)-C(40)-H(40)	120.7
H(26A)-C(26)-H(26C)	109.5	C(40)-C(41)-C(42)	120.3(3)
H(26B)-C(26)-H(26C)	109.5	C(40)-C(41)-H(41)	119.9
C(29)-C(27)-C(30)	107.9(3)	C(42)-C(41)-H(41)	119.9
C(29)-C(27)-C(28)	107.9(3)	C(41)-C(42)-C(37)	122.0(3)
C(30)-C(27)-C(28)	109.8(3)	C(41)-C(42)-H(42)	119.0
C(29)-C(27)-P(2)	106.7(2)	C(37)-C(42)-H(42)	119.0
C(30)-C(27)-P(2)	111.5(2)	H(28A)-C(28)-H(28B)	109.5
C(28)-C(27)-P(2)	112.8(2)	C(27)-C(28)-H(28C)	109.5

Table 3.9. (cont.)

C(27)-C(28)-H(28A)	109.5	H(28A)-C(28)-H(28C)	109.5
C(27)-C(28)-H(28B)	109.5	H(28B)-C(28)-H(28C)	109.5
C(27)-C(29)-H(29A)	109.5		

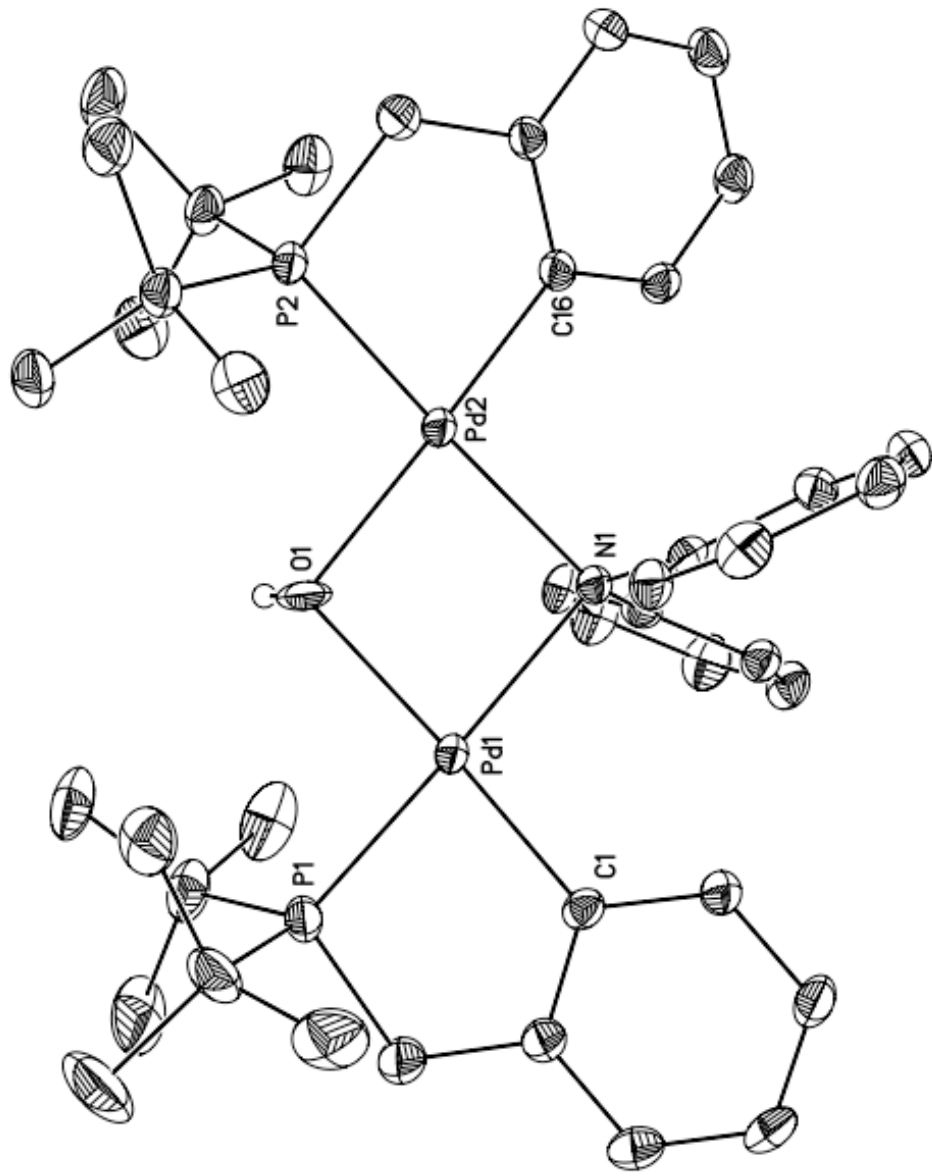


Figure 3.12. ORTEP diagram of **3.13** with 35 % probability ellipsoids.

3.5 References

- (1) Hanley, P. S.; Markovic, D.; Hartwig, J. F. *J. Am. Chem. Soc.* **2010**, *132*, 6302.
- (2) Hartwig, J. F. *Organotransition metal chemistry : from bonding to catalysis*; University Science Books: Sausalito, Calif., 2010.
- (3) Zhao, P. J.; Krug, C.; Hartwig, J. F. *J. Am. Chem. Soc.* **2005**, *127*, 12066.
- (4) Barshop, B. A.; Wrenn, R. F.; Frieden, C. *Anal. Biochem.* **1983**, *130*, 134.
- (5) Zimmerle, C. T.; Frieden, C. *Biochem. J.* **1989**, *258*, 381.
- (6) M. J. Frisch, G. W. T., H. B. Schlegel, G. E. Scuseria, M. A. Robb, J. R. Cheeseman, G. Scalmani, V. Barone, B. Mennucci, G. A. Petersson, H. Nakatsuji, M. Caricato, X. Li, H. P. Hratchian, A. F. Izmaylov, J. Bloino, G. Zheng, J. L. Sonnenberg, M. Hada, M. Ehara, K. Toyota, R. Fukuda, J. Hasegawa, M. Ishida, T. Nakajima, Y. Honda, O. Kitao, H. Nakai, T. Vreven, J. A. Montgomery, Jr., J. E. Peralta, F. Ogliaro, M. Bearpark, J. J. Heyd, E. Brothers, K. N. Kudin, V. N. Staroverov, R. Kobayashi, J. Normand, K. Raghavachari, A. Rendell, J. C. Burant, S. S. Iyengar, J. Tomasi, M. Cossi, N. Rega, J. M. Millam, M. Klene, J. E. Knox, J. B. Cross, V. Bakken, C. Adamo, J. Jaramillo, R. Gomperts, R. E. Stratmann, O. Yazyev, A. J. Austin, R. Cammi, C. Pomelli, J. W. Ochterski, R. L. Martin, K. Morokuma, V. G. Zakrzewski, G. A. Voth, P. Salvador, J. J. Dannenberg, S. Dapprich, A. D. Daniels, Ö. Farkas, J. B. Foresman, J. V. Ortiz, J. Cioslowski, and D. J. Fox. In *Gaussian 09, Revision A.1*; Gaussian, Inc.: Wallingford CT, 2009.
- (7) Roy, L. E.; Hay, P. J.; Martin, R. L. *J. Chem. Theory Comput.* **2008**, *4*, 1029.
- (8) Ariaafard, A.; Hyland, C. J. T.; Carty, A. J.; Sharma, M.; Brookes, N. J.; Yates, B. F. *Inorg. Chem.* **2010**, *49*, 11249.

- (9) Bercaw, J. E.; Chen, G. S.; Labinger, J. A.; Lin, B. L. *Organometallics* **2010**, *29*, 4354.
- (10) Ledford, J.; Shultz, C. S.; Gates, D. P.; White, P. S.; DeSimone, J. M.; Brookhart, M. *Organometallics* **2001**, *20*, 5266.
- (11) Burger, B. J.; Santarsiero, B. D.; Trimmer, M. S.; Bercaw, J. E. *J. Am. Chem. Soc.* **1988**, *110*, 3134.
- (12) Faller, J. W.; Chase, K. J. *Organometallics* **1995**, *14*, 1592.
- (13) Malinoski, J. M.; White, P. S.; Brookhart, M. *Organometallics* **2003**, *22*, 621.
- (14) Wang, L.; Flood, T. C. *J. Am. Chem. Soc.* **1992**, *114*, 3169.
- (15) Rix, F. C.; Brookhart, M. *J. Am. Chem. Soc.* **1995**, *117*, 1137.
- (16) Brookhart, M.; Volpe, A. F.; Lincoln, D. M.; Horvath, I. T.; Millar, J. M. *J. Am. Chem. Soc.* **1990**, *112*, 5634.
- (17) Malinoski, J. M.; Brookhart, M. *Organometallics* **2003**, *22*, 5324.
- (18) Chan, M. S. W.; Deng, L. Q.; Ziegler, T. *Organometallics* **2000**, *19*, 2741.
- (19) Gagne, M. R.; Stern, C. L.; Marks, T. J. *J. Am. Chem. Soc.* **1992**, *114*, 275.
- (20) Motta, A.; Lanza, G.; Fragala, I. L.; Marks, T. J. *Organometallics* **2004**, *23*, 4097.
- (21) Stubbert, B. D.; Marks, T. J. *J. Am. Chem. Soc.* **2007**, *129*, 6149.
- (22) Huffman, J. C.; Moloy, K. G.; Marsella, J. A.; Caulton, K. G. *J. Am. Chem. Soc.* **1980**, *102*, 3009.
- (23) Schock, L. E.; Marks, T. J. *J. Am. Chem. Soc.* **1988**, *110*, 7701.
- (24) Ban, E.; Hughes, R. P.; Powell, J. J. *Organomet. Chem.* **1974**, *69*, 455.
- (25) Miki, K.; Shiotani, O.; Kai, Y.; Kasai, N.; Kanatani, H.; Kurosawa, H. *Organometallics* **1983**, *2*, 585.

- (26) Rix, F. C.; Brookhart, M.; White, P. S. *J. Am. Chem. Soc.* **1996**, *118*, 2436.
- (27) Halpern, J.; Okamoto, T. *Inorg. Chim. A. Let.* **1984**, *89*, L53.
- (28) Doherty, N. M.; Bercaw, J. E. *J. Am. Chem. Soc.* **1985**, *107*, 2670.
- (29) Barluenga, J.; Fernandez, M. A.; Aznar, F.; Valdes, C. *Chem. Comm.* **2002**, 2362.
- (30) Pawluc, P.; Hreczycho, G.; Szudkowska, J.; Kubicki, M.; Marciniec, B. *Org. Lett.* **2009**, *11*, 3390.

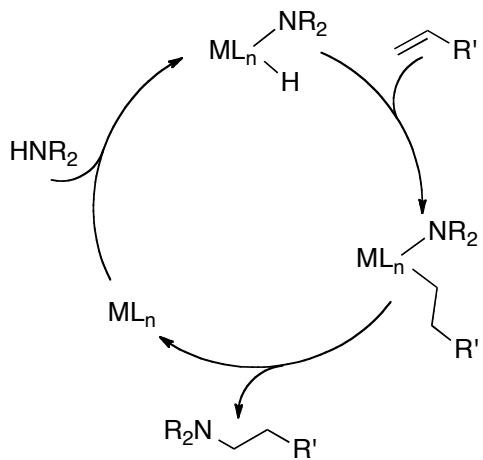
Chapter 4: Reductive Elimination of Alkylamines from Low-Valent Alkylpalladium(II)

Amido Complexes*

4.1 Introduction

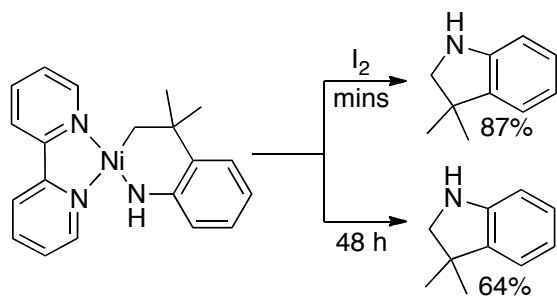
Reductive elimination is a fundamental organometallic transformation that is proposed to be the product-forming step in numerous catalytic cycles.¹ Under the umbrella of the anti-Markovnikov hydroamination subgroup within CENTC (Center for Enabling New Technologies Through Catalysis), we desired to develop a system that would undergo the facile reductive elimination of an alkylamine from a low-valent metal center. The mechanism illustrated in Scheme 4.1 describes a proposed catalytic cycle for the hydroamination of an alkene that would generate products with anti-Markovnikov selectivity. Upon formation a hydrido amido complex from the oxidative addition of an amine to M⁰ complex, an olefin may undergo migratory insertion into the M-H bond to form an alkyl amido complex. Reductive elimination of an alkylamine from the alkylmetal amido complex would release products with the desired anti-Markovnikov selectivity. Although C-N bond-forming reductive eliminations of arylamines from a variety of transition metal-amido complexes are known, reductive elimination of an alkylamine from an isolated metal-amido complex has only been observed in a few cases.

* Part of this chapter was previously published in Hanley, P. S.; Marquard, S. L.; Cundari, T. R.; Hartwig, J. F. *J. Am. Chem. Soc.* **2012**, *134*, 15281.



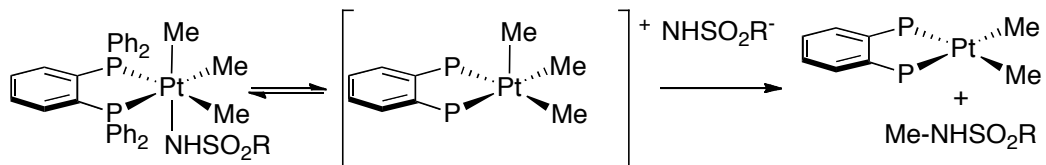
Scheme 4.1. Proposed mechanism of anti-Markovnikov hydroamination of alkenes

Hillhouse has reported the intramolecular reductive elimination of an indoline from a nickel amide in the presence and absence of an oxidant (Scheme 4.2).²⁻³ The bipyridine ligated alkynickel(II) amido complex was synthesized *in situ*, and stirring of this species in benzene for 48 h at room temperature generated 64% of indoline. In the presence of I_2 , the reaction was complete in minutes forming 87% of the indoline product. Because the reaction occurs rapidly in the presence of oxidant, it is unclear if the slow reaction in the absence of added oxidant is a purely unimolecular, thermal process or catalyzed by a low concentration of oxidant.



Scheme 4.2. Reductive elimination of Nickel-amido complex prepared by Hillhouse

Goldberg has reported the reductive elimination of a sulfonamide from a methylplatinum(IV) sulfonamido complex by dissociation of the sulfonamide ligand (Scheme 4.3).⁴ However, high-valent platinum(IV) is necessary for facile reductive elimination, and it remains unclear if reductive elimination of an alkylamine from a low-valent metal center is a reasonable transformation.

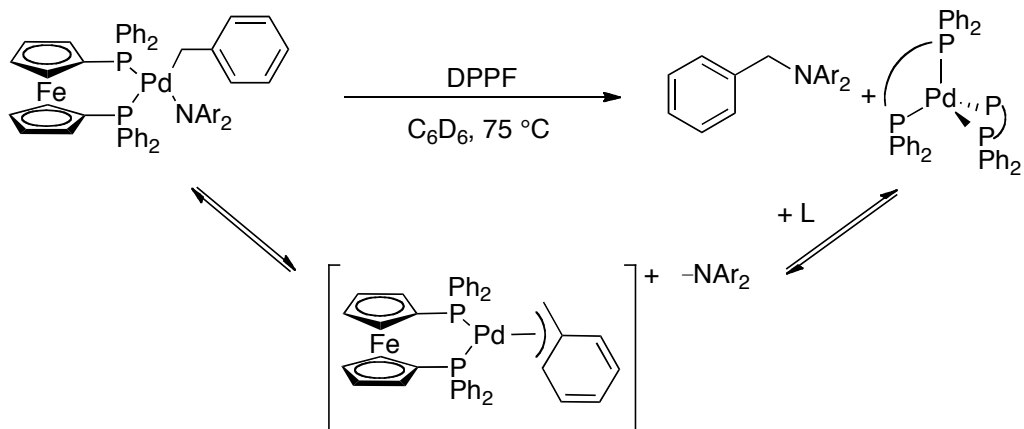


Scheme 4.3. Reductive elimination of a sulfonamide from Pt(IV)

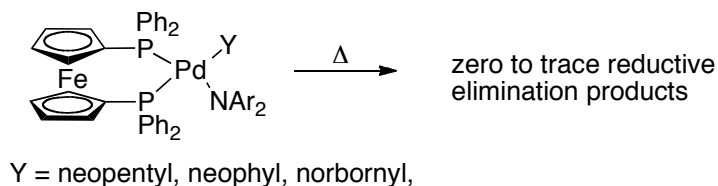
Several palladium-catalyzed reactions have been proposed to occur by reductive elimination from a palladium amido complex to form new C(sp³)-N bonds. Several C(sp³)-H amidation reactions with added oxidants have been reported.⁵⁻⁸ These reactions presumably generate a palladium(IV) intermediate that would be prone to C-N reductive elimination. In addition, several palladium-catalyzed reactions that form C(sp³)-N bonds without external oxidant have been reported, including the palladium-catalyzed formation of norbornyl indoline,⁹⁻¹⁰ and an intermolecular amination of C-H bonds.¹¹ The species that undergoes the reductive elimination step has not been observed directly in these systems.

Recently, our group reported examples of C(sp³)-N and C(sp³)-O bond-forming reductive elimination of benzylamines and benzyl ethers from isolated benzylpalladium(II) amido and phenoxide complexes ligated by a chelating phosphine ligand, as shown in Scheme 4.4.¹²⁻¹³ Kinetic and stereochemical studies implied that these reactions proceed by a stepwise pathway that involves dissociation of the diarylamido ligand, followed by nucleophilic attack of the amide onto a proposed η^3 -benzylpalladium intermediate. However, reductive elimination to form an

alkyl-nitrogen bond from an isolated palladium complex has not been reported, despite significant effort.¹⁴⁻¹⁵ Thermolysis of 1,1'-Bis(diphenylphosphino)ferrocene (DPPF)-ligated alkylpalladium amido complexes that are analogs of the benzylpalladium amido complexes did not generate products from reductive elimination (Scheme 4.5).¹⁶



Scheme 4.4. Proposed mechanism for the reductive elimination of benzylamines and benzylethers



Scheme 4.5. Attempted reductive elimination of alkylamines

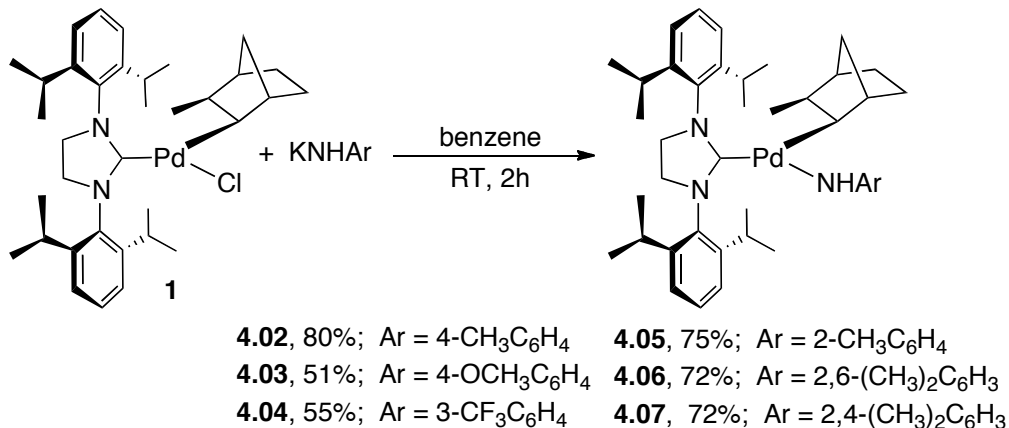
In chapter 4, we report a series of isolated and fully characterized three-coordinate palladium-alkylamido complexes ligated by bulky, monodentate N-heterocyclic carbene ligands that undergo direct thermal reductive eliminations of an N -alkylamine. The stereochemical outcome of the norbornylamine products from the reductive elimination step implies that these reactions occur by a concerted reductive elimination. Reductive elimination products were also

formed from reactions of (COD)Pd(2-CH₃-norbornyl)(Cl) with bulky monodentate phosphine ligands and KNHAr, but in the species undergoing the reductive elimination has not been determined.

4.2 Results and Discussion

4.2.1 Synthesis and Reactivity of NHC-Ligated Palladium Amido Complexes

Synthesis of the palladium-amido complexes in this study is summarized in Scheme 4.6. To isolate palladium alkylamido complexes that are stable to β -hydrogen elimination, norbornylpalladium complexes were prepared. The β -hydrogen atoms in the norbornyl ligand are known to be resistant to β -hydrogen elimination.¹⁷ The SIPr-ligated palladium chloride complex **4.1** was prepared by ligand substitution of (COD)Pd((2-CH₃-norbornyl)Cl)¹⁷ with 1,3-bis(2,6-diisopropylphenyl)imidazolidin-2-ylidene (SIPr) in THF at room temperature. X-ray crystallographic analysis showed that complex **4.1** exists as a stable, three-coordinate chloride complex in the solid state. Palladium anilido complexes (**4.02-4.07**) were synthesized in good yields from the reaction of chloride **4.1** with KNHAr salts in benzene over 2-4 h at room temperature. In solution, the SIPr ligand of each Pd-amido complex rotates freely about the Pd-C bond, as evidenced by two doublet resonances and 1 triplet resonance observed in the ¹H NMR spectrum between δ 7.32-7.03 each integrating to two hydrogen atoms.



Scheme 4.6. Preparation of SIPr-Ligated Norbornylpalladium Amido complexes **4.02-4.07**

The solid-state structure of **4.03** was determined by single-crystal X-ray diffraction, and an ORTEP drawing is shown in Figure 4.1. Complex **4.03** is a stable, three-coordinate palladium amide that possesses a distorted T-shaped geometry and does not form an *N*-bridged dimeric palladium amido structure, which is common among metal-anilido complexes.¹⁸⁻²⁰ The carbene ligand is oriented *cis* to the open coordination site, and the 2-methylnorbornyl ligand has the *syn-exo* configuration. Previously prepared three-coordinate arylpalladium diarylamido complexes ligated by tri-*tert*-butylphosphine possessed C-Pd-N angles between 88.75 and 93.46 degrees and P-Pd-N angles between 166.00 and 170.66 degrees.²¹ Complex **4.03** is more distorted from a true T-shaped geometry than these previous complexes. The C(norbornyl)-Pd-N angle is 109.15 degrees, and the C(NHC)-Pd-C(norbornyl) angle is 161.28 degrees. The Pd-N distance is ~0.041 Å shorter and the Pd-C(alkyl) distance is ~0.057 Å longer than those of $(\text{P}(t\text{-Bu})_3)\text{Pd}(\text{Ar})\text{NAr}'_2$ complexes (2.078 and 1.987 Å).

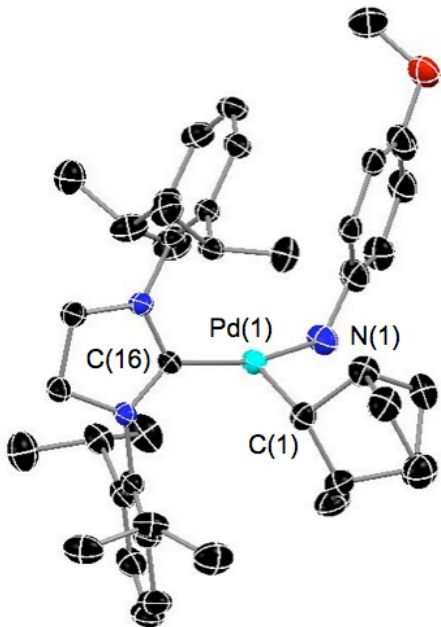


Figure 4.1. ORTEP drawing of complex **4.03** with 35% probability ellipsoids. Hydrogen atoms are omitted for clarity. Selected bond angles (degrees) and lengths (\AA): C(16)-Pd(1)-N(1) 161.28(12); C(16)-Pd(1)-C(1), 89.35(12); N(1)-Pd(1)-C(1), 109.15(13); Pd-C(16), 1.974(3); Pd-N, 2.037(3); Pd-C(1), 2.044(3).

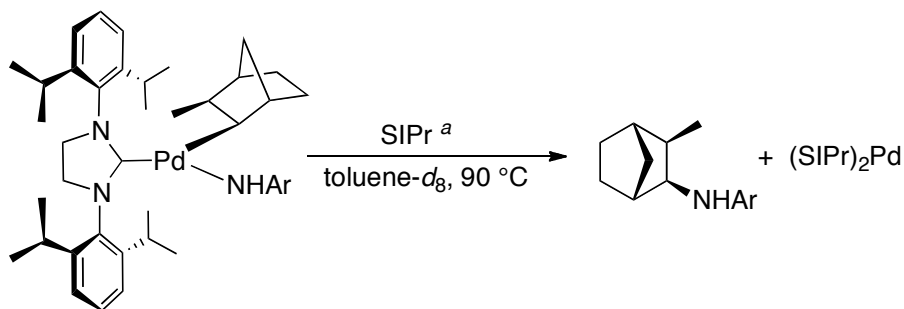
Warming of the SPr-ligated Pd-norbornyl complexes **4.02-4.07** resulted in the reductive elimination of norbornylamines in good yields. The yields and rate constants for these reactions are shown in Table 4.1. The decomposition of Pd-amide **4.02** at 90 °C formed 3-methyl-2-(4-methylanilino)norbornane product in 85% yield. The reductive elimination of **4.02** was conducted in both THF and toluene. The reaction was slightly faster in THF-*d*₈ than toluene-*d*₈ at 50 °C, but by less than a factor of two. In the presence of one equiv of SPr, the reaction generated (SPr)₂Pd⁰ as the metal product in 89% yield.

The decay of the Pd-amides was monitored by ¹H NMR spectroscopy over time in the presence of 1 equiv of the *N*-heterocyclic carbene. The decay curves fit well to a first-order

exponential decay from which the rate constants for reductive elimination were determined. The reductive elimination was found to be zero-order in the concentration of added NHC, as the rate constant for the reaction of **2.02** at 90 °C in the presence of excess (10 equiv) SiPr was 1.0×10^{-3} s⁻¹.

The data in Table 4.1 reveal the electronic and steric effects of the anilido ligand on the rate of reductive elimination: complexes containing more electron-donating anilido ligands reacted faster than complexes containing less electron-donating anilide ligands. Complex **4.03** containing the most electron-donating *para*-anisylamido ligand reacted approximately 2 times faster than complex **4.02** containing the *para*-tolylamido ligand, and an order of magnitude faster than complex **2.04** containing the less electron-donation *meta*-trifluoromethylamido ligand. The magnitude of the observed electronic effect on the rate of reductive elimination of alkylamines is similar to that observed on the reductive elimination of benzylamines¹² and *N*-methyldiarylamines²² from isolated benzyl palladium and arylpalladium amido complexes.

Table 4.1. Reductive Elimination of Norbornylamines from Pd-amide **4.02-4.07**.



entry	complex	Yield ^b	$k_{obs} (\times 10^{-4} \text{ s}^{-1})$
1	4.02 ; Ar = 4-CH ₃ C ₆ H ₄	85%	11 ± 1
2	4.03 ; Ar = 4-OCH ₃ C ₆ H ₄	77%	18
3	4.04 ; Ar = 3-CF ₃ C ₆ H	70%	1.2 ± 0.1
4	4.05 ; Ar = 2-CH ₃ C ₆ H ₄	79%	2.4 ± 0.2
5	4.06 ; Ar = 2,6-(CH ₃) ₂ C ₆ H ₃	84%	7.2 ± 0.5
6	4.07 ; Ar = 2,4-(CH ₃) ₂ C ₆ H ₃	95%	4.8

^aReactions were conducted in NMR tubes with 0.013 mmol Pd-amide, 0.013 mmol SiPr, and 0.013 mmol trimethoxybenzene (TMB) in 0.4 mL toluene-*d*₈ at 90 °C.

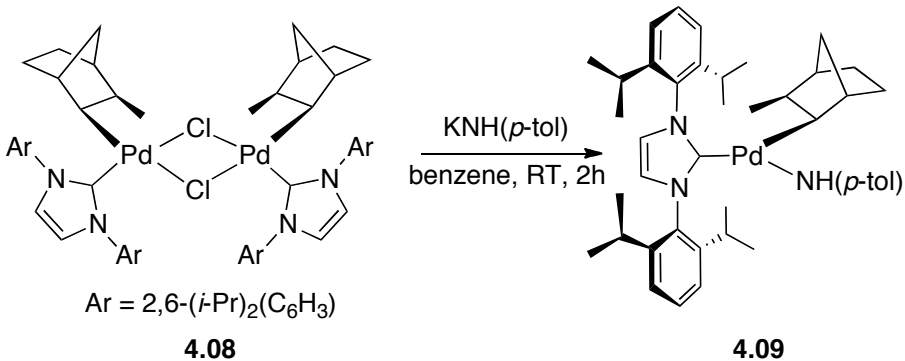
^bYields determined by comparison of the integrated aryl resonances of norbornylamine and TMB standard.

Complexes ligated by more hindered anilido ligands reacted more slowly than complexes containing less sterically hindered anilido ligands; however, the overall steric effect imparted by the anilido ligand on the rate of reductive elimination was small. The reductive elimination of complex **2.05** containing an *ortho*-tolyl substituent was almost an order of magnitude slower than that of complex **4.02** containing a *para*-tolyl group, but the reductive eliminations of complexes **2.06** and **2.07** containing a 2,6-dimethylanilido and 2,4-dimethylanilido ligands, respectively, were faster than that of complex **2.05** and slower than that of complex **4.02**. We propose that

compensating steric and electronic effects of the substituents of the anilido ligand of **2.06** and **2.07** result in intermediate rate constants for the reductive elimination of the corresponding *N*-aryl norbornylamines.

To examine the effects of the ancillary NHC ligand on the rate of reductive elimination, we prepared a norbornylamido complex ligated by the unsaturated NHC, 1,3-bis(2,6-diisopropylphenyl)imidazol-2-ylidene (IPr). Like that of **4.01**, the synthesis of the chloride complex **4.08** for conversion to the anilide was accomplished by the reaction of 1 equiv of IPr with (COD)Pd(2-CH₃-norbornyl)Cl in THF. X-ray crystallography showed that **4.08** exists as a dimeric palladium complex with the two palladium centers bridging through the chloride ligands. In solution, two sets of resonances in the ¹H NMR spectra suggest that **4.08** exists as a mixture of *cis* and *trans* diastereomers at room temperature. At 90 °C, a single set of resonances is observed that likely indicates rapid interconversion between the *cis* and *trans* diastereomers. Signer molecular weight analysis in benzene confirmed that the **4.08** adopts a dimeric structure at room temperature.

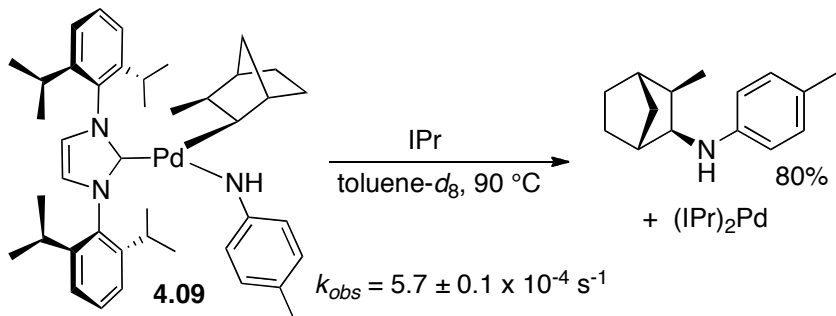
IPr-ligated complex **4.09** was isolated in 41% yield from the reaction of **4.08** with 1 equiv of KNH(4-CH₃C₆H₅) in benzene (Scheme 4.7). Solid-state structural analysis confirmed that the IPr-ligated norbornylamido complex is a stable three-coordinate monomer. Pd-amide **4.08** crystallized as two distinct molecules within the unit cell, both of which are less distorted from a true T-shape than the SIPr-ligated Pd-amide **4.02**. Complex **4.09** contains C(NHC)-Pd-N angles of 163.42 and 163.83 degrees, C(norbornyl)-Pd-N angles of 91.05 and 92.05 degrees, and C-Pd-C angles of 105.06 and 103.67 degrees.



Scheme 4.7. Preparation of IPr-Ligated Norbornylpalladium Amido Complex **4.09**

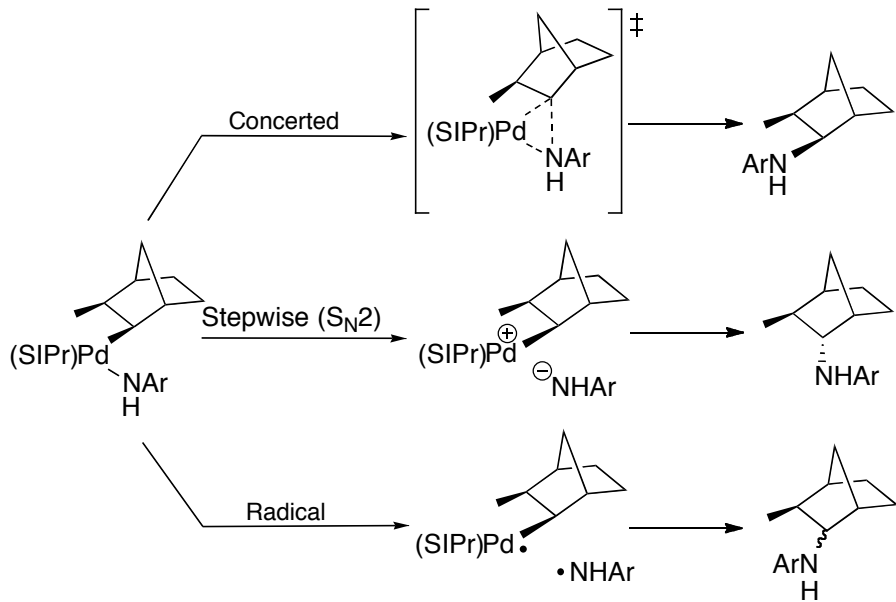
The preparation of analogous norbornylpalladium amido complexes ligated by 1,3-bis(2,4,6-trimethylphenyl)imidazol-2-ylidene (IMes) did not lead to an isolable amido complex. The reaction of (IMes)Pd(2-CH₃-norbornyl)Cl with KNHAr generated a mixture of products that we were unable to identify by ¹H NMR spectroscopy. The IMes ligand lacks the bulky isopropyl groups of SIPr and IPr that are likely necessary for the formation of stable, three-coordinate amido complexes.

Warming of IPr-ligated **4.09** in toluene at 90 °C in the presence of 1 equiv of IPr resulted in the reductive elimination of the norbornylamine product in 80% yield and (IPr)₂Pd° in 92% yield (Scheme 4.8). The rate constant for the reductive elimination *N*-norbornyl toluidine from **4.09** ($5.7 \pm 0.1 \times 10^{-4} \text{ s}^{-1}$) was 5 times smaller than the rate constant for the analogous reductive elimination from complex **4.02**. In contrast to reductive eliminations of benzylamines from four-coordinate benzylpalladium amido complexes,¹² this result indicates that the reductive elimination of alkylamine is faster from complexes ligated by more electron-donating ancillary NHC ligands.



Scheme 4.8. Reductive Elimination of Norbornylamine from Pd-Amide **4.09**

The stable stereochemical configuration of the norbornyl ligand of the alkylpalladium amido complexes provides a means to assess the mechanism of the reductive elimination step. The mechanism of the reductive elimination of the norbornylamines could proceed by one of the three pathways depicted in Scheme 4.9. A concerted reductive elimination would lead to retention of the configuration of the norbornyl ligand in Pd-amide **4.02** and form the *syn*- *exo*-3-methyl-*exo*-2-(4-methylanilino)norbornane. A stepwise pathway involving dissociation of the amido ligand and backside nucleophilic attack onto the *endo* face of the norboryl ligand would result in inversion of the configuration, forming only the *anti*-*exo*-3-methyl-*endo*-2-(4-methylanilino)-norbornane. Finally, a radical pathway would result in an erosion of the configuration and the formation of multiple isomers of the norbornylamine product.



Scheme 4.9. Possible Mechanisms for the Reductive Elimination of Norbornylamines from (SIPr)Pd(2-CH₃C₇H₁₀)NHArc Complexes

To assess whether the stereochemical outcome of the reaction would be biased by the relative stabilities of the diastereomeric products, we computed the energies of the different stereoisomers. Energy minimizations by DFT indicate that the ground state free energy of the *syn-exo*-3-methyl-*exo*-2-anilinonorbornane isomer **4.12** is higher than that of either *anti* diastereomer **4.10** or **4.11** by about 1.4 and 1.7 kcal/mol (Figure 4.2). Thus, the product that would be formed by a concerted pathway is the least stable of the diastereomers.

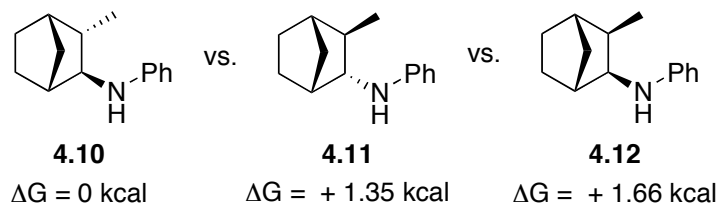


Figure 4.2. Computed relative ground-state free energies (ΔG) of three diastereomers of 3-methyl-2-anilinonorbornane

Reductive eliminations from Pd-amides **4.02-4.07** and **4.09** formed a single diastereomer. Independent preparation of *syn* and *anti* norbornylamine isomers (see the experimental section for procedures) revealed that the *syn-exo,exo* diastereomer **4.12** is formed. The stereochemical outcome implies that reductive elimination of the norbornylamine from the three-coordinate (SIPr)Pd(2-CH₃C₇H₁₀)NAr complexes occur by a concerted pathway.

Because a direct, concerted reductive elimination from an alkylpalladium amide has not been documented previously, we sought to determine if the barrier we measured for such a process is consistent with that computed for a concerted reductive elimination. Hybrid quantum/molecular mechanics (QM/MM) calculations were performed on a full chemical model of **2.07**. The transition-state structure computed for a concerted reductive elimination is illustrated in Figure 4.3. The QM/MM simulations indicated that this transition state lies 25.3 kcal/mol (ΔH^\ddagger) and 23.9 kcal/mol (ΔG^\ddagger) kcal/mol above the ground state of **2.07** at 363 K. These barriers are similar to the 26 kcal/mol barrier measured experimentally and are, therefore, consistent with the proposed concerted reductive elimination mechanism.

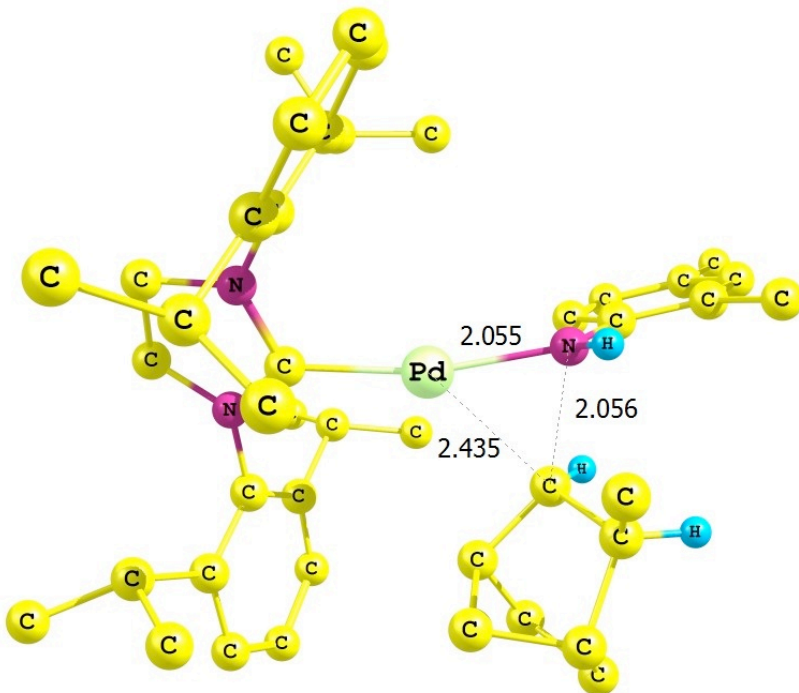


Figure 4.3. Computed transition-state structure of complex **4.07**

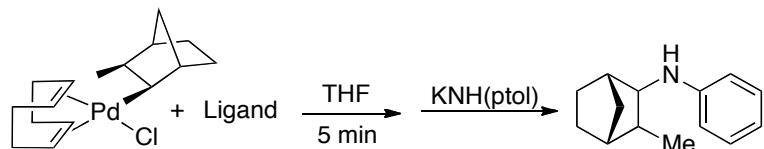
4.2.2 Reactions of $(COD)Pd(2\text{-CH}_3\text{-norbornyl})Cl$ Complexes with Monodentate Phosphines and $KNH(p\text{-tol})$

The ability of the NHC-ligated alkylpalladium amido complexes to undergo thermal reductive elimination of alkylamines is mostly likely facilitated by the three-coordinate T-shaped geometry about the palladium center. Three-coordinate palladium complexes have been shown to undergo C-C and C-N bond forming reductive elimination faster than related four coordinate complexes.²¹ To determine if three-coordinate alkylpalladium amido complexes ligated by alternate bulky ligands undergo facile reductive elimination of alkylamines, we aimed to synthesize and observe the reactivity of a series of Pd-amides ligated by a variety of bulky monodentate ligands. Thus, reactions involving the combination of $(COD)Pd(2\text{-CH}_3\text{-norbornyl})Cl$ complexes with monodentate phosphines and $KNH(p\text{-tol})$ were conducted to

explore the scope of low-valent palladium complexes that undergo reductive elimination of alkylamines.

To identify new complexes prone to reductive elimination of alkylamines, reactions of *in situ* generated alkylpalladium amido complexes were conducted with bulky, monodentate phosphines. The results from the initial reaction screen are described in Table 4.2. Phosphine ligands were allowed to react with (COD)Pd(2-CH₃-norbornyl)Cl for 5 mins at room temperature in THF to displace the COD and form a phosphine ligated palladium complex, followed by the addition of a THF solution containing 1 equiv of KNH(*p*-tol). The reaction mixture was heated for 5 h at 80 °C, filtered through celite, and the crude reaction mixture was submitted to GCMS analysis to identify products from reductive elimination.

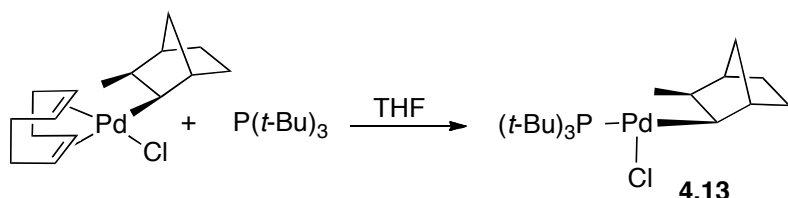
Table 4.2. Reactions of (COD)Pd(2-CH₃-norbornyl)Cl, ligands, and KNH(*p*-tol)



Entry	Ligand	Yield R.E. product
1	SIPr	42%
2	P(<i>t</i> -Bu) ₃	~50%
3	P(<i>o</i> -tol) ₃	0%
4	MorDalPhos	0%
5	PMes ₃	0%
6	PCy ₃	0%
7	P(<i>t</i> -Bu) ₂ Bn	15%
8	QPhos	24%
9	P(<i>t</i> -Bu) ₂ Me	0%

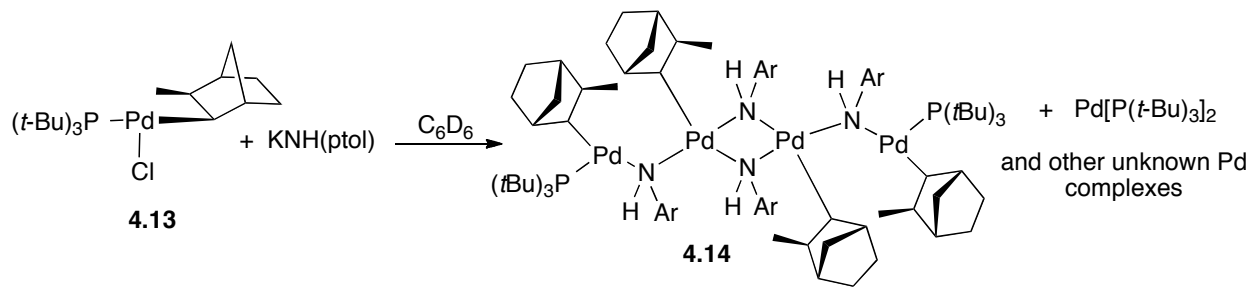
To ensure that this method of screening would generate complexes that undergo reductive elimination of alkylamines, a reaction with SIPr was implemented as a model reaction to test the reaction conditions. Moderate yield of norbornylamine was observed when SIPr was allowed to react with (COD)Pd(2-CH₃-norbornyl)Cl and KNH(*p*-tol) (entry 1). Reactions conducted with the bulky trialkylphosphines P(*t*-Bu)₃, P(*t*-Bu)₂Bn, and QPhos also generated low to moderate yield of reductive elimination product. Reactions utilizing the slightly less bulky P(*t*-Bu)₂Me did not form any reductive elimination products. In addition, reactions conducted with phosphine ligands containing cyclohexyl or aryl groups did not generate any alkylamine products.

To determine what species is undergoing reductive elimination in entries 2, 7, and 8 (Table 4.2), we sought to isolate and characterize an alkylpalladium amido complex ligated by $\text{P}(t\text{-Bu})_3$. The chloride complex $(\text{P}(t\text{-Bu})_3)\text{Pd}(\text{2-CH}_3\text{-norbornyl})\text{Cl}$ (**4.13**) was prepared from the reaction of $(\text{COD})\text{Pd}(\text{2-CH}_3\text{-norbornyl})\text{Cl}$ and $\text{P}(t\text{-Bu})_3$ in THF at room temperature (Scheme 4.10), and fully characterized by ^1H NMR spectroscopy. The structure of this complex is unknown; it may exist as dimer or as a three-coordinate chloride complex similar to **4.01**.



Scheme 4.10. Preparation of $(\text{P}(t\text{-Bu})_3)\text{Pd}(\text{2-CH}_3\text{-norbornyl})\text{Cl}$ (**4.13**)

Treatment of $(\text{P}(t\text{-Bu})_3)\text{Pd}(\text{2-CH}_3\text{-norbornyl})\text{Cl}$ with $\text{KNH}(p\text{-tol})$ in benzene- d_6 forms immediately a deep red solution (Scheme 4.11). ^{31}P and ^1H NMR spectroscopy revealed the formation $\text{Pd}[\text{P}(t\text{-Bu})_3]_2$, norbornylamine, and multiple new complexes of which the identity is unknown. Upon the addition of pentane to the reaction mixture and cooling to -35 °C, red crystals formed. X-ray crystallographic analysis revealed the formation of a tetrameric alkylpalladium amido complex (Figure 4.4). Two of the palladium centers possess three-coordinate geometry and are ligated by $\text{P}(t\text{-Bu})_3$. The other two palladiums are square planar, four-coordinate complexes and are not ligated by $\text{P}(t\text{-Bu})_3$. Dissolution of the crystals in benzene- d_6 forms a red solution from which ^{31}P NMR spectroscopy reveals two resonances at δ 68.9 and 63.9 ppm that decay at different rates at room temperature. The species undergoing reductive elimination is unknown at this time.



Scheme 4.11. Reaction of $(\text{P}(t\text{-Bu})_3)\text{Pd}(2\text{-CH}_3\text{-norbornyl})\text{Cl}$ and $\text{KNH}(p\text{-tol})$

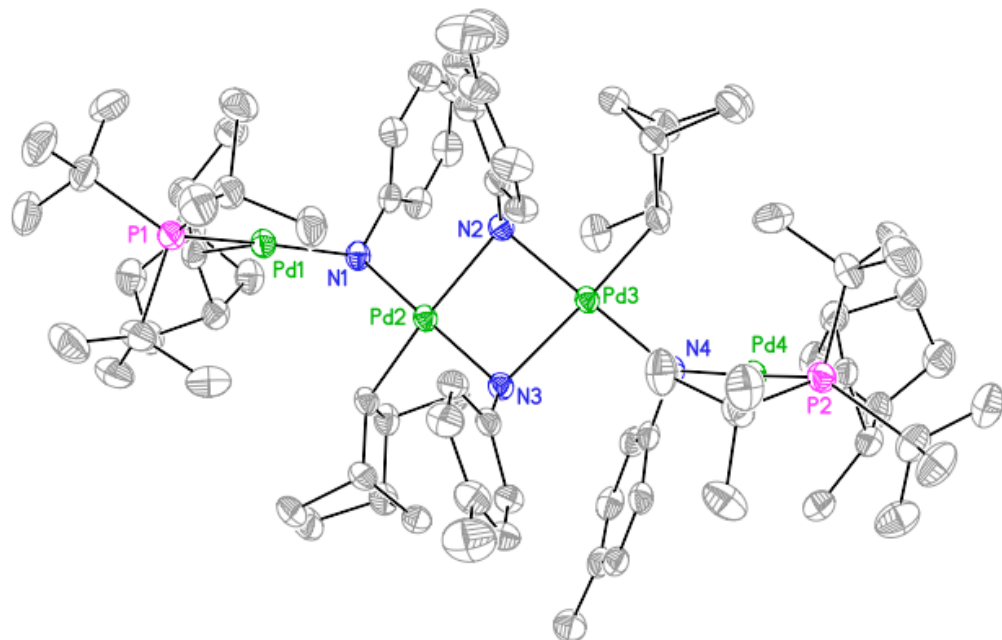


Figure 4.4. ORTEP drawing of complex **4.14** with 35% probability ellipsoids. Hydrogen atoms are omitted for clarity.

4.3 Summary

In summary, we report discrete, low-valent palladium complexes that undergo reductive elimination of alkylamines. The steric bulk of the SPr and IPr ligands leads to the formation of

stable three-coordinate palladium amido complexes, which undergo reductive elimination of alkylamine upon heating without an external oxidant to create a higher-valent intermediate. The stereochemical configuration of the norbornylamine products implies that these reductive eliminations occur by a concerted mechanism. This mechanism contrasts the stepwise mechanism for the reductive elimination of benzylamines from four-coordinate DPPF-ligated benzylpalladium complexes.

Amido complexes ligated by bulky monophosphines also undergo reductive elimination to generate alkylamines, but the structure of the complex undergoing reductive elimination is unknown. A tetrameric alkylpalladium amido complex was isolated, but it is unclear if this complex undergoes reductive elimination to form alkylamine or is first converted to another species that eliminates alkylamine. Future work will examine the reductive elimination of alkylamines from complexes ligated with a range of ancillary ligands, and the development of new catalytic reactions involving this class of reductive elimination.

4.4 Experimental

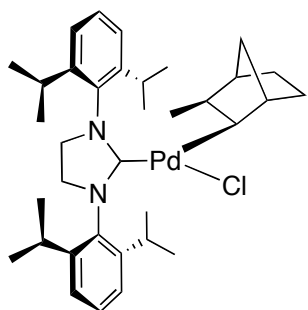
4.4.1 General Experimental Details

Unless otherwise noted, all manipulations were carried out under an inert atmosphere in a nitrogen-filled glovebox or by standard Schlenk techniques. THF, benzene, toluene and pentane were degassed by purging with argon for 45 minutes and dried with a solvent purification system containing a 1 m column of activated alumina. Potassium anilide salts were prepared by addition 1.1 equiv of HMDS to 1 equiv of arylamine in toluene. The precipitated anilide was collected by filtration and washed with toluene and pentane. (COD)Pd(2-CH₃-norbornyl)Cl was prepared according to literature procedure.

Analytical gas chromatography (GC) was performed using a Hewlett-Packard 5890 Gas Chromatograph fitted with a flame ionization detector and a Hewlett-Packard HP5 (30m x 0.32 mm) capillary column. NMR spectra were acquired on 500 MHz or 400 MHz Varian Unity or 500 MHz Innova instruments at the University of Illinois VOICE NMR facility. Chemical shifts are reported in ppm relative to residual chloroform (7.26 ppm for ¹H; 77.0 ppm for ¹³C), toluene (2.09 ppm for ¹H; 20.4 ppm for ¹³C), benzene (7.15 ppm for ¹H; 128.0 ppm for ¹³C), or THF (3.58 ppm for ¹H) or to an external standard (85% H₃PO₄ = 0 ppm for ³¹P or CFCI₃ = 0 ppm for ¹⁹F). Coupling constants are reported in Hertz. Elemental analyses were performed by Roberston-Microlit Laboratories, Inc. (Ledgewood, NJ).

4.4.2 Preparation and Characterization of New Palladium Complexes

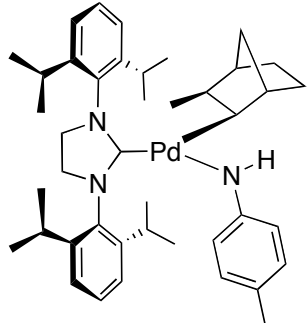
Preparation of (SiPr)Pd(2-CH₃-norbornyl)Cl (4.01)



(COD)Pd(2-CH₃-norbornyl)Cl (0.150 g, 0.418 mmol) and SiPr (0.177g, 0.459 mmol) were added to a 20 mL scintillation vial and the reaction mixture was dissolved in 3 mL of THF. The reaction was stirred at room temperature for 2 h. After 2 h, 15 mL of pentane was added to precipitate an orange solid. The orange solid was collected by filtration and washed with (5 × 3 mL) pentane and dried by vacuum. Collected 0.245 g; 92 %. ¹H NMR (CDCl₃, 500 MHz): δ 7.42 (t, *J* = 7.5 Hz, 2H), 7.28 (d, *J* = 7.5 Hz, 2H), 7.25 (d, *J* = 7.5 Hz, 2H), 4.07-4.00 (m, 4H), 3.23 (hept, *J* = 7.0 Hz, 2H), 3.16 (hept, *J* = 7.0 Hz, 2H), 3.10 (d, *J* = 7.5 Hz, 1H), 2.07 (d, *J* = 10.0 Hz, 1H), 1.99 (d, *J* = 3.5 Hz, 1H), 1.56 (d, *J* = 6.5 Hz, 6H), 1.47 (d, *J* = 3.0 Hz, 1H), 1.44 (d, *J* = 6.5 Hz, 6H), 1.30 (d, *J* = 7.0 Hz, 6H), 1.28 (d, *J* = 6.5 Hz, 6H), 1.22-1.18 (m, 1H), 0.85-0.79 (m, 4H), 0.71-0.66 (m, 2H), 0.56- 0.42 (m, 2H). ¹³C[¹H] NMR (CDCl₃, 126

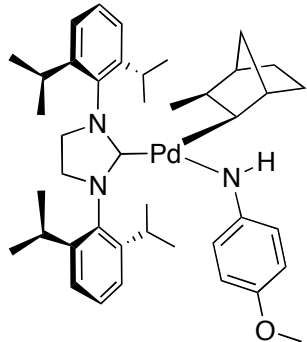
MHz): δ 200.5, 146.9, 146.6, 134.1, 129.8, 124.8, 124.6, 57.9, 53.6, 47.8, 46.1, 45.9, 34.9, 29.1, 29.0, 28.7, 28.4, 26.1, 26.0, 23.9, 23.8, 23.3. Anal. Calc'd. for $C_{35}H_{51}N_2ClPd$: C, 65.51; H, 8.01; N, 4.37; found, C, 65.39; H, 8.20; N, 4.11.

Preparation of (SiPr)Pd(2-CH₃-norbornyl)NH(4-CH₃C₆H₄) (4.02)



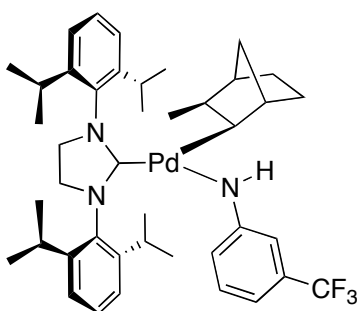
(SiPr)Pd(2-CH₃-norbornyl)Cl (0.120 g, 0.187 mmol) and KNH(*p*-CH₃) (0.0272 g, 0.187 mmol) were added to a 20 mL scintillation vial and the reaction mixture was dissolved in 3 mL of benzene. The reaction mixture was stirred for 2 h and the color changed to dark red/purple. After 2h, the reaction mixture was filtered through a syringe filter and the volatiles were removed by vacuum. A 1.5 mL aliquot of pentane was added to the residue and after 2 minutes dark crystals appeared. The reaction mixture was placed into a freezer (-35 °C) overnight to increase the yield of crystallized product. The supernatant liquid was removed with a pipette and the crystals were dried vacuum. Yield 0.107 g, 80%. ¹H NMR (C_6D_6 , 500 MHz): δ 7.34 (t, J = 7.5 Hz, 2H), 7.25 (d, J = 7.5 Hz, 2H), 7.09 (d, J = 8.0 Hz, 2H), 6.85 (d, J = 8.0 Hz, 2H), 6.19 (d, J = 8.0 Hz, 2H), 3.86 (s, 1H), 3.48-3.34 (m, 6H), 3.11-3.03 (m, 3H), 2.28 (s, 3H), 2.11 (s, 1H), 1.77 (d, J = 9.5 Hz, 1H), 1.66 (d, J = 6.5 Hz, 6H), 1.56 (s, 1H), 1.33- 0.95 (m, 22H), 0.80 (bs, 4H), 0.65 (d, J = 9.5 Hz, 1H). ¹³C[¹H] NMR (C_6D_6 , 126 MHz): δ 210.5, 157.8, 147.5, 146.9, 136.4, 129.5, 129.3, 124.9, 124.8, 120.8, 117.8, 53.4, 48.1, 47.2, 45.4, 44.5, 35.0, 29.8, 29.5, 29.3, 29.1, 26.3, 25.8, 24.4, 24.1, 23.6, 21.0. Anal. Calc'd. for $C_{42}H_{59}N_3Pd$: C, 70.81; H, 8.35; N, 5.90; found, C, 70.58; H, 8.31; N, 5.72.

Preparation of (SiPr)Pd(2-CH₃-norbornyl)NH(4-OCH₃C₆H₄) (4.03)



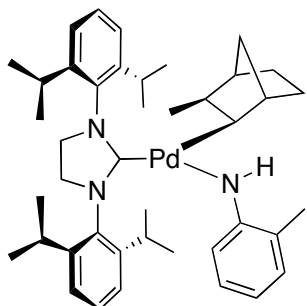
(SiPr)Pd(2-CH₃-norbornyl)Cl (0.100 g, 0.157 mmol) and KNH(*p*-OCH₃) (0.0253 g, 0.157 mmol) were added to a 20 mL scintillation vial and the reaction mixture was dissolved in 3 mL of benzene. The reaction mixture was stirred for 2 h and the color changed to dark red/purple. After 2h, the reaction mixture was filtered through a syringe filter and the volatiles were removed by vacuum. A 1.5 mL aliquot of pentane was added to the residue and after 2 minutes dark crystals appeared. The reaction mixture was placed into a freezer (-35 °C) overnight to increase the yield of crystallized product. The supernatant liquid was removed with a pipette and the crystals were dried vacuum. Yield 0.0581 g, 51%. ¹H NMR (C₆D₆, 500 MHz): δ 7.30 (d, *J* = 8.0 Hz, 2H), 7.22 (d, *J* = 7.5Hz, 2H), 7.08 (d, *J* = 8.0 Hz, 2H), 6.69 (d, *J* = 8.5Hz, 2H), 6.16 (d, *J* = 8.5 Hz, 2H), 3.84 (s, 1H), 3.48 (s, 3H), 3.46-3.35 (m, 6H), 3.09 (hept, *J* = 7.0 Hz, 2H), 3.02 (s, 1H), 2.09 (d, *J* = 3.0 Hz, 1H), 1.77 (d, *J* = 10 Hz, 1H), 1.65 (d, *J* = 7.0 Hz, 6H), 1.61 (d, *J* = 7.0 Hz, 1H), 1.59 (d, *J* = 3.5 Hz, 1H), 1.51 (d, *J* = 7.0 Hz, 1H), 1.35-1.29 (m, 7 H), 1.16 (d, *J* = 7.0 Hz, 6H), 1.11-1.06 (m, 7H), 1.00-0.96 (m, 1H), 0.81 (s, 3H), 0.68 (d, *J* = 7.5Hz, 1H). ¹³C[¹H] NMR (C₆D₆, 126 MHz): δ 210.7, 154.22, 149.9, 147.5, 146.9, 136.3, 129.5, 124.90, 124.8, 118.1, 114.9, 55.7, 53.4, 47.8, 47.2, 45.4, 44.5, 35.0, 29.9, 29.5, 29.3, 29.1, 26.3, 25.8, 24.5, 24.1, 23.6. Anal. Calc'd. for C₄₂H₅₉N₃OPd: C, 69.26; H, 8.16; N, 5.77; found, C, 68.97; H, 8.30; N, 5.50.

Preparation of (SiPr)Pd(2-CH₃-norbornyl)NH(3-CF₃C₆H₄) (4.04)



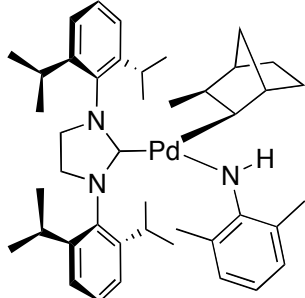
(SiPr)Pd(2-CH₃-norbornyl)Cl (0.100 g, 0.156 mmol) and KNH(3-CF₃C₆H₄) (0.0310 g, 0.156 mmol) were added to a 20 mL scintillation vial and the reaction mixture was dissolved in 3 mL of benzene. The reaction mixture was stirred for 2 h and the color changed to dark red/purple. After 2h, the reaction mixture was filtered through a syringe filter and the volatiles were removed by vacuum. A 1.5 mL aliquot of pentane was added to the residue and after 2 minutes dark crystals appeared. The reaction mixture was placed into a freezer (-35 °C) overnight to increase the yield of crystallized product. The supernatant liquid was removed with a pipette and the crystals were dried vacuum. Yield: 0.0662 g; 55%. ¹H NMR (C₆D₆, 500 MHz): δ 7.31 (t, *J* = 8.0 Hz, 2H), 7.23 (d, *J* = 7.5 Hz, 2H), 7.05 (d, *J* = 7.5Hz, 2H), 6.85 (t, *J* = 8.0 Hz, 1H), 6.74 (d, *J* = 7.0 Hz, 1H), 6.57 (s, 1H), 6.16 (d, *J* = 6.5 Hz, 1H), 3.72 (s, 1H), 3.45-3.22 (m, 6H), 3.14-2.99 (m, 3H), 2.05 (s, 1H), 1.64 (s, 1H), 1.62 (d, *J* = 7.0 Hz, 6H), 1.48 (d, *J* = 3.0 Hz, 1H), 1.30-0.94 (m, 22 H), 0.77 (d, *J* = 7.0 Hz, 3H), 0.72-0.67 (m, 1H), 0.56 (d, *J* = 10.0 Hz, 1H). ¹³C[¹H] NMR (C₆D₆, 126 MHz): δ 208.7, 160.3, 147.2, 146.7, 135.9, 130.8 (q, *J* = 28.2 Hz), 129.8, 128.9, 126.3 (q, *J* = 274 Hz), 125.1, 124.9, 120.6, 113.0, 108.1, 53.4, 49.8, 47.4, 45.5, 44.8, 34.7, 29.5, 29.4, 29.2, 29.1, 26.2, 25.7, 24.1, 24.0, 23.6. ¹⁹F NMR (C₆D₆, 470 MHz): δ -61.9. Anal. Calc'd. for C₄₂H₅₆F₃N₃Pd: C, 65.83; H, 7.37; N, 5.48; found, C, 65.59; H, 7.46; N, 5.27.

Preparation of (SiPr)Pd(2-CH₃-norbornyl)NH(2-CH₃C₆H₄) (4.05)



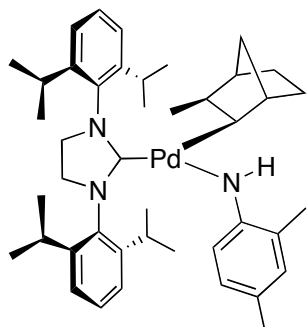
(SiPr)Pd(2-CH₃-norbornyl)Cl (0.120 g, 0.187 mmol) and KNH(CH₃) (0.0272 g, 0.187 mmol) were added to a 20 mL scintillation vial and the reaction mixture was dissolved in 3 mL of benzene. The reaction mixture was stirred for 2 h and the color changed to dark red/purple. After 2h, the reaction mixture was filtered through a syringe filter and the volatiles were removed by vacuum. A 1.5 mL aliquot of pentane was added to the residue and after 2 minutes dark crystals appeared. The reaction mixture was placed into a freezer (-35 °C) overnight to increase the yield of crystallized product. The supernatant liquid was removed with a pipette and the crystals were dried vacuum. Yield 0.100 g, 75%. ¹H NMR (C₆D₆, 500 MHz): δ 7.32 (t, *J* = 8.0 Hz, 2H), 7.24 (d, *J* = 8.0 Hz, 2H), 7.09-7.05 (m, 3H), 6.99 (t, *J* = 7.5 Hz, 1H), 6.62 (t, *J* = 7.5 Hz, 1H), 6.20 (d, *J* = 8.0 Hz, 1H), 3.96 (s, 1H), 3.48-3.34 (m, 6H), 3.12-3.04 (m, 3H), 2.11 (bs, 4H), 1.66 (d, *J* = 7.0 Hz, 6H), 1.65 (bs, 1H), 1.56 (d, *J* = 4.0 Hz, 1H), 1.32- 1.26 (m, 7H), 1.16 (d, *J* = 7.0 Hz, 6H), 1.10-0.90 (m, 12H), 0.78 (p, *J* = 7.0 Hz, 1H), 0.57 (d, *J* = 10.0 Hz, 1H). ¹³C[¹H] NMR (C₆D₆, 126 MHz): δ 210.3, 157.9, 147.5, 146.9, 136.3, 129.8, 129.6, 127.1, 125.0, 124.9, 121.7, 118.1, 112.8, 53.4, 48.5, 47.2, 45.6, 44.5, 34.8, 29.7, 29.4, 29.2, 26.3, 25.8, 24.6, 24.1, 23.7, 18.8. Anal. Calc'd. for C₄₂H₅₉N₃Pd: C, 70.81; H, 8.35; N, 5.90; found, C, 70.89; H, 8.35; N, 5.71.

Preparation of (SiPr)Pd(2-CH₃-norbornyl)NH(2,6-(CH₃)₂C₆H₄) (4.06)



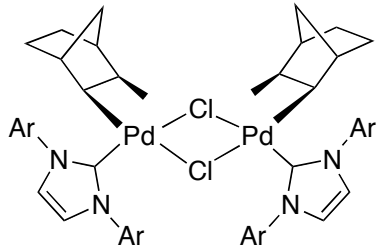
(SiPr)Pd(2-CH₃-norbornyl)Cl (0.120 g, 0.187 mmol) and KNH(2,6-(CH₃)₂C₆H₃) (0.0444 g, 0.187 mmol) were added to a 20 mL scintillation vial and the reaction mixture was dissolved in 3 mL of benzene. The reaction mixture was stirred for 2 h and the color changed to dark red/purple. After 2h, the reaction mixture was filtered through a syringe filter and the volatiles were removed by vacuum. A 1.5 mL aliquot of pentane was added to the residue and after 2 minutes dark crystals appeared. The reaction mixture was placed into a freezer (-35 °C) overnight to complete the crystallization of the product. The supernatant liquid was removed with a pipette and the crystals were dried vacuum. Yield: 0.108 g, 72%. ¹H NMR (C₆D₆, 500 MHz): δ 7.26 (t, *J* = 7.5 Hz, 2H), 7.20 (d, *J* = 8.0 Hz, 2H), 7.10 (d, *J* = 7.5 Hz, 2H), 7.03 (d, *J* = 8.0 Hz, 2H), 6.27 (t, *J* = 7.0 Hz, 1H), 4.62 (s, 1H), 3.52-3.36 (m, 6H), 3.14-3.04 (m, 3H), 2.20 (s, 6H), 2.16 (d, *J* = 3.0 Hz, 1H), 1.66 (d, *J* = 7.0 Hz, 6H), 1.51 (d, *J* = 3.0 Hz, 1H), 1.46 (d, *J* = 9.0 Hz, 1H), 1.30-0.95 (m, 22H), 0.84 (d, *J* = 7.0 Hz, 3H), 0.72 (p, *J* = 6.5 Hz, 1H), 0.55 (d, *J* = 9.5 Hz, 1H). ¹³C[¹H] NMR (C₆D₆, 126 MHz): δ 210.1, 156.3, 147.3, 146.6, 136.8, 129.6, 128.7, 125.2, 125.0, 123.7, 113.1, 53.6, 49.2, 46.8, 46.3, 45.6, 34.5, 30.1, 29.3, 29.2, 29.0, 26.2, 25.9, 25.1, 24.0, 23.8, 20.1. Anal. Calc'd. for C₄₃H₆₁N₃Pd: C, 71.10; H, 8.46; N, 5.78; found, C, 70.86; H, 8.55; N, 5.64.

Preparation of (SiPr)Pd(2-CH₃-norbornyl)NH(2,4-(CH₃)₂C₆H₄) (4.07)



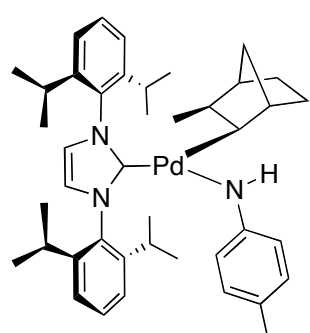
(SiPr)Pd(2-CH₃-norbornyl)Cl (0.100 g, 0.156 mmol) and KNH(2,4-(CH₃)C₆H₃) (0.0248 g, 0.156 mmol) were added to a 20 mL scintillation vial and the reaction mixture was dissolved in 3 mL of benzene. The reaction mixture was stirred for 2 h and the color changed to dark red/purple. After 2h, the reaction mixture was filtered through a syringe filter and the volatiles were removed by vacuum. A 1.5 mL aliquot of pentane was added to the residue and after 2 minutes dark crystals appeared. The reaction mixture was placed into a freezer (-35 °C) overnight to increase the yield of crystallized product. The supernatant liquid was removed with a pipette and the crystals were dried vacuum. Yield: 0.0684 g, 72%. ¹H NMR (C₆D₆, 500 MHz): δ 7.34 (t, *J* = 8.0 Hz, 2H), 7.27 (d, *J* = 8.0 Hz, 2H), 7.09 (d, *J* = 8.0 Hz, 2H), 6.83 (s, 1H), 6.80 (d, *J* = 7.5 Hz, 1H), 6.14 (d, *J* = 8.0 Hz, 1H), 3.99 (s, 1H), 3.49-3.37 (m, 6H), 3.13-3.05 (m, 3H), 2.32 (s, 3H), 2.11 (bs, 4H), 1.68 (d, *J* = 6.5 Hz, 6H), 1.62 (d, *J* = 9.5 Hz, 1H), 1.56 (d, *J* = 5.0 Hz, 1H), 1.33 (d, *J* = 6.5 Hz, 6H), 1.31-0.94 (m, 16 H), 0.90 (d, *J* = 7.0 Hz, 3H), 0.87 (p, *J* = 7.0 Hz, 1H), 0.58 (d, *J* = 9.5 Hz, 1H). ¹³C[¹H] NMR (C₆D₆, 126 MHz): δ 210.7, 155.5, 147.5, 146.9, 136.4, 130.6, 129.5, 127.6, 124.9, 124.8, 121.7, 120.8, 118.3, 53.4, 48.0, 47.1, 45.5, 44.4, 34.7, 29.8, 29.4, 29.3, 29.2, 26.3, 25.8, 24.8, 24.1, 23.6, 21.1, 18.8. Anal. Calc'd. for C₄₃H₆₁N₃Pd: C, 71.10; H, 8.46; N, 5.78; found, C, 71.37; H, 8.71; N, 5.55.

Preparation of (IPr)Pd(2-CH₃-norbornyl)Cl (4.08)



To a 20 mL scintillation vial was added (COD)Pd(2-CH₃-norbornyl)Cl (0.130 g, 0.362 mmol) and IPr (0.141 g, 0.363 mmol). The reaction mixture was dissolved in 5 mL benzene and stirred for 3 h. The reaction mixture was filtered through a syringe filter to remove Pd° black, and the volatiles were removed by vacuum. To the yellow residue was added 2 mL and pentane, and the reaction mixture was placed into the freezer (-35 °C) overnight. The supernatant liquid was removed from the light yellow precipitate with a pipette and the solid was dried by vacuum. Yield 0.208 g, 90%. ¹H NMR (C₆D₆, 500 MHz, 90°C): δ 7.24 (t, *J* = 8.0 Hz, 2H), 7.12 (d, *J* = 7.5 Hz, 4H), 6.60 (s, 2H), 2.84 (hept, *J* = 7.0 Hz, 4H), 2.66 (d, *J* = 9.5 Hz, 1H), 2.14 (s, 1H), 1.59 (bs, 1H), 1.42 (d, *J* = 6.5 Hz, 6H), 1.41 (d, *J* = 6.5 Hz, 6H), 1.29-1.24 (m, 4H), 1.03 (d, *J* = 6.5 Hz, 6H), 1.02 (d, *J* = 6.5 Hz, 6H), 0.86-0.77 (m, 4H), 0.63 (p, *J* = 6.5 Hz, 1H), 0.51 (bs, 1H). ¹³C[¹H] NMR (C₆D₆, 126 MHz, 90°C): δ 146.3, 130.9, 128.6, 124.8, 124.7, 124.1, 48.7, 47.0, 46.9, 34.9, 29.8, 29.6, 25.7, 25.5, 24.5, 23.4. Anal. Calc'd. for C₃₅H₄₉N₂ClPd: C, 65.72; H, 7.72; N, 4.38; found, C, 65.80; H, 7.72; N, 4.32.

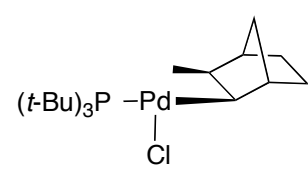
Preparation of (IPr)Pd(2-CH₃-norbornyl)NH(4-CH₃C₆H₄) (4.09)



(SIPr)Pd(2-CH₃-norbornyl)Cl (0.100 g, 0.156 mmol) and KNH(*p*-CH₃) (0.0227 g, 0.156 mmol) were added to a 20 mL scintillation vial and the reaction mixture was dissolved in 3 mL of benzene. The reaction mixture was stirred for 3 h and the color changed to dark red/purple. After 2h, the reaction mixture was filtered through a syringe filter and the volatiles were removed by vacuum. The residue was dissolved in 15 mL of

pentane and was filtered through a syringe filter to remove a small amount of palladium byproduct. The volatiles were removed by vacuum and 1.5 mL of pentane was added to the residue and after 2 minutes dark crystals appeared. The reaction mixture was placed into a freezer (-35 °C) overnight to increase the yield of crystallized product. The supernatant liquid was removed with a pipette and the crystals were dried vacuum. Yield 0.0452 g, 41%. ¹H NMR (C₆D₆, 500 MHz): δ 7.36 (t, *J* = 8.0 Hz, 2H), 7.26 (d, *J* = 8.0 Hz, 2H), 7.11 (d, *J* = 8.0 Hz, 2H), 6.89 (d, *J* = 8.0 Hz, 2H), 6.48 (s, 2H), 6.35 (d, *J* = 8.5 Hz, 2H), 3.85 (s, 1H), 3.10 (d, *J* = 7.5 Hz, 1H) 3.05 (hept, *J* = 7.0 Hz, 2H), 2.65 (hept, *J* = 2.65 Hz, 2H), 2.31 (s, 3H), 2.11 (d, *J* = 3.0 Hz, 1H), 1.83 (d, *J* = 9.5 Hz, 1H), 1.58 (d, *J* = 3.0 Hz, 1H), 1.55 (d, *J* = 7.0 Hz, 6H), 1.32-1.17 (m, 8H), 1.08-0.96 (m, 14H), 0.94 (d, *J* = 7.0 Hz, 3H), 0.74-0.69 (m, 2H). ¹³C[¹H] NMR (C₆D₆, 126 MHz): δ 185.7, 157.9, 146.3, 146.0, 136.1, 130.3, 129.4, 124.5, 124.4, 123.2, 120.7, 117.8, 47.6, 47.4, 45.4, 44.4, 35.0, 29.7, 29.6, 29.3, 29.2, 25.8, 25.1, 24.6, 23.4, 23.2, 21.1. Anal. Calc'd. for C₄₂H₅₇N₃Pd: C, 70.91; H, 8.22; N, 5.91; found, C, 71.27; H, 8.36; N, 5.65.

*Preparation of (P(*t*-Bu)₃)Pd(2-CH₃-norbornyl)Cl (4.13)*



(COD)Pd(2-CH₃-norbornyl)Cl (0.200 g, 0.557 mmol) and P(*t*-Bu)₃Cl (0.118 g, 0.585 mmol) were added to a 20 mL scintillation vial and the reaction mixture was dissolved in 4 mL of THF. The dark orange reaction mixture was stirred 2 h and filtered through celite. The volatiles were removed by vacuum. Pentane (15 mL) was added to the residue and an orange solid was collected by filtration and dried by vacuum. Yield: 0.217 g; 86%. ¹H NMR (C₆D₆, 500 MHz): δ 4.21 (dd, *J* = 17.5, 7 Hz, 1H), 3.32 (d, *J* = 10 Hz, 1H), 2.83 (s, 1H), 2.01 (d, *J* = 7Hz, 3H), 1.92 (bs, 1H), 1.49-1.36 (m, 2H), 1.19-1.13 (m, 2H), 1.09 (d, *J* = 12.0Hz, 18H), 1.05-0.97 (m, 2H). ¹³C[¹H] NMR

(C₆D₆, 126 MHz): δ 57.1, 49.3, 47.0, 46.7, 38.7, 35.5, 32.0, 29.7, 29.6, 25.1. ³¹P NMR (C₆D₆, 202 MHz): δ 70.5 s. Anal. Calc'd. for C₂₀H₄₀ClPPd: C, 52.98; H, 8.89; found, C, 52.94; H, 8.63.

4.4.3 General Procedure for Kinetic Analysis of Reductive Elimination from Norbornylamido Complexes

In an N₂ filled glovebox, (SiPr)Pd(2-CH₃-norbornyl)NHArc (0.130 mmol), SiPr (0.130 mmol), and trimethoxybenzene (0.130 mmol) was added to a 4 mL vial and the reaction mixture was dissolved into 0.4 mL toluene-*d*₈. The reaction mixture was carefully transferred to an NMR tube and inserted into a 500 MHz NMR probe that was pre-warmed to 90 °C. An array was collected with scans every 45 s until the complex had reacted greater than three half-lives. The spectra were integrated and fit to an exponential decay to determine the rate constant for reductive elimination. The yields of the norbornylamine products were determined by comparing the integration of the aryl proton resonances to those of trimethoxybenzene in the ¹H NMR spectrum following completion of the reaction.

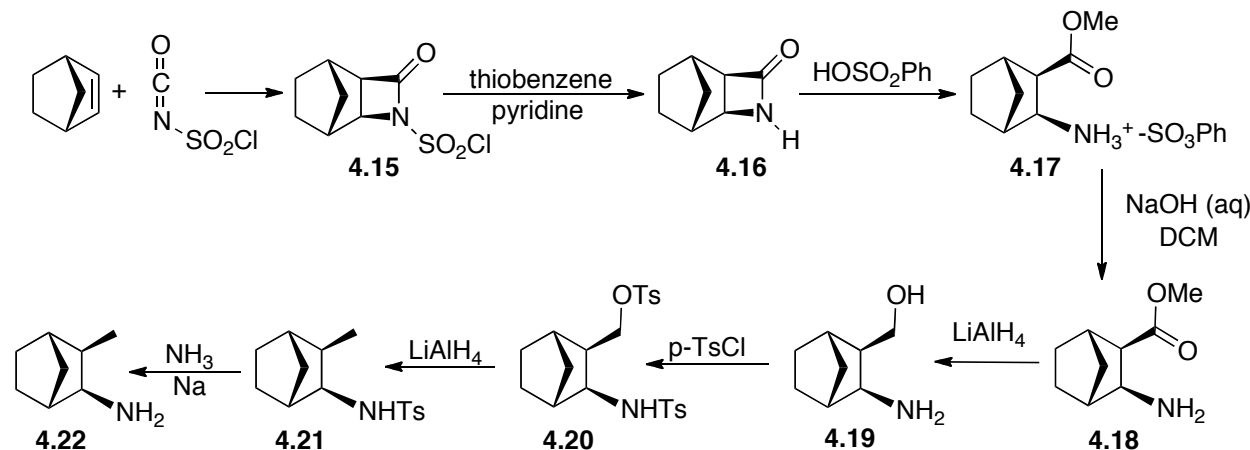
4.4.4 Effect of Solvent on the Reductive Elimination from Norbornylamido Complexes

In an N₂ filled glovebox, (SiPr)Pd(2-CH₃-norbornyl)NH(4-CH₃C₆H₄) (0.130 mmol), SiPr (0.130 mmol), and trimethoxybenzene (0.130 mmol) were added to a 4 mL vial, and the reaction mixture was dissolved in ether 0.4 mL toluene-*d*₈ or 0.4 mL THF-*d*₈. The reaction mixture was carefully transferred to an NMR tube, and an initial ¹H NMR spectrum was obtained. The NMR tube was placed into an oil bath at 50 °C. ¹H NMR spectra were obtained every 45 to 135 minutes by ¹H NMR spectroscopy. The spectra were integrated and fit to an exponential decay to

determine the rate constant for reductive elimination. The rate constant for reductive elimination was found to be $1.3 \times 10^{-4} \text{ s}^{-1}$ in THF-*d*₈ and $7.8 \times 10^{-5} \text{ s}^{-1}$ in toluene-*d*₈.

4.4.5 Synthesis of *syn*-*exo*-3-methyl-*exo*-2-aminonorbornane

The preparation of the parent norbornylamine, *syn*-*exo*-3-methyl-*exo*-2-aminonorbornane, was conducted by a modified procedure illustrated below. Intermediates **4.15**-**4.17** were prepared from a procedure reported by Moriconi,²³ and the aminoester **4.18** was revealed by the reaction of **7.17** with NaOH in dichloromethane. Intermediate **4.18** was carried on to the parent norbornylamine product by a previously described procedure.²⁴



General Procedure for the Preparation of the N-arylnorbornylamine Products

Two different procedures were employed to synthesize the N-arylnorbornylamine products from intermediate **4.22**.²⁵⁻²⁶

- 1) In an N₂ filled glovebox, 4 mL vial was charged with 3-methylbicyclo[2.2.1]heptan-2-amine (0.069 g; 0.55 mmol), 3-bromobenzotrifluoride (0.113 g; 0.050 mmol), NaOtBu (0.067 g; 0.70 mmol), Pd(OAc)₂ (0.0056 g; 0.025 mmol) and Josiphos - CyPF-*t*-Bu (0.014 g; 0.025 mmol). The reaction mixture was dissolved in 0.50 mL anhydrous DME

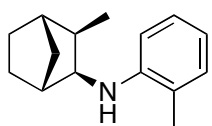
and heated to 100 °C for 18 h. The reaction mixture was cooled to RT and filtered through celite. The product was purified by column chromatography (hexane/ethylacetate).

2) In an N₂ filled glovebox, 4 mL vial was charged with 3-methylbicyclo[2.2.1]heptan-2-amine (0.069 g; 0.55 mmol), 1-bromo-2,4-dimethylbenzene (0.0925 g; 0.050 mmol), NaOtBu (0.067 g; 0.70 mmol), Chloro[2-(dicyclohexylphosphino)-3,6-dimethoxy-2',4',6'-triisopropyl-1,1'-biphenyl][2-(2-aminoethyl)phenyl]palladium(II) (0.0200 g; 0.025 mmol) and 2-(Dicyclohexylphosphino)3,6-dimethoxy-2',4',6'-triisopropyl-1,1'-biphenyl (0.0134 g; 0.025 mmol). The reaction mixture was dissolved in 0.5 mL Bu₂O and stirred at 110 °C for 4 h. The reaction mixture was cooled to room temperature and filtered through celite. The reaction mixture was purified by column chromatography (hexane/ethylacetate). This procedure is adapted from a method described by Buchwald.

Preparation of syn-exo-3-methyl-endo-2-(4-methylanilino)norbornane

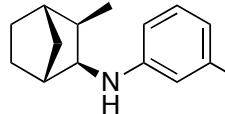
Prepared according to procedure 1 using 3-methylbicyclo[2.2.1]heptan-2-amine (0.090 g; 0.72 mmol), 4-bromotoluene (0.123 g; 0.72 mmol), Pd(OAc)₂ (0.0016 g; 0.0072 mmol), Josiphos - CyPF-*t*-Bu (0.0040 g; 0.0072 mmol), and NaOtBu (0.097 g; 1.0 mmol). Collected 0.061 g; 40%. ¹H NMR (C₆D₆, 500 MHz): δ 7.01 (d, *J* = 8.0 Hz, 2H), 6.45 (d, *J* = 8.5 Hz, 2H), 3.27 (s, 1H), 3.13 (bs, 1H), 2.22 (s, 3H), 1.92 (s, 1H), 1.69-1.64 (m, 2H), 1.38-1.31 (m, 3H), 1.06-1.01 (m, 2H), 0.84 (dt, *J* = 10.5, 1.5 Hz, 1H), 0.80 (d, *J* = 7.5 Hz, 3H). Anal. Calc'd. for C₁₅H₂₁N: C, 83.67; H, 9.83; N, 6.50; found, C, 83.66; H, 9.65; N, 6.40.

Preparation of syn-exo-3-methyl-endo-2-(2-methylanilino)norbornane



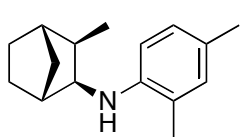
Prepared according to procedure 1 using 3-methylbicyclo[2.2.1]heptan-2-amine (0.069 g; 0.55 mmol), 2-bromotoluene (0.855 g; 0.050 mmol), NaOtBu (0.067 g; 0.70 mmol), Pd(OAc)₂ (0.0056 g; 0.025 mmol) and Josiphos - CyPF-*t*-Bu (0.014 g; 0.025 mmol). Collected 13.4 mg; 12%. ¹H NMR (C₆D₆, 500 MHz): δ 7.22 (t, *J* = 7.5 Hz, 1H), 7.05 (d, *J* = 7.5 Hz, 1H), 6.78 (t, *J* = 7.5 Hz, 1H), 6.61 (d, *J* = 8.5 Hz, 1H), 3.38 (bs, 1H), 3.19 (d, *J* = 7.0 Hz, 1H), 2.01 (bs, 1H), 1.91 (s, 3H), 1.71-1.69 (m, 2H), 1.44 (d, *J* = 10.0 Hz, 1H), 1.36-1.33 (m, 2H), 1.06 (d, *J* = 9.5 Hz, 2H), 0.87 (d, *J* = 10.0 Hz, 1H), 0.81 (d, *J* = 7.5 Hz, 3H). ¹³C[¹H] NMR (C₆D₆, 126 MHz): δ 146.6, 130.3, 127.6, 121.3, 116.8, 110.4, 59.3, 44.0, 43.3, 42.3, 33.0, 29.4, 27.1, 17.4, 14.4. HRMS (EI⁺) m/z calc'd for C₁₆H₂₁N for [M+]: 215.1674, found 215.1673.

Preparation of syn-exo-3-methyl-endo-2-(3-trifluoromethylanilino)norbornane



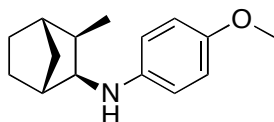
A 4 ml vial was charged with 3-methylbicyclo[2.2.1]heptan-2-amine (0.069 g; 0.55 mmol), 3-bromobenzotrifluoride (0.113 g; 0.050 mmol), Pd(OAc)₂ (0.0056 g; 0.025 mmol), Josiphos - CyPF-*t*-Bu (0.014 g; 0.025 mmol), and NaOtBu (0.067 g; 0.70 mmol). Collected 0.022 g; 16 %. ¹H NMR (C₆D₆, 500 MHz): δ 6.95-6.90 (m, 2H), 6.67 (s, 1H), 6.28 (d, *J* = 7.5 Hz, 1H), 3.30 (d, *J* = 6.0 Hz, 1H), 2.92 (d, *J* = 7.0 Hz, 1H), 1.76 (s, 1H), 1.63 (s, 1H), 1.56 (p, *J* = 7.5 Hz, 1H), 1.35-1.21 (m, 3H), 0.99-0.91 (m, 2H), 0.80 (dt, *J* = 10 Hz, 1.5 Hz, 1H), 0.64 (d, *J* = 7.5 Hz, 3H). ¹³C[¹H] NMR (C₆D₆, 126 MHz): δ 148.9, 131.7 (q, *J* = 31.4 Hz), 129.9, 127.5 (q, *J* = 273 Hz), 115.3, 113.0, 109.2, 59.3, 43.9, 43.3, 42.5, 33.0, 29.1, 27.1, 14.6. ¹⁹F NMR (C₆D₆, 470 MHz): δ -62.8. Anal. Calc'd. for C₁₅H₁₈F₃N: C, 66.90; H, 6.74; N, 5.20; found, C, 67.14; H, 7.06; N, 4.95.

Preparation of syn-exo-3-methyl-endo-2-(2,4-dimethylanilino)norbornane



Prepared according to procedure 2 using 3-methylbicyclo[2.2.1]heptan-2-amine (0.069 g; 0.55 mmol), 1-bromo-2,4-dimethylbenzene (0.0925 g; 0.050 mmol), NaOtBu (0.067 g; 0.70 mmol), Chloro[2-(dicyclohexylphosphino)-3,6-dimethoxy-2',4',6'-triisopropyl-1,1'-biphenyl][2-(2-aminoethyl)phenyl]palladium(II) (0.0200 g; 0.025 mmol) and 2-(Dicyclohexylphosphino)3,6-dimethoxy-2',4',6'-triisopropyl-1,1'-biphenyl (0.0134 g; 0.025 mmol). Collected 0.033 g; 29%. ^1H NMR (C_6D_6 , 500 MHz): δ 7.04 (d, $J = 8.5$ Hz, 1H), 6.87 (s, 1H), 6.58 (d, $J = 8.5$ Hz, 1H), 3.29 (s, 1H), 3.22, (t, $J = 6.5$ Hz, 1H), 2.26 (s, 3H), 2.04 (s, 1H), 1.95 (s, 3H), 1.74-1.71 (m, 2H), 1.47 (dt, $J = 10.0, 2.0$ Hz, 1H), 1.36-1.33 (m, 2H), 1.09-1.06 (m, 2H), 0.88 (dt, $J = 10.0, 1.5$ Hz, 1H), 0.84 (d, $J = 7.5$ Hz, 3H). ^{13}C [1H] NMR (CDCl_3 , 126 MHz): δ 144.0, 130.8, 127.3, 125.1, 121.3, 109.9, 59.3, 43.7, 42.9, 42.0, 32.8, 29.1, 26.9, 20.3, 17.4, 14.4. HRMS (EI $^+$) m/z calc'd for $\text{C}_{16}\text{H}_{23}\text{N}$ for [M+]: 229.1831, found 229.1839.

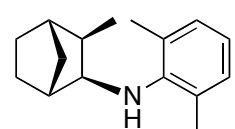
Preparation of syn-exo-3-methyl-endo-2-(4-methoxyanilino)norbornane



Prepared according to procedure 2 using 3-methylbicyclo[2.2.1]heptan-2-amine (0.150 g; 1.20 mmol), 4-bromoanisole (0.187 g; 1.00 mmol), NaOtBu (0.135 g; 1.40 mmol), Chloro[2-(dicyclohexylphosphino)-3,6-dimethoxy-2',4',6'-triisopropyl-1,1'-biphenyl][2-(2-aminoethyl)phenyl]palladium(II) (0.0399 g; 0.050 mmol) and 2-(Dicyclohexylphosphino)3,6-dimethoxy-2',4',6'-triisopropyl-1,1'-biphenyl (0.0268 g; 0.050 mmol). Collected 0.034 g; 16%. ^1H NMR (C_6D_6 , 500 MHz): δ 6.84 (d, $J = 9.0$ Hz, 2H), 6.42 (d, $J = 9.0$ Hz, 2H), 3.43 (s, 3H), 3.15 (bs, 1H), 3.10 (d, $J = 7.5$ Hz, 1H), 1.95 (s, 1H), 1.71-1.68 (m, 2H), 1.40-1.33 (m, 3H), 1.07-1.04 (m, 2H), 0.86 (d, $J = 9.5$ Hz, 1H), 0.82 (d, $J = 7.5$ Hz, 3H).

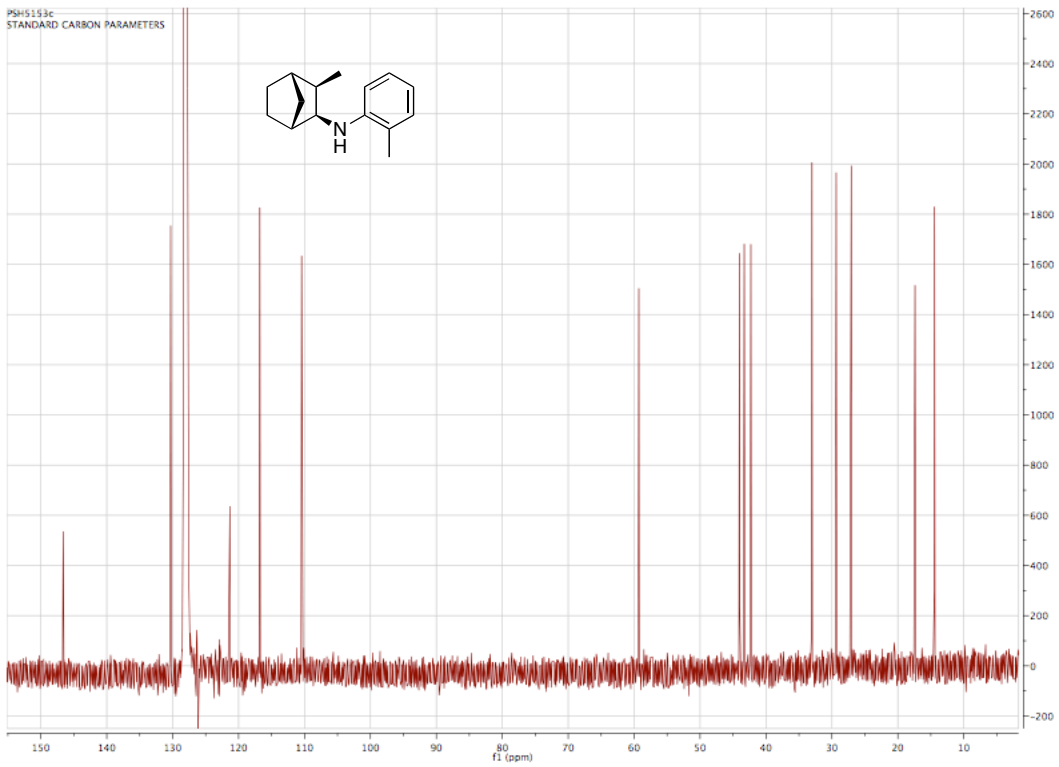
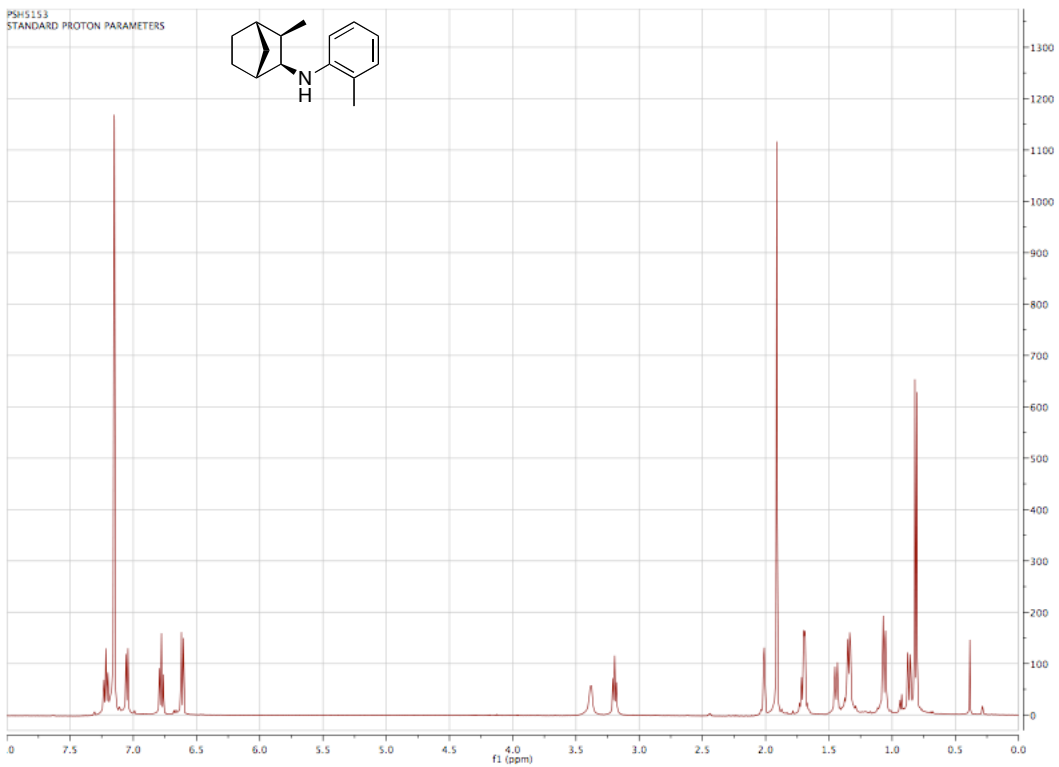
$^{13}\text{C}[\text{H}]$ NMR (C_6D_6 , 126 MHz): δ 152.3, 143.3, 115.2, 114.0, 60.3, 55.4, 44.1, 43.3, 42.6, 33.0, 29.3, 27.3, 14.8. HRMS (EI $^+$) m/z calc'd for $\text{C}_{16}\text{H}_{21}\text{NO}$ for [M+]: 231.1623, found 231.1617.

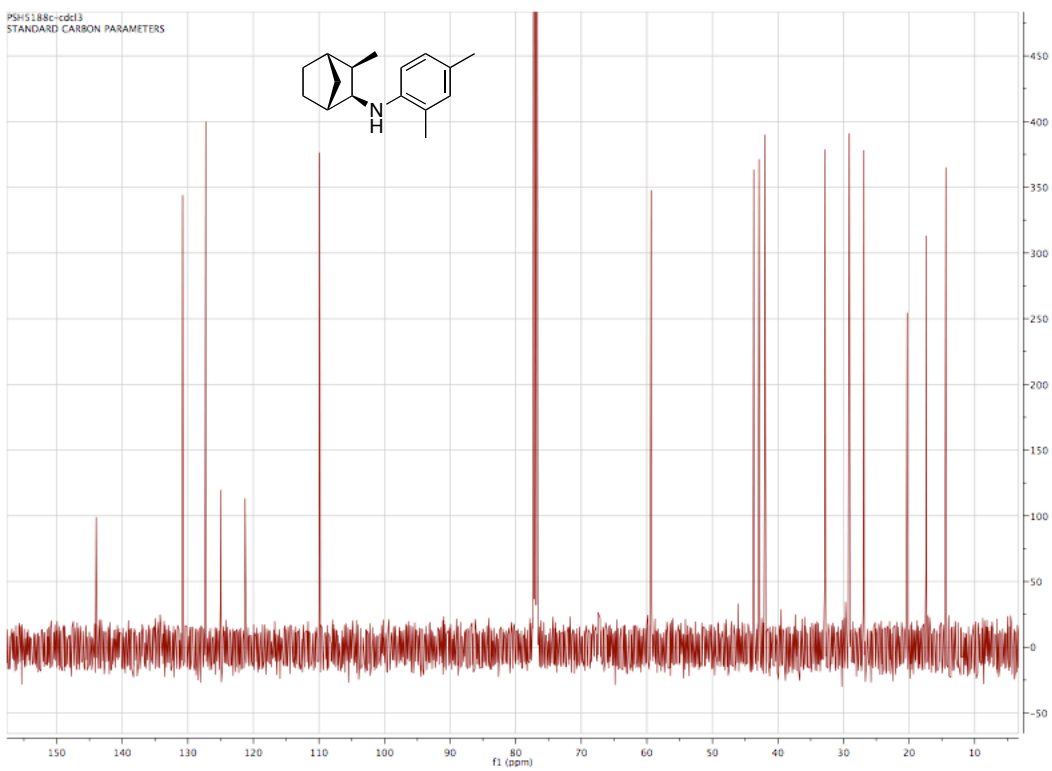
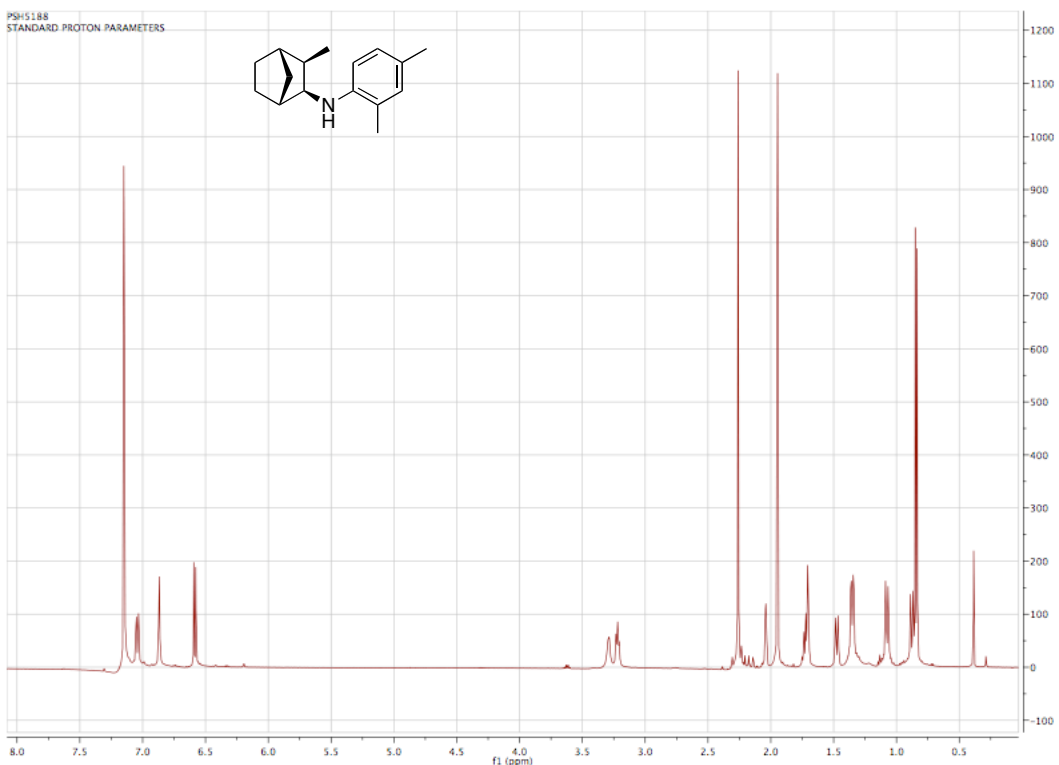
Preparation of syn-exo-3-methyl-endo-2-(2,6-dimethylanilino)norbornane

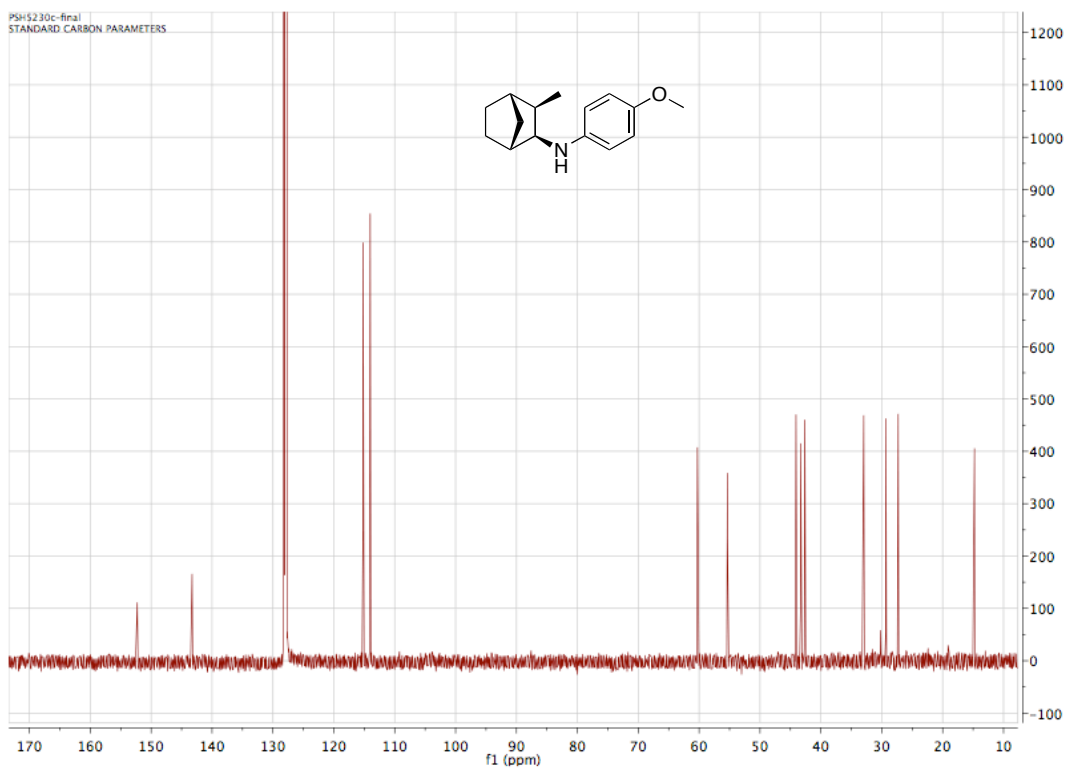
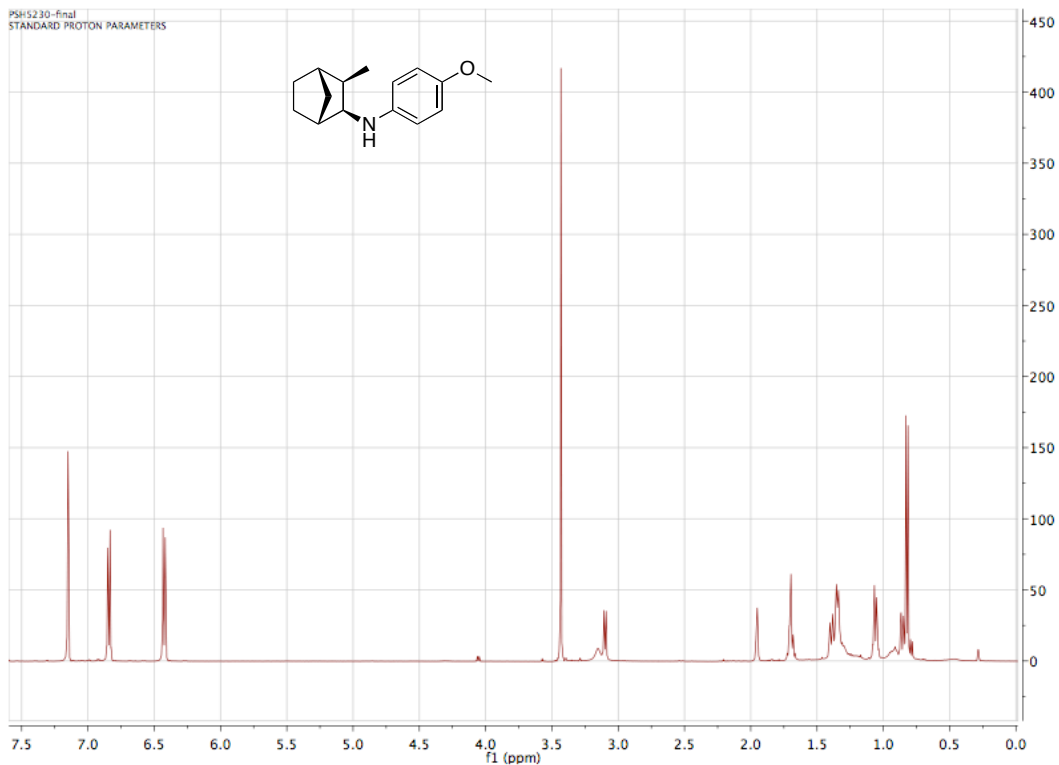


Prepared according to procedure 2 using 3-methylbicyclo[2.2.1]heptan-2-amine (0.150 g; 1.20 mmol), 1-bromo-2,6-dimethylbenzene (0.185 g; 1.00 mmol), NaOtBu (0.135 g; 1.40 mmol), Chloro[2-(dicyclohexylphosphino)-3,6-dimethoxy-2',4',6'-triisopropyl-1,1'-biphenyl][2-(2-aminoethyl)phenyl]palladium(II) (0.0399 g; 0.050 mmol) and 2-(Dicyclohexylphosphino)3,6-dimethoxy-2',4',6'-triisopropyl-1,1'-biphenyl (0.0268 g; 0.050 mmol). This compound could not be cleanly isolated; GCMS indicated the major product of this reaction has an M/Z of 229. The aryl resonances and methyl groups in ^1H NMR spectrum of the crude product in benzene- d_6 matched those of the product formed from the reductive elimination of **2e**. ^1H NMR (C_6D_6 , 500 MHz): δ 7.01 (d, J = 7.5 Hz, 2H), 6.87 (d, J = 7.5 Hz, 1H), 2.18 (s, 6H), 1.04 (d, J = 6.0 Hz, 3H). ^1H and ^{13}C NMR spectrum of the same material was collected in CDCl_3 and included below. ^{13}C NMR [^1H] (101 MHz, CDCl_3) δ 146.33, 128.94, 127.99, 120.48, 63.33, 43.64, 42.51, 41.66, 32.32, 29.21, 26.91, 19.17, 15.05.

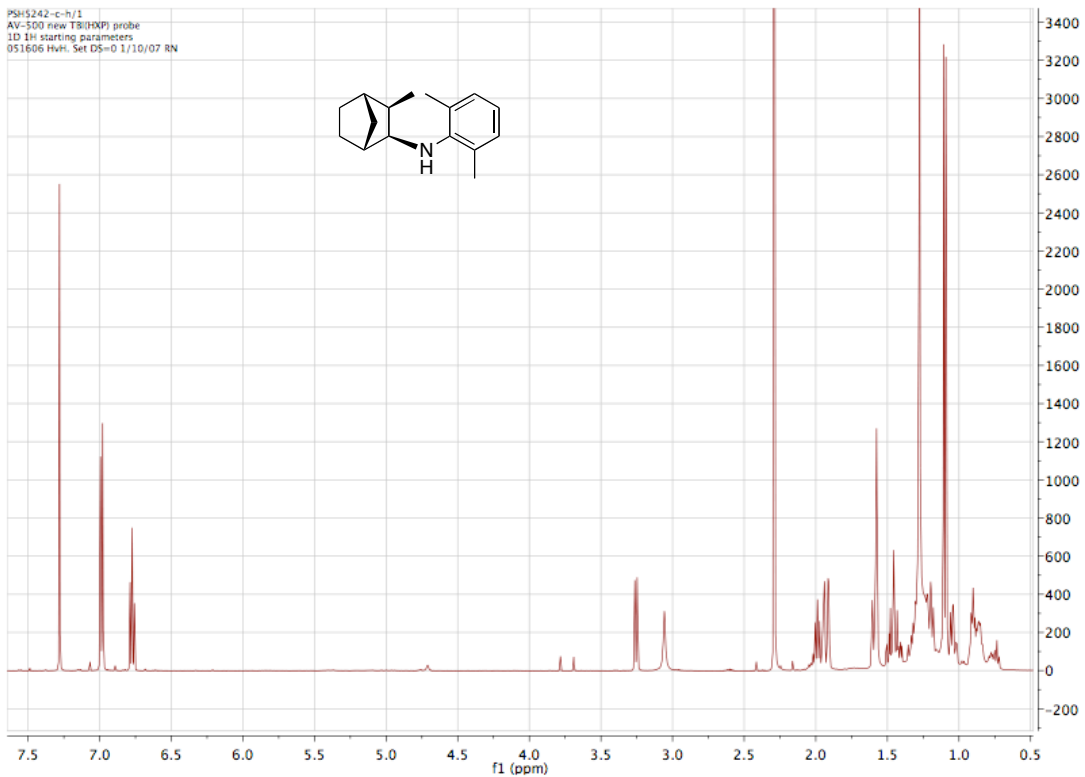
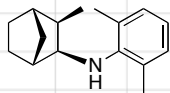
NMR Spectra for Norbornylamine Products



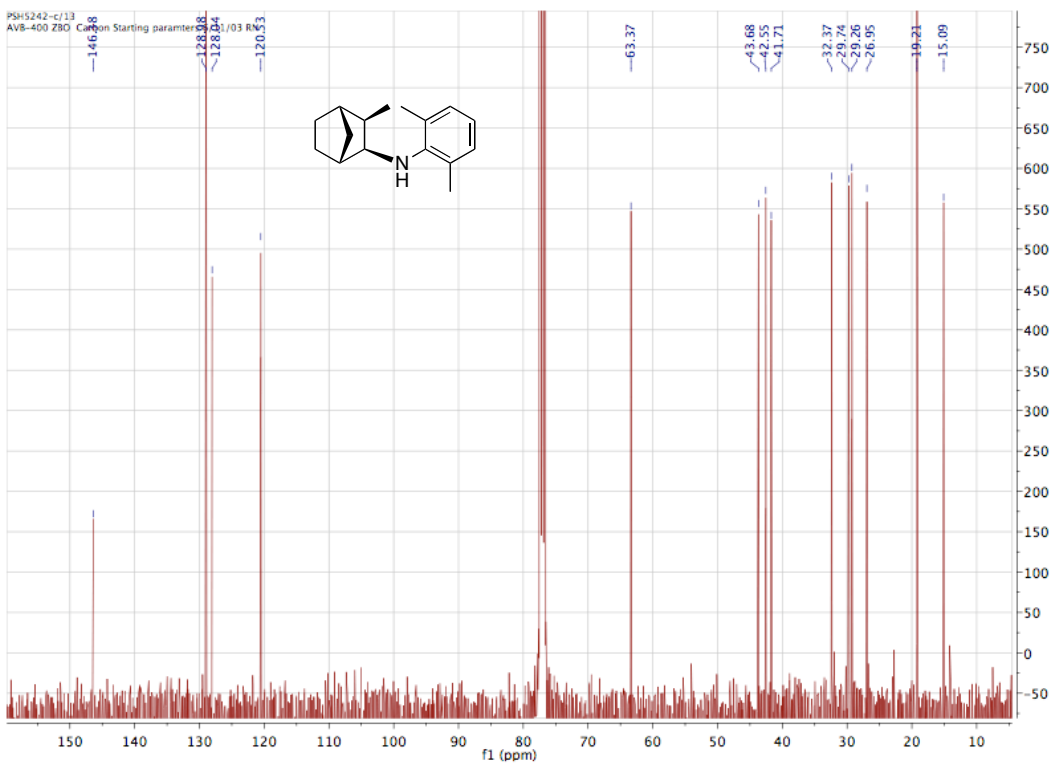
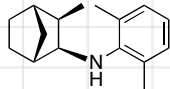




PSI5242-c-h/1
AV8-400 new TSP(exp) probe
1D 1H starting parameters:
05.1606 HvrL Set DS=0 1/10/07 RN



PSI5242-c/13
AV8-400 ZBO Carbon Starting parameter
05.1606 HvrL Set DS=0 1/10/07 RN

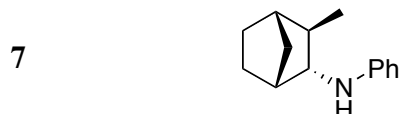


4.4.6 Computational Details

Computations of the relative ground state free energies of the norbornylamine products were conducted with density functional theory with the Gaussian 09 package.²⁷ The B3LYP functional with polarized triple- basis sets was used.



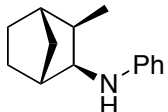
C	-2.200749	1.8111536	-0.270478	C	-1.175489	1.024110	0.576922
C	-0.728934	-0.216805	-0.256311	C	-1.971149	-1.166495	-0.163267
C	-3.005536	-0.308267	0.613388	C	-3.467948	0.896927	-0.237243
C	-2.086712	0.381496	1.643371	H	-1.839049	1.992389	-1.286924
H	-2.405321	2.787430	0.176734	H	-0.339160	1.621691	0.940079
H	-0.561178	0.075075	-1.297694	H	-3.827830	-0.900579	1.020266
H	-4.304501	1.402937	0.251659	H	-3.810400	0.609385	-1.232908
H	-1.564222	-0.322666	2.297628	H	-2.603485	1.115334	2.267992
H	-1.698454	-2.000996	0.495775	C	-2.415093	-1.768112	-1.495549
H	-1.610585	-2.370855	-1.926076	H	-2.678055	-0.999688	-2.227285
H	-3.285996	-2.417822	-1.365767	N	0.470076	-0.895450	0.203918
H	0.339502	-1.528231	0.978211	C	1.756462	-0.390419	0.074265
C	2.062691	0.717429	-0.736222	C	3.380506	1.147161	-0.874942
C	4.422269	0.506059	-0.211790	C	4.123869	-0.587581	0.602861
C	2.817466	-1.030772	0.745386	H	1.275631	1.246657	-1.257516
H	3.588213	2.002675	-1.509027	H	5.443554	0.850003	-0.322401
H	4.918154	-1.102813	1.132561	H	2.602723	-1.889381	1.374914



C	-3.151942	-0.892169	-1.001991	C	-2.904007	0.568874	-0.561939
C	-1.389182	0.878352	-0.697909	C	-0.770467	0.091264	0.528031
C	-2.001066	-0.634168	1.132767	C	-2.525619	-1.721168	0.165733
C	-3.079144	0.455751	0.969619	C	-1.068690	2.375689	-0.699817
H	-2.693509	-1.111149	-1.969943	H	-4.222035	-1.094733	-1.096726
H	-3.544175	1.294543	-1.067929	H	-1.000481	0.443131	-1.624546

H	-1.816963	-0.996429	2.145068	H	-3.282760	-2.327731	0.668866
H	-1.753522	-2.419403	-0.167435	H	-2.848724	1.377815	1.509402
H	-4.077258	0.120921	1.264782	H	-1.536799	2.874100	-1.554285
H	0.008465	2.548631	-0.763904	H	-1.432772	2.867027	0.208361
N	0.337438	-0.800247	0.246115	H	0.096016	-1.614460	-0.297487
H	-0.423264	0.812012	1.272287	C	1.668349	-0.420875	0.124825
C	2.164747	0.818856	0.566261	C	3.522466	1.113323	0.466987
C	4.422203	0.201174	-0.076130	C	3.936769	-1.028872	-0.522022
C	2.587876	-1.337182	-0.425010	H	1.496111	1.556657	0.989081
H	3.875180	2.077499	0.817868	H	5.475779	0.441018	-0.153039
H	4.616204	-1.757965	-0.950665	H	2.228684	-2.302846	-0.768997

8



C	3.644953	0.323905	0.841331	C	2.896864	0.665812	-0.466016
C	1.454103	1.125491	-0.114011	C	0.758246	-0.233789	0.328954
C	1.910921	-1.259171	0.188270	C	2.944279	-0.992154	1.307424
C	2.657339	-0.738882	-1.058408	C	0.764361	1.853988	-1.268937
N	-0.388817	-0.627678	-0.477981	H	3.570466	1.126918	1.578850
H	4.707991	0.156206	0.648745	H	3.427185	1.373024	-1.106659
H	1.487062	1.804353	0.745148	H	0.438760	-0.171054	1.374393
H	1.556083	-2.291959	0.160558	H	3.656300	-1.818606	1.370989
H	2.470172	-0.897125	2.287445	H	2.048838	-0.733424	-1.965871
H	3.583210	-1.283698	-1.263328	H	1.296661	2.783440	-1.492566
H	-0.269343	2.107998	-1.026067	H	0.743243	1.248791	-2.177841
H	-0.263408	-1.463486	-1.027596	C	-1.703465	-0.342070	-0.146997
C	-2.047535	0.659465	0.779272	C	-3.384420	0.924227	1.068140
C	-4.409771	0.216194	0.448866	C	-4.075167	-0.774784	-0.475794
C	-2.748673	-1.053033	-0.770428	H	-1.273787	1.239714	1.265701
H	-3.621172	1.701822	1.786728	H	-5.446732	0.430365	0.677729
H	-4.856925	-1.340885	-0.971087	H	-2.505094	-1.829848	-1.489400

Computations of the alkylpalladium amido complex **4.07** were conducted at the Department of Chemistry and Center for Advanced Scientific Computing and Modeling, University of North Texas, Denton, TX, 76203. The Dipp substituents of SIPr and the methyl groups of the anilido ligand were modeled with the UFF force field,²⁸ while the remainder of the complex was modeled with the M06 functional in conjunction with the 6-311++G(d,p) basis set for main group atoms and the Stevens pseudopotentials and valence basis sets²⁹ for palladium. QM/MM calculations employed the ONION formalism.³⁰ Initial conformational searches were performed at a lower level of theory to identify the lowest energy conformations of the various stationary points.

Ground State **4.07**

Pd	-0.117956000	-0.717837000	-0.061356000
C	0.612173000	1.152437000	0.403411000
N	1.780641000	1.508566000	0.977118000
N	-0.143898000	2.263132000	0.387900000
N	-1.110248000	-2.518259000	-0.306032000
H	-0.796102000	-3.203971000	0.373901000
C	0.517184000	3.460334000	0.913511000
H	-0.113030000	3.991500000	1.631370000
H	0.778400000	4.154641000	0.106903000
C	1.758946000	2.856985000	1.564210000
H	2.661931000	3.425485000	1.333955000
H	1.659329000	2.804568000	2.655477000
C	-1.445239000	2.286507000	-0.154595000
C	-2.560345000	2.020482000	0.683627000
C	-1.644546000	2.632723000	-1.518059000
C	-3.852915000	2.060063000	0.131009000
C	-2.957843000	2.691877000	-2.019275000
C	-4.046541000	2.400084000	-1.203863000
H	-4.721315000	1.839559000	0.737791000
H	-3.145308000	2.968867000	-3.048148000
H	-5.049498000	2.439408000	-1.609171000
C	2.760906000	0.560153000	1.343246000
C	2.538234000	-0.323270000	2.438267000
C	4.007033000	0.541109000	0.657270000
C	3.531469000	-1.265732000	2.762425000
C	4.977133000	-0.405169000	1.034034000
C	4.730112000	-1.311256000	2.059302000
H	3.387793000	-1.962171000	3.577944000
H	5.940008000	-0.437523000	0.542397000
H	5.486590000	-2.036058000	2.331309000

C	1.287561000	-0.236296000	3.311761000
C	1.650393000	0.104017000	4.762855000
C	0.457018000	-1.522870000	3.243047000
H	0.625188000	0.579658000	2.970366000
H	2.266075000	1.028446000	4.793783000
H	0.726453000	0.284571000	5.353083000
H	2.216023000	-0.722251000	5.242584000
H	0.126307000	-1.702895000	2.200865000
H	1.037253000	-2.400432000	3.597086000
H	-0.451839000	-1.424820000	3.874092000
C	-2.389761000	1.724002000	2.170737000
C	-2.811429000	0.289715000	2.499013000
C	-3.152526000	2.736108000	3.034998000
H	-1.326651000	1.813516000	2.468224000
H	-2.186640000	-0.420011000	1.919994000
H	-2.653986000	0.081453000	3.578678000
H	-3.881190000	0.117795000	2.256236000
H	-2.854133000	3.770698000	2.760874000
H	-4.250476000	2.631090000	2.908420000
H	-2.908630000	2.578567000	4.107452000
C	-0.476419000	2.982310000	-2.435825000
C	-0.500474000	4.471214000	-2.799795000
C	-0.468705000	2.115006000	-3.700383000
H	0.490867000	2.790504000	-1.927391000
H	-0.494858000	5.089834000	-1.877283000
H	0.398708000	4.731528000	-3.398118000
H	-1.405736000	4.723138000	-3.392202000
H	-0.553756000	1.047140000	-3.424838000
H	-1.308476000	2.375290000	-4.378248000
H	0.484297000	2.257767000	-4.253399000
C	4.346044000	1.571256000	-0.419395000
C	4.807225000	0.919699000	-1.730481000
C	5.410845000	2.548247000	0.093946000
H	3.450520000	2.174145000	-0.677014000
H	4.047031000	0.204756000	-2.093400000
H	4.940491000	1.697829000	-2.512142000
H	5.772119000	0.385868000	-1.606660000
H	5.075988000	3.017915000	1.042943000
H	6.374505000	2.026711000	0.276973000
H	5.579936000	3.354722000	-0.651218000
C	-2.457614000	-2.242534000	-0.218767000
C	-2.990395000	-1.352859000	-1.182566000
C	-3.372662000	-2.762976000	0.737105000
C	-4.322231000	-0.998192000	-1.209792000
H	-2.309849000	-0.969011000	-1.939601000
C	-4.713569000	-2.387574000	0.689034000
C	-5.212823000	-1.502656000	-0.263264000
H	-4.659932000	-0.324977000	-1.994771000
H	-5.402874000	-2.787833000	1.431800000
C	-2.899589000	-3.696120000	1.823082000
H	-2.475326000	-4.616215000	1.369242000
H	-2.122411000	-3.193724000	2.436381000
H	-3.727979000	-3.997043000	2.499060000
C	-6.660159000	-1.106877000	-0.252784000
H	-6.889465000	-0.393087000	-1.072504000
H	-7.295181000	-2.008615000	-0.380202000

H	-6.905829000	-0.621536000	0.715254000
C	1.351511000	-1.172442000	-1.478015000
C	0.740283000	-1.572165000	-2.824956000
C	2.357849000	-2.308406000	-1.168331000
H	1.839555000	-0.197507000	-1.545362000
C	0.827807000	-3.096367000	-2.815824000
C	1.803623000	-1.223198000	-3.884330000
H	-0.249099000	-1.163787000	-3.029853000
C	2.320311000	-3.120208000	-2.480729000
H	3.356036000	-1.869666000	-1.022971000
H	0.609661000	-3.533048000	-3.797881000
H	0.169918000	-3.538785000	-2.064606000
H	1.379785000	-1.333740000	-4.889506000
H	2.162989000	-0.192043000	-3.795441000
C	2.906293000	-2.281567000	-3.622394000
H	2.780541000	-4.108323000	-2.371922000
H	3.071302000	-2.903049000	-4.509378000
H	3.874086000	-1.841517000	-3.356978000
C	2.080685000	-3.214569000	0.021049000
H	2.932692000	-3.884470000	0.185900000
H	1.195804000	-3.834762000	-0.147277000
H	1.912756000	-2.643831000	0.935508000

Transition State 4.07

Pd	-0.355200000	0.239651000	-0.336865000
C	1.432038000	0.639396000	0.621613000
N	2.288925000	-0.045013000	1.408738000
N	1.727907000	1.940214000	0.828407000
N	-2.283108000	0.199326000	-1.046902000
C	2.889022000	2.182884000	1.688333000
C	3.115049000	0.793519000	2.284797000
C	1.100371000	2.959094000	0.082959000
C	1.539800000	3.255249000	-1.236138000
C	0.026052000	3.688334000	0.655962000
C	0.882677000	4.266404000	-1.960814000
C	-0.584504000	4.707860000	-0.096584000
C	-0.163403000	4.986405000	-1.392776000
C	2.410279000	-1.448608000	1.368231000
C	3.373460000	-2.047546000	0.511698000
C	1.598991000	-2.261382000	2.205087000
C	3.469766000	-3.450157000	0.470584000
C	1.758878000	-3.658691000	2.158503000
C	2.671254000	-4.243762000	1.286996000
C	4.325547000	-1.208362000	-0.336738000
C	4.103997000	-1.450283000	-1.832716000
C	5.786575000	-1.467015000	0.051861000
C	2.702559000	2.508407000	-1.883285000
C	3.836134000	3.465465000	-2.271982000
C	2.229012000	1.692071000	-3.089936000
C	-0.484001000	3.386202000	2.061339000
C	-1.970851000	3.010567000	2.043114000
C	-0.227663000	4.567992000	3.003099000
C	0.570127000	-1.658135000	3.154804000
C	1.015360000	-1.829193000	4.610923000

C	-0.824167000	-2.263667000	2.936341000
C	-3.454548000	0.007008000	-0.342503000
C	-3.340116000	-0.296897000	1.025200000
C	-4.759304000	0.072176000	-0.889575000
C	-4.438444000	-0.535719000	1.822881000
C	-5.857784000	-0.146951000	-0.058322000
C	-5.724688000	-0.460717000	1.290910000
C	-4.986343000	0.393923000	-2.345748000
C	-6.941457000	-0.700812000	2.136594000
C	-1.478432000	-1.668345000	-1.350467000
C	-0.240316000	-2.560400000	-1.080528000
C	-1.737795000	-1.861676000	-2.861716000
C	0.469386000	-2.616722000	-2.427725000
C	-0.808302000	-3.988324000	-0.986146000
C	-0.787961000	-3.029352000	-3.196568000
C	-1.233990000	-4.286732000	-2.442590000
C	-1.441110000	-0.666857000	-3.770747000
H	-2.401292000	0.493053000	-2.005315000
H	2.678843000	2.931495000	2.456593000
H	3.753611000	2.525903000	1.105390000
H	4.168272000	0.500595000	2.271859000
H	2.758146000	0.735252000	3.320384000
H	1.184478000	4.507585000	-2.971556000
H	-1.399024000	5.287912000	0.316925000
H	-0.651434000	5.767339000	-1.961736000
H	4.182148000	-3.936634000	-0.182568000
H	1.169107000	-4.305075000	2.794571000
H	2.769527000	-5.321189000	1.253475000
H	4.151400000	-0.127690000	-0.169997000
H	4.779554000	-0.799839000	-2.428426000
H	4.298616000	-2.508366000	-2.106693000
H	3.060787000	-1.191522000	-2.100141000
H	6.093031000	-2.504789000	-0.197074000
H	6.454273000	-0.764588000	-0.491452000
H	5.924766000	-1.302060000	1.141897000
H	3.146775000	1.784028000	-1.174772000
H	4.715448000	2.886685000	-2.627474000
H	3.522575000	4.157125000	-3.081803000
H	4.148910000	4.061897000	-1.388257000
H	1.448710000	0.971848000	-2.768009000
H	1.812810000	2.347735000	-3.883466000
H	3.076318000	1.114447000	-3.517030000
H	0.050023000	2.514337000	2.493592000
H	-2.150542000	2.224623000	1.282168000
H	-2.276250000	2.614854000	3.035296000
H	-2.607916000	3.887894000	1.803845000
H	-0.533224000	4.302824000	4.037793000
H	0.855041000	4.816752000	3.013786000
H	-0.798589000	5.466029000	2.685182000
H	0.467752000	-0.567456000	2.976668000
H	0.293492000	-1.328902000	5.291294000
H	1.076998000	-2.903730000	4.885932000
H	2.013094000	-1.363911000	4.760214000
H	-0.874087000	-3.311720000	3.298737000
H	-1.584602000	-1.671507000	3.488892000
H	-1.083653000	-2.251859000	1.857656000

H	-2.336331000	-0.292930000	1.442315000
H	-4.274515000	-0.762874000	2.873586000
H	-6.860815000	-0.082387000	-0.477412000
H	-4.536703000	1.379212000	-2.589901000
H	-4.528676000	-0.392948000	-2.978403000
H	-6.067868000	0.442014000	-2.594167000
H	-7.520283000	-1.553804000	1.723984000
H	-6.664398000	-0.937202000	3.186015000
H	-7.581224000	0.206707000	2.136460000
H	-2.303229000	-1.997685000	-0.718203000
H	0.355058000	-2.277341000	-0.219838000
H	-2.783603000	-2.165109000	-3.011456000
H	0.874438000	-1.653445000	-2.745834000
H	1.264038000	-3.371210000	-2.457271000
H	-0.017088000	-4.671379000	-0.653314000
H	-1.629139000	-4.064959000	-0.266403000
H	-0.673191000	-3.175258000	-4.274993000
H	-0.727287000	-5.176007000	-2.832275000
H	-2.311948000	-4.457400000	-2.542818000
H	-0.583560000	-0.087710000	-3.417188000
H	-1.222831000	-1.013175000	-4.786469000
H	-2.288555000	0.020001000	-3.858062000

4.4.7 Crystallographic Data for 4.01

Table 4.3. Crystal data and structure refinement for 4.01.

Identification code	4.01
Empirical formula	C ₄₀ H ₆₃ ClN ₂ Pd
Formula weight	713.77
Temperature	193(2) K
Wavelength	1.54178 Å
Crystal system	Orthorhombic
Space group	P 21 21 21
Unit cell dimensions	a = 9.7615(3) Å b = 13.4772(5) Å c = 29.0572(13) Å
Volume	3822.7(3) Å ³
Z	4
Density (calculated)	1.240 Mg/m ³
Absorption coefficient	4.753 mm ⁻¹
F(000)	1520
Crystal size	0.42 x 0.134 x 0.045 mm ³
Theta range for data collection	4.47 to 67.54°
Index ranges	-11<=h<=11, -16<=k<=15, -20<=l<=34
Reflections collected	30073
Independent reflections	6751 [R(int) = 0.1238]
Completeness to theta = 67.54°	99.1 %
Absorption correction	Integration
Max. and min. transmission	0.8439 and 0.3790
Refinement method	Full-matrix least-squares on F ²
Data / restraints / parameters	6751 / 364 / 457
Goodness-of-fit on F ²	1.058
Final R indices [I>2sigma(I)]	R1 = 0.0586, wR2 = 0.1453
R indices (all data)	R1 = 0.0694, wR2 = 0.1540
Absolute structure parameter	0.444(9)
Largest diff. peak and hole	0.709 and -1.677 e.Å ⁻³

Table 4.4. Atomic coordinates ($\times 10^4$) and equivalent isotropic displacement parameters ($\text{\AA}^2 \times 10^3$) for **4.01**. U(eq) is defined as one third of the trace of the orthogonalized U^{ij} tensor.

	x	y	z	U(eq)
Pd(1)	9133(1)	7726(1)	8314(1)	47(1)
Cl(1)	11371(1)	7484(1)	8052(1)	71(1)
N(1)	6269(3)	7114(2)	8256(2)	54(1)
N(2)	6368(3)	8692(2)	8426(1)	50(1)
C(1)	9213(5)	8010(3)	8994(2)	57(1)
C(2)	9890(5)	7122(4)	9244(2)	70(1)
C(3)	9462(6)	7227(5)	9759(2)	86(2)
C(4)	10282(6)	8122(5)	9925(2)	83(2)
C(5)	11089(5)	8436(4)	9492(2)	75(1)
C(6)	10096(5)	8928(4)	9139(2)	60(1)
C(7)	11369(5)	7433(4)	9265(2)	70(1)
C(8)	10837(6)	9498(4)	8785(2)	70(2)
C(1B)	9198(10)	7643(6)	9007(2)	64(2)
C(2B)	9990(9)	8482(7)	9256(3)	67(2)
C(3B)	9586(13)	8412(9)	9774(3)	79(2)
C(4B)	10337(15)	7489(9)	9946(3)	79(2)
C(5B)	11027(10)	7091(6)	9504(3)	72(2)
C(6B)	9925(10)	6671(6)	9169(4)	68(2)
C(7B)	11421(9)	8063(8)	9266(5)	71(2)
C(8B)	10500(20)	5970(10)	8832(5)	72(5)
C(9)	7120(3)	7869(3)	8354(2)	43(1)
C(10)	4829(4)	7454(3)	8233(2)	69(2)
C(11)	4929(4)	8540(3)	8336(2)	61(1)
C(12)	6643(4)	6129(3)	8128(2)	54(1)
C(13)	6569(5)	5364(3)	8442(2)	61(2)
C(14)	6876(5)	4414(3)	8305(2)	72(2)
C(15)	7263(5)	4219(4)	7861(2)	69(2)
C(16)	7326(5)	4963(4)	7555(2)	66(2)
C(17)	6993(5)	5952(3)	7663(2)	59(1)
C(18)	6104(6)	5552(4)	8937(2)	70(2)
C(19)	7052(7)	5051(5)	9284(3)	95(2)
C(20)	4614(6)	5182(6)	9001(3)	88(2)
C(21)	7010(3)	6759(4)	7304(2)	66(2)
C(22)	5660(8)	6850(30)	7030(4)	91(5)
C(23)	8241(8)	7098(18)	7010(5)	70(5)
C(22B)	6062(6)	6526(6)	6892(2)	85(2)
C(23B)	8494(5)	6912(6)	7137(3)	78(2)
C(24)	6911(4)	9683(3)	8450(2)	50(1)
C(25)	7529(4)	10107(3)	8058(2)	53(1)
C(26)	7986(5)	11085(3)	8091(2)	63(1)
C(27)	7838(5)	11628(4)	8486(2)	69(2)
C(28)	7210(5)	11209(4)	8862(2)	68(2)
C(29)	6702(5)	10220(3)	8857(2)	59(1)
C(30)	7690(5)	9555(3)	7590(2)	61(1)
C(31)	9138(5)	9641(4)	7406(2)	68(1)
C(32)	6662(5)	9956(5)	7247(2)	77(2)
C(33)	5987(5)	9795(4)	9271(2)	64(1)
C(34)	6753(7)	9970(5)	9722(2)	86(2)

Table 4.4. (cont.)

C(35)	4603(6)	10251(5)	9318(2)	87(2)
-------	---------	----------	---------	-------

Table 4.5. Bond lengths [\AA] and angles [$^\circ$] for **4.01**.

Pd(1)-C(9)	1.978(3)	C(8)-H(8C)	0.9800
Pd(1)-C(1)	2.014(4)	C(1B)-C(2B)	1.549(9)
Pd(1)-C(1B)	2.016(7)	C(1B)-C(6B)	1.564(9)
Pd(1)-Cl(1)	2.3364(11)	C(1B)-H(1B)	1.0000
N(1)-C(9)	1.344(5)	C(2B)-C(7B)	1.506(10)
N(1)-C(12)	1.426(6)	C(2B)-C(3B)	1.559(10)
N(1)-C(10)	1.480(5)	C(2B)-H(2B)	1.0000
N(2)-C(9)	1.346(5)	C(3B)-C(4B)	1.528(11)
N(2)-C(24)	1.439(5)	C(3B)-H(3C)	0.9900
N(2)-C(11)	1.443(5)	C(3B)-H(3D)	0.9900
C(1)-C(2)	1.549(7)	C(4B)-C(5B)	1.544(10)
C(1)-C(6)	1.565(6)	C(4B)-H(4C)	0.9900
C(1)-H(1A)	1.0000	C(4B)-H(4D)	0.9900
C(2)-C(7)	1.504(7)	C(5B)-C(7B)	1.530(10)
C(2)-C(3)	1.560(7)	C(5B)-C(6B)	1.557(10)
C(2)-H(2A)	1.0000	C(5B)-H(5B)	1.0000
C(3)-C(4)	1.526(9)	C(6B)-C(8B)	1.474(11)
C(3)-H(3A)	0.9900	C(6B)-H(6B)	1.0000
C(3)-H(3B)	0.9900	C(7B)-H(7C)	0.9900
C(4)-C(5)	1.544(7)	C(7B)-H(7D)	0.9900
C(4)-H(4A)	0.9900	C(8B)-H(8D)	0.9800
C(4)-H(4B)	0.9900	C(8B)-H(8E)	0.9800
C(5)-C(7)	1.530(7)	C(8B)-H(8F)	0.9800
C(5)-C(6)	1.561(7)	C(10)-C(11)	1.497(6)
C(5)-H(5A)	1.0000	C(10)-H(10A)	0.9900
C(6)-C(8)	1.472(8)	C(10)-H(10B)	0.9900
C(6)-H(6A)	1.0000	C(11)-H(11A)	0.9900
C(7)-H(7A)	0.9900	C(11)-H(11B)	0.9900
C(7)-H(7B)	0.9900	C(12)-C(13)	1.379(7)
C(8)-H(8A)	0.9800	C(12)-C(17)	1.413(8)
C(8)-H(8B)	0.9800	C(22B)-H(22D)	0.9800
C(13)-C(14)	1.373(7)	C(22B)-H(22E)	0.9800
C(13)-C(18)	1.529(8)	C(22B)-H(22F)	0.9800
C(14)-C(15)	1.371(9)	C(23B)-H(23D)	0.9800
C(14)-H(14A)	0.9500	C(23B)-H(23E)	0.9800
C(15)-C(16)	1.340(8)	C(23B)-H(23F)	0.9800
C(15)-H(15A)	0.9500	C(24)-C(29)	1.401(7)
C(16)-C(17)	1.407(7)	C(24)-C(25)	1.411(7)
C(16)-H(16A)	0.9500	C(25)-C(26)	1.396(6)
C(17)-C(21)	1.507(8)	C(25)-C(30)	1.556(8)
C(18)-C(19)	1.526(9)	C(26)-C(27)	1.369(8)
C(18)-C(20)	1.549(8)	C(26)-H(26A)	0.9500
C(18)-H(18A)	1.0000	C(27)-C(28)	1.374(8)
C(19)-H(19A)	0.9800	C(27)-H(27A)	0.9500
C(19)-H(19B)	0.9800	C(28)-C(29)	1.423(7)
C(19)-H(19C)	0.9800	C(28)-H(28A)	0.9500
C(20)-H(20A)	0.9800	C(29)-C(33)	1.503(8)
C(20)-H(20B)	0.9800	C(30)-C(32)	1.516(8)
C(20)-H(20C)	0.9800	C(30)-C(31)	1.516(7)
C(21)-C(23B)	1.542(6)	C(30)-H(30A)	1.0000
C(21)-C(22)	1.543(8)	C(31)-H(31A)	0.9800
C(21)-C(23)	1.544(8)	C(31)-H(31B)	0.9800
C(21)-C(22B)	1.546(6)	C(31)-H(31C)	0.9800

Table 4.5. (cont.)

C(21)-H(21A)	1.0000	C(32)-H(32A)	0.9800
C(21)-H(21B)	0.9602	C(32)-H(32B)	0.9800
C(22)-H(22A)	0.9800	C(32)-H(32C)	0.9800
C(22)-H(22B)	0.9800	C(33)-C(35)	1.491(8)
C(22)-H(22C)	0.9800	C(33)-C(34)	1.526(8)
C(23)-H(23A)	0.9800	C(33)-H(33A)	1.0000
C(23)-H(23B)	0.9800	C(34)-H(34A)	0.9800
C(23)-H(23C)	0.9800	C(35)-H(35A)	0.9800
C(34)-H(34B)	0.9800	C(35)-H(35B)	0.9800
C(34)-H(34C)	0.9800	C(35)-H(35C)	0.9800
C(9)-Pd(1)-C(1)	87.89(18)	C(3)-C(4)-H(4A)	111.2
C(9)-Pd(1)-C(1B)	88.8(3)	C(5)-C(4)-H(4A)	111.2
C(1)-Pd(1)-C(1B)	14.2(3)	C(3)-C(4)-H(4B)	111.2
C(9)-Pd(1)-Cl(1)	164.07(13)	C(5)-C(4)-H(4B)	111.2
C(1)-Pd(1)-Cl(1)	108.04(14)	H(4A)-C(4)-H(4B)	109.1
C(1B)-Pd(1)-Cl(1)	106.7(3)	C(7)-C(5)-C(4)	101.6(5)
C(9)-N(1)-C(12)	127.0(3)	C(7)-C(5)-C(6)	101.6(4)
C(9)-N(1)-C(10)	111.2(3)	C(4)-C(5)-C(6)	109.6(4)
C(12)-N(1)-C(10)	121.3(3)	C(7)-C(5)-H(5A)	114.2
C(9)-N(2)-C(24)	124.9(3)	C(4)-C(5)-H(5A)	114.2
C(9)-N(2)-C(11)	112.7(3)	C(6)-C(5)-H(5A)	114.2
C(24)-N(2)-C(11)	119.9(3)	C(8)-C(6)-C(5)	112.0(4)
C(2)-C(1)-C(6)	104.5(4)	C(8)-C(6)-C(1)	119.7(4)
C(2)-C(1)-Pd(1)	109.3(3)	C(5)-C(6)-C(1)	100.6(4)
C(6)-C(1)-Pd(1)	115.8(3)	C(8)-C(6)-H(6A)	108.0
C(2)-C(1)-H(1A)	109.0	C(5)-C(6)-H(6A)	108.0
C(6)-C(1)-H(1A)	109.0	C(1)-C(6)-H(6A)	108.0
Pd(1)-C(1)-H(1A)	109.0	C(2)-C(7)-C(5)	95.3(4)
C(7)-C(2)-C(1)	102.3(4)	C(2)-C(7)-H(7A)	112.7
C(7)-C(2)-C(3)	101.2(4)	C(5)-C(7)-H(7A)	112.7
C(1)-C(2)-C(3)	105.4(4)	C(2)-C(7)-H(7B)	112.7
C(7)-C(2)-H(2A)	115.4	C(5)-C(7)-H(7B)	112.7
C(1)-C(2)-H(2A)	115.4	H(7A)-C(7)-H(7B)	110.2
C(3)-C(2)-H(2A)	115.4	C(2B)-C(1B)-C(6B)	104.1(6)
C(4)-C(3)-C(2)	103.6(5)	C(2B)-C(1B)-Pd(1)	116.2(6)
C(4)-C(3)-H(3A)	111.0	C(6B)-C(1B)-Pd(1)	111.3(6)
C(2)-C(3)-H(3A)	111.0	C(2B)-C(1B)-H(1B)	108.3
C(4)-C(3)-H(3B)	111.0	C(6B)-C(1B)-H(1B)	108.3
C(2)-C(3)-H(3B)	111.0	Pd(1)-C(1B)-H(1B)	108.3
H(3A)-C(3)-H(3B)	109.0	C(7B)-C(2B)-C(1B)	101.4(7)
C(3)-C(4)-C(5)	103.1(4)	C(2B)-C(7B)-C(5B)	95.6(6)
C(7B)-C(2B)-C(3B)	101.1(7)	C(2B)-C(7B)-H(7C)	112.6
C(1B)-C(2B)-C(3B)	106.3(7)	C(5B)-C(7B)-H(7C)	112.6
C(7B)-C(2B)-H(2B)	115.4	C(2B)-C(7B)-H(7D)	112.6
C(1B)-C(2B)-H(2B)	115.4	C(5B)-C(7B)-H(7D)	112.6
C(3B)-C(2B)-H(2B)	115.4	H(7C)-C(7B)-H(7D)	110.1
C(4B)-C(3B)-C(2B)	104.1(7)	C(6B)-C(8B)-H(8D)	109.5
C(4B)-C(3B)-H(3C)	110.9	C(6B)-C(8B)-H(8E)	109.5
C(2B)-C(3B)-H(3C)	110.9	H(8D)-C(8B)-H(8E)	109.5
C(4B)-C(3B)-H(3D)	110.9	C(6B)-C(8B)-H(8F)	109.5
C(2B)-C(3B)-H(3D)	110.9	H(8D)-C(8B)-H(8F)	109.5
H(3C)-C(3B)-H(3D)	109.0	H(8E)-C(8B)-H(8F)	109.5
C(3B)-C(4B)-C(5B)	102.7(7)	N(1)-C(9)-N(2)	108.7(3)

Table 4.5. (cont.)

C(3B)-C(4B)-H(4C)	111.2	N(1)-C(9)-Pd(1)	121.9(3)
C(5B)-C(4B)-H(4C)	111.2	N(2)-C(9)-Pd(1)	129.1(3)
C(3B)-C(4B)-H(4D)	111.2	N(1)-C(10)-C(11)	103.4(3)
C(5B)-C(4B)-H(4D)	111.2	N(1)-C(10)-H(10A)	111.1
H(4C)-C(4B)-H(4D)	109.1	C(11)-C(10)-H(10A)	111.1
C(7B)-C(5B)-C(4B)	100.9(7)	N(1)-C(10)-H(10B)	111.1
C(7B)-C(5B)-C(6B)	101.6(7)	C(11)-C(10)-H(10B)	111.1
C(4B)-C(5B)-C(6B)	110.1(8)	H(10A)-C(10)-H(10B)	109.1
C(7B)-C(5B)-H(5B)	114.2	N(2)-C(11)-C(10)	103.8(3)
C(4B)-C(5B)-H(5B)	114.2	N(2)-C(11)-H(11A)	111.0
C(6B)-C(5B)-H(5B)	114.2	C(10)-C(11)-H(11A)	111.0
C(8B)-C(6B)-C(5B)	112.7(9)	N(2)-C(11)-H(11B)	111.0
C(8B)-C(6B)-C(1B)	120.6(9)	C(10)-C(11)-H(11B)	111.0
C(5B)-C(6B)-C(1B)	101.4(6)	H(11A)-C(11)-H(11B)	109.0
C(8B)-C(6B)-H(6B)	107.1	C(13)-C(12)-C(17)	121.2(4)
C(5B)-C(6B)-H(6B)	107.1	C(13)-C(12)-N(1)	120.7(5)
C(1B)-C(6B)-H(6B)	107.1	C(18)-C(20)-H(20B)	109.5
C(17)-C(12)-N(1)	117.9(4)	H(20A)-C(20)-H(20B)	109.5
C(14)-C(13)-C(12)	119.7(6)	C(18)-C(20)-H(20C)	109.5
C(14)-C(13)-C(18)	119.4(5)	H(20A)-C(20)-H(20C)	109.5
C(12)-C(13)-C(18)	120.9(4)	H(20B)-C(20)-H(20C)	109.5
C(15)-C(14)-C(13)	120.7(6)	C(17)-C(21)-C(23B)	109.0(4)
C(15)-C(14)-H(14A)	119.7	C(17)-C(21)-C(22)	113.8(11)
C(13)-C(14)-H(14A)	119.7	C(23B)-C(21)-C(22)	129.0(7)
C(16)-C(15)-C(14)	119.5(5)	C(17)-C(21)-C(23)	127.2(7)
C(16)-C(15)-H(15A)	120.2	C(22)-C(21)-C(23)	110.9(8)
C(14)-C(15)-H(15A)	120.2	C(17)-C(21)-C(22B)	112.5(4)
C(15)-C(16)-C(17)	123.4(6)	C(23B)-C(21)-C(22B)	110.2(5)
C(15)-C(16)-H(16A)	118.3	C(23)-C(21)-C(22B)	95.6(7)
C(17)-C(16)-H(16A)	118.3	C(17)-C(21)-H(21A)	99.5
C(16)-C(17)-C(12)	115.4(5)	C(23B)-C(21)-H(21A)	99.7
C(16)-C(17)-C(21)	121.8(5)	C(22)-C(21)-H(21A)	99.5
C(12)-C(17)-C(21)	122.8(4)	C(23)-C(21)-H(21A)	99.5
C(19)-C(18)-C(13)	111.6(5)	C(22B)-C(21)-H(21A)	124.5
C(19)-C(18)-C(20)	110.3(5)	C(17)-C(21)-H(21B)	107.8
C(13)-C(18)-C(20)	109.8(5)	C(23B)-C(21)-H(21B)	111.7
C(19)-C(18)-H(18A)	108.3	C(22)-C(21)-H(21B)	80.4
C(13)-C(18)-H(18A)	108.3	C(23)-C(21)-H(21B)	106.0
C(20)-C(18)-H(18A)	108.3	C(22B)-C(21)-H(21B)	105.6
C(18)-C(19)-H(19A)	109.5	C(21)-C(22)-H(22A)	109.5
C(18)-C(19)-H(19B)	109.5	C(21)-C(22)-H(22B)	109.5
H(19A)-C(19)-H(19B)	109.5	C(21)-C(22)-H(22C)	109.5
C(18)-C(19)-H(19C)	109.5	C(21)-C(23)-H(23A)	109.5
H(19A)-C(19)-H(19C)	109.5	C(21)-C(23)-H(23B)	109.5
H(19B)-C(19)-H(19C)	109.5	C(21)-C(23)-H(23C)	109.5
C(18)-C(20)-H(20A)	109.5	C(28)-C(29)-C(33)	120.8(5)
C(21)-C(22B)-H(22D)	109.5	C(32)-C(30)-C(31)	110.9(5)
C(21)-C(22B)-H(22E)	109.5	C(32)-C(30)-C(25)	109.7(4)
H(22D)-C(22B)-H(22E)	109.5	C(31)-C(30)-C(25)	111.5(4)
C(21)-C(22B)-H(22F)	109.5	C(32)-C(30)-H(30A)	108.2
H(22D)-C(22B)-H(22F)	109.5	C(31)-C(30)-H(30A)	108.2
H(22E)-C(22B)-H(22F)	109.5	C(25)-C(30)-H(30A)	108.2
C(21)-C(23B)-H(23D)	109.5	C(30)-C(31)-H(31A)	109.5
C(21)-C(23B)-H(23E)	109.5	C(30)-C(31)-H(31B)	109.5
H(23D)-C(23B)-H(23E)	109.5	H(31A)-C(31)-H(31B)	109.5

Table 4.5. (cont.)

C(21)-C(23B)-H(23F)	109.5	C(30)-C(31)-H(31C)	109.5
H(23D)-C(23B)-H(23F)	109.5	H(31A)-C(31)-H(31C)	109.5
H(23E)-C(23B)-H(23F)	109.5	H(31B)-C(31)-H(31C)	109.5
C(29)-C(24)-C(25)	122.4(4)	C(30)-C(32)-H(32A)	109.5
C(29)-C(24)-N(2)	117.9(4)	C(30)-C(32)-H(32B)	109.5
C(25)-C(24)-N(2)	119.5(4)	H(32A)-C(32)-H(32B)	109.5
C(26)-C(25)-C(24)	117.6(5)	C(30)-C(32)-H(32C)	109.5
C(26)-C(25)-C(30)	118.6(5)	H(32A)-C(32)-H(32C)	109.5
C(24)-C(25)-C(30)	123.7(4)	H(32B)-C(32)-H(32C)	109.5
C(27)-C(26)-C(25)	121.9(5)	C(35)-C(33)-C(29)	109.7(5)
C(27)-C(26)-H(26A)	119.0	C(35)-C(33)-C(34)	107.5(5)
C(25)-C(26)-H(26A)	119.0	C(29)-C(33)-C(34)	113.6(5)
C(26)-C(27)-C(28)	119.6(5)	C(35)-C(33)-H(33A)	108.6
C(26)-C(27)-H(27A)	120.2	C(29)-C(33)-H(33A)	108.6
C(28)-C(27)-H(27A)	120.2	C(34)-C(33)-H(33A)	108.6
C(27)-C(28)-C(29)	122.2(6)	C(33)-C(34)-H(34A)	109.5
C(27)-C(28)-H(28A)	118.9	C(33)-C(34)-H(34B)	109.5
C(29)-C(28)-H(28A)	118.9	H(34A)-C(34)-H(34B)	109.5
C(24)-C(29)-C(28)	116.1(5)	C(33)-C(34)-H(34C)	109.5
C(24)-C(29)-C(33)	123.1(4)	H(35A)-C(35)-H(35B)	109.5
H(34A)-C(34)-H(34C)	109.5	C(33)-C(35)-H(35C)	109.5
H(34B)-C(34)-H(34C)	109.5	H(35A)-C(35)-H(35C)	109.5
C(33)-C(35)-H(35A)	109.5	H(35B)-C(35)-H(35C)	109.5
C(33)-C(35)-H(35B)	109.5		

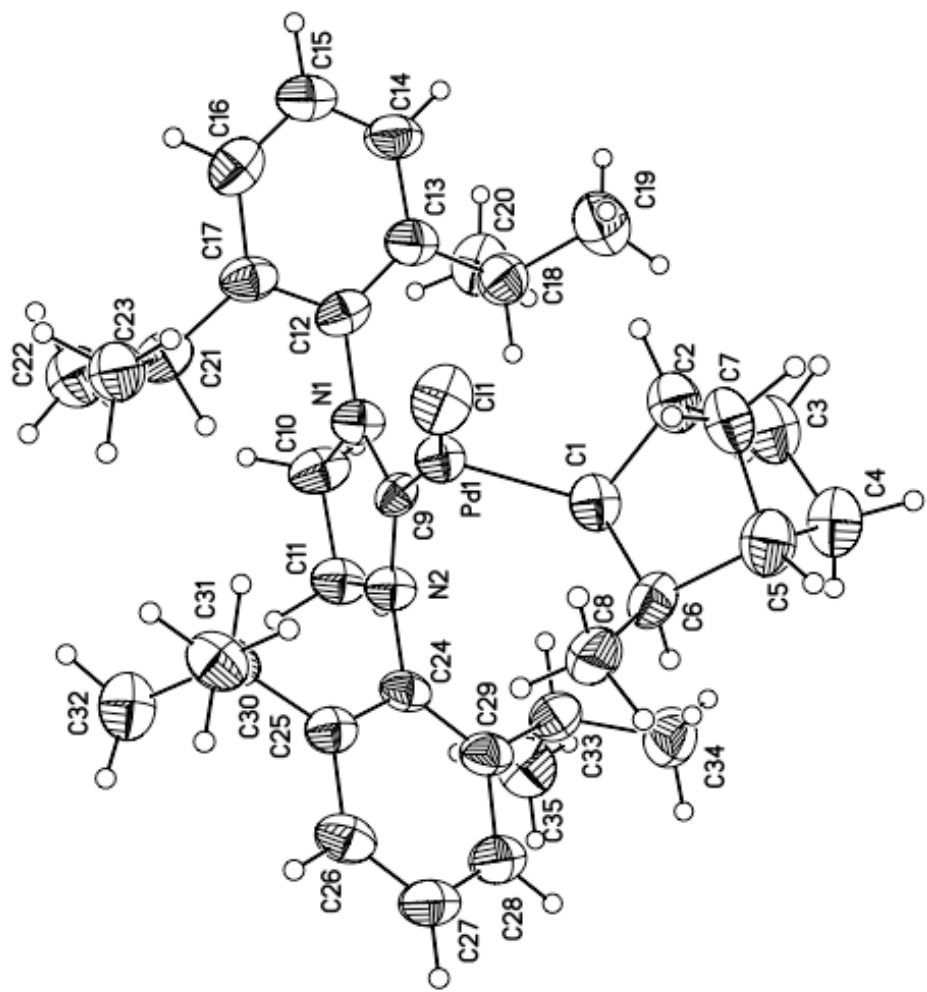


Figure 4.5. ORTEP diagram of **4.01** with 35% probability ellipsoids.

4.4.8 Crystallographic Data for 4.03

Table 4.6. Crystal data and structure refinement for 4.03.

Identification code	4.03
Empirical formula	C ₄₂ H ₅₉ N ₃ OPd
Formula weight	728.32
Temperature	193(2) K
Wavelength	1.54178 Å
Crystal system	Monoclinic
Space group	P2(1)/n
Unit cell dimensions	a = 12.8298(3) Å b = 15.9470(3) Å c = 19.8577(4) Å
Volume	3859.92(14) Å ³
Z	4
Density (calculated)	1.253 Mg/m ³
Absorption coefficient	4.128 mm ⁻¹
F(000)	1544
Crystal size	0.378 x 0.198 x 0.064 mm ³
Theta range for data collection	3.63 to 67.96°
Index ranges	-15<=h<=15, -18<=k<=17, -23<=l<=23
Reflections collected	33291
Independent reflections	6914 [R(int) = 0.0387]
Completeness to theta = 67.96°	98.2 %
Absorption correction	Integration
Max. and min. transmission	0.8404 and 0.3866
Refinement method	Full-matrix least-squares on F ²
Data / restraints / parameters	6914 / 385 / 530
Goodness-of-fit on F ²	1.071
Final R indices [I>2sigma(I)]	R1 = 0.0390, wR2 = 0.1023
R indices (all data)	R1 = 0.0437, wR2 = 0.1056
Largest diff. peak and hole	1.499 and -0.491 e.Å ⁻³

Table 4.7. Atomic coordinates ($\times 10^4$) and equivalent isotropic displacement parameters ($\text{\AA}^2 \times 10^3$) for **4.03**. $U(\text{eq})$ is defined as one third of the trace of the orthogonalized U^{ij} tensor.

	x	y	z	$U(\text{eq})$
Pd(1)	2136(1)	1951(1)	4083(1)	35(1)
N(2)	3586(2)	2927(1)	5331(1)	33(1)
N(3)	1868(2)	3287(2)	5019(1)	33(1)
C(1)	2988(3)	2591(2)	3532(2)	42(1)
C(2)	2159(3)	2904(2)	2826(2)	54(1)
C(3)	2774(3)	3595(2)	2544(2)	64(1)
C(4)	3604(4)	3078(3)	2300(2)	68(1)
C(5)	3385(3)	2185(2)	2476(2)	57(1)
C(6)	3810(3)	2056(2)	3291(2)	51(1)
C(7)	2134(3)	2192(3)	2324(2)	62(1)
C(8)	3931(3)	1146(3)	3506(2)	67(1)
N(1)	1347(2)	964(2)	3489(2)	54(1)
C(9)	212(4)	945(7)	3117(4)	49(2)
C(10)	-330(6)	1711(6)	3000(5)	40(1)
C(11)	-1464(6)	1737(5)	2696(6)	44(2)
C(12)	-2054(3)	996(6)	2510(4)	54(2)
C(13)	-1512(6)	229(5)	2628(7)	58(2)
C(14)	-378(6)	204(6)	2931(7)	58(2)
O(1)	-3212(5)	1024(8)	2194(6)	62(2)
C(15)	-3740(10)	1387(11)	2678(8)	82(3)
C(9B)	238(5)	993(11)	3089(6)	50(2)
C(10B)	-395(11)	1690(9)	3122(9)	51(2)
C(11B)	-1529(10)	1658(11)	2823(9)	52(2)
C(12B)	-2030(5)	929(12)	2492(7)	59(2)
C(13B)	-1396(10)	233(9)	2459(8)	57(2)
C(14B)	-263(10)	265(9)	2758(8)	52(2)
O(1B)	-3182(8)	820(11)	2293(11)	72(3)
C(15B)	-3746(15)	1554(14)	2449(15)	88(5)
C(16)	2602(2)	2792(2)	4848(1)	30(1)
C(17)	3521(2)	3465(2)	5922(2)	41(1)
C(18)	2357(2)	3797(2)	5654(2)	42(1)
C(19)	4540(2)	2430(2)	5386(2)	36(1)
C(20)	4570(2)	1592(2)	5614(2)	42(1)
C(21)	5511(3)	1128(2)	5648(2)	52(1)
C(22)	6373(3)	1479(2)	5476(2)	59(1)
C(23)	6334(3)	2301(3)	5276(2)	57(1)
C(24)	5419(2)	2801(2)	5230(2)	44(1)
C(25)	3678(3)	1211(2)	5861(2)	48(1)
C(26)	4085(4)	1096(3)	6673(2)	72(1)
C(27)	3256(4)	387(2)	5492(2)	68(1)
C(28)	5440(3)	3728(2)	5054(2)	52(1)
C(29)	6150(3)	4200(2)	5704(2)	64(1)
C(30)	5826(4)	3907(3)	4415(3)	74(1)
C(31)	714(2)	3330(2)	4621(2)	34(1)
C(32)	12(2)	2710(2)	4734(2)	42(1)
C(33)	-1103(3)	2784(2)	4348(2)	52(1)
C(34)	-1487(3)	3428(2)	3878(2)	52(1)

Table 4.7. (cont.)

C(35)	-779(2)	4035(2)	3780(2)	46(1)
C(36)	343(2)	3999(2)	4153(2)	38(1)
C(37)	405(3)	2003(2)	5254(2)	57(1)
C(38)	-205(12)	2042(9)	5814(6)	63(4)
C(39)	333(13)	1134(5)	4941(8)	71(4)
C(38B)	190(20)	2180(9)	5956(6)	68(5)
C(39B)	-65(19)	1152(6)	4959(8)	65(5)
C(38C)	620(30)	2232(12)	6023(5)	60(5)
C(39C)	-330(20)	1229(10)	5042(12)	63(5)
C(40)	1081(2)	4694(2)	4051(2)	38(1)
C(41)	821(3)	5513(2)	4363(2)	54(1)
C(42)	984(3)	4839(2)	3277(2)	59(1)

Table 4.8. Bond lengths [Å] and angles [°] for **4.03**.

Pd(1)-C(16)	1.974(3)	C(5)-H(5)	1.0000
Pd(1)-N(1)	2.037(3)	C(6)-C(8)	1.508(5)
Pd(1)-C(1)	2.044(3)	C(6)-H(6)	1.0000
N(2)-C(16)	1.343(3)	C(7)-H(7A)	0.9900
N(2)-C(19)	1.435(4)	C(7)-H(7B)	0.9900
N(2)-C(17)	1.476(4)	C(8)-H(8A)	0.9800
N(3)-C(16)	1.350(4)	C(8)-H(8B)	0.9800
N(3)-C(31)	1.447(3)	C(8)-H(8C)	0.9800
N(3)-C(18)	1.468(4)	N(1)-C(9B)	1.397(7)
C(1)-C(6)	1.545(4)	N(1)-C(9)	1.412(5)
C(1)-C(2)	1.555(5)	N(1)-H(1A)	0.8799(10)
C(1)-H(1)	1.0000	C(9)-C(10)	1.3900
C(2)-C(7)	1.505(5)	C(9)-C(14)	1.3900
C(2)-C(3)	1.556(5)	C(10)-C(11)	1.3900
C(2)-H(2)	1.0000	C(10)-H(10A)	0.9500
C(3)-C(4)	1.541(6)	C(11)-C(12)	1.3900
C(3)-H(3A)	0.9900	C(11)-H(11A)	0.9500
C(3)-H(3B)	0.9900	C(12)-C(13)	1.3900
C(4)-C(5)	1.513(5)	C(12)-O(1)	1.421(5)
C(4)-H(4A)	0.9900	C(13)-C(14)	1.3900
C(4)-H(4B)	0.9900	C(13)-H(13A)	0.9500
C(5)-C(7)	1.537(6)	C(14)-H(14A)	0.9500
C(5)-C(6)	1.550(5)	C(18)-H(18A)	0.9900
O(1)-C(15)	1.458(9)	C(18)-H(18B)	0.9900
C(15)-H(15A)	0.9800	C(19)-C(24)	1.391(4)
C(15)-H(15B)	0.9800	C(19)-C(20)	1.407(4)
C(15)-H(15C)	0.9800	C(20)-C(21)	1.399(5)
C(9B)-C(10B)	1.3900	C(20)-C(25)	1.507(5)
C(9B)-C(14B)	1.3900	C(21)-C(22)	1.376(6)
C(10B)-C(11B)	1.3900	C(21)-H(21)	0.9500
C(10B)-H(10B)	0.9500	C(22)-C(23)	1.367(6)
C(11B)-C(12B)	1.3900	C(22)-H(22)	0.9500
C(11B)-H(11B)	0.9500	C(23)-C(24)	1.399(5)
C(12B)-C(13B)	1.3900	C(23)-H(23)	0.9500
C(12B)-O(1B)	1.417(7)	C(24)-C(28)	1.521(5)
C(13B)-C(14B)	1.3900	C(25)-C(27)	1.521(5)
C(13B)-H(13B)	0.9500	C(25)-C(26)	1.542(5)
C(14B)-H(14B)	0.9500	C(25)-H(25)	1.0000
O(1B)-C(15B)	1.459(11)	C(26)-H(26A)	0.9800
C(15B)-H(15D)	0.9800	C(26)-H(26B)	0.9800
C(15B)-H(15E)	0.9800	C(26)-H(26C)	0.9800
C(15B)-H(15F)	0.9800	C(27)-H(27A)	0.9800
C(17)-C(18)	1.517(4)	C(27)-H(27B)	0.9800
C(17)-H(17A)	0.9900	C(27)-H(27C)	0.9800
C(17)-H(17B)	0.9900	C(37)-C(39B)	1.526(7)
C(28)-C(30)	1.524(6)	C(37)-C(38B)	1.529(8)
C(28)-C(29)	1.527(5)	C(37)-C(39C)	1.533(8)
C(28)-H(28)	1.0000	C(37)-C(38)	1.548(7)
C(29)-H(29A)	0.9800	C(37)-H(37A)	1.0000
C(29)-H(29B)	0.9800	C(37)-H(37B)	1.0000
C(29)-H(29C)	0.9800	C(37)-H(37C)	0.9999
C(30)-H(30A)	0.9800	C(38)-H(38A)	0.9800
C(30)-H(30B)	0.9800	C(38)-H(38B)	0.9800

Table 4.8. (cont.)

C(30)-H(30C)	0.9800	C(38)-H(38C)	0.9800
C(31)-C(36)	1.398(4)	C(39)-H(39A)	0.9800
C(31)-C(32)	1.401(4)	C(39)-H(39B)	0.9800
C(32)-C(33)	1.401(5)	C(39)-H(39C)	0.9800
C(32)-C(37)	1.506(5)	C(38B)-H(38D)	0.9800
C(33)-C(34)	1.371(6)	C(38B)-H(38E)	0.9800
C(33)-H(33)	0.9500	C(38B)-H(38F)	0.9800
C(34)-C(35)	1.383(5)	C(39B)-H(39D)	0.9800
C(34)-H(34)	0.9500	C(39B)-H(39E)	0.9800
C(35)-C(36)	1.399(4)	C(39B)-H(39F)	0.9800
C(35)-H(35)	0.9500	C(38C)-H(38G)	0.9800
C(36)-C(40)	1.513(4)	C(38C)-H(38H)	0.9800
C(37)-C(39)	1.510(7)	C(38C)-H(38I)	0.9800
C(37)-C(38C)	1.511(8)	C(41)-H(41A)	0.9800
C(39C)-H(39G)	0.9800	C(41)-H(41B)	0.9800
C(39C)-H(39H)	0.9800	C(41)-H(41C)	0.9800
C(39C)-H(39I)	0.9800	C(42)-H(42A)	0.9800
C(40)-C(42)	1.520(5)	C(42)-H(42B)	0.9800
C(40)-C(41)	1.527(4)	C(42)-H(42C)	0.9800
C(40)-H(40)	1.0000		

C(16)-Pd(1)-N(1)	161.28(12)	C(2)-C(3)-H(3A)	111.3
C(16)-Pd(1)-C(1)	89.35(12)	C(4)-C(3)-H(3B)	111.3
N(1)-Pd(1)-C(1)	109.15(13)	C(2)-C(3)-H(3B)	111.3
C(16)-N(2)-C(19)	123.7(2)	H(3A)-C(3)-H(3B)	109.2
C(16)-N(2)-C(17)	112.8(2)	C(5)-C(4)-C(3)	103.6(3)
C(19)-N(2)-C(17)	121.3(2)	C(5)-C(4)-H(4A)	111.0
C(16)-N(3)-C(31)	124.4(2)	C(3)-C(4)-H(4A)	111.0
C(16)-N(3)-C(18)	113.3(2)	C(5)-C(4)-H(4B)	111.0
C(31)-N(3)-C(18)	122.3(2)	C(3)-C(4)-H(4B)	111.0
C(6)-C(1)-C(2)	103.8(3)	H(4A)-C(4)-H(4B)	109.0
C(6)-C(1)-Pd(1)	114.9(2)	C(4)-C(5)-C(7)	101.8(3)
C(2)-C(1)-Pd(1)	108.3(2)	C(4)-C(5)-C(6)	109.6(3)
C(6)-C(1)-H(1)	109.9	C(7)-C(5)-C(6)	102.3(3)
C(2)-C(1)-H(1)	109.9	C(4)-C(5)-H(5)	114.0
Pd(1)-C(1)-H(1)	109.9	C(7)-C(5)-H(5)	114.0
C(7)-C(2)-C(1)	102.9(3)	C(6)-C(5)-H(5)	114.0
C(7)-C(2)-C(3)	101.8(3)	C(8)-C(6)-C(1)	117.6(3)
C(1)-C(2)-C(3)	105.7(3)	C(8)-C(6)-C(5)	113.3(3)
C(7)-C(2)-H(2)	114.9	C(1)-C(6)-C(5)	101.5(3)
C(1)-C(2)-H(2)	114.9	C(8)-C(6)-H(6)	108.0
C(3)-C(2)-H(2)	114.9	C(1)-C(6)-H(6)	108.0
C(4)-C(3)-C(2)	102.2(3)	C(5)-C(6)-H(6)	108.0
C(4)-C(3)-H(3A)	111.3	C(11)-C(10)-H(10A)	120.0
C(2)-C(7)-C(5)	94.0(3)	C(10)-C(11)-C(12)	120.0
C(2)-C(7)-H(7A)	112.9	C(10)-C(11)-H(11A)	120.0
C(5)-C(7)-H(7A)	112.9	C(12)-C(11)-H(11A)	120.0
C(2)-C(7)-H(7B)	112.9	C(13)-C(12)-C(11)	120.0
C(5)-C(7)-H(7B)	112.9	C(13)-C(12)-O(1)	120.1(7)
H(7A)-C(7)-H(7B)	110.3	C(11)-C(12)-O(1)	119.9(7)
C(6)-C(8)-H(8A)	109.5	C(12)-C(13)-C(14)	120.0
C(6)-C(8)-H(8B)	109.5	C(12)-C(13)-H(13A)	120.0
H(8A)-C(8)-H(8B)	109.5	C(14)-C(13)-H(13A)	120.0
C(6)-C(8)-H(8C)	109.5	C(13)-C(14)-C(9)	120.0

Table 4.8. (cont.)

H(8A)-C(8)-H(8C)	109.5	C(13)-C(14)-H(14A)	120.0
H(8B)-C(8)-H(8C)	109.5	C(9)-C(14)-H(14A)	120.0
C(9B)-N(1)-Pd(1)	122.5(7)	C(12)-O(1)-C(15)	111.0(8)
C(9)-N(1)-Pd(1)	124.4(5)	C(10B)-C(9B)-C(14B)	120.0
C(9B)-N(1)-H(1A)	126(3)	C(10B)-C(9B)-N(1)	120.5(11)
C(9)-N(1)-H(1A)	124(3)	C(14B)-C(9B)-N(1)	118.6(11)
Pd(1)-N(1)-H(1A)	110(3)	C(11B)-C(10B)-C(9B)	120.0
C(10)-C(9)-C(14)	120.0	C(11B)-C(10B)-H(10B)	120.0
C(10)-C(9)-N(1)	116.7(7)	C(9B)-C(10B)-H(10B)	120.0
C(14)-C(9)-N(1)	123.0(7)	C(10B)-C(11B)-C(12B)	120.0
C(9)-C(10)-C(11)	120.0	C(10B)-C(11B)-H(11B)	120.0
C(9)-C(10)-H(10A)	120.0	C(18)-C(17)-H(17A)	111.2
C(12B)-C(11B)-H(11B)	120.0	N(2)-C(17)-H(17B)	111.2
C(13B)-C(12B)-C(11B)	120.0	C(18)-C(17)-H(17B)	111.2
C(13B)-C(12B)-O(1B)	117.6(11)	H(17A)-C(17)-H(17B)	109.2
C(11B)-C(12B)-O(1B)	121.5(11)	N(3)-C(18)-C(17)	102.5(2)
C(14B)-C(13B)-C(12B)	120.0	N(3)-C(18)-H(18A)	111.3
C(14B)-C(13B)-H(13B)	120.0	C(17)-C(18)-H(18A)	111.3
C(12B)-C(13B)-H(13B)	120.0	N(3)-C(18)-H(18B)	111.3
C(13B)-C(14B)-C(9B)	120.0	C(17)-C(18)-H(18B)	111.3
C(13B)-C(14B)-H(14B)	120.0	H(18A)-C(18)-H(18B)	109.2
C(9B)-C(14B)-H(14B)	120.0	C(24)-C(19)-C(20)	122.3(3)
C(12B)-O(1B)-C(15B)	112.6(10)	C(24)-C(19)-N(2)	118.6(3)
O(1B)-C(15B)-H(15D)	109.5	C(20)-C(19)-N(2)	119.1(3)
O(1B)-C(15B)-H(15E)	109.5	C(21)-C(20)-C(19)	117.0(3)
H(15D)-C(15B)-H(15E)	109.5	C(21)-C(20)-C(25)	120.2(3)
O(1B)-C(15B)-H(15F)	109.5	C(19)-C(20)-C(25)	122.7(3)
H(15D)-C(15B)-H(15F)	109.5	C(22)-C(21)-C(20)	121.5(3)
H(15E)-C(15B)-H(15F)	109.5	C(22)-C(21)-H(21)	119.3
N(2)-C(16)-N(3)	107.5(2)	C(20)-C(21)-H(21)	119.3
N(2)-C(16)-Pd(1)	130.5(2)	C(23)-C(22)-C(21)	120.2(3)
N(3)-C(16)-Pd(1)	121.54(19)	C(23)-C(22)-H(22)	119.9
N(2)-C(17)-C(18)	102.6(2)	C(21)-C(22)-H(22)	119.9
N(2)-C(17)-H(17A)	111.2	H(27A)-C(27)-H(27C)	109.5
C(22)-C(23)-C(24)	121.3(3)	H(27B)-C(27)-H(27C)	109.5
C(22)-C(23)-H(23)	119.4	C(24)-C(28)-C(30)	114.1(3)
C(24)-C(23)-H(23)	119.4	C(24)-C(28)-C(29)	109.4(3)
C(19)-C(24)-C(23)	117.7(3)	C(30)-C(28)-C(29)	110.4(3)
C(19)-C(24)-C(28)	122.7(3)	C(24)-C(28)-H(28)	107.6
C(23)-C(24)-C(28)	119.5(3)	C(30)-C(28)-H(28)	107.6
C(20)-C(25)-C(27)	112.5(3)	C(29)-C(28)-H(28)	107.6
C(20)-C(25)-C(26)	110.2(3)	C(28)-C(29)-H(29A)	109.5
C(27)-C(25)-C(26)	110.8(3)	C(28)-C(29)-H(29B)	109.5
C(20)-C(25)-H(25)	107.7	H(29A)-C(29)-H(29B)	109.5
C(27)-C(25)-H(25)	107.7	C(28)-C(29)-H(29C)	109.5
C(26)-C(25)-H(25)	107.7	H(29A)-C(29)-H(29C)	109.5
C(25)-C(26)-H(26A)	109.5	H(29B)-C(29)-H(29C)	109.5
C(25)-C(26)-H(26B)	109.5	C(28)-C(30)-H(30A)	109.5
H(26A)-C(26)-H(26B)	109.5	C(28)-C(30)-H(30B)	109.5
C(25)-C(26)-H(26C)	109.5	H(30A)-C(30)-H(30B)	109.5
H(26A)-C(26)-H(26C)	109.5	C(28)-C(30)-H(30C)	109.5
H(26B)-C(26)-H(26C)	109.5	H(30A)-C(30)-H(30C)	109.5
C(25)-C(27)-H(27A)	109.5	H(30B)-C(30)-H(30C)	109.5
C(25)-C(27)-H(27B)	109.5	C(36)-C(31)-C(32)	122.8(3)
H(27A)-C(27)-H(27B)	109.5	C(36)-C(31)-N(3)	118.5(3)

Table 4.8. (cont.)

C(25)-C(27)-H(27C)	109.5	C(39)-C(37)-C(38B)	122.6(9)
C(32)-C(31)-N(3)	118.6(3)	C(39B)-C(37)-C(38B)	110.6(8)
C(31)-C(32)-C(33)	116.8(3)	C(32)-C(37)-C(39C)	111.6(8)
C(31)-C(32)-C(37)	122.9(3)	C(38C)-C(37)-C(39C)	111.9(9)
C(33)-C(32)-C(37)	120.3(3)	C(38B)-C(37)-C(39C)	97.3(11)
C(34)-C(33)-C(32)	121.6(3)	C(32)-C(37)-C(38)	109.0(5)
C(34)-C(33)-H(33)	119.2	C(39)-C(37)-C(38)	110.7(8)
C(32)-C(33)-H(33)	119.2	C(39B)-C(37)-C(38)	94.8(11)
C(33)-C(34)-C(35)	120.5(3)	C(39C)-C(37)-C(38)	79.7(15)
C(33)-C(34)-H(34)	119.7	C(32)-C(37)-H(37A)	106.8
C(35)-C(34)-H(34)	119.7	C(39)-C(37)-H(37A)	106.8
C(34)-C(35)-C(36)	120.6(3)	C(38C)-C(37)-H(37A)	67.1
C(34)-C(35)-H(35)	119.7	C(39B)-C(37)-H(37A)	124.5
C(36)-C(35)-H(35)	119.7	C(38B)-C(37)-H(37A)	87.0
C(31)-C(36)-C(35)	117.7(3)	C(39C)-C(37)-H(37A)	136.2
C(31)-C(36)-C(40)	123.5(2)	C(38)-C(37)-H(37A)	106.8
C(35)-C(36)-C(40)	118.8(3)	C(32)-C(37)-H(37B)	106.9
C(32)-C(37)-C(39)	116.1(7)	C(39)-C(37)-H(37B)	87.7
C(32)-C(37)-C(38C)	115.3(7)	C(38C)-C(37)-H(37B)	87.5
C(39)-C(37)-C(38C)	127.4(10)	C(39B)-C(37)-H(37B)	106.9
C(32)-C(37)-C(39B)	113.2(6)	C(38B)-C(37)-H(37B)	107.0
C(38C)-C(37)-C(39B)	121.9(10)	C(39C)-C(37)-H(37B)	121.8
C(32)-C(37)-C(38B)	111.7(6)	H(39D)-C(39B)-H(39E)	109.5
C(38)-C(37)-H(37B)	125.5	C(37)-C(39B)-H(39F)	109.5
C(32)-C(37)-H(37C)	105.7	H(39D)-C(39B)-H(39F)	109.5
C(39)-C(37)-H(37C)	69.8	H(39E)-C(39B)-H(39F)	109.5
C(38C)-C(37)-H(37C)	105.7	C(37)-C(38C)-H(38G)	109.5
C(39B)-C(37)-H(37C)	89.6	C(37)-C(38C)-H(38H)	109.5
C(38B)-C(37)-H(37C)	124.2	C(37)-C(38C)-H(38I)	109.5
C(39C)-C(37)-H(37C)	105.7	C(37)-C(39C)-H(39G)	109.5
C(38)-C(37)-H(37C)	139.7	C(37)-C(39C)-H(39H)	109.5
C(37)-C(38)-H(38A)	109.5	C(37)-C(39C)-H(39I)	109.5
C(37)-C(38)-H(38B)	109.5	C(36)-C(40)-C(42)	112.9(3)
C(37)-C(38)-H(38C)	109.5	C(36)-C(40)-C(41)	110.3(3)
C(37)-C(39)-H(39A)	109.5	C(42)-C(40)-C(41)	108.8(3)
C(37)-C(39)-H(39B)	109.5	C(36)-C(40)-H(40)	108.2
C(37)-C(39)-H(39C)	109.5	C(42)-C(40)-H(40)	108.2
C(37)-C(38B)-H(38D)	109.5	C(41)-C(40)-H(40)	108.2
C(37)-C(38B)-H(38E)	109.5	C(40)-C(41)-H(41A)	109.5
H(38D)-C(38B)-H(38E)	109.5	C(40)-C(41)-H(41B)	109.5
C(37)-C(38B)-H(38F)	109.5	H(41A)-C(41)-H(41B)	109.5
H(38D)-C(38B)-H(38F)	109.5	C(40)-C(41)-H(41C)	109.5
H(38E)-C(38B)-H(38F)	109.5	H(41A)-C(41)-H(41C)	109.5
C(37)-C(39B)-H(39D)	109.5	H(41B)-C(41)-H(41C)	109.5
C(37)-C(39B)-H(39E)	109.5	C(40)-C(42)-H(42C)	109.5
C(40)-C(42)-H(42A)	109.5	H(42A)-C(42)-H(42C)	109.5
C(40)-C(42)-H(42B)	109.5	H(42B)-C(42)-H(42C)	109.5
H(42A)-C(42)-H(42B)	109.5		

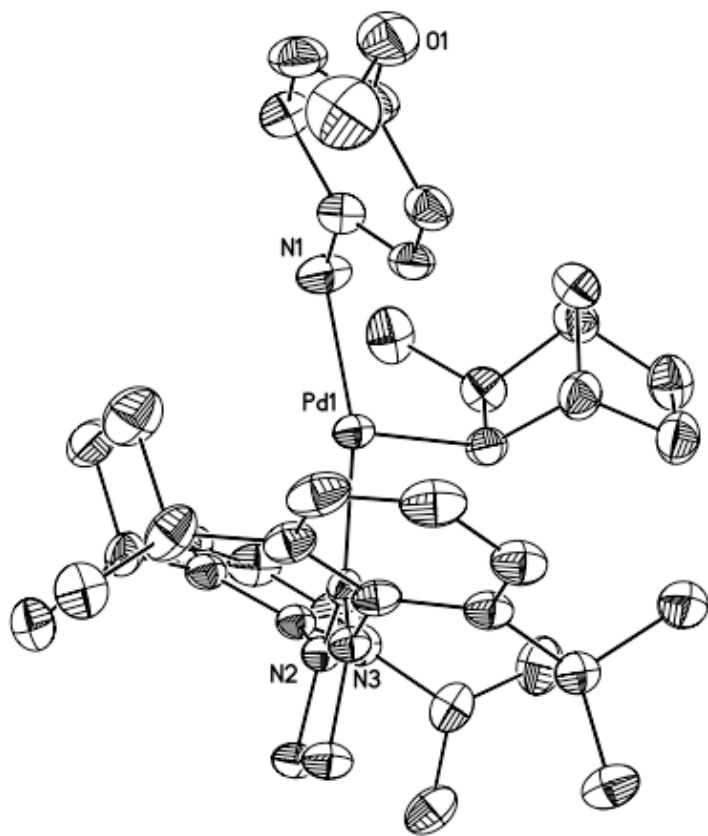


Figure 4.6. ORTEP drawing of **4.03** with 35% probability ellipsoids.

4.4.9 Crystallographic Data for 4.08

Table 4.9. Crystal data and structure refinement for 4.08.

Empirical formula	C ₈₅ H ₁₁₆ Cl ₂ N ₄ Pd ₂		
Formula weight	1477.52		
Temperature	193(1) K		
Wavelength	1.54178 Å		
Crystal system	Triclinic		
Space group	P-1		
Unit cell dimensions	a = 11.7161(5) Å	b = 14.8135(6) Å	c = 23.0484(13) Å
			a = 102.478(3)°. b = 92.417(3)°. g = 109.701(2)°.
Volume	3648.2(3) Å ³		
Z	2		
Density (calculated)	1.345 Mg/m ³		
Absorption coefficient	5.005 mm ⁻¹		
F(000)	1560		
Crystal size	0.315 x 0.131 x 0.045 mm ³		
Theta range for data collection	1.98 to 67.93°.		
Index ranges	-10<=h<=13, -17<=k<=17, -26<=l<=27		
Reflections collected	12743		
Independent reflections	12743 [R(int) = 0.0684]		
Completeness to theta = 67.93°	95.9 %		
Absorption correction	Integration		
Max. and min. transmission	0.8232 and 0.3926		
Refinement method	Full-matrix least-squares on F ²		
Data / restraints / parameters	12743 / 43 / 742		
Goodness-of-fit on F ²	1.031		
Final R indices [I>2sigma(I)]	R1 = 0.0399, wR2 = 0.1041		
R indices (all data)	R1 = 0.0679, wR2 = 0.1205		
Largest diff. peak and hole	0.947 and -1.044 e.Å ⁻³		

Table 4.10. Atomic coordinates ($\times 10^4$) and equivalent isotropic displacement parameters ($\text{\AA}^2 \times 10^3$) for **4.08**. U(eq) is defined as one third of the trace of the orthogonalized U_{ij}^2 tensor.

	x	y	z	U(eq)
Pd(1)	3632(1)	7410(1)	3338(1)	24(1)
Pd(2)	5057(1)	9159(1)	2443(1)	25(1)
Cl(1)	3292(1)	7560(1)	2285(1)	31(1)
Cl(2)	5237(1)	8959(1)	3431(1)	40(1)
N(1)	1151(3)	5748(2)	2940(1)	27(1)
N(2)	2627(3)	5202(2)	3011(1)	26(1)
N(3)	4007(3)	9880(2)	1520(1)	29(1)
N(4)	4463(3)	8627(2)	1083(1)	31(1)
C(1)	2373(3)	6055(3)	3137(2)	25(1)
C(2)	685(4)	4742(3)	2689(2)	35(1)
C(3)	1606(4)	4402(3)	2727(2)	33(1)
C(4)	388(3)	6348(3)	3036(2)	30(1)
C(5)	-91(3)	6574(3)	2546(2)	35(1)
C(6)	-819(4)	7153(3)	2659(2)	43(1)
C(7)	-1071(4)	7474(3)	3222(2)	48(1)
C(8)	-638(4)	7195(3)	3697(2)	43(1)
C(9)	88(3)	6617(3)	3619(2)	34(1)
C(10)	70(4)	6166(3)	1906(2)	42(1)
C(11)	-1083(5)	5253(4)	1610(2)	62(1)
C(12)	318(4)	6915(4)	1520(2)	53(1)
C(13)	461(4)	6238(3)	4130(2)	38(1)
C(14)	-333(4)	5145(3)	4055(2)	49(1)
C(15)	380(4)	6823(4)	4750(2)	48(1)
C(16)	3744(3)	5111(3)	3230(2)	27(1)
C(17)	3730(3)	4727(3)	3736(2)	29(1)
C(18)	4795(4)	4631(3)	3948(2)	35(1)
C(19)	5841(4)	4925(3)	3675(2)	41(1)
C(20)	5828(4)	5297(3)	3174(2)	40(1)
C(21)	4781(3)	5391(3)	2932(2)	31(1)
C(22)	2578(4)	4384(3)	4033(2)	32(1)
C(23)	2020(4)	3252(3)	3890(2)	44(1)
C(24)	2797(4)	4799(3)	4715(2)	46(1)
C(25)	4755(4)	5714(3)	2355(2)	36(1)
C(26)	5800(4)	6660(3)	2365(2)	49(1)
C(27)	4751(5)	4875(4)	1828(2)	54(1)
C(28)	4059(3)	7321(3)	4200(2)	27(1)
C(29)	5453(4)	7691(3)	4402(2)	34(1)
C(30)	5628(4)	7179(3)	4898(2)	44(1)
C(31)	5061(5)	7650(3)	5423(2)	47(1)
C(32)	4725(4)	8442(3)	5178(2)	42(1)
C(33)	3577(4)	7912(3)	4706(2)	35(1)
C(34)	5742(4)	8747(3)	4785(2)	41(1)
C(35)	3064(4)	8649(3)	4532(2)	39(1)
C(36)	6484(3)	10505(3)	2622(2)	31(1)
C(37)	6522(4)	11223(3)	3236(2)	40(1)
C(38)	7210(5)	12274(3)	3171(2)	51(1)
C(39)	8535(4)	12279(3)	3120(2)	55(1)
C(40)	8458(4)	11267(3)	3227(2)	48(1)

Table 4.10. (cont.)

C(41)	7794(4)	10453(3)	2656(2)	41(1)
C(42)	7493(4)	11104(3)	3652(2)	47(1)
C(43)	7884(4)	9454(3)	2691(2)	48(1)
C(44)	4601(3)	9265(3)	1625(2)	26(1)
C(45)	3474(4)	9594(3)	925(2)	37(1)
C(46)	3761(4)	8825(3)	653(2)	37(1)
C(47)	4020(3)	10771(3)	1936(2)	31(1)
C(48)	3286(4)	10698(3)	2397(2)	35(1)
C(49)	3346(4)	11580(3)	2785(2)	44(1)
C(50)	4087(4)	12479(3)	2714(2)	46(1)
C(51)	4789(4)	12530(3)	2251(2)	44(1)
C(52)	4769(4)	11675(3)	1845(2)	37(1)
C(53)	2355(4)	9720(3)	2450(2)	41(1)
C(54)	2460(20)	9660(15)	3110(4)	54(3)
C(55)	1064(8)	9671(14)	2247(12)	53(3)
C(54B)	2110(30)	9490(30)	3062(9)	53(6)
C(55B)	1145(15)	9524(19)	2066(13)	39(5)
C(56)	5509(4)	11775(3)	1319(2)	44(1)
C(57)	4983(6)	12248(4)	894(2)	64(1)
C(58)	6865(5)	12365(4)	1512(3)	70(2)
C(59)	5044(4)	7907(3)	927(2)	31(1)
C(60)	6321(4)	8256(3)	917(2)	38(1)
C(61)	6849(5)	7548(4)	741(2)	54(1)
C(62)	6179(5)	6566(4)	560(3)	63(1)
C(63)	4925(5)	6233(3)	553(2)	50(1)
C(64)	4320(4)	6897(3)	736(2)	40(1)
C(65)	7072(4)	9351(3)	1051(2)	44(1)
C(66)	8451(5)	9582(4)	1195(2)	63(1)
C(67)	6881(5)	9775(4)	520(2)	57(1)
C(68)	2950(4)	6503(3)	706(2)	41(1)
C(69)	2343(5)	6196(4)	51(2)	55(1)
C(70)	2467(5)	5616(3)	983(2)	49(1)

Table 4.11. Bond lengths [Å] and angles [°] for **4.08**.

Pd(1)-C(1)	1.991(4)	C(4)-C(5)	1.392(5)
Pd(1)-C(28)	2.071(3)	C(4)-C(9)	1.410(6)
Pd(1)-Cl(2)	2.3858(10)	C(5)-C(6)	1.395(6)
Pd(1)-Cl(1)	2.5125(8)	C(5)-C(10)	1.514(6)
Pd(2)-C(44)	1.991(3)	C(6)-C(7)	1.364(7)
Pd(2)-C(36)	2.068(4)	C(6)-H(6A)	0.9500
Pd(2)-Cl(2)	2.3682(9)	C(7)-C(8)	1.385(6)
Pd(2)-Cl(1)	2.5058(9)	C(7)-H(7A)	0.9500
N(1)-C(1)	1.371(5)	C(8)-C(9)	1.388(5)
N(1)-C(2)	1.381(5)	C(8)-H(8A)	0.9500
N(1)-C(4)	1.451(4)	C(9)-C(13)	1.516(5)
N(2)-C(1)	1.368(4)	C(10)-C(12)	1.529(6)
N(2)-C(3)	1.381(5)	C(10)-C(11)	1.552(7)
N(2)-C(16)	1.441(4)	C(10)-H(10A)	1.0000
N(3)-C(44)	1.372(5)	C(11)-H(11A)	0.9800
N(3)-C(45)	1.396(5)	C(11)-H(11B)	0.9800
N(3)-C(47)	1.449(5)	C(11)-H(11C)	0.9800
N(4)-C(44)	1.360(5)	C(12)-H(12A)	0.9800
N(4)-C(46)	1.401(5)	C(12)-H(12B)	0.9800
N(4)-C(59)	1.441(5)	C(12)-H(12C)	0.9800
C(2)-C(3)	1.342(5)	C(13)-C(15)	1.528(6)
C(2)-H(2A)	0.9500	C(13)-C(14)	1.538(6)
C(3)-H(3A)	0.9500	C(23)-H(23B)	0.9800
C(13)-H(13A)	1.0000	C(23)-H(23C)	0.9800
C(14)-H(14A)	0.9800	C(24)-H(24A)	0.9800
C(14)-H(14B)	0.9800	C(24)-H(24B)	0.9800
C(14)-H(14C)	0.9800	C(24)-H(24C)	0.9800
C(15)-H(15A)	0.9800	C(25)-C(26)	1.513(6)
C(15)-H(15B)	0.9800	C(25)-C(27)	1.537(6)
C(15)-H(15C)	0.9800	C(25)-H(25A)	1.0000
C(16)-C(17)	1.402(5)	C(26)-H(26A)	0.9800
C(16)-C(21)	1.404(5)	C(26)-H(26B)	0.9800
C(17)-C(18)	1.385(5)	C(26)-H(26C)	0.9800
C(17)-C(22)	1.522(5)	C(27)-H(27A)	0.9800
C(18)-C(19)	1.381(6)	C(27)-H(27B)	0.9800
C(18)-H(18A)	0.9500	C(27)-H(27C)	0.9800
C(19)-C(20)	1.384(6)	C(28)-C(33)	1.547(5)
C(19)-H(19A)	0.9500	C(28)-C(29)	1.552(5)
C(20)-C(21)	1.387(5)	C(28)-H(28A)	1.0000
C(20)-H(20A)	0.9500	C(29)-C(34)	1.536(5)
C(21)-C(25)	1.512(5)	C(29)-C(30)	1.542(5)
C(22)-C(23)	1.533(6)	C(29)-H(29A)	1.0000
C(22)-C(24)	1.535(5)	C(30)-C(31)	1.552(6)
C(22)-H(22A)	1.0000	C(30)-H(30A)	0.9900
C(23)-H(23A)	0.9800	C(38)-H(38B)	0.9900
C(30)-H(30B)	0.9900	C(39)-C(40)	1.544(6)
C(31)-C(32)	1.558(6)	C(39)-H(39A)	0.9900
C(31)-H(31A)	0.9900	C(39)-H(39B)	0.9900
C(31)-H(31B)	0.9900	C(40)-C(42)	1.519(6)
C(32)-C(34)	1.533(6)	C(40)-C(41)	1.546(6)
C(32)-C(33)	1.552(6)	C(40)-H(40A)	1.0000
C(32)-H(32A)	1.0000	C(41)-C(43)	1.537(6)
C(33)-C(35)	1.523(5)	C(41)-H(41A)	1.0000

Table 4.11. (cont).

C(33)-H(33A)	1.0000	C(42)-H(42A)	0.9900
C(34)-H(34A)	0.9900	C(42)-H(42B)	0.9900
C(34)-H(34B)	0.9900	C(43)-H(43A)	0.9800
C(35)-H(35A)	0.9800	C(43)-H(43B)	0.9800
C(35)-H(35B)	0.9800	C(43)-H(43C)	0.9800
C(35)-H(35C)	0.9800	C(45)-C(46)	1.331(6)
C(36)-C(41)	1.562(5)	C(45)-H(45A)	0.9500
C(36)-C(37)	1.564(5)	C(46)-H(46A)	0.9500
C(36)-H(36A)	1.0000	C(47)-C(48)	1.395(5)
C(37)-C(42)	1.537(6)	C(47)-C(52)	1.397(6)
C(37)-C(38)	1.537(6)	C(48)-C(49)	1.392(6)
C(37)-H(37A)	1.0000	C(48)-C(53)	1.525(6)
C(38)-C(39)	1.559(7)	C(49)-C(50)	1.372(6)
C(38)-H(38A)	0.9900	C(55B)-H(55E)	0.9800
C(49)-H(49A)	0.9500	C(55B)-H(55F)	0.9800
C(50)-C(51)	1.373(6)	C(56)-C(58)	1.524(7)
C(50)-H(50A)	0.9500	C(56)-C(57)	1.538(7)
C(51)-C(52)	1.395(6)	C(56)-H(56A)	1.0000
C(51)-H(51A)	0.9500	C(57)-H(57A)	0.9800
C(52)-C(56)	1.525(6)	C(57)-H(57B)	0.9800
C(53)-C(55)	1.537(7)	C(57)-H(57C)	0.9800
C(53)-C(55B)	1.543(8)	C(58)-H(58A)	0.9800
C(53)-C(54)	1.545(7)	C(58)-H(58B)	0.9800
C(53)-C(54B)	1.538(8)	C(58)-H(58C)	0.9800
C(53)-H(53A)	1.0000	C(59)-C(64)	1.406(6)
C(53)-H(53B)	0.9601	C(59)-C(60)	1.412(6)
C(54)-H(54A)	0.9800	C(60)-C(61)	1.387(6)
C(54)-H(54B)	0.9800	C(60)-C(65)	1.516(6)
C(54)-H(54C)	0.9800	C(61)-C(62)	1.358(7)
C(55)-H(55A)	0.9800	C(61)-H(61A)	0.9500
C(55)-H(55B)	0.9800	C(62)-C(63)	1.382(7)
C(55)-H(55C)	0.9800	C(62)-H(62A)	0.9500
C(54B)-H(54D)	0.9800	C(63)-C(64)	1.403(6)
C(54B)-H(54E)	0.9800	C(63)-H(63A)	0.9500
C(54B)-H(54F)	0.9800	C(64)-C(68)	1.504(6)
C(55B)-H(55D)	0.9800	C(68)-C(69)	1.544(6)
C(65)-C(67)	1.531(6)	C(68)-H(68A)	1.0000
C(65)-C(66)	1.540(6)	C(69)-H(69A)	0.9800
C(65)-H(65A)	1.0000	C(69)-H(69D)	0.9800
C(66)-H(66A)	0.9800	C(69)-H(69B)	0.9800
C(66)-H(66B)	0.9800	C(70)-H(70D)	0.9800
C(66)-H(66C)	0.9800	C(70)-H(70A)	0.9800
C(67)-H(67A)	0.9800	C(70)-H(70B)	0.9800
C(67)-H(67B)	0.9800	C(68)-C(70)	1.533(6)
C(67)-H(67C)	0.9800		

C(1)-Pd(1)-C(28)	91.96(14)	C(44)-N(4)-C(46)	110.8(3)
C(1)-Pd(1)-Cl(2)	171.15(10)	C(44)-N(4)-C(59)	127.0(3)
C(28)-Pd(1)-Cl(2)	94.40(11)	C(46)-N(4)-C(59)	121.9(3)
C(1)-Pd(1)-Cl(1)	90.93(9)	N(2)-C(1)-N(1)	103.8(3)
C(28)-Pd(1)-Cl(1)	175.50(11)	N(2)-C(1)-Pd(1)	124.4(2)
Cl(2)-Pd(1)-Cl(1)	82.36(3)	N(1)-C(1)-Pd(1)	129.7(2)
C(44)-Pd(2)-C(36)	92.06(15)	C(3)-C(2)-N(1)	107.4(3)
C(44)-Pd(2)-Cl(2)	170.20(10)	C(3)-C(2)-H(2A)	126.3

Table 4.11. (cont.).

C(36)-Pd(2)-Cl(2)	94.58(11)	N(1)-C(2)-H(2A)	126.3
C(44)-Pd(2)-Cl(1)	90.23(10)	C(2)-C(3)-N(2)	106.9(3)
C(36)-Pd(2)-Cl(1)	176.69(11)	C(2)-C(3)-H(3A)	126.6
Cl(2)-Pd(2)-Cl(1)	82.85(3)	N(2)-C(3)-H(3A)	126.6
Pd(2)-Cl(1)-Pd(1)	93.84(3)	C(5)-C(4)-C(9)	122.6(3)
Pd(2)-Cl(2)-Pd(1)	100.89(3)	C(5)-C(4)-N(1)	119.0(3)
C(1)-N(1)-C(2)	110.8(3)	C(9)-C(4)-N(1)	118.2(3)
C(1)-N(1)-C(4)	126.1(3)	C(4)-C(5)-C(6)	117.2(4)
C(2)-N(1)-C(4)	122.8(3)	C(4)-C(5)-C(10)	123.3(4)
C(1)-N(2)-C(3)	111.1(3)	C(6)-C(5)-C(10)	119.4(4)
C(1)-N(2)-C(16)	124.8(3)	C(7)-C(6)-C(5)	121.7(4)
C(3)-N(2)-C(16)	123.4(3)	C(7)-C(6)-H(6A)	119.1
C(44)-N(3)-C(45)	110.6(3)	C(5)-C(6)-H(6A)	119.1
C(44)-N(3)-C(47)	126.2(3)	C(6)-C(7)-C(8)	120.0(4)
C(45)-N(3)-C(47)	122.9(3)	H(12A)-C(12)-H(12B)	109.5
C(6)-C(7)-H(7A)	120.0	C(10)-C(12)-H(12C)	109.5
C(8)-C(7)-H(7A)	120.0	H(12A)-C(12)-H(12C)	109.5
C(7)-C(8)-C(9)	121.4(4)	H(12B)-C(12)-H(12C)	109.5
C(7)-C(8)-H(8A)	119.3	C(9)-C(13)-C(15)	114.0(3)
C(9)-C(8)-H(8A)	119.3	C(9)-C(13)-C(14)	110.1(3)
C(8)-C(9)-C(4)	116.9(4)	C(15)-C(13)-C(14)	108.7(4)
C(8)-C(9)-C(13)	120.9(4)	C(9)-C(13)-H(13A)	108.0
C(4)-C(9)-C(13)	122.0(3)	C(15)-C(13)-H(13A)	108.0
C(5)-C(10)-C(12)	114.1(4)	C(14)-C(13)-H(13A)	108.0
C(5)-C(10)-C(11)	109.4(4)	C(13)-C(14)-H(14A)	109.5
C(12)-C(10)-C(11)	109.4(4)	C(13)-C(14)-H(14B)	109.5
C(5)-C(10)-H(10A)	107.9	H(14A)-C(14)-H(14B)	109.5
C(12)-C(10)-H(10A)	107.9	C(13)-C(14)-H(14C)	109.5
C(11)-C(10)-H(10A)	107.9	H(14A)-C(14)-H(14C)	109.5
C(10)-C(11)-H(11A)	109.5	H(14B)-C(14)-H(14C)	109.5
C(10)-C(11)-H(11B)	109.5	C(13)-C(15)-H(15A)	109.5
H(11A)-C(11)-H(11B)	109.5	C(13)-C(15)-H(15B)	109.5
C(10)-C(11)-H(11C)	109.5	H(15A)-C(15)-H(15B)	109.5
H(11A)-C(11)-H(11C)	109.5	C(13)-C(15)-H(15C)	109.5
H(11B)-C(11)-H(11C)	109.5	H(15A)-C(15)-H(15C)	109.5
C(10)-C(12)-H(12A)	109.5	H(15B)-C(15)-H(15C)	109.5
C(10)-C(12)-H(12B)	109.5	C(23)-C(22)-H(22A)	107.8
C(17)-C(16)-C(21)	122.8(3)	C(24)-C(22)-H(22A)	107.8
C(17)-C(16)-N(2)	117.2(3)	C(22)-C(23)-H(23A)	109.5
C(21)-C(16)-N(2)	119.9(3)	C(22)-C(23)-H(23B)	109.5
C(18)-C(17)-C(16)	117.8(4)	H(23A)-C(23)-H(23B)	109.5
C(18)-C(17)-C(22)	120.2(3)	C(22)-C(23)-H(23C)	109.5
C(16)-C(17)-C(22)	122.0(3)	H(23A)-C(23)-H(23C)	109.5
C(19)-C(18)-C(17)	120.8(4)	H(23B)-C(23)-H(23C)	109.5
C(19)-C(18)-H(18A)	119.6	C(22)-C(24)-H(24A)	109.5
C(17)-C(18)-H(18A)	119.6	C(22)-C(24)-H(24B)	109.5
C(18)-C(19)-C(20)	120.3(4)	H(24A)-C(24)-H(24B)	109.5
C(18)-C(19)-H(19A)	119.9	C(22)-C(24)-H(24C)	109.5
C(20)-C(19)-H(19A)	119.9	H(24A)-C(24)-H(24C)	109.5
C(19)-C(20)-C(21)	121.7(4)	H(24B)-C(24)-H(24C)	109.5
C(19)-C(20)-H(20A)	119.2	C(21)-C(25)-C(26)	112.9(4)
C(21)-C(20)-H(20A)	119.2	C(21)-C(25)-C(27)	109.5(3)
C(20)-C(21)-C(16)	116.7(4)	C(26)-C(25)-C(27)	110.7(4)
C(20)-C(21)-C(25)	120.8(4)	C(21)-C(25)-H(25A)	107.8
C(16)-C(21)-C(25)	122.4(3)	C(26)-C(25)-H(25A)	107.8

Table 4.11. (cont).

C(17)-C(22)-C(23)	111.3(3)	C(27)-C(25)-H(25A)	107.8
C(17)-C(22)-C(24)	112.8(3)	C(25)-C(26)-H(26A)	109.5
C(23)-C(22)-C(24)	109.2(3)	C(25)-C(26)-H(26B)	109.5
C(17)-C(22)-H(22A)	107.8	C(29)-C(30)-C(31)	103.3(3)
H(26A)-C(26)-H(26B)	109.5	C(29)-C(30)-H(30A)	111.1
C(25)-C(26)-H(26C)	109.5	C(31)-C(30)-H(30A)	111.1
H(26A)-C(26)-H(26C)	109.5	C(29)-C(30)-H(30B)	111.1
H(26B)-C(26)-H(26C)	109.5	C(31)-C(30)-H(30B)	111.1
C(25)-C(27)-H(27A)	109.5	H(30A)-C(30)-H(30B)	109.1
C(25)-C(27)-H(27B)	109.5	C(30)-C(31)-C(32)	102.7(3)
H(27A)-C(27)-H(27B)	109.5	C(30)-C(31)-H(31A)	111.2
C(25)-C(27)-H(27C)	109.5	C(32)-C(31)-H(31A)	111.2
H(27A)-C(27)-H(27C)	109.5	C(30)-C(31)-H(31B)	111.2
H(27B)-C(27)-H(27C)	109.5	C(32)-C(31)-H(31B)	111.2
C(33)-C(28)-C(29)	103.8(3)	H(31A)-C(31)-H(31B)	109.1
C(33)-C(28)-Pd(1)	116.5(2)	C(34)-C(32)-C(33)	102.0(3)
C(29)-C(28)-Pd(1)	113.5(2)	C(34)-C(32)-C(31)	101.1(4)
C(33)-C(28)-H(28A)	107.5	C(33)-C(32)-C(31)	108.9(3)
C(29)-C(28)-H(28A)	107.5	C(34)-C(32)-H(32A)	114.4
Pd(1)-C(28)-H(28A)	107.5	C(33)-C(32)-H(32A)	114.5
C(34)-C(29)-C(30)	99.6(3)	C(31)-C(32)-H(32A)	114.4
C(34)-C(29)-C(28)	103.7(3)	C(35)-C(33)-C(28)	116.0(3)
C(30)-C(29)-C(28)	106.7(3)	C(35)-C(33)-C(32)	111.4(3)
C(34)-C(29)-H(29A)	115.0	C(28)-C(33)-C(32)	102.1(3)
C(30)-C(29)-H(29A)	115.0	C(35)-C(33)-H(33A)	109.0
C(28)-C(29)-H(29A)	115.0	C(38)-C(37)-C(36)	106.4(4)
C(28)-C(33)-H(33A)	109.0	C(42)-C(37)-H(37A)	115.0
C(32)-C(33)-H(33A)	109.0	C(38)-C(37)-H(37A)	115.0
C(32)-C(34)-C(29)	94.4(3)	C(36)-C(37)-H(37A)	115.0
C(32)-C(34)-H(34A)	112.8	C(37)-C(38)-C(39)	102.5(4)
C(29)-C(34)-H(34A)	112.8	C(37)-C(38)-H(38A)	111.3
C(32)-C(34)-H(34B)	112.8	C(39)-C(38)-H(38A)	111.3
C(29)-C(34)-H(34B)	112.8	C(37)-C(38)-H(38B)	111.3
H(34A)-C(34)-H(34B)	110.3	C(39)-C(38)-H(38B)	111.3
C(33)-C(35)-H(35A)	109.5	H(38A)-C(38)-H(38B)	109.2
C(33)-C(35)-H(35B)	109.5	C(40)-C(39)-C(38)	103.2(4)
H(35A)-C(35)-H(35B)	109.5	C(40)-C(39)-H(39A)	111.1
C(33)-C(35)-H(35C)	109.5	C(38)-C(39)-H(39A)	111.1
H(35A)-C(35)-H(35C)	109.5	C(40)-C(39)-H(39B)	111.1
H(35B)-C(35)-H(35C)	109.5	C(38)-C(39)-H(39B)	111.1
C(41)-C(36)-C(37)	102.8(3)	H(39A)-C(39)-H(39B)	109.1
C(41)-C(36)-Pd(2)	115.6(3)	C(42)-C(40)-C(39)	101.6(4)
C(37)-C(36)-Pd(2)	114.5(3)	C(42)-C(40)-C(41)	101.9(3)
C(41)-C(36)-H(36A)	107.8	C(39)-C(40)-C(41)	108.7(4)
C(37)-C(36)-H(36A)	107.8	C(42)-C(40)-H(40A)	114.4
Pd(2)-C(36)-H(36A)	107.8	C(39)-C(40)-H(40A)	114.4
C(42)-C(37)-C(38)	99.8(4)	C(41)-C(40)-H(40A)	114.4
C(42)-C(37)-C(36)	103.9(3)	C(46)-C(45)-H(45A)	126.4
C(43)-C(41)-C(40)	111.2(4)	N(3)-C(45)-H(45A)	126.4
C(43)-C(41)-C(36)	116.5(3)	C(45)-C(46)-N(4)	107.1(3)
C(40)-C(41)-C(36)	102.3(3)	C(45)-C(46)-H(46A)	126.4
C(43)-C(41)-H(41A)	108.8	N(4)-C(46)-H(46A)	126.4
C(40)-C(41)-H(41A)	108.8	C(48)-C(47)-C(52)	122.9(4)
C(36)-C(41)-H(41A)	108.8	C(48)-C(47)-N(3)	119.7(4)
C(40)-C(42)-C(37)	94.7(3)	C(52)-C(47)-N(3)	117.4(3)

Table 4.11. (cont.).

C(40)-C(42)-H(42A)	112.8	C(49)-C(48)-C(47)	117.0(4)
C(37)-C(42)-H(42A)	112.8	C(49)-C(48)-C(53)	120.0(4)
C(40)-C(42)-H(42B)	112.8	C(47)-C(48)-C(53)	122.8(4)
C(37)-C(42)-H(42B)	112.8	C(50)-C(49)-C(48)	121.5(4)
H(42A)-C(42)-H(42B)	110.2	C(50)-C(49)-H(49A)	119.3
C(41)-C(43)-H(43A)	109.5	C(48)-C(49)-H(49A)	119.3
C(41)-C(43)-H(43B)	109.5	C(49)-C(50)-C(51)	120.4(4)
H(43A)-C(43)-H(43B)	109.5	C(49)-C(50)-H(50A)	119.8
C(41)-C(43)-H(43C)	109.5	C(51)-C(50)-H(50A)	119.8
H(43A)-C(43)-H(43C)	109.5	C(50)-C(51)-C(52)	121.1(4)
H(43B)-C(43)-H(43C)	109.5	C(50)-C(51)-H(51A)	119.5
N(4)-C(44)-N(3)	104.2(3)	C(52)-C(51)-H(51A)	119.5
N(4)-C(44)-Pd(2)	130.3(3)	C(51)-C(52)-C(47)	117.1(4)
N(3)-C(44)-Pd(2)	123.1(3)	C(51)-C(52)-C(56)	118.9(4)
C(46)-C(45)-N(3)	107.1(3)	C(53)-C(55)-H(55A)	109.5
C(47)-C(52)-C(56)	123.9(4)	C(53)-C(55)-H(55B)	109.5
C(48)-C(53)-C(55)	109.3(6)	C(53)-C(55)-H(55C)	109.5
C(48)-C(53)-C(55B)	108.7(10)	C(53)-C(54B)-H(54D)	109.5
C(48)-C(53)-C(54)	108.7(9)	C(53)-C(54B)-H(54E)	109.5
C(55)-C(53)-C(54)	110.0(6)	H(54D)-C(54B)-H(54E)	109.5
C(55B)-C(53)-C(54)	124.4(10)	C(53)-C(54B)-H(54F)	109.5
C(48)-C(53)-C(54B)	121.6(16)	H(54D)-C(54B)-H(54F)	109.5
C(55)-C(53)-C(54B)	97.3(12)	H(54E)-C(54B)-H(54F)	109.5
C(55B)-C(53)-C(54B)	110.5(10)	C(53)-C(55B)-H(55D)	109.5
C(48)-C(53)-H(53A)	109.6	C(53)-C(55B)-H(55E)	109.5
C(55)-C(53)-H(53A)	109.6	H(55D)-C(55B)-H(55E)	109.5
C(55B)-C(53)-H(53A)	94.5	C(53)-C(55B)-H(55F)	109.5
C(54)-C(53)-H(53A)	109.6	H(55D)-C(55B)-H(55F)	109.5
C(54B)-C(53)-H(53A)	108.5	H(55E)-C(55B)-H(55F)	109.5
C(48)-C(53)-H(53B)	105.9	C(58)-C(56)-C(52)	113.0(4)
C(55)-C(53)-H(53B)	118.1	C(58)-C(56)-C(57)	110.0(4)
C(55B)-C(53)-H(53B)	103.1	C(52)-C(56)-C(57)	110.0(4)
C(54)-C(53)-H(53B)	104.3	C(58)-C(56)-H(56A)	107.9
C(54B)-C(53)-H(53B)	105.3	C(52)-C(56)-H(56A)	107.9
C(53)-C(54)-H(54A)	109.5	C(57)-C(56)-H(56A)	107.9
C(53)-C(54)-H(54B)	109.5	C(56)-C(57)-H(57A)	109.5
C(53)-C(54)-H(54C)	109.5	C(63)-C(62)-H(62A)	119.8
C(56)-C(57)-H(57B)	109.5	C(62)-C(63)-C(64)	120.8(5)
H(57A)-C(57)-H(57B)	109.5	C(62)-C(63)-H(63A)	119.6
C(56)-C(57)-H(57C)	109.5	C(64)-C(63)-H(63A)	119.6
H(57A)-C(57)-H(57C)	109.5	C(63)-C(64)-C(59)	117.1(4)
H(57B)-C(57)-H(57C)	109.5	C(63)-C(64)-C(68)	119.0(4)
C(56)-C(58)-H(58A)	109.5	C(59)-C(64)-C(68)	123.9(4)
C(56)-C(58)-H(58B)	109.5	C(60)-C(65)-C(67)	110.5(4)
H(58A)-C(58)-H(58B)	109.5	C(60)-C(65)-C(66)	113.2(4)
C(56)-C(58)-H(58C)	109.5	C(67)-C(65)-C(66)	108.2(4)
H(58A)-C(58)-H(58C)	109.5	C(60)-C(65)-H(65A)	108.3
H(58B)-C(58)-H(58C)	109.5	C(67)-C(65)-H(65A)	108.3
C(64)-C(59)-C(60)	122.3(4)	C(66)-C(65)-H(65A)	108.3
C(64)-C(59)-N(4)	119.5(3)	C(65)-C(66)-H(66A)	109.5
C(60)-C(59)-N(4)	117.9(4)	C(65)-C(66)-H(66B)	109.5
C(61)-C(60)-C(59)	116.7(4)	H(66A)-C(66)-H(66B)	109.5
C(61)-C(60)-C(65)	121.3(4)	C(65)-C(66)-H(66C)	109.5
C(59)-C(60)-C(65)	121.9(4)	H(66A)-C(66)-H(66C)	109.5
C(62)-C(61)-C(60)	122.4(5)	H(66B)-C(66)-H(66C)	109.5

Table 4.11. (cont).

C(62)-C(61)-H(61A)	118.8	C(65)-C(67)-H(67A)	109.5
C(60)-C(61)-H(61A)	118.8	C(65)-C(67)-H(67B)	109.5
C(61)-C(62)-C(63)	120.5(4)	H(67A)-C(67)-H(67B)	109.5
C(61)-C(62)-H(62A)	119.8	C(68)-C(69)-H(69A)	109.5
C(65)-C(67)-H(67C)	109.5	C(68)-C(69)-H(69D)	109.5
H(67A)-C(67)-H(67C)	109.5	H(69A)-C(69)-H(69D)	109.5
H(67B)-C(67)-H(67C)	109.5	C(68)-C(69)-H(69B)	109.5
C(64)-C(68)-C(70)	113.3(4)	H(69A)-C(69)-H(69B)	109.5
C(64)-C(68)-C(69)	110.8(4)	H(69D)-C(69)-H(69B)	109.5
C(70)-C(68)-C(69)	108.4(4)	C(68)-C(70)-H(70D)	109.5
C(64)-C(68)-H(68A)	108.1	C(68)-C(70)-H(70A)	109.5
C(70)-C(68)-H(68A)	108.1	H(70D)-C(70)-H(70A)	109.5
C(69)-C(68)-H(68A)	108.1	C(68)-C(70)-H(70B)	109.5
H(70A)-C(70)-H(70B)	109.5	H(70D)-C(70)-H(70B)	109.5

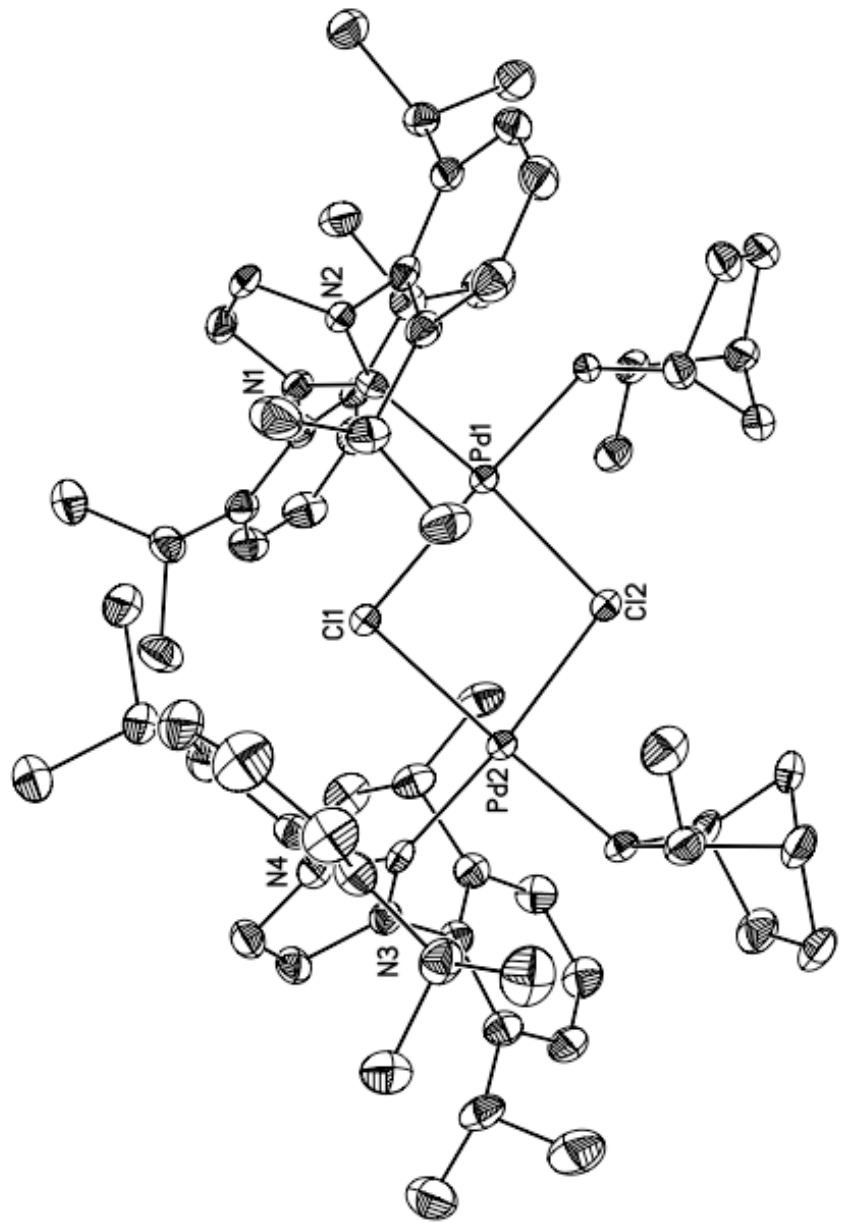


Figure 4.7. ORTEP drawing **4.08** with 35% probability ellipsoids

4.4.10 Crystallographic Data for 4.09

Table 4.12. Crystal data and structure refinement for 4.09.

Identification code	4.09
Empirical formula	C ₁₇₃ H ₂₄₀ N ₁₂ Pd ₄
Formula weight	2913.37
Temperature	183(2) K
Wavelength	0.71073 Å
Crystal system	Monoclinic
Space group	P2(1)/n
Unit cell dimensions	a = 10.517(5) Å b = 22.963(11) Å c = 32.741(16) Å
Volume	7835(7) Å ³
Z	2
Density (calculated)	1.235 Mg/m ³
Absorption coefficient	0.506 mm ⁻¹
F(000)	3092
Crystal size	0.56 x 0.23 x 0.099 mm ³
Theta range for data collection	1.09 to 25.37°
Index ranges	-12<=h<=12, -27<=k<=27, -39<=l<=39
Reflections collected	74015
Independent reflections	14240 [R(int) = 0.0886]
Completeness to theta = 25.37°	99.1 %
Absorption correction	Integration
Max. and min. transmission	0.9688 and 0.8744
Refinement method	Full-matrix least-squares on F ²
Data / restraints / parameters	14240 / 477 / 949
Goodness-of-fit on F ²	1.061
Final R indices [I>2sigma(I)]	R1 = 0.0468, wR2 = 0.0979
R indices (all data)	R1 = 0.0791, wR2 = 0.1081
Largest diff. peak and hole	0.882 and -0.523 e.Å ⁻³

Table 4.13. Atomic coordinates ($\times 10^4$) and equivalent isotropic displacement parameters ($\text{\AA}^2 \times 10^3$) for **4.09**. U(eq) is defined as one third of the trace of the orthogonalized U^{ij} tensor.

	x	y	z	U(eq)
Pd(1)	3060(1)	1814(1)	549(1)	36(1)
N(1)	4578(3)	2172(2)	331(1)	49(1)
N(2)	262(3)	1670(1)	357(1)	31(1)
N(3)	729(3)	1507(1)	1008(1)	33(1)
C(1)	3723(3)	1040(2)	810(1)	40(1)
C(2)	4417(4)	680(2)	504(1)	50(1)
C(3)	4428(4)	52(2)	649(1)	61(1)
C(4)	5382(4)	71(2)	1062(2)	68(1)
C(5)	5817(4)	698(2)	1090(1)	62(1)
C(6)	4730(4)	1088(2)	1203(1)	52(1)
C(7)	5839(4)	854(2)	637(1)	64(1)
C(8)	5211(5)	1692(2)	1334(1)	73(2)
C(9)	5086(12)	2031(8)	-24(3)	43(2)
C(10)	6328(11)	2187(6)	-80(3)	48(2)
C(11)	6815(10)	2023(5)	-437(3)	51(2)
C(12)	6059(11)	1702(5)	-738(2)	41(2)
C(13)	4817(11)	1546(5)	-682(3)	42(2)
C(14)	4331(11)	1710(7)	-325(3)	43(2)
C(15)	6577(14)	1504(6)	-1130(3)	58(3)
C(9B)	4970(20)	1995(14)	-54(5)	46(2)
C(10B)	6190(20)	2112(11)	-145(5)	46(2)
C(11B)	6563(16)	1918(9)	-514(5)	47(2)
C(12B)	5703(19)	1608(8)	-792(4)	45(3)
C(13B)	4475(18)	1492(9)	-701(5)	44(2)
C(14B)	4106(18)	1685(13)	-332(6)	45(2)
C(15B)	6120(30)	1401(10)	-1205(5)	65(4)
C(16)	1291(3)	1636(2)	662(1)	33(1)
C(17)	-893(3)	1566(2)	508(1)	40(1)
C(18)	-603(3)	1469(2)	912(1)	38(1)
C(19)	374(3)	1870(2)	-60(1)	34(1)
C(20)	467(3)	1457(2)	-363(1)	40(1)
C(21)	541(4)	1668(2)	-762(1)	52(1)
C(22)	516(4)	2256(2)	-840(1)	62(1)
C(23)	440(4)	2651(2)	-531(1)	53(1)
C(24)	358(3)	2470(2)	-130(1)	42(1)
C(25)	456(4)	810(2)	-278(1)	48(1)
C(26)	-929(4)	577(2)	-382(1)	63(1)
C(27)	1388(5)	460(2)	-501(1)	66(1)
C(28)	249(3)	2913(2)	204(1)	48(1)
C(29)	-872(13)	3320(7)	29(8)	66(4)
C(30)	1476(12)	3265(8)	345(7)	50(4)
C(29B)	-929(14)	3323(8)	173(10)	51(5)
C(30B)	1501(15)	3271(10)	242(10)	56(5)
C(31)	1405(3)	1467(2)	1424(1)	36(1)
C(32)	1988(4)	1972(2)	1608(1)	42(1)
C(33)	2616(4)	1915(2)	2007(1)	53(1)
C(34)	2622(4)	1396(2)	2222(1)	58(1)

Table 4.13. (cont.)

C(35)	2010(4)	917(2)	2039(1)	53(1)
C(36)	1400(4)	936(2)	1631(1)	40(1)
C(37)	1816(4)	2565(2)	1400(1)	50(1)
C(38)	432(7)	2797(6)	1376(5)	58(3)
C(39)	2791(10)	3024(5)	1588(6)	53(3)
C(38B)	572(14)	2822(8)	1528(8)	54(5)
C(39B)	2929(17)	3004(10)	1493(10)	81(7)
C(40)	756(4)	389(2)	1447(1)	40(1)
C(41)	-470(4)	253(2)	1640(1)	56(1)
C(42)	1656(4)	-135(2)	1502(1)	50(1)
Pd(2)	6928(1)	526(1)	3472(1)	35(1)
N(4)	5427(3)	922(1)	3680(1)	43(1)
N(5)	9531(3)	765(1)	3306(1)	29(1)
N(6)	9412(3)	-166(1)	3316(1)	32(1)
C(43)	6086(3)	-43(2)	3043(1)	41(1)
C(44)	4969(4)	246(2)	2757(1)	46(1)
C(45)	4762(4)	-123(2)	2361(1)	56(1)
C(46)	4194(4)	-707(2)	2508(1)	67(1)
C(47)	4093(4)	-579(2)	2967(1)	57(1)
C(48)	5427(4)	-589(2)	3218(1)	52(1)
C(49)	3783(3)	77(2)	2949(1)	48(1)
C(50)	5349(4)	-585(2)	3682(1)	68(1)
C(51)	4719(3)	1383(2)	3503(1)	35(1)
C(52)	3499(3)	1528(2)	3601(1)	42(1)
C(53)	2812(4)	2000(2)	3421(1)	42(1)
C(54)	3290(4)	2356(2)	3135(1)	37(1)
C(55)	4503(4)	2217(2)	3038(1)	40(1)
C(56)	5203(3)	1745(2)	3214(1)	37(1)
C(57)	2527(4)	2865(2)	2941(1)	53(1)
C(58)	8684(3)	320(2)	3349(1)	29(1)
C(59)	10735(3)	561(2)	3259(1)	34(1)
C(60)	10663(3)	-20(2)	3266(1)	36(1)
C(61)	9199(3)	1374(2)	3347(1)	30(1)
C(62)	9152(4)	1593(2)	3744(1)	38(1)
C(63)	8841(4)	2180(2)	3774(1)	50(1)
C(64)	8610(4)	2525(2)	3430(1)	50(1)
C(65)	8649(4)	2290(2)	3043(1)	46(1)
C(66)	8940(3)	1710(2)	2990(1)	33(1)
C(67)	9453(4)	1232(2)	4133(1)	47(1)
C(68)	10784(4)	1370(2)	4351(1)	75(2)
C(69)	8463(5)	1314(3)	4429(1)	86(2)
C(70)	8924(4)	1448(2)	2561(1)	42(1)
C(71)	9238(5)	1872(2)	2242(1)	71(2)
C(72)	7582(4)	1169(2)	2421(1)	72(2)
C(73)	8979(3)	-757(2)	3359(1)	37(1)
C(74)	8695(4)	-1098(2)	3006(1)	44(1)
C(75)	8271(4)	-1667(2)	3060(2)	60(1)
C(76)	8146(4)	-1870(2)	3447(2)	66(1)
C(77)	8445(4)	-1539(2)	3787(2)	58(1)
C(78)	8906(4)	-969(2)	3759(1)	46(1)
C(79)	8873(4)	-879(2)	2580(1)	49(1)
C(80)	10188(4)	-1064(2)	2467(1)	63(1)
C(81)	7821(4)	-1085(2)	2237(1)	68(1)
C(82)	9381(4)	-628(2)	4141(1)	59(1)
C(83)	10491(8)	-980(5)	4390(2)	87(3)

Table 4.13. (cont.)

C(84)	8409(7)	-452(5)	4427(3)	89(3)
C(83B)	10826(8)	-618(15)	4284(7)	94(7)
C(84B)	8580(20)	-786(14)	4485(6)	83(7)

Table 4.14. Bond lengths [Å] and angles [°] for **4.09**.

Pd(1)-C(16)	1.988(4)	C(4)-H(4B)	0.9900
Pd(1)-N(1)	2.011(3)	C(5)-C(7)	1.527(6)
Pd(1)-C(1)	2.053(4)	C(5)-C(6)	1.538(6)
N(1)-C(9)	1.382(5)	C(5)-H(5A)	1.0000
N(1)-C(9B)	1.436(7)	C(6)-C(8)	1.517(6)
N(1)-H(1A)	0.8800	C(6)-H(6A)	1.0000
N(2)-C(16)	1.371(4)	C(7)-H(7A)	0.9900
N(2)-C(17)	1.394(4)	C(7)-H(7B)	0.9900
N(2)-C(19)	1.459(4)	C(8)-H(8A)	0.9800
N(3)-C(16)	1.379(4)	C(8)-H(8B)	0.9800
N(3)-C(18)	1.397(4)	C(8)-H(8C)	0.9800
N(3)-C(31)	1.450(4)	C(9)-C(10)	1.3900
C(1)-C(2)	1.555(5)	C(9)-C(14)	1.3900
C(1)-C(6)	1.558(5)	C(10)-C(11)	1.3900
C(1)-H(1B)	1.0000	C(10)-H(10A)	0.9500
C(2)-C(3)	1.520(6)	C(11)-C(12)	1.3900
C(2)-C(7)	1.553(6)	C(11)-H(11A)	0.9500
C(2)-H(2A)	1.0000	C(12)-C(13)	1.3900
C(3)-C(4)	1.570(6)	C(12)-C(15)	1.531(6)
C(3)-H(3A)	0.9900	C(13)-C(14)	1.3900
C(3)-H(3B)	0.9900	C(13)-H(13A)	0.9500
C(4)-C(5)	1.509(6)	C(14)-H(14A)	0.9500
C(4)-H(4A)	0.9900	C(20)-C(21)	1.405(5)
C(15)-H(15A)	0.9800	C(20)-C(25)	1.512(5)
C(15)-H(15B)	0.9800	C(21)-C(22)	1.374(6)
C(15)-H(15C)	0.9800	C(21)-H(21A)	0.9500
C(9B)-C(10B)	1.3900	C(22)-C(23)	1.367(6)
C(9B)-C(14B)	1.3900	C(22)-H(22A)	0.9500
C(10B)-C(11B)	1.3900	C(23)-C(24)	1.390(5)
C(10B)-H(10B)	0.9500	C(23)-H(23A)	0.9500
C(11B)-C(12B)	1.3900	C(24)-C(28)	1.511(5)
C(11B)-H(11B)	0.9500	C(25)-C(27)	1.529(6)
C(12B)-C(13B)	1.3900	C(25)-C(26)	1.546(6)
C(12B)-C(15B)	1.552(8)	C(25)-H(25A)	1.0000
C(13B)-C(14B)	1.3900	C(26)-H(26A)	0.9800
C(13B)-H(13B)	0.9500	C(26)-H(26B)	0.9800
C(14B)-H(14B)	0.9500	C(26)-H(26C)	0.9800
C(15B)-H(15D)	0.9800	C(27)-H(27A)	0.9800
C(15B)-H(15E)	0.9800	C(27)-H(27B)	0.9800
C(15B)-H(15F)	0.9800	C(27)-H(27C)	0.9800
C(17)-C(18)	1.335(5)	C(28)-C(30)	1.540(6)
C(17)-H(17A)	0.9500	C(28)-C(30B)	1.544(7)
C(18)-H(18A)	0.9500	C(28)-C(29B)	1.548(7)
C(19)-C(20)	1.388(5)	C(28)-C(29)	1.552(6)
C(19)-C(24)	1.397(5)	C(35)-H(35A)	0.9500
C(28)-H(28A)	1.0000	C(36)-C(40)	1.512(5)
C(29)-H(29A)	0.9800	C(37)-C(39)	1.539(6)
C(29)-H(29B)	0.9800	C(37)-C(38)	1.541(6)
C(29)-H(29C)	0.9800	C(37)-C(39B)	1.543(7)
C(30)-H(30A)	0.9800	C(37)-C(38B)	1.543(7)
C(30)-H(30B)	0.9800	C(37)-H(37A)	1.0000
C(30)-H(30C)	0.9800	C(38)-H(38A)	0.9800
C(29B)-H(29D)	0.9800	C(38)-H(38B)	0.9800

Table 4.14. (cont.)

C(29B)-H(29E)	0.9800	C(38)-H(38C)	0.9800
C(29B)-H(29F)	0.9800	C(39)-H(39A)	0.9800
C(30B)-H(30D)	0.9800	C(39)-H(39B)	0.9800
C(30B)-H(30E)	0.9800	C(39)-H(39C)	0.9800
C(30B)-H(30F)	0.9800	C(38B)-H(38D)	0.9800
C(31)-C(36)	1.395(5)	C(38B)-H(38E)	0.9800
C(31)-C(32)	1.409(5)	C(38B)-H(38F)	0.9800
C(32)-C(33)	1.388(5)	C(39B)-H(39D)	0.9800
C(32)-C(37)	1.523(5)	C(39B)-H(39E)	0.9800
C(33)-C(34)	1.382(6)	C(39B)-H(39F)	0.9800
C(33)-H(33A)	0.9500	C(40)-C(42)	1.527(5)
C(34)-C(35)	1.371(6)	C(40)-C(41)	1.543(5)
C(34)-H(34A)	0.9500	C(40)-H(40A)	1.0000
C(35)-C(36)	1.403(5)	C(44)-H(44A)	1.0000
C(41)-H(41A)	0.9800	C(45)-C(46)	1.570(6)
C(41)-H(41B)	0.9800	C(45)-H(45A)	0.9900
C(41)-H(41C)	0.9800	C(45)-H(45B)	0.9900
C(42)-H(42A)	0.9800	C(46)-C(47)	1.546(6)
C(42)-H(42B)	0.9800	C(46)-H(46A)	0.9900
C(42)-H(42C)	0.9800	C(46)-H(46B)	0.9900
Pd(2)-C(58)	2.001(3)	C(47)-C(48)	1.527(5)
Pd(2)-N(4)	2.018(3)	C(47)-C(49)	1.541(6)
Pd(2)-C(43)	2.032(4)	C(47)-H(47A)	1.0000
N(4)-C(51)	1.376(5)	C(48)-C(50)	1.534(6)
N(4)-H(4C)	0.8800	C(48)-H(48A)	1.0000
N(5)-C(58)	1.375(4)	C(49)-H(49A)	0.9900
N(5)-C(59)	1.378(4)	C(49)-H(49B)	0.9900
N(5)-C(61)	1.451(4)	C(50)-H(50A)	0.9800
N(6)-C(58)	1.367(4)	C(50)-H(50B)	0.9800
N(6)-C(60)	1.389(4)	C(50)-H(50C)	0.9800
N(6)-C(73)	1.443(5)	C(51)-C(52)	1.404(5)
C(43)-C(44)	1.549(5)	C(51)-C(56)	1.406(5)
C(43)-C(48)	1.577(5)	C(52)-C(53)	1.388(5)
C(43)-H(43A)	1.0000	C(52)-H(52A)	0.9500
C(44)-C(49)	1.520(5)	C(53)-C(54)	1.389(5)
C(44)-C(45)	1.539(5)	C(66)-C(70)	1.524(5)
C(53)-H(53A)	0.9500	C(67)-C(68)	1.516(6)
C(54)-C(55)	1.393(5)	C(67)-C(69)	1.526(6)
C(54)-C(57)	1.508(5)	C(67)-H(67A)	1.0000
C(55)-C(56)	1.391(5)	C(68)-H(68A)	0.9800
C(55)-H(55A)	0.9500	C(68)-H(68B)	0.9800
C(56)-H(56A)	0.9500	C(68)-H(68C)	0.9800
C(57)-H(57A)	0.9800	C(69)-H(69A)	0.9800
C(57)-H(57B)	0.9800	C(69)-H(69B)	0.9800
C(57)-H(57C)	0.9800	C(69)-H(69C)	0.9800
C(59)-C(60)	1.336(5)	C(70)-C(71)	1.498(5)
C(59)-H(59A)	0.9500	C(70)-C(72)	1.561(5)
C(60)-H(60A)	0.9500	C(70)-H(70A)	1.0000
C(61)-C(66)	1.398(5)	C(71)-H(71A)	0.9800
C(61)-C(62)	1.402(5)	C(71)-H(71B)	0.9800
C(62)-C(63)	1.392(5)	C(71)-H(71C)	0.9800
C(62)-C(67)	1.516(5)	C(72)-H(72A)	0.9800
C(63)-C(64)	1.372(5)	C(72)-H(72B)	0.9800
C(63)-H(63A)	0.9500	C(72)-H(72C)	0.9800
C(64)-C(65)	1.384(5)	C(73)-C(74)	1.395(5)

Table 4.14. (cont.)

C(64)-H(64A)	0.9500	C(73)-C(78)	1.408(5)
C(65)-C(66)	1.385(5)	C(74)-C(75)	1.399(6)
C(65)-H(65A)	0.9500	C(82)-H(82B)	0.9602
C(74)-C(79)	1.518(6)	C(83)-H(83A)	0.9800
C(75)-C(76)	1.372(6)	C(83)-H(83B)	0.9800
C(75)-H(75A)	0.9500	C(83)-H(83C)	0.9800
C(76)-C(77)	1.351(6)	C(84)-H(84A)	0.9800
C(76)-H(76A)	0.9500	C(84)-H(84B)	0.9800
C(77)-C(78)	1.404(6)	C(84)-H(84C)	0.9800
C(77)-H(77A)	0.9500	C(83B)-H(83D)	0.9800
C(78)-C(82)	1.503(6)	C(83B)-H(83E)	0.9800
C(79)-C(80)	1.539(5)	C(83B)-H(83F)	0.9800
C(79)-C(81)	1.540(5)	C(84B)-H(84D)	0.9800
C(79)-H(79A)	1.0000	C(84B)-H(84E)	0.9800
C(80)-H(80A)	0.9800	C(84B)-H(84F)	0.9800
C(80)-H(80B)	0.9800	C(82)-C(83B)	1.528(7)
C(80)-H(80C)	0.9800	C(82)-C(84)	1.530(6)
C(81)-H(81A)	0.9800	C(82)-C(84B)	1.536(7)
C(81)-H(81B)	0.9800	C(82)-C(83)	1.556(6)
C(81)-H(81C)	0.9800	C(82)-H(82A)	1.0000
C(16)-Pd(1)-N(1)	163.42(13)	C(3)-C(2)-H(2A)	115.3
C(16)-Pd(1)-C(1)	91.05(15)	C(7)-C(2)-H(2A)	115.3
N(1)-Pd(1)-C(1)	105.06(14)	C(1)-C(2)-H(2A)	115.3
C(9)-N(1)-Pd(1)	128.2(6)	C(2)-C(3)-C(4)	102.8(4)
C(9B)-N(1)-Pd(1)	122.0(10)	C(2)-C(3)-H(3A)	111.2
C(9)-N(1)-H(1A)	115.9	C(4)-C(3)-H(3A)	111.2
C(9B)-N(1)-H(1A)	122.1	C(2)-C(3)-H(3B)	111.2
Pd(1)-N(1)-H(1A)	115.9	C(4)-C(3)-H(3B)	111.2
C(16)-N(2)-C(17)	111.7(3)	H(3A)-C(3)-H(3B)	109.1
C(16)-N(2)-C(19)	122.9(3)	C(5)-C(4)-C(3)	103.4(4)
C(17)-N(2)-C(19)	124.9(3)	C(5)-C(4)-H(4A)	111.1
C(16)-N(3)-C(18)	110.9(3)	C(3)-C(4)-H(4A)	111.1
C(16)-N(3)-C(31)	125.1(3)	C(5)-C(4)-H(4B)	111.1
C(18)-N(3)-C(31)	123.8(3)	C(3)-C(4)-H(4B)	111.1
C(2)-C(1)-C(6)	104.2(3)	H(4A)-C(4)-H(4B)	109.0
C(2)-C(1)-Pd(1)	110.8(3)	C(4)-C(5)-C(7)	102.1(4)
C(6)-C(1)-Pd(1)	115.9(3)	C(4)-C(5)-C(6)	110.0(4)
C(2)-C(1)-H(1B)	108.6	C(7)-C(5)-C(6)	101.9(3)
C(6)-C(1)-H(1B)	108.6	C(4)-C(5)-H(5A)	113.9
Pd(1)-C(1)-H(1B)	108.6	C(7)-C(5)-H(5A)	113.9
C(3)-C(2)-C(7)	100.9(3)	C(6)-C(5)-H(5A)	113.9
C(3)-C(2)-C(1)	106.6(3)	C(8)-C(6)-C(5)	111.8(4)
C(7)-C(2)-C(1)	101.6(3)	C(9)-C(10)-H(10A)	120.0
C(8)-C(6)-C(1)	117.5(3)	C(10)-C(11)-C(12)	120.0
C(5)-C(6)-C(1)	101.7(3)	C(10)-C(11)-H(11A)	120.0
C(8)-C(6)-H(6A)	108.5	C(12)-C(11)-H(11A)	120.0
C(5)-C(6)-H(6A)	108.5	C(11)-C(12)-C(13)	120.0
C(1)-C(6)-H(6A)	108.5	C(11)-C(12)-C(15)	121.3(5)
C(5)-C(7)-C(2)	94.2(3)	C(13)-C(12)-C(15)	118.7(5)
C(5)-C(7)-H(7A)	112.9	C(14)-C(13)-C(12)	120.0
C(2)-C(7)-H(7A)	112.9	C(14)-C(13)-H(13A)	120.0
C(5)-C(7)-H(7B)	112.9	C(12)-C(13)-H(13A)	120.0
C(2)-C(7)-H(7B)	112.9	C(13)-C(14)-C(9)	120.0

Table 4.14. (cont.)

H(7A)-C(7)-H(7B)	110.3	C(13)-C(14)-H(14A)	120.0
C(6)-C(8)-H(8A)	109.5	C(9)-C(14)-H(14A)	120.0
C(6)-C(8)-H(8B)	109.5	C(10B)-C(9B)-C(14B)	120.0
H(8A)-C(8)-H(8B)	109.5	C(10B)-C(9B)-N(1)	121.0(13)
C(6)-C(8)-H(8C)	109.5	C(14B)-C(9B)-N(1)	118.9(14)
H(8A)-C(8)-H(8C)	109.5	C(11B)-C(10B)-C(9B)	120.0
H(8B)-C(8)-H(8C)	109.5	C(11B)-C(10B)-H(10B)	120.0
N(1)-C(9)-C(10)	121.8(8)	C(9B)-C(10B)-H(10B)	120.0
N(1)-C(9)-C(14)	118.2(8)	C(10B)-C(11B)-C(12B)	120.0
C(10)-C(9)-C(14)	120.0	C(10B)-C(11B)-H(11B)	120.0
C(11)-C(10)-C(9)	120.0	C(12B)-C(11B)-H(11B)	120.0
C(11)-C(10)-H(10A)	120.0	C(17)-C(18)-H(18A)	126.3
C(11B)-C(12B)-C(13B)	120.0	N(3)-C(18)-H(18A)	126.3
C(11B)-C(12B)-C(15B)	119.6(10)	C(20)-C(19)-C(24)	123.7(3)
C(13B)-C(12B)-C(15B)	120.4(9)	C(20)-C(19)-N(2)	118.5(3)
C(14B)-C(13B)-C(12B)	120.0	C(24)-C(19)-N(2)	117.7(3)
C(14B)-C(13B)-H(13B)	120.0	C(19)-C(20)-C(21)	116.7(4)
C(12B)-C(13B)-H(13B)	120.0	C(19)-C(20)-C(25)	122.4(3)
C(13B)-C(14B)-C(9B)	120.0	C(21)-C(20)-C(25)	120.9(4)
C(13B)-C(14B)-H(14B)	120.0	C(22)-C(21)-C(20)	120.6(4)
C(9B)-C(14B)-H(14B)	120.0	C(22)-C(21)-H(21A)	119.7
C(12B)-C(15B)-H(15D)	109.5	C(20)-C(21)-H(21A)	119.7
C(12B)-C(15B)-H(15E)	109.5	C(23)-C(22)-C(21)	121.1(4)
H(15D)-C(15B)-H(15E)	109.5	C(23)-C(22)-H(22A)	119.4
C(12B)-C(15B)-H(15F)	109.5	C(21)-C(22)-H(22A)	119.4
H(15D)-C(15B)-H(15F)	109.5	C(22)-C(23)-C(24)	121.1(4)
H(15E)-C(15B)-H(15F)	109.5	C(22)-C(23)-H(23A)	119.4
N(2)-C(16)-N(3)	103.2(3)	C(24)-C(23)-H(23A)	119.4
N(2)-C(16)-Pd(1)	121.2(2)	C(23)-C(24)-C(19)	116.8(4)
N(3)-C(16)-Pd(1)	135.4(2)	C(23)-C(24)-C(28)	120.3(4)
C(18)-C(17)-N(2)	106.7(3)	C(19)-C(24)-C(28)	122.9(3)
C(18)-C(17)-H(17A)	126.6	C(20)-C(25)-C(27)	114.1(4)
N(2)-C(17)-H(17A)	126.6	C(20)-C(25)-C(26)	109.2(3)
C(17)-C(18)-N(3)	107.5(3)	C(30)-C(28)-C(29)	111.1(7)
C(27)-C(25)-C(26)	110.9(4)	C(30B)-C(28)-C(29)	107.8(15)
C(20)-C(25)-H(25A)	107.4	C(24)-C(28)-H(28A)	108.3
C(27)-C(25)-H(25A)	107.4	C(30)-C(28)-H(28A)	108.3
C(26)-C(25)-H(25A)	107.4	C(30B)-C(28)-H(28A)	120.5
C(25)-C(26)-H(26A)	109.5	C(29B)-C(28)-H(28A)	92.7
C(25)-C(26)-H(26B)	109.5	C(29)-C(28)-H(28A)	108.3
H(26A)-C(26)-H(26B)	109.5	C(28)-C(29)-H(29A)	109.5
C(25)-C(26)-H(26C)	109.5	C(28)-C(29)-H(29B)	109.5
H(26A)-C(26)-H(26C)	109.5	C(28)-C(29)-H(29C)	109.5
H(26B)-C(26)-H(26C)	109.5	C(28)-C(30)-H(30A)	109.5
C(25)-C(27)-H(27A)	109.5	C(28)-C(30)-H(30B)	109.5
C(25)-C(27)-H(27B)	109.5	C(28)-C(30)-H(30C)	109.5
H(27A)-C(27)-H(27B)	109.5	C(28)-C(29B)-H(29D)	109.5
C(25)-C(27)-H(27C)	109.5	C(28)-C(29B)-H(29E)	109.5
H(27A)-C(27)-H(27C)	109.5	H(29D)-C(29B)-H(29E)	109.5
H(27B)-C(27)-H(27C)	109.5	C(28)-C(29B)-H(29F)	109.5
C(24)-C(28)-C(30)	115.3(10)	H(29D)-C(29B)-H(29F)	109.5
C(24)-C(28)-C(30B)	105.6(11)	H(29E)-C(29B)-H(29F)	109.5
C(24)-C(28)-C(29B)	120.0(11)	C(28)-C(30B)-H(30D)	109.5
C(30)-C(28)-C(29B)	109.4(14)	C(28)-C(30B)-H(30E)	109.5
C(30B)-C(28)-C(29B)	110.3(9)	H(30D)-C(30B)-H(30E)	109.5

Table 4.14. (cont.)

C(24)-C(28)-C(29)	105.3(10)	C(32)-C(37)-C(38)	112.7(6)
C(28)-C(30B)-H(30F)	109.5	C(39)-C(37)-C(38)	110.9(6)
H(30D)-C(30B)-H(30F)	109.5	C(32)-C(37)-C(39B)	117.0(12)
H(30E)-C(30B)-H(30F)	109.5	C(38)-C(37)-C(39B)	118.1(13)
C(36)-C(31)-C(32)	122.8(3)	C(32)-C(37)-C(38B)	106.0(7)
C(36)-C(31)-N(3)	118.6(3)	C(39)-C(37)-C(38B)	100.0(10)
C(32)-C(31)-N(3)	118.6(3)	C(39B)-C(37)-C(38B)	110.2(9)
C(33)-C(32)-C(31)	116.7(4)	C(32)-C(37)-H(37A)	106.3
C(33)-C(32)-C(37)	121.2(4)	C(39)-C(37)-H(37A)	106.3
C(31)-C(32)-C(37)	121.8(3)	C(38)-C(37)-H(37A)	106.3
C(34)-C(33)-C(32)	122.0(4)	C(39B)-C(37)-H(37A)	93.0
C(34)-C(33)-H(33A)	119.0	C(38B)-C(37)-H(37A)	124.8
C(32)-C(33)-H(33A)	119.0	C(37)-C(38)-H(38A)	109.5
C(35)-C(34)-C(33)	120.0(4)	C(37)-C(38)-H(38B)	109.5
C(35)-C(34)-H(34A)	120.0	H(38A)-C(38)-H(38B)	109.5
C(33)-C(34)-H(34A)	120.0	C(37)-C(38)-H(38C)	109.5
C(34)-C(35)-C(36)	121.2(4)	H(38A)-C(38)-H(38C)	109.5
C(34)-C(35)-H(35A)	119.4	H(38B)-C(38)-H(38C)	109.5
C(36)-C(35)-H(35A)	119.4	C(37)-C(39)-H(39A)	109.5
C(31)-C(36)-C(35)	117.3(4)	C(37)-C(39)-H(39B)	109.5
C(31)-C(36)-C(40)	124.3(3)	C(37)-C(39)-H(39C)	109.5
C(35)-C(36)-C(40)	118.4(4)	C(37)-C(38B)-H(38D)	109.5
C(32)-C(37)-C(39)	113.6(7)	H(41B)-C(41)-H(41C)	109.5
C(37)-C(38B)-H(38E)	109.5	C(40)-C(42)-H(42A)	109.5
H(38D)-C(38B)-H(38E)	109.5	C(40)-C(42)-H(42B)	109.5
C(37)-C(38B)-H(38F)	109.5	H(42A)-C(42)-H(42B)	109.5
H(38D)-C(38B)-H(38F)	109.5	C(40)-C(42)-H(42C)	109.5
H(38E)-C(38B)-H(38F)	109.5	H(42A)-C(42)-H(42C)	109.5
C(37)-C(39B)-H(39D)	109.5	H(42B)-C(42)-H(42C)	109.5
C(37)-C(39B)-H(39E)	109.5	C(58)-Pd(2)-N(4)	163.83(13)
H(39D)-C(39B)-H(39E)	109.5	C(58)-Pd(2)-C(43)	92.04(15)
C(37)-C(39B)-H(39F)	109.5	N(4)-Pd(2)-C(43)	103.67(14)
H(39D)-C(39B)-H(39F)	109.5	C(51)-N(4)-Pd(2)	127.4(2)
H(39E)-C(39B)-H(39F)	109.5	C(51)-N(4)-H(4C)	116.3
C(36)-C(40)-C(42)	111.8(3)	Pd(2)-N(4)-H(4C)	116.3
C(36)-C(40)-C(41)	111.1(3)	C(58)-N(5)-C(59)	112.0(3)
C(42)-C(40)-C(41)	109.3(3)	C(58)-N(5)-C(61)	122.6(3)
C(36)-C(40)-H(40A)	108.2	C(59)-N(5)-C(61)	125.1(3)
C(42)-C(40)-H(40A)	108.2	C(58)-N(6)-C(60)	111.1(3)
C(41)-C(40)-H(40A)	108.2	C(58)-N(6)-C(73)	124.9(3)
C(40)-C(41)-H(41A)	109.5	C(60)-N(6)-C(73)	123.7(3)
C(40)-C(41)-H(41B)	109.5	C(44)-C(43)-C(48)	103.0(3)
H(41A)-C(41)-H(41B)	109.5	C(44)-C(43)-Pd(2)	111.5(3)
C(40)-C(41)-H(41C)	109.5	C(48)-C(43)-Pd(2)	115.6(3)
H(41A)-C(41)-H(41C)	109.5	C(48)-C(47)-C(46)	109.9(4)
C(44)-C(43)-H(43A)	108.8	C(49)-C(47)-C(46)	101.0(4)
C(48)-C(43)-H(43A)	108.8	C(48)-C(47)-H(47A)	114.2
Pd(2)-C(43)-H(43A)	108.8	C(49)-C(47)-H(47A)	114.2
C(49)-C(44)-C(45)	100.2(3)	C(46)-C(47)-H(47A)	114.2
C(49)-C(44)-C(43)	103.8(3)	C(47)-C(48)-C(50)	111.4(4)
C(45)-C(44)-C(43)	106.5(3)	C(47)-C(48)-C(43)	102.1(3)
C(49)-C(44)-H(44A)	114.9	C(50)-C(48)-C(43)	116.1(3)
C(45)-C(44)-H(44A)	114.9	C(47)-C(48)-H(48A)	109.0
C(43)-C(44)-H(44A)	114.9	C(50)-C(48)-H(48A)	109.0
C(44)-C(45)-C(46)	103.2(3)	C(43)-C(48)-H(48A)	109.0

Table 4.14. (cont.)

C(44)-C(45)-H(45A)	111.1	C(44)-C(49)-C(47)	94.8(3)
C(46)-C(45)-H(45A)	111.1	C(44)-C(49)-H(49A)	112.8
C(44)-C(45)-H(45B)	111.1	C(47)-C(49)-H(49A)	112.8
C(46)-C(45)-H(45B)	111.1	C(44)-C(49)-H(49B)	112.8
H(45A)-C(45)-H(45B)	109.1	C(47)-C(49)-H(49B)	112.8
C(47)-C(46)-C(45)	102.4(3)	H(49A)-C(49)-H(49B)	110.2
C(47)-C(46)-H(46A)	111.3	C(48)-C(50)-H(50A)	109.5
C(45)-C(46)-H(46A)	111.3	C(48)-C(50)-H(50B)	109.5
C(47)-C(46)-H(46B)	111.3	H(50A)-C(50)-H(50B)	109.5
C(45)-C(46)-H(46B)	111.3	C(48)-C(50)-H(50C)	109.5
H(46A)-C(46)-H(46B)	109.2	H(50A)-C(50)-H(50C)	109.5
C(48)-C(47)-C(49)	102.0(3)	C(54)-C(57)-H(57C)	109.5
H(50B)-C(50)-H(50C)	109.5	H(57A)-C(57)-H(57C)	109.5
N(4)-C(51)-C(52)	123.0(3)	H(57B)-C(57)-H(57C)	109.5
N(4)-C(51)-C(56)	120.9(3)	N(6)-C(58)-N(5)	102.9(3)
C(52)-C(51)-C(56)	116.0(3)	N(6)-C(58)-Pd(2)	138.7(3)
C(53)-C(52)-C(51)	121.8(4)	N(5)-C(58)-Pd(2)	118.2(3)
C(53)-C(52)-H(52A)	119.1	C(60)-C(59)-N(5)	106.5(3)
C(51)-C(52)-H(52A)	119.1	C(60)-C(59)-H(59A)	126.8
C(52)-C(53)-C(54)	122.2(4)	N(5)-C(59)-H(59A)	126.8
C(52)-C(53)-H(53A)	118.9	C(59)-C(60)-N(6)	107.5(3)
C(54)-C(53)-H(53A)	118.9	C(59)-C(60)-H(60A)	126.3
C(53)-C(54)-C(55)	116.3(4)	N(6)-C(60)-H(60A)	126.3
C(53)-C(54)-C(57)	121.4(3)	C(66)-C(61)-C(62)	123.4(3)
C(55)-C(54)-C(57)	122.3(4)	C(66)-C(61)-N(5)	118.4(3)
C(56)-C(55)-C(54)	122.4(4)	C(62)-C(61)-N(5)	118.2(3)
C(56)-C(55)-H(55A)	118.8	C(63)-C(62)-C(61)	116.8(3)
C(54)-C(55)-H(55A)	118.8	C(63)-C(62)-C(67)	119.7(3)
C(55)-C(56)-C(51)	121.3(3)	C(61)-C(62)-C(67)	123.5(4)
C(55)-C(56)-H(56A)	119.3	C(64)-C(63)-C(62)	121.3(4)
C(51)-C(56)-H(56A)	119.3	C(64)-C(63)-H(63A)	119.3
C(54)-C(57)-H(57A)	109.5	C(62)-C(63)-H(63A)	119.3
C(54)-C(57)-H(57B)	109.5	C(63)-C(64)-C(65)	120.2(4)
H(57A)-C(57)-H(57B)	109.5	H(69A)-C(69)-H(69B)	109.5
C(63)-C(64)-H(64A)	119.9	C(67)-C(69)-H(69C)	109.5
C(65)-C(64)-H(64A)	119.9	H(69A)-C(69)-H(69C)	109.5
C(64)-C(65)-C(66)	121.6(4)	H(69B)-C(69)-H(69C)	109.5
C(64)-C(65)-H(65A)	119.2	C(71)-C(70)-C(66)	114.2(3)
C(66)-C(65)-H(65A)	119.2	C(71)-C(70)-C(72)	109.8(4)
C(65)-C(66)-C(61)	116.6(3)	C(66)-C(70)-C(72)	109.2(3)
C(65)-C(66)-C(70)	121.3(3)	C(71)-C(70)-H(70A)	107.8
C(61)-C(66)-C(70)	122.0(3)	C(66)-C(70)-H(70A)	107.8
C(62)-C(67)-C(68)	110.8(3)	C(72)-C(70)-H(70A)	107.8
C(62)-C(67)-C(69)	112.5(4)	C(70)-C(71)-H(71A)	109.5
C(68)-C(67)-C(69)	109.9(3)	C(70)-C(71)-H(71B)	109.5
C(62)-C(67)-H(67A)	107.8	H(71A)-C(71)-H(71B)	109.5
C(68)-C(67)-H(67A)	107.8	C(70)-C(71)-H(71C)	109.5
C(69)-C(67)-H(67A)	107.8	H(71A)-C(71)-H(71C)	109.5
C(67)-C(68)-H(68A)	109.5	H(71B)-C(71)-H(71C)	109.5
C(67)-C(68)-H(68B)	109.5	C(70)-C(72)-H(72A)	109.5
H(68A)-C(68)-H(68B)	109.5	C(70)-C(72)-H(72B)	109.5
C(67)-C(68)-H(68C)	109.5	H(72A)-C(72)-H(72B)	109.5
H(68A)-C(68)-H(68C)	109.5	C(70)-C(72)-H(72C)	109.5
H(68B)-C(68)-H(68C)	109.5	H(72A)-C(72)-H(72C)	109.5
C(67)-C(69)-H(69A)	109.5	H(72B)-C(72)-H(72C)	109.5

Table 4.14. (cont.)

C(67)-C(69)-H(69B)	109.5	C(80)-C(79)-H(79A)	107.8
C(74)-C(73)-C(78)	122.9(4)	C(81)-C(79)-H(79A)	107.8
C(74)-C(73)-N(6)	118.7(3)	C(79)-C(80)-H(80A)	109.5
C(78)-C(73)-N(6)	118.3(3)	C(79)-C(80)-H(80B)	109.5
C(73)-C(74)-C(75)	117.2(4)	H(80A)-C(80)-H(80B)	109.5
C(73)-C(74)-C(79)	122.4(4)	C(79)-C(80)-H(80C)	109.5
C(75)-C(74)-C(79)	120.4(4)	H(80A)-C(80)-H(80C)	109.5
C(76)-C(75)-C(74)	120.3(4)	H(80B)-C(80)-H(80C)	109.5
C(76)-C(75)-H(75A)	119.8	C(79)-C(81)-H(81A)	109.5
C(74)-C(75)-H(75A)	119.8	C(79)-C(81)-H(81B)	109.5
C(77)-C(76)-C(75)	122.0(5)	H(81A)-C(81)-H(81B)	109.5
C(77)-C(76)-H(76A)	119.0	C(79)-C(81)-H(81C)	109.5
C(75)-C(76)-H(76A)	119.0	H(81A)-C(81)-H(81C)	109.5
C(76)-C(77)-C(78)	120.9(4)	H(81B)-C(81)-H(81C)	109.5
C(76)-C(77)-H(77A)	119.5	C(78)-C(82)-C(83B)	117.9(10)
C(78)-C(77)-H(77A)	119.5	C(78)-C(82)-C(84)	118.1(5)
C(77)-C(78)-C(73)	116.5(4)	C(83B)-C(82)-C(84)	121.9(10)
C(77)-C(78)-C(82)	120.6(4)	C(78)-C(82)-C(84B)	109.5(10)
C(73)-C(78)-C(82)	122.7(4)	C(83B)-C(82)-C(84B)	113.4(10)
C(74)-C(79)-C(80)	110.9(3)	C(78)-C(82)-C(83)	107.8(4)
C(74)-C(79)-C(81)	113.7(4)	C(84)-C(82)-C(83)	109.4(5)
C(80)-C(79)-C(81)	108.7(4)	C(84B)-C(82)-C(83)	86.5(10)
C(74)-C(79)-H(79A)	107.8	C(82)-C(84)-H(84C)	109.5
C(78)-C(82)-H(82A)	107.0	H(82B)-C(84)-H(84C)	144.0
C(83B)-C(82)-H(82A)	69.8	C(82)-C(83B)-H(83D)	109.5
C(84)-C(82)-H(82A)	107.0	C(82)-C(83B)-H(83E)	109.5
C(84B)-C(82)-H(82A)	134.7	H(83D)-C(83B)-H(83E)	109.5
C(83)-C(82)-H(82A)	107.0	C(82)-C(83)-H(83C)	109.5
C(78)-C(82)-H(82B)	105.1	C(82)-C(84)-H(84A)	109.5
C(83B)-C(82)-H(82B)	104.3	H(82B)-C(84)-H(84A)	83.8
C(84)-C(82)-H(82B)	74.9	C(82)-C(84)-H(84B)	109.5
C(84B)-C(82)-H(82B)	105.4	H(82B)-C(84)-H(84B)	96.2
C(83)-C(82)-H(82B)	138.7	C(82)-C(83)-H(83B)	109.5
C(82)-C(83)-H(83A)	109.5	C(82)-C(84B)-H(84E)	109.5
C(82)-C(83B)-H(83F)	109.5	H(84D)-C(84B)-H(84E)	109.5
H(83D)-C(83B)-H(83F)	109.5	C(82)-C(84B)-H(84F)	109.5
H(83E)-C(83B)-H(83F)	109.5	H(84D)-C(84B)-H(84F)	109.5
C(82)-C(84B)-H(84D)	109.5	H(84E)-C(84B)-H(84F)	109.5

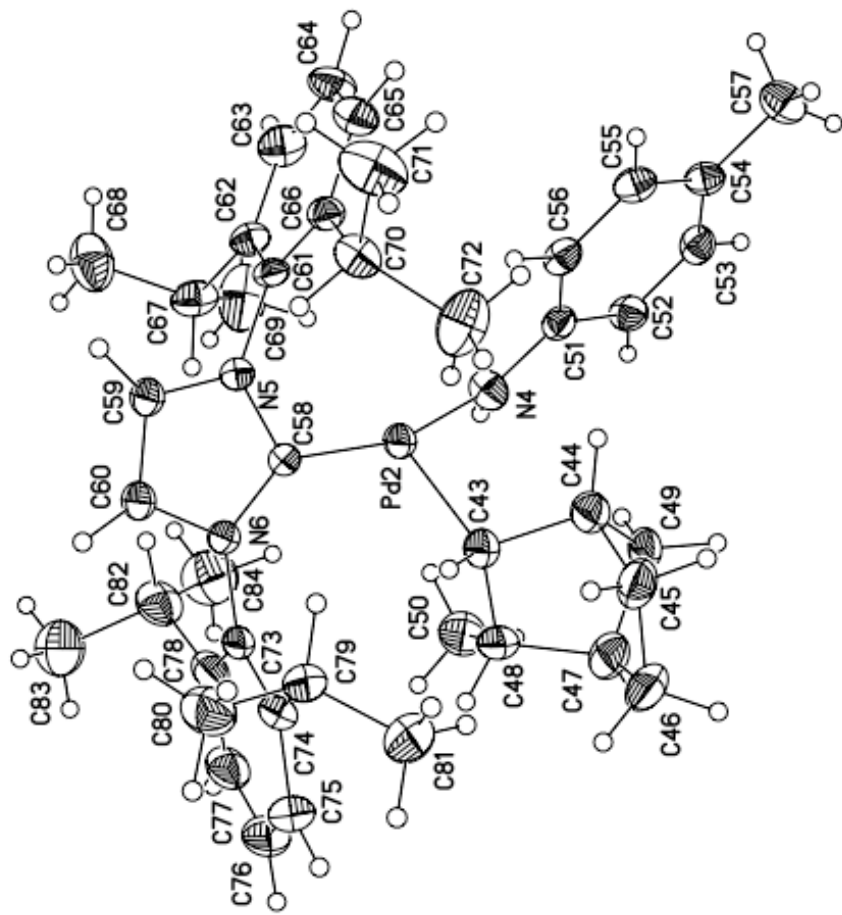


Figure 4.8. ORTEP drawing of **4.09** with 35% probability ellipsoids

4.4.11 Crystallographic Data for 4.14

Table 4.15. Crystal data and structure refinement for 4.14.

Identification code	4.14
Empirical formula	C ₉₄ H ₁₆₂ N ₄ P ₂ Pd ₄
Formula weight	1835.82
Temperature	193(2) K
Wavelength	0.71073 Å
Crystal system	Triclinic
Space group	P-1
Unit cell dimensions	a = 14.9127(3) Å b = 15.4821(3) Å c = 21.1941(4) Å
Volume	4667.86(16) Å ³
Z	2
Density (calculated)	1.306 Mg/m ³
Absorption coefficient	0.836 mm ⁻¹
F(000)	1936
Crystal size	0.536 x 0.23 x 0.222 mm ³
Theta range for data collection	1.36 to 25.39°.
Index ranges	-17<=h<=17, -18<=k<=18, -25<=l<=25
Reflections collected	64392
Independent reflections	17083 [R(int) = 0.0365]
Completeness to theta = 25.39°	99.5 %
Absorption correction	Integration
Max. and min. transmission	0.8909 and 0.8105
Refinement method	Full-matrix least-squares on F ²
Data / restraints / parameters	17083 / 1079 / 1169
Goodness-of-fit on F ²	1.080
Final R indices [I>2sigma(I)]	R1 = 0.0310, wR2 = 0.0787
R indices (all data)	R1 = 0.0392, wR2 = 0.0823
Largest diff. peak and hole	0.867 and -0.684 e.Å ⁻³

Table 4.16. Atomic coordinates ($\times 10^4$) and equivalent isotropic displacement parameters ($\text{\AA}^2 \times 10^3$) for **4.14**. U(eq) is defined as one third of the trace of the orthogonalized U^{ij} tensor.

	x	y	z	U(eq)
Pd(1)	10335(1)	6833(1)	3386(1)	37(1)
Pd(2)	8312(1)	7535(1)	3204(1)	31(1)
Pd(3)	6949(1)	8399(1)	2424(1)	32(1)
Pd(4)	4733(1)	8574(1)	1889(1)	37(1)
P(1)	10637(1)	5399(1)	2944(1)	41(1)
P(2)	3796(1)	7777(1)	919(1)	39(1)
N(1)	9743(1)	8007(1)	3594(1)	36(1)
N(2)	8196(1)	7998(1)	2250(1)	32(1)
N(3)	6901(1)	7257(1)	2938(1)	34(1)
N(4)	5769(1)	8984(2)	2714(1)	36(1)
C(1)	10065(2)	5242(2)	2046(1)	47(1)
C(2)	11870(2)	5138(2)	2950(2)	59(1)
C(3)	9999(2)	4579(2)	3326(2)	54(1)
C(4)	9230(2)	5751(2)	2067(2)	60(1)
C(5)	10699(2)	5730(2)	1694(2)	63(1)
C(6)	9758(3)	4283(2)	1636(2)	63(1)
C(7)	12461(2)	5961(3)	2863(2)	73(1)
C(8)	11968(3)	4315(3)	2413(2)	79(1)
C(9)	12294(3)	4985(3)	3615(2)	75(1)
C(10)	10143(3)	3587(2)	3094(2)	74(1)
C(11)	10287(3)	4876(2)	4079(2)	63(1)
C(12)	8972(2)	4662(2)	3186(2)	65(1)
C(13)	11314(2)	7084(3)	4237(2)	45(1)
C(14)	12210(2)	7731(3)	4325(2)	54(1)
C(15)	12277(3)	8306(3)	5023(2)	57(1)
C(16)	12444(3)	7727(3)	5524(2)	64(1)
C(17)	11494(3)	7171(3)	5439(2)	60(1)
C(18)	10915(3)	7467(2)	4870(2)	47(1)
C(19)	12275(3)	8296(3)	3836(2)	64(1)
C(20)	11277(3)	8464(2)	5038(2)	56(1)
C(13B)	11412(8)	7155(9)	4157(5)	51(3)
C(14B)	11413(10)	7148(10)	4876(6)	51(3)
C(15B)	12095(10)	7990(11)	5206(6)	60(3)
C(16B)	13041(9)	7880(15)	5014(9)	65(3)
C(17B)	12944(8)	8059(15)	4318(8)	66(3)
C(18B)	11892(9)	8098(11)	4160(7)	55(3)
C(19B)	10522(10)	7137(14)	5128(8)	54(5)
C(20B)	11756(12)	8661(9)	4820(8)	58(3)
C(21)	10108(2)	8786(2)	3427(1)	37(1)
C(22)	10169(2)	9648(2)	3844(1)	46(1)
C(23)	10521(2)	10397(2)	3664(2)	55(1)
C(24)	10824(2)	10345(2)	3071(2)	57(1)
C(25)	10774(2)	9492(2)	2662(2)	54(1)
C(26)	10429(2)	8731(2)	2838(1)	42(1)
C(27)	11179(3)	11173(2)	2877(2)	88(1)
C(28)	8334(2)	7180(2)	4079(1)	36(1)

Table 4.16. (cont.)

C(29)	8367(2)	7993(2)	4697(1)	44(1)
C(30)	7712(2)	7596(2)	5084(1)	54(1)
C(31)	8134(3)	6850(2)	5353(2)	63(1)
C(32)	8009(2)	6062(2)	4723(1)	54(1)
C(33)	7587(2)	6482(2)	4168(1)	44(1)
C(34)	8073(2)	8845(2)	4544(1)	50(1)
C(35)	6946(2)	7056(2)	4534(1)	56(1)
C(36)	8277(2)	7512(2)	1622(1)	34(1)
C(37)	7563(2)	6892(2)	1227(1)	40(1)
C(38)	7652(2)	6354(2)	623(1)	52(1)
C(39)	8469(2)	6432(2)	375(1)	52(1)
C(40)	9147(2)	7090(2)	744(1)	49(1)
C(41)	9073(2)	7623(2)	1348(1)	40(1)
C(42)	8574(3)	5832(3)	-271(2)	85(1)
C(43)	6452(2)	6388(2)	2666(1)	34(1)
C(44)	5639(2)	6069(2)	2849(1)	41(1)
C(45)	5153(2)	5240(2)	2529(2)	49(1)
C(46)	5453(2)	4665(2)	2029(2)	52(1)
C(47)	6294(2)	4943(2)	1884(1)	50(1)
C(48)	6789(2)	5778(2)	2198(1)	41(1)
C(49)	4893(3)	3777(2)	1655(2)	82(1)
C(50)	7083(2)	9440(2)	1984(1)	38(1)
C(51)	7533(2)	10364(2)	2457(2)	49(1)
C(52)	8150(2)	10757(2)	2034(2)	62(1)
C(53)	7541(3)	10947(2)	1447(2)	71(1)
C(54)	7205(3)	10007(2)	986(2)	64(1)
C(55)	7603(2)	9379(2)	1392(1)	49(1)
C(56)	8075(2)	10313(2)	3110(2)	58(1)
C(57)	8540(2)	9914(2)	1706(2)	60(1)
C(58)	5556(13)	8861(9)	3323(2)	38(2)
C(59)	5899(9)	9477(7)	3920(3)	44(1)
C(60)	5687(5)	9325(5)	4509(3)	50(1)
C(61)	5139(5)	8568(4)	4524(2)	47(1)
C(62)	4765(5)	7962(4)	3925(3)	44(1)
C(63)	4966(5)	8113(5)	3335(2)	41(1)
C(64)	4969(6)	8384(5)	5171(3)	62(2)
C(58B)	5640(50)	8910(30)	3354(8)	41(3)
C(59B)	6020(30)	9590(20)	3909(11)	44(3)
C(60B)	5948(18)	9496(15)	4541(9)	49(3)
C(61B)	5474(16)	8750(14)	4642(7)	48(3)
C(62B)	5081(12)	8062(13)	4088(8)	42(3)
C(63B)	5169(17)	8144(19)	3458(8)	43(3)
C(64B)	5450(20)	8632(16)	5332(8)	64(5)
C(65)	4141(4)	9738(3)	1953(3)	43(1)
C(66)	3485(3)	10000(3)	2449(2)	47(1)
C(67)	3872(3)	10994(3)	2773(2)	56(1)
C(68)	3726(3)	11542(3)	2262(2)	68(1)
C(69)	4434(3)	11273(3)	1818(2)	64(1)
C(70)	4878(3)	10562(3)	2117(2)	51(1)
C(71)	3421(3)	9470(3)	2965(2)	54(1)
C(72)	4908(3)	10970(3)	2854(2)	58(1)
C(65B)	4064(10)	9696(6)	2102(6)	46(3)
C(66B)	4299(7)	10564(6)	1870(5)	46(2)

Table 4.16. (cont.)

C(67B)	4259(7)	11302(6)	2500(5)	57(2)
C(68B)	3283(7)	11272(7)	2624(7)	61(2)
C(69B)	3135(7)	10435(8)	2892(6)	60(2)
C(70B)	4032(7)	10038(7)	2842(5)	51(2)
C(71B)	5223(7)	10730(8)	1665(6)	54(3)
C(72B)	4711(8)	10905(9)	3049(6)	53(3)
C(73)	4050(2)	6606(2)	946(1)	46(1)
C(76)	5064(2)	6696(2)	1269(2)	62(1)
C(77)	3513(3)	6243(2)	1416(2)	70(1)
C(78)	3901(2)	5898(2)	288(2)	60(1)
C(74)	2502(3)	7762(4)	751(4)	54(1)
C(79)	2165(5)	7811(4)	1410(4)	66(2)
C(80)	1971(4)	6934(4)	227(4)	65(2)
C(81)	2246(5)	8604(5)	526(4)	70(2)
C(74B)	2522(6)	7772(14)	973(10)	55(4)
C(79B)	2338(15)	7867(13)	1686(11)	64(5)
C(80B)	1904(12)	6943(13)	498(11)	67(5)
C(81B)	2109(15)	8579(14)	775(12)	73(5)
C(75)	4280(6)	8051(4)	194(3)	46(2)
C(82)	3722(7)	7590(7)	-499(4)	67(2)
C(83)	4350(6)	9078(4)	288(3)	57(2)
C(84)	5274(5)	7837(5)	201(4)	61(2)
C(75B)	3996(15)	8156(13)	154(6)	54(3)
C(82B)	3375(19)	7579(19)	-480(12)	72(6)
C(83B)	3939(16)	9158(13)	205(10)	70(5)
C(84B)	4990(15)	7971(12)	133(13)	66(5)

Table 4.17. Bond lengths [\AA] and angles [$^\circ$] for 4.14.

Pd(1)-C(13B)	2.047(9)	C(1)-C(4)	1.537(4)
Pd(1)-C(13)	2.079(3)	C(2)-C(9)	1.535(5)
Pd(1)-N(1)	2.083(2)	C(2)-C(8)	1.537(4)
Pd(1)-P(1)	2.3174(7)	C(2)-C(7)	1.540(5)
Pd(2)-C(28)	2.047(2)	C(3)-C(12)	1.539(5)
Pd(2)-N(3)	2.072(2)	C(3)-C(11)	1.539(4)
Pd(2)-N(1)	2.162(2)	C(3)-C(10)	1.548(4)
Pd(2)-N(2)	2.2823(19)	C(4)-H(4A)	0.9800
Pd(2)-Pd(3)	3.0288(3)	C(4)-H(4B)	0.9800
Pd(3)-C(50)	2.046(3)	C(4)-H(4C)	0.9800
Pd(3)-N(2)	2.073(2)	C(5)-H(5A)	0.9800
Pd(3)-N(4)	2.161(2)	C(5)-H(5B)	0.9800
Pd(3)-N(3)	2.280(2)	C(5)-H(5C)	0.9800
Pd(4)-C(65)	2.068(4)	C(6)-H(6A)	0.9800
Pd(4)-C(65B)	2.081(8)	C(6)-H(6B)	0.9800
Pd(4)-N(4)	2.085(2)	C(6)-H(6C)	0.9800
Pd(4)-P(2)	2.3133(7)	C(7)-H(7A)	0.9800
P(1)-C(3)	1.908(3)	C(7)-H(7B)	0.9800
P(1)-C(1)	1.917(3)	C(7)-H(7C)	0.9800
P(1)-C(2)	1.919(3)	C(8)-H(8A)	0.9800
P(2)-C(73)	1.897(3)	C(8)-H(8B)	0.9800
P(2)-C(75B)	1.899(8)	C(8)-H(8C)	0.9800
P(2)-C(74)	1.907(4)	C(9)-H(9A)	0.9800
P(2)-C(75)	1.908(4)	C(9)-H(9B)	0.9800
P(2)-C(74B)	1.920(8)	C(9)-H(9C)	0.9800
N(1)-C(21)	1.415(3)	C(10)-H(10A)	0.9800
N(1)-H(1A)	0.8800	C(10)-H(10B)	0.9800
N(2)-C(36)	1.401(3)	C(10)-H(10C)	0.9800
N(2)-H(2A)	0.8800	C(11)-H(11A)	0.9800
N(3)-C(43)	1.395(3)	C(11)-H(11B)	0.9800
N(3)-H(3A)	0.8800	C(11)-H(11C)	0.9800
N(4)-C(58)	1.424(4)	C(12)-H(12A)	0.9800
N(4)-C(58B)	1.428(8)	C(12)-H(12B)	0.9800
N(4)-H(4D)	0.8800	C(12)-H(12C)	0.9800
C(1)-C(6)	1.527(4)	C(13)-C(14)	1.552(5)
C(1)-C(5)	1.535(4)	C(17B)-H(17D)	0.9900
C(13)-C(18)	1.564(5)	C(18B)-C(20B)	1.522(10)
C(13)-H(13A)	1.0000	C(18B)-H(18B)	1.0000
C(14)-C(19)	1.509(5)	C(19B)-H(19D)	0.9800
C(14)-C(15)	1.525(5)	C(19B)-H(19E)	0.9800
C(14)-H(14A)	1.0000	C(19B)-H(19F)	0.9800
C(15)-C(20)	1.538(5)	C(20B)-H(20C)	0.9900
C(15)-C(16)	1.546(5)	C(20B)-H(20D)	0.9900
C(15)-H(15A)	1.0000	C(21)-C(26)	1.391(4)
C(16)-C(17)	1.550(5)	C(21)-C(22)	1.408(4)
C(16)-H(16A)	0.9900	C(22)-C(23)	1.382(4)
C(16)-H(16B)	0.9900	C(22)-H(22A)	0.9500
C(17)-C(18)	1.558(5)	C(23)-C(24)	1.386(4)
C(17)-H(17A)	0.9900	C(23)-H(23A)	0.9500
C(17)-H(17B)	0.9900	C(24)-C(25)	1.393(4)
C(18)-C(20)	1.528(5)	C(24)-C(27)	1.506(5)

Table 4.17. (cont.)

C(18)-H(18A)	1.0000	C(25)-C(26)	1.390(4)
C(19)-H(19A)	0.9800	C(25)-H(25A)	0.9500
C(19)-H(19B)	0.9800	C(26)-H(26A)	0.9500
C(19)-H(19C)	0.9800	C(27)-H(27A)	0.9800
C(20)-H(20A)	0.9900	C(27)-H(27B)	0.9800
C(20)-H(20B)	0.9900	C(27)-H(27C)	0.9800
C(13B)-C(14B)	1.526(9)	C(28)-C(33)	1.541(4)
C(13B)-C(18B)	1.562(10)	C(28)-C(29)	1.587(4)
C(13B)-H(13B)	1.0000	C(28)-H(28A)	1.0000
C(14B)-C(19B)	1.503(10)	C(29)-C(34)	1.517(4)
C(14B)-C(15B)	1.531(10)	C(29)-C(30)	1.536(4)
C(14B)-H(14B)	1.0000	C(29)-H(29A)	1.0000
C(15B)-C(20B)	1.538(10)	C(30)-C(35)	1.531(4)
C(15B)-C(16B)	1.540(10)	C(30)-C(31)	1.544(4)
C(15B)-H(15B)	1.0000	C(30)-H(30A)	1.0000
C(16B)-C(17B)	1.552(11)	C(31)-C(32)	1.563(5)
C(16B)-H(16C)	0.9900	C(31)-H(31A)	0.9900
C(16B)-H(16D)	0.9900	C(31)-H(31B)	0.9900
C(17B)-C(18B)	1.564(10)	C(32)-C(33)	1.552(4)
C(17B)-H(17C)	0.9900	C(49)-H(49B)	0.9800
C(32)-H(32A)	0.9900	C(49)-H(49C)	0.9800
C(32)-H(32B)	0.9900	C(50)-C(55)	1.560(4)
C(33)-C(35)	1.541(4)	C(50)-C(51)	1.569(4)
C(33)-H(33A)	1.0000	C(50)-H(50A)	1.0000
C(34)-H(34A)	0.9800	C(51)-C(56)	1.518(4)
C(34)-H(34B)	0.9800	C(51)-C(52)	1.552(4)
C(34)-H(34C)	0.9800	C(51)-H(51A)	1.0000
C(35)-H(35A)	0.9900	C(52)-C(53)	1.531(5)
C(35)-H(35B)	0.9900	C(52)-C(57)	1.541(5)
C(36)-C(37)	1.388(4)	C(52)-H(52A)	1.0000
C(36)-C(41)	1.411(4)	C(53)-C(54)	1.546(5)
C(37)-C(38)	1.392(4)	C(53)-H(53A)	0.9900
C(37)-H(37A)	0.9500	C(53)-H(53B)	0.9900
C(38)-C(39)	1.402(4)	C(54)-C(55)	1.542(4)
C(38)-H(38A)	0.9500	C(54)-H(54A)	0.9900
C(39)-C(40)	1.371(4)	C(54)-H(54B)	0.9900
C(39)-C(42)	1.507(4)	C(55)-C(57)	1.527(5)
C(40)-C(41)	1.381(4)	C(55)-H(55A)	1.0000
C(40)-H(40A)	0.9500	C(56)-H(56A)	0.9800
C(41)-H(41A)	0.9500	C(56)-H(56B)	0.9800
C(42)-H(42A)	0.9800	C(56)-H(56C)	0.9800
C(42)-H(42B)	0.9800	C(57)-H(57A)	0.9900
C(42)-H(42C)	0.9800	C(57)-H(57B)	0.9900
C(43)-C(48)	1.392(4)	C(58)-C(59)	1.391(4)
C(43)-C(44)	1.408(4)	C(58)-C(63)	1.393(5)
C(44)-C(45)	1.382(4)	C(59)-C(60)	1.397(5)
C(44)-H(44A)	0.9500	C(59)-H(59A)	0.9500
C(45)-C(46)	1.380(4)	C(60)-C(61)	1.372(6)
C(45)-H(45A)	0.9500	C(60)-H(60A)	0.9500
C(46)-C(47)	1.386(4)	C(61)-C(62)	1.397(6)
C(46)-C(49)	1.517(4)	C(61)-C(64)	1.514(5)
C(47)-C(48)	1.392(4)	C(62)-C(63)	1.393(5)
C(47)-H(47A)	0.9500	C(62)-H(62A)	0.9500

Table 4.17. (cont.)

C(48)-H(48A)	0.9500	C(63)-H(63A)	0.9500
C(49)-H(49A)	0.9800	C(71)-H(71B)	0.9800
C(64)-H(64A)	0.9800	C(71)-H(71C)	0.9800
C(64)-H(64B)	0.9800	C(72)-H(72A)	0.9900
C(64)-H(64C)	0.9800	C(72)-H(72B)	0.9900
C(58B)-C(59B)	1.393(9)	C(65B)-C(70B)	1.546(10)
C(58B)-C(63B)	1.394(9)	C(65B)-C(66B)	1.560(11)
C(59B)-C(60B)	1.398(9)	C(65B)-H(65B)	1.0000
C(59B)-H(59B)	0.9500	C(66B)-C(71B)	1.522(9)
C(60B)-C(61B)	1.373(10)	C(66B)-C(67B)	1.559(9)
C(60B)-H(60B)	0.9500	C(66B)-H(66B)	1.0000
C(61B)-C(62B)	1.400(10)	C(67B)-C(68B)	1.516(9)
C(61B)-C(64B)	1.520(9)	C(67B)-C(72B)	1.534(10)
C(62B)-C(63B)	1.395(9)	C(67B)-H(67B)	1.0000
C(62B)-H(62B)	0.9500	C(68B)-C(69B)	1.540(10)
C(63B)-H(63B)	0.9500	C(68B)-H(68C)	0.9900
C(64B)-H(64D)	0.9800	C(68B)-H(68D)	0.9900
C(64B)-H(64E)	0.9800	C(69B)-C(70B)	1.532(9)
C(64B)-H(64F)	0.9800	C(69B)-H(69C)	0.9900
C(65)-C(70)	1.541(6)	C(69B)-H(69D)	0.9900
C(65)-C(66)	1.554(6)	C(70B)-C(72B)	1.536(10)
C(65)-H(65A)	1.0000	C(70B)-H(70B)	1.0000
C(66)-C(71)	1.518(5)	C(71B)-H(71D)	0.9800
C(66)-C(67)	1.551(5)	C(71B)-H(71E)	0.9800
C(66)-H(66A)	1.0000	C(71B)-H(71F)	0.9800
C(67)-C(68)	1.525(6)	C(72B)-H(72C)	0.9900
C(67)-C(72)	1.535(6)	C(72B)-H(72D)	0.9900
C(67)-H(67A)	1.0000	C(73)-C(78)	1.536(4)
C(68)-C(69)	1.542(6)	C(73)-C(77)	1.536(4)
C(68)-H(68A)	0.9900	C(73)-C(76)	1.544(4)
C(68)-H(68B)	0.9900	C(76)-H(76A)	0.9800
C(69)-C(70)	1.544(5)	C(76)-H(76B)	0.9800
C(69)-H(69A)	0.9900	C(76)-H(76C)	0.9800
C(69)-H(69B)	0.9900	C(77)-H(77A)	0.9800
C(70)-C(72)	1.537(6)	C(77)-H(77B)	0.9800
C(70)-H(70A)	1.0000	C(77)-H(77C)	0.9800
C(71)-H(71A)	0.9800	C(83)-H(83C)	0.9800
C(78)-H(78A)	0.9800	C(84)-H(84A)	0.9800
C(78)-H(78B)	0.9800	C(84)-H(84B)	0.9800
C(78)-H(78C)	0.9800	C(84)-H(84C)	0.9800
C(74)-C(79)	1.542(5)	C(75B)-C(84B)	1.541(7)
C(74)-C(81)	1.548(5)	C(75B)-C(83B)	1.542(7)
C(74)-C(80)	1.549(5)	C(75B)-C(82B)	1.545(7)
C(79)-H(79A)	0.9800	C(82B)-H(82D)	0.9800
C(79)-H(79B)	0.9800	C(82B)-H(82E)	0.9800
C(79)-H(79C)	0.9800	C(82B)-H(82F)	0.9800
C(80)-H(80A)	0.9800	C(83B)-H(83D)	0.9800
C(80)-H(80B)	0.9800	C(83B)-H(83E)	0.9800
C(80)-H(80C)	0.9800	C(83B)-H(83F)	0.9800
C(81)-H(81A)	0.9800	C(84B)-H(84D)	0.9800
C(81)-H(81B)	0.9800	C(84B)-H(84E)	0.9800
C(81)-H(81C)	0.9800	C(84B)-H(84F)	0.9800
C(74B)-C(79B)	1.553(7)	C(81B)-H(81E)	0.9800

Table 4.17. (cont.)

C(74B)-C(80B)	1.555(7)	C(81B)-H(81F)	0.9800
C(74B)-C(81B)	1.558(7)	C(75)-C(83)	1.548(5)
C(79B)-H(79D)	0.9800	C(75)-C(84)	1.548(5)
C(79B)-H(79E)	0.9800	C(75)-C(82)	1.550(5)
C(79B)-H(79F)	0.9800	C(82)-H(82A)	0.9800
C(80B)-H(80D)	0.9800	C(82)-H(82B)	0.9800
C(80B)-H(80E)	0.9800	C(82)-H(82C)	0.9800
C(80B)-H(80F)	0.9800	C(83)-H(83A)	0.9800
C(81B)-H(81D)	0.9800	C(83)-H(83B)	0.9800
C(13B)-Pd(1)-C(13)	7.6(5)	C(1)-P(1)-Pd(1)	99.86(9)
C(13B)-Pd(1)-N(1)	98.7(4)	C(2)-P(1)-Pd(1)	121.05(11)
C(13)-Pd(1)-N(1)	98.64(12)	C(73)-P(2)-C(75B)	116.4(7)
C(13B)-Pd(1)-P(1)	96.6(4)	C(73)-P(2)-C(74)	108.6(2)
C(13)-Pd(1)-P(1)	96.24(10)	C(75B)-P(2)-C(74)	95.0(7)
N(1)-Pd(1)-P(1)	164.54(6)	C(73)-P(2)-C(75)	106.6(2)
C(28)-Pd(2)-N(3)	93.89(9)	C(74)-P(2)-C(75)	108.5(3)
C(28)-Pd(2)-N(1)	83.37(10)	C(73)-P(2)-C(74B)	105.5(7)
N(3)-Pd(2)-N(1)	170.91(8)	C(75B)-P(2)-C(74B)	108.1(9)
C(28)-Pd(2)-N(2)	175.34(9)	C(75)-P(2)-C(74B)	121.9(7)
N(3)-Pd(2)-N(2)	83.02(8)	C(73)-P(2)-Pd(4)	99.03(9)
N(1)-Pd(2)-N(2)	99.15(8)	C(75B)-P(2)-Pd(4)	115.3(5)
C(28)-Pd(2)-Pd(3)	132.36(7)	C(74)-P(2)-Pd(4)	123.7(2)
N(3)-Pd(2)-Pd(3)	48.80(6)	C(75)-P(2)-Pd(4)	109.0(2)
N(1)-Pd(2)-Pd(3)	128.26(6)	C(74B)-P(2)-Pd(4)	112.2(6)
N(2)-Pd(2)-Pd(3)	43.15(5)	C(21)-N(1)-Pd(1)	120.72(16)
C(50)-Pd(3)-N(2)	93.85(9)	C(21)-N(1)-Pd(2)	116.07(16)
C(50)-Pd(3)-N(4)	83.61(9)	Pd(1)-N(1)-Pd(2)	102.13(9)
N(2)-Pd(3)-N(4)	171.50(8)	C(21)-N(1)-H(1A)	105.5
C(50)-Pd(3)-N(3)	176.27(9)	Pd(1)-N(1)-H(1A)	105.5
N(2)-Pd(3)-N(3)	83.07(8)	Pd(2)-N(1)-H(1A)	105.5
N(4)-Pd(3)-N(3)	99.14(8)	C(36)-N(2)-Pd(3)	119.93(16)
C(50)-Pd(3)-Pd(2)	133.12(8)	C(36)-N(2)-Pd(2)	128.30(16)
N(2)-Pd(3)-Pd(2)	48.86(5)	Pd(3)-N(2)-Pd(2)	87.99(7)
N(4)-Pd(3)-Pd(2)	128.60(5)	C(36)-N(2)-H(2A)	106.0
N(3)-Pd(3)-Pd(2)	43.14(5)	Pd(3)-N(2)-H(2A)	106.0
C(65)-Pd(4)-C(65B)	10.2(5)	Pd(2)-N(2)-H(2A)	106.0
C(65)-Pd(4)-N(4)	99.73(15)	C(43)-N(3)-Pd(2)	122.35(16)
C(65B)-Pd(4)-N(4)	95.8(4)	C(43)-N(3)-Pd(3)	126.24(15)
C(65)-Pd(4)-P(2)	95.93(14)	Pd(2)-N(3)-Pd(3)	88.06(8)
C(65B)-Pd(4)-P(2)	100.0(4)	C(43)-N(3)-H(3A)	105.9
N(4)-Pd(4)-P(2)	164.16(6)	Pd(2)-N(3)-H(3A)	105.9
C(3)-P(1)-C(1)	109.45(14)	Pd(3)-N(3)-H(3A)	105.9
C(3)-P(1)-C(2)	108.88(15)	C(58)-N(4)-Pd(4)	117.4(6)
C(1)-P(1)-C(2)	107.91(13)	C(58B)-N(4)-Pd(4)	123(2)
C(3)-P(1)-Pd(1)	109.02(10)	H(5A)-C(5)-H(5C)	109.5
C(58)-N(4)-Pd(3)	115.0(9)	H(5B)-C(5)-H(5C)	109.5
C(58B)-N(4)-Pd(3)	112(4)	C(1)-C(6)-H(6A)	109.5
Pd(4)-N(4)-Pd(3)	105.83(9)	C(1)-C(6)-H(6B)	109.5
C(58)-N(4)-H(4D)	105.9	H(6A)-C(6)-H(6B)	109.5
C(58B)-N(4)-H(4D)	102.8	C(1)-C(6)-H(6C)	109.5

Table 4.17. (cont.)

Pd(4)-N(4)-H(4D)	105.9	H(6A)-C(6)-H(6C)	109.5
Pd(3)-N(4)-H(4D)	105.9	H(6B)-C(6)-H(6C)	109.5
C(6)-C(1)-C(5)	109.2(3)	C(2)-C(7)-H(7A)	109.5
C(6)-C(1)-C(4)	109.1(3)	C(2)-C(7)-H(7B)	109.5
C(5)-C(1)-C(4)	105.1(3)	H(7A)-C(7)-H(7B)	109.5
C(6)-C(1)-P(1)	117.3(2)	C(2)-C(7)-H(7C)	109.5
C(5)-C(1)-P(1)	109.4(2)	H(7A)-C(7)-H(7C)	109.5
C(4)-C(1)-P(1)	106.07(18)	H(7B)-C(7)-H(7C)	109.5
C(9)-C(2)-C(8)	107.3(3)	C(2)-C(8)-H(8A)	109.5
C(9)-C(2)-C(7)	105.9(3)	C(2)-C(8)-H(8B)	109.5
C(8)-C(2)-C(7)	108.9(3)	H(8A)-C(8)-H(8B)	109.5
C(9)-C(2)-P(1)	111.6(2)	C(2)-C(8)-H(8C)	109.5
C(8)-C(2)-P(1)	114.2(3)	H(8A)-C(8)-H(8C)	109.5
C(7)-C(2)-P(1)	108.6(2)	H(8B)-C(8)-H(8C)	109.5
C(12)-C(3)-C(11)	105.6(3)	C(2)-C(9)-H(9A)	109.5
C(12)-C(3)-C(10)	109.7(3)	C(2)-C(9)-H(9B)	109.5
C(11)-C(3)-C(10)	108.4(3)	H(9A)-C(9)-H(9B)	109.5
C(12)-C(3)-P(1)	108.2(2)	C(2)-C(9)-H(9C)	109.5
C(11)-C(3)-P(1)	108.8(2)	H(9A)-C(9)-H(9C)	109.5
C(10)-C(3)-P(1)	115.7(2)	H(9B)-C(9)-H(9C)	109.5
C(1)-C(4)-H(4A)	109.5	C(3)-C(10)-H(10A)	109.5
C(1)-C(4)-H(4B)	109.5	C(3)-C(10)-H(10B)	109.5
H(4A)-C(4)-H(4B)	109.5	H(10A)-C(10)-H(10B)	109.5
C(1)-C(4)-H(4C)	109.5	C(3)-C(10)-H(10C)	109.5
H(4A)-C(4)-H(4C)	109.5	H(10A)-C(10)-H(10C)	109.5
H(4B)-C(4)-H(4C)	109.5	H(10B)-C(10)-H(10C)	109.5
C(1)-C(5)-H(5A)	109.5	C(3)-C(11)-H(11A)	109.5
C(1)-C(5)-H(5B)	109.5	C(3)-C(11)-H(11B)	109.5
H(5A)-C(5)-H(5B)	109.5	H(11A)-C(11)-H(11B)	109.5
C(1)-C(5)-H(5C)	109.5	C(18)-C(17)-H(17A)	111.2
C(3)-C(11)-H(11C)	109.5	C(16)-C(17)-H(17B)	111.2
H(11A)-C(11)-H(11C)	109.5	C(18)-C(17)-H(17B)	111.2
H(11B)-C(11)-H(11C)	109.5	H(17A)-C(17)-H(17B)	109.1
C(3)-C(12)-H(12A)	109.5	C(20)-C(18)-C(17)	100.8(3)
C(3)-C(12)-H(12B)	109.5	C(20)-C(18)-C(13)	102.9(3)
H(12A)-C(12)-H(12B)	109.5	C(17)-C(18)-C(13)	106.0(3)
C(3)-C(12)-H(12C)	109.5	C(20)-C(18)-H(18A)	115.2
H(12A)-C(12)-H(12C)	109.5	C(17)-C(18)-H(18A)	115.2
H(12B)-C(12)-H(12C)	109.5	C(13)-C(18)-H(18A)	115.2
C(14)-C(13)-C(18)	103.1(3)	C(18)-C(20)-C(15)	94.0(3)
C(14)-C(13)-Pd(1)	121.0(3)	C(18)-C(20)-H(20A)	112.9
C(18)-C(13)-Pd(1)	112.2(2)	C(15)-C(20)-H(20A)	112.9
C(14)-C(13)-H(13A)	106.6	C(18)-C(20)-H(20B)	112.9
C(18)-C(13)-H(13A)	106.6	C(15)-C(20)-H(20B)	112.9
Pd(1)-C(13)-H(13A)	106.6	H(20A)-C(20)-H(20B)	110.4
C(19)-C(14)-C(15)	111.7(3)	C(14B)-C(13B)-C(18B)	106.5(7)
C(19)-C(14)-C(13)	117.9(3)	C(14B)-C(13B)-Pd(1)	128.7(9)
C(15)-C(14)-C(13)	102.3(3)	C(18B)-C(13B)-Pd(1)	106.6(8)
C(19)-C(14)-H(14A)	108.1	C(14B)-C(13B)-H(13B)	104.3
C(15)-C(14)-H(14A)	108.1	C(18B)-C(13B)-H(13B)	104.3
C(13)-C(14)-H(14A)	108.1	Pd(1)-C(13B)-H(13B)	104.3
C(14)-C(15)-C(20)	101.8(3)	C(19B)-C(14B)-C(13B)	119.2(12)
C(14)-C(15)-C(16)	109.9(3)	C(19B)-C(14B)-C(15B)	113.9(11)

Table 4.17. (cont.)

C(20)-C(15)-C(16)	102.3(3)	C(13B)-C(14B)-C(15B)	99.1(7)
C(14)-C(15)-H(15A)	113.9	C(19B)-C(14B)-H(14B)	108.0
C(20)-C(15)-H(15A)	113.9	C(13B)-C(14B)-H(14B)	108.0
C(16)-C(15)-H(15A)	113.9	C(15B)-C(14B)-H(14B)	108.0
C(15)-C(16)-C(17)	102.8(3)	C(14B)-C(15B)-C(20B)	101.8(9)
C(15)-C(16)-H(16A)	111.2	C(14B)-C(15B)-C(16B)	110.7(11)
C(17)-C(16)-H(16A)	111.2	C(20B)-C(15B)-C(16B)	102.2(9)
C(15)-C(16)-H(16B)	111.2	C(14B)-C(15B)-H(15B)	113.7
C(17)-C(16)-H(16B)	111.2	C(20B)-C(15B)-H(15B)	113.7
H(16A)-C(16)-H(16B)	109.1	C(16B)-C(15B)-H(15B)	113.7
C(16)-C(17)-C(18)	102.9(3)	C(15B)-C(16B)-C(17B)	104.0(8)
C(16)-C(17)-H(17A)	111.2	C(22)-C(23)-C(24)	122.4(3)
C(15B)-C(16B)-H(16C)	111.0	C(22)-C(23)-H(23A)	118.8
C(17B)-C(16B)-H(16C)	111.0	C(24)-C(23)-H(23A)	118.8
C(15B)-C(16B)-H(16D)	111.0	C(23)-C(24)-C(25)	116.6(3)
C(17B)-C(16B)-H(16D)	111.0	C(23)-C(24)-C(27)	121.5(3)
H(16C)-C(16B)-H(16D)	109.0	C(25)-C(24)-C(27)	121.8(3)
C(16B)-C(17B)-C(18B)	101.1(8)	C(26)-C(25)-C(24)	121.6(3)
C(16B)-C(17B)-H(17C)	111.5	C(26)-C(25)-H(25A)	119.2
C(18B)-C(17B)-H(17C)	111.5	C(24)-C(25)-H(25A)	119.2
C(16B)-C(17B)-H(17D)	111.5	C(25)-C(26)-C(21)	121.6(3)
C(18B)-C(17B)-H(17D)	111.5	C(25)-C(26)-H(26A)	119.2
H(17C)-C(17B)-H(17D)	109.4	C(21)-C(26)-H(26A)	119.2
C(20B)-C(18B)-C(13B)	101.8(9)	C(24)-C(27)-H(27A)	109.5
C(20B)-C(18B)-C(17B)	99.7(9)	C(24)-C(27)-H(27B)	109.5
C(13B)-C(18B)-C(17B)	106.0(10)	H(27A)-C(27)-H(27B)	109.5
C(20B)-C(18B)-H(18B)	115.7	C(24)-C(27)-H(27C)	109.5
C(13B)-C(18B)-H(18B)	115.7	H(27A)-C(27)-H(27C)	109.5
C(17B)-C(18B)-H(18B)	115.7	H(27B)-C(27)-H(27C)	109.5
C(14B)-C(19B)-H(19D)	109.5	C(33)-C(28)-C(29)	102.8(2)
C(14B)-C(19B)-H(19E)	109.5	C(33)-C(28)-Pd(2)	121.38(18)
H(19D)-C(19B)-H(19E)	109.5	C(29)-C(28)-Pd(2)	114.56(18)
C(14B)-C(19B)-H(19F)	109.5	C(33)-C(28)-H(28A)	105.6
H(19D)-C(19B)-H(19F)	109.5	C(29)-C(28)-H(28A)	105.6
H(19E)-C(19B)-H(19F)	109.5	Pd(2)-C(28)-H(28A)	105.6
C(18B)-C(20B)-C(15B)	94.0(7)	C(34)-C(29)-C(30)	111.1(2)
C(18B)-C(20B)-H(20C)	112.9	C(34)-C(29)-C(28)	115.8(2)
C(15B)-C(20B)-H(20C)	112.9	C(30)-C(29)-C(28)	102.0(2)
C(18B)-C(20B)-H(20D)	112.9	C(34)-C(29)-H(29A)	109.2
C(15B)-C(20B)-H(20D)	112.9	C(30)-C(29)-H(29A)	109.2
H(20C)-C(20B)-H(20D)	110.3	C(28)-C(29)-H(29A)	109.2
C(26)-C(21)-C(22)	116.7(3)	C(35)-C(30)-C(29)	102.0(2)
C(26)-C(21)-N(1)	121.0(2)	C(35)-C(30)-C(31)	101.9(3)
C(22)-C(21)-N(1)	122.3(2)	C(29)-C(30)-C(31)	109.6(3)
C(23)-C(22)-C(21)	121.0(3)	C(35)-C(30)-H(30A)	114.0
C(23)-C(22)-H(22A)	119.5	C(29)-C(30)-H(30A)	114.0
C(21)-C(22)-H(22A)	119.5	C(36)-C(37)-H(37A)	118.9
C(31)-C(30)-H(30A)	114.0	C(38)-C(37)-H(37A)	118.9
C(30)-C(31)-C(32)	102.7(2)	C(37)-C(38)-C(39)	121.1(3)
C(30)-C(31)-H(31A)	111.2	C(37)-C(38)-H(38A)	119.5
C(32)-C(31)-H(31A)	111.2	C(39)-C(38)-H(38A)	119.5
C(30)-C(31)-H(31B)	111.2	C(40)-C(39)-C(38)	116.3(3)
C(32)-C(31)-H(31B)	111.2	C(40)-C(39)-C(42)	122.6(3)

Table 4.17. (cont.)

H(31A)-C(31)-H(31B)	109.1	C(38)-C(39)-C(42)	121.1(3)
C(33)-C(32)-C(31)	103.0(2)	C(39)-C(40)-C(41)	123.2(3)
C(33)-C(32)-H(32A)	111.2	C(39)-C(40)-H(40A)	118.4
C(31)-C(32)-H(32A)	111.2	C(41)-C(40)-H(40A)	118.4
C(33)-C(32)-H(32B)	111.2	C(40)-C(41)-C(36)	120.9(3)
C(31)-C(32)-H(32B)	111.2	C(40)-C(41)-H(41A)	119.5
H(32A)-C(32)-H(32B)	109.1	C(36)-C(41)-H(41A)	119.5
C(35)-C(33)-C(28)	103.5(2)	C(39)-C(42)-H(42A)	109.5
C(35)-C(33)-C(32)	99.8(2)	C(39)-C(42)-H(42B)	109.5
C(28)-C(33)-C(32)	107.4(2)	H(42A)-C(42)-H(42B)	109.5
C(35)-C(33)-H(33A)	114.8	C(39)-C(42)-H(42C)	109.5
C(28)-C(33)-H(33A)	114.8	H(42A)-C(42)-H(42C)	109.5
C(32)-C(33)-H(33A)	114.8	H(42B)-C(42)-H(42C)	109.5
C(29)-C(34)-H(34A)	109.5	C(48)-C(43)-N(3)	121.9(2)
C(29)-C(34)-H(34B)	109.5	C(48)-C(43)-C(44)	115.7(3)
H(34A)-C(34)-H(34B)	109.5	N(3)-C(43)-C(44)	122.4(2)
C(29)-C(34)-H(34C)	109.5	C(45)-C(44)-C(43)	121.7(3)
H(34A)-C(34)-H(34C)	109.5	C(45)-C(44)-H(44A)	119.1
H(34B)-C(34)-H(34C)	109.5	C(43)-C(44)-H(44A)	119.1
C(30)-C(35)-C(33)	94.5(2)	C(46)-C(45)-C(44)	122.1(3)
C(30)-C(35)-H(35A)	112.8	C(46)-C(45)-H(45A)	119.0
C(33)-C(35)-H(35A)	112.8	C(44)-C(45)-H(45A)	119.0
C(30)-C(35)-H(35B)	112.8	C(45)-C(46)-C(47)	116.4(3)
C(33)-C(35)-H(35B)	112.8	C(45)-C(46)-C(49)	121.9(3)
H(35A)-C(35)-H(35B)	110.3	C(47)-C(46)-C(49)	121.7(3)
C(37)-C(36)-N(2)	121.3(2)	C(46)-C(47)-C(48)	122.2(3)
C(37)-C(36)-C(41)	115.9(2)	C(46)-C(47)-H(47A)	118.9
N(2)-C(36)-C(41)	122.8(2)	C(48)-C(47)-H(47A)	118.9
C(36)-C(37)-C(38)	122.3(3)	C(53)-C(54)-H(54A)	111.2
C(43)-C(48)-C(47)	121.4(3)	C(55)-C(54)-H(54B)	111.2
C(43)-C(48)-H(48A)	119.3	C(53)-C(54)-H(54B)	111.2
C(47)-C(48)-H(48A)	119.3	H(54A)-C(54)-H(54B)	109.1
C(46)-C(49)-H(49A)	109.5	C(57)-C(55)-C(54)	100.4(3)
C(46)-C(49)-H(49B)	109.5	C(57)-C(55)-C(50)	103.6(2)
H(49A)-C(49)-H(49B)	109.5	C(54)-C(55)-C(50)	106.9(2)
C(46)-C(49)-H(49C)	109.5	C(57)-C(55)-H(55A)	114.8
H(49A)-C(49)-H(49C)	109.5	C(54)-C(55)-H(55A)	114.8
H(49B)-C(49)-H(49C)	109.5	C(50)-C(55)-H(55A)	114.8
C(55)-C(50)-C(51)	102.6(2)	C(51)-C(56)-H(56A)	109.5
C(55)-C(50)-Pd(3)	120.98(18)	C(51)-C(56)-H(56B)	109.5
C(51)-C(50)-Pd(3)	115.33(18)	H(56A)-C(56)-H(56B)	109.5
C(55)-C(50)-H(50A)	105.6	C(51)-C(56)-H(56C)	109.5
C(51)-C(50)-H(50A)	105.6	H(56A)-C(56)-H(56C)	109.5
Pd(3)-C(50)-H(50A)	105.6	H(56B)-C(56)-H(56C)	109.5
C(56)-C(51)-C(52)	111.8(3)	C(55)-C(57)-C(52)	94.5(2)
C(56)-C(51)-C(50)	115.3(2)	C(55)-C(57)-H(57A)	112.8
C(52)-C(51)-C(50)	102.6(2)	C(52)-C(57)-H(57A)	112.8
C(56)-C(51)-H(51A)	109.0	C(55)-C(57)-H(57B)	112.8
C(52)-C(51)-H(51A)	109.0	C(52)-C(57)-H(57B)	112.8
C(50)-C(51)-H(51A)	109.0	H(57A)-C(57)-H(57B)	110.3
C(53)-C(52)-C(57)	101.8(3)	C(59)-C(58)-C(63)	117.4(4)
C(53)-C(52)-C(51)	108.9(3)	C(59)-C(58)-N(4)	122.4(5)
C(57)-C(52)-C(51)	100.9(2)	C(63)-C(58)-N(4)	120.1(5)

Table 4.17. (cont.)

C(53)-C(52)-H(52A)	114.6	C(58)-C(59)-C(60)	120.8(4)
C(57)-C(52)-H(52A)	114.6	C(58)-C(59)-H(59A)	119.6
C(51)-C(52)-H(52A)	114.6	C(60)-C(59)-H(59A)	119.6
C(52)-C(53)-C(54)	103.6(3)	C(61)-C(60)-C(59)	121.7(4)
C(52)-C(53)-H(53A)	111.0	C(61)-C(60)-H(60A)	119.1
C(54)-C(53)-H(53A)	111.0	C(59)-C(60)-H(60A)	119.1
C(52)-C(53)-H(53B)	111.0	C(60)-C(61)-C(62)	117.9(4)
C(54)-C(53)-H(53B)	111.0	C(60)-C(61)-C(64)	121.0(4)
H(53A)-C(53)-H(53B)	109.0	C(62)-C(61)-C(64)	121.1(4)
C(55)-C(54)-C(53)	102.9(3)	C(63)-C(62)-C(61)	120.7(4)
C(55)-C(54)-H(54A)	111.2	C(71)-C(66)-C(67)	111.1(3)
C(63)-C(62)-H(62A)	119.7	C(71)-C(66)-C(65)	118.0(3)
C(61)-C(62)-H(62A)	119.7	C(67)-C(66)-C(65)	101.4(3)
C(62)-C(63)-C(58)	121.4(4)	C(71)-C(66)-H(66A)	108.6
C(62)-C(63)-H(63A)	119.3	C(67)-C(66)-H(66A)	108.6
C(58)-C(63)-H(63A)	119.3	C(65)-C(66)-H(66A)	108.6
C(59B)-C(58B)-C(63B)	117.0(9)	C(68)-C(67)-C(72)	101.5(4)
C(59B)-C(58B)-N(4)	120.5(18)	C(68)-C(67)-C(66)	109.4(4)
C(63B)-C(58B)-N(4)	122.4(17)	C(72)-C(67)-C(66)	102.1(3)
C(58B)-C(59B)-C(60B)	121.0(11)	C(68)-C(67)-H(67A)	114.2
C(58B)-C(59B)-H(59B)	119.5	C(72)-C(67)-H(67A)	114.2
C(60B)-C(59B)-H(59B)	119.5	C(66)-C(67)-H(67A)	114.2
C(61B)-C(60B)-C(59B)	121.9(10)	C(67)-C(68)-C(69)	103.8(3)
C(61B)-C(60B)-H(60B)	119.1	C(67)-C(68)-H(68A)	111.0
C(59B)-C(60B)-H(60B)	119.1	C(69)-C(68)-H(68A)	111.0
C(60B)-C(61B)-C(62B)	117.8(9)	C(67)-C(68)-H(68B)	111.0
C(60B)-C(61B)-C(64B)	121.3(11)	C(69)-C(68)-H(68B)	111.0
C(62B)-C(61B)-C(64B)	120.7(11)	H(68A)-C(68)-H(68B)	109.0
C(63B)-C(62B)-C(61B)	120.4(10)	C(68)-C(69)-C(70)	102.5(4)
C(63B)-C(62B)-H(62B)	119.8	C(68)-C(69)-H(69A)	111.3
C(61B)-C(62B)-H(62B)	119.8	C(70)-C(69)-H(69A)	111.3
C(58B)-C(63B)-C(62B)	121.9(10)	C(68)-C(69)-H(69B)	111.3
C(58B)-C(63B)-H(63B)	119.1	C(70)-C(69)-H(69B)	111.3
C(62B)-C(63B)-H(63B)	119.1	H(69A)-C(69)-H(69B)	109.2
C(61B)-C(64B)-H(64D)	109.5	C(72)-C(70)-C(65)	103.7(4)
C(61B)-C(64B)-H(64E)	109.5	C(72)-C(70)-C(69)	100.6(3)
H(64D)-C(64B)-H(64E)	109.5	C(65)-C(70)-C(69)	106.0(4)
C(61B)-C(64B)-H(64F)	109.5	C(72)-C(70)-H(70A)	115.0
H(64D)-C(64B)-H(64F)	109.5	C(65)-C(70)-H(70A)	115.0
H(64E)-C(64B)-H(64F)	109.5	C(69)-C(70)-H(70A)	115.0
C(70)-C(65)-C(66)	104.0(3)	C(67)-C(72)-C(70)	93.7(3)
C(70)-C(65)-Pd(4)	110.9(3)	C(67)-C(72)-H(72A)	113.0
C(66)-C(65)-Pd(4)	121.0(3)	C(70)-C(72)-H(72A)	113.0
C(70)-C(65)-H(65A)	106.7	C(67)-C(72)-H(72B)	113.0
C(66)-C(65)-H(65A)	106.7	C(70)-C(72)-H(72B)	113.0
Pd(4)-C(65)-H(65A)	106.7	C(72B)-C(70B)-H(70B)	115.0
H(72A)-C(72)-H(72B)	110.4	C(65B)-C(70B)-H(70B)	115.0
C(70B)-C(65B)-C(66B)	104.3(6)	C(66B)-C(71B)-H(71D)	109.5
C(70B)-C(65B)-Pd(4)	113.7(7)	C(66B)-C(71B)-H(71E)	109.5
C(66B)-C(65B)-Pd(4)	123.5(8)	H(71D)-C(71B)-H(71E)	109.5
C(70B)-C(65B)-H(65B)	104.5	C(66B)-C(71B)-H(71F)	109.5
C(66B)-C(65B)-H(65B)	104.5	H(71D)-C(71B)-H(71F)	109.5
Pd(4)-C(65B)-H(65B)	104.5	H(71E)-C(71B)-H(71F)	109.5

Table 4.17. (cont.)

C(71B)-C(66B)-C(67B)	108.7(8)	C(67B)-C(72B)-C(70B)	94.3(6)
C(71B)-C(66B)-C(65B)	118.8(9)	C(67B)-C(72B)-H(72C)	112.9
C(67B)-C(66B)-C(65B)	101.1(6)	C(70B)-C(72B)-H(72C)	112.9
C(71B)-C(66B)-H(66B)	109.2	C(67B)-C(72B)-H(72D)	112.9
C(67B)-C(66B)-H(66B)	109.2	C(70B)-C(72B)-H(72D)	112.9
C(65B)-C(66B)-H(66B)	109.2	H(72C)-C(72B)-H(72D)	110.3
C(68B)-C(67B)-C(72B)	101.3(8)	C(78)-C(73)-C(77)	108.6(3)
C(68B)-C(67B)-C(66B)	109.3(8)	C(78)-C(73)-C(76)	107.9(3)
C(72B)-C(67B)-C(66B)	102.0(7)	C(77)-C(73)-C(76)	104.7(3)
C(68B)-C(67B)-H(67B)	114.3	C(78)-C(73)-P(2)	117.5(2)
C(72B)-C(67B)-H(67B)	114.3	C(77)-C(73)-P(2)	110.6(2)
C(66B)-C(67B)-H(67B)	114.3	C(76)-C(73)-P(2)	106.8(2)
C(67B)-C(68B)-C(69B)	104.0(7)	C(73)-C(76)-H(76A)	109.5
C(67B)-C(68B)-H(68C)	111.0	C(73)-C(76)-H(76B)	109.5
C(69B)-C(68B)-H(68C)	111.0	H(76A)-C(76)-H(76B)	109.5
C(67B)-C(68B)-H(68D)	111.0	C(73)-C(76)-H(76C)	109.5
C(69B)-C(68B)-H(68D)	111.0	H(76A)-C(76)-H(76C)	109.5
H(68C)-C(68B)-H(68D)	109.0	H(76B)-C(76)-H(76C)	109.5
C(70B)-C(69B)-C(68B)	102.8(7)	C(73)-C(77)-H(77A)	109.5
C(70B)-C(69B)-H(69C)	111.2	C(73)-C(77)-H(77B)	109.5
C(68B)-C(69B)-H(69C)	111.2	H(77A)-C(77)-H(77B)	109.5
C(70B)-C(69B)-H(69D)	111.2	C(73)-C(77)-H(77C)	109.5
C(68B)-C(69B)-H(69D)	111.2	H(77A)-C(77)-H(77C)	109.5
H(69C)-C(69B)-H(69D)	109.1	H(77B)-C(77)-H(77C)	109.5
C(69B)-C(70B)-C(72B)	99.6(7)	C(73)-C(78)-H(78A)	109.5
C(69B)-C(70B)-C(65B)	107.3(8)	C(73)-C(78)-H(78B)	109.5
C(72B)-C(70B)-C(65B)	103.0(8)	H(78A)-C(78)-H(78B)	109.5
C(69B)-C(70B)-H(70B)	115.0	C(84)-C(75)-C(82)	107.6(4)
C(73)-C(78)-H(78C)	109.5	C(83)-C(75)-P(2)	107.2(4)
H(78A)-C(78)-H(78C)	109.5	C(84)-C(75)-P(2)	111.6(4)
H(78B)-C(78)-H(78C)	109.5	C(82)-C(75)-P(2)	116.0(5)
C(79)-C(74)-C(81)	106.4(4)	C(84B)-C(75B)-C(83B)	109.6(10)
C(79)-C(74)-C(80)	109.5(4)	C(84B)-C(75B)-C(82B)	108.6(10)
C(81)-C(74)-C(80)	107.4(4)	C(83B)-C(75B)-C(82B)	110.3(11)
C(79)-C(74)-P(2)	107.3(4)	C(84B)-C(75B)-P(2)	100.5(12)
C(81)-C(74)-P(2)	111.0(4)	C(83B)-C(75B)-P(2)	114.3(12)
C(80)-C(74)-P(2)	114.9(4)	C(82B)-C(75B)-P(2)	112.9(15)
C(79B)-C(74B)-C(80B)	110.2(10)	C(75B)-C(82B)-H(82D)	109.5
C(79B)-C(74B)-C(81B)	102.8(10)	C(75B)-C(82B)-H(82E)	109.5
C(80B)-C(74B)-C(81B)	103.5(10)	H(82D)-C(82B)-H(82E)	109.5
C(79B)-C(74B)-P(2)	112.7(10)	C(75B)-C(82B)-H(82F)	109.5
C(80B)-C(74B)-P(2)	113.2(11)	H(82D)-C(82B)-H(82F)	109.5
C(81B)-C(74B)-P(2)	113.6(13)	H(82E)-C(82B)-H(82F)	109.5
C(74B)-C(79B)-H(79D)	109.5	C(75B)-C(83B)-H(83D)	109.5
C(74B)-C(79B)-H(79E)	109.5	C(75B)-C(83B)-H(83E)	109.5
H(79D)-C(79B)-H(79E)	109.5	H(83D)-C(83B)-H(83E)	109.5
C(74B)-C(79B)-H(79F)	109.5	C(75B)-C(83B)-H(83F)	109.5
H(79D)-C(79B)-H(79F)	109.5	H(83D)-C(83B)-H(83F)	109.5
H(79E)-C(79B)-H(79F)	109.5	H(83E)-C(83B)-H(83F)	109.5
C(74B)-C(80B)-H(80D)	109.5	C(75B)-C(84B)-H(84D)	109.5
C(74B)-C(80B)-H(80E)	109.5	C(75B)-C(84B)-H(84E)	109.5
H(80D)-C(80B)-H(80E)	109.5	H(84D)-C(84B)-H(84E)	109.5
C(74B)-C(80B)-H(80F)	109.5	C(75B)-C(84B)-H(84F)	109.5

Table 4.17. (cont.)

H(80D)-C(80B)-H(80F)	109.5	H(84D)-C(84B)-H(84F)	109.5
H(80E)-C(80B)-H(80F)	109.5	H(84E)-C(84B)-H(84F)	109.5
C(74B)-C(81B)-H(81D)	109.5	H(81D)-C(81B)-H(81F)	109.5
C(74B)-C(81B)-H(81E)	109.5	H(81E)-C(81B)-H(81F)	109.5
H(81D)-C(81B)-H(81E)	109.5	C(83)-C(75)-C(84)	105.1(4)
C(74B)-C(81B)-H(81F)	109.5	C(83)-C(75)-C(82)	108.7(5)

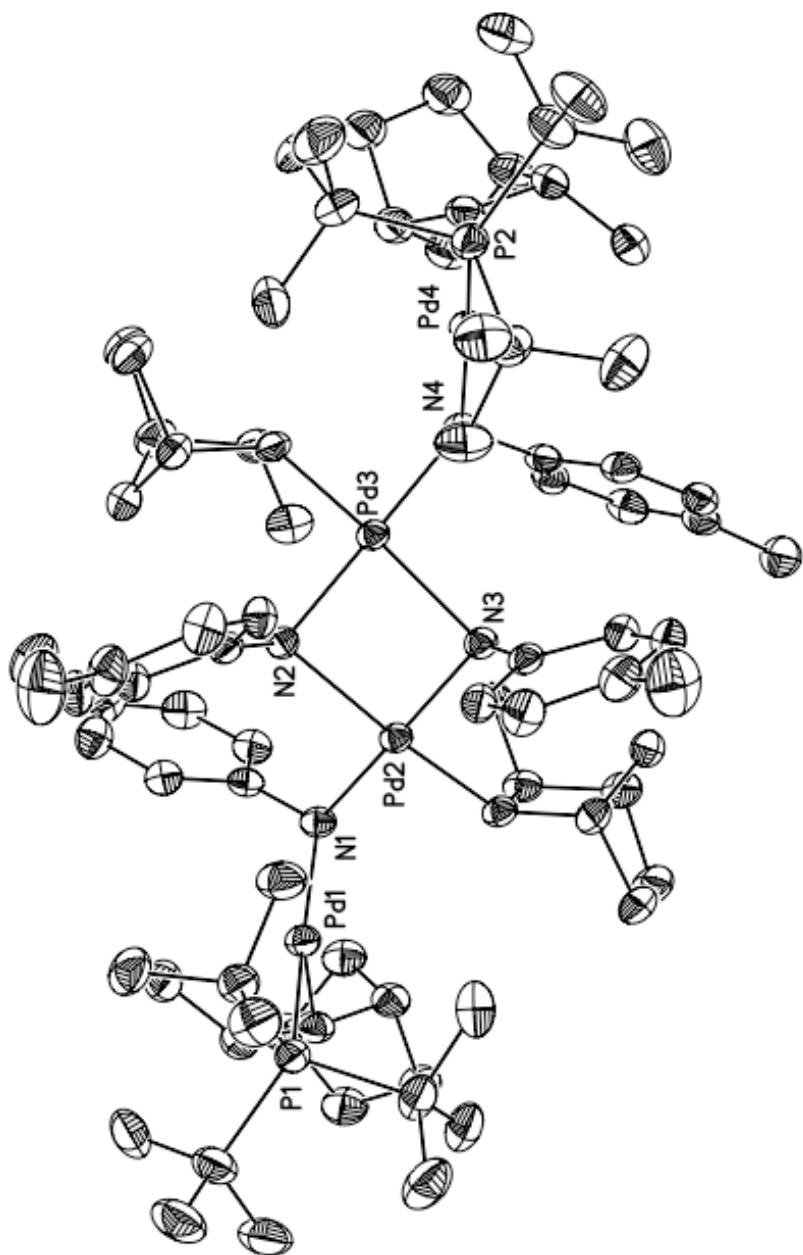


Figure 4.9. ORTEP drawing of **4.14** with 35% probability ellipsoids.

4.5 References

- (1) Hartwig, J. F. *Organotransition metal chemistry: from bonding to catalysis*; University Science Books: Sausalito, Calif., 2010.
- (2) Koo, K.; Hillhouse, G. L. *Organometallics* **1995**, *14*, 4421.
- (3) Lin, B. L.; Clough, C. R.; Hillhouse, G. L. *J. Am. Chem. Soc.* **2002**, *124*, 2890.
- (4) Pawlikowski, A. V.; Getty, A. D.; Goldberg, K. I. *J. Am. Chem. Soc.* **2007**, *129*, 10382.
- (5) Iglesias, A.; Alvarez, R.; de Lera, A. R.; Muniz, K. *Angew. Chem., Int. Ed.* **2012**, *51*, 2225.
- (6) Neumann, J. J.; Rakshit, S.; Droge, T.; Glorius, F. *Angew. Chem., Int. Ed.* **2009**, *48*, 6892.
- (7) Mei, T. S.; Wang, X. S.; Yu, J. Q. *J. Am. Chem. Soc.* **2009**, *131*, 10806.
- (8) Brice, J. L.; Harang, J. E.; Timokhin, V. I.; Anastasi, N. R.; Stahl, S. S. *J Am Chem Soc* **2005**, *127*, 2868.
- (9) Lautens, M.; Paquin, J. F.; Piguil, S.; Dahlmann, M. *J. Org. Chem.* **2001**, *66*, 8127.
- (10) Catellani, M.; Del Rio, A. *Russ. Chem. Bull.* **1998**, *47*, 928.
- (11) Pan, J.; Su, M. J.; Buchwald, S. L. *Angew. Chem., Int. Ed.* **2011**, *50*, 8647.
- (12) Marquard, S. L.; Rosenfeld, D. C.; Hartwig, J. F. *Angew. Chem., Int. Ed.* **2010**, *49*, 793.
- (13) Marquard, S. L.; Hartwig, J. F. *Angew. Chem., Int. Ed.* **2011**, *50*, 7119.
- (14) Esposito, O.; Gois, P. M. P.; Lewis, A. K. D. K.; Caddick, S.; Cloke, F. G. N.; Hitchcock, P. B. *Organometallics* **2008**, *27*, 6411.

- (15) Esposito, O.; Lewis, A. K. D. K.; Hitchcock, P. B.; Caddick, S.; Cloke, F. G. N. *Chem. Commun.* **2007**, 1157.
- (16) Marquard, S. L., University of Illinois at Urbana-Champaign, 2011.
- (17) Kang, M.; Sen, A. *Organometallics* **2004**, *23*, 5396.
- (18) Villanueva, L. A.; Abboud, K. A.; Boncella, J. M. *Organometallics* **1994**, *13*, 3921.
- (19) Driver, M. S.; Hartwig, J. F. *J. Am. Chem. Soc.* **1996**, *118*, 4206.
- (20) Driver, M. S.; Hartwig, J. F. *Organometallics* **1997**, *16*, 5706.
- (21) Yamashita, M.; Hartwig, J. F. *J. Am. Chem. Soc.* **2004**, *126*, 5344.
- (22) Yamashita, M.; Vicario, J. V. C.; Hartwig, J. F. *J. Am. Chem. Soc.* **2003**, *125*, 16347.
- (23) Moriconi, E. J.; Crawford, W. C. *J. Org. Chem.* **1968**, *33*, 370.
- (24) Kirmse, W.; Hartmann, M.; Siegfried, R.; Wroblowsky, H. J.; Zang, B.; Zellmer, V. *Chem. Ber-Recl.* **1981**, *114*, 1793.
- (25) Fors, B. P.; Watson, D. A.; Bischoe, M. R.; Buchwald, S. L. *J. Am. Chem. Soc.* **2008**, *130*, 13552.
- (26) Shen, Q.; Ogata, T.; Hartwig, J. F. *J. Am. Chem. Soc.* **2008**, *130*, 6586.
- (27) M. J. Frisch, G. W. T., H. B. Schlegel, G. E. Scuseria, M. A. Robb, J. R. Cheeseman, G. Scalmani, V. Barone, B. Mennucci, G. A. Petersson, H. Nakatsuji, M. Caricato, X. Li, H. P. Hratchian, A. F. Izmaylov, J. Bloino, G. Zheng, J. L. Sonnenberg, M. Hada, M. Ehara, K. Toyota, R. Fukuda, J. Hasegawa, M. Ishida, T. Nakajima, Y. Honda, O. Kitao, H. Nakai, T. Vreven, J. A. Montgomery, Jr., J. E. Peralta, F. Ogliaro, M. Bearpark, J. J. Heyd, E. Brothers, K. N. Kudin, V. N. Staroverov, R. Kobayashi, J. Normand, K. Raghavachari, A.

Rendell, J. C. Burant, S. S. Iyengar, J. Tomasi, M. Cossi, N. Rega, J. M. Millam, M. Klene, J. E. Knox, J. B. Cross, V. Bakken, C. Adamo, J. Jaramillo, R. Gomperts, R. E. Stratmann, O. Yazyev, A. J. Austin, R. Cammi, C. Pomelli, J. W. Ochterski, R. L. Martin, K. Morokuma, V. G. Zakrzewski, G. A. Voth, P. Salvador, J. J. Dannenberg, S. Dapprich, A. D. Daniels, Ö. Farkas, J. B. Foresman, J. V. Ortiz, J. Cioslowski, and D. J. Fox. In *Gaussian 09, Revision A.1*; Gaussian, Inc.: Wallingford CT, 2009.

- (28) Rappe, A. K.; Casewit, C. J.; Colwell, K. S.; Goddard, W. A.; Skiff, W. M. *J. Am. Chem. Soc.* **1992**, *114*, 10024.
- (29) Stevens, W. J.; Krauss, M.; Basch, H.; Jasien, P. G. *Can. J. Chem.* **1992**, *70*, 612.
- (30) Svensson, M.; Humbel, S.; Froese, R. D. J.; Matsubara, T.; Sieber, S.; Morokuma, K. *J. Phys. Chem.* **1996**, *100*, 19357.